UNIVERSITY OF CALIFORNIA SAN DIEGO

Novel signaling mechanisms downstream of NIPI-3/Tribbles regulate development in *Caenorhabditis elegans*

A dissertation submitted in partial satisfaction of the requirements for the degree Doctor of Philosophy

in

Biology

by

Rose Aria Malinow

Committee in charge:

Professor Yishi Jin, Chair
Professor Susan Ackerman
Professor Christopher Glass
Professor James Kadonaga
Professor Emily Troemel

2022

The dissertation of Rose Aria Malinow is approved, and it is acceptable in quality and form for publication on microfilm and electronically.

University of California San Diego

2022

TABLE OF CONTENTS

LIST OF FIGURES

LIST OF TABLES

ACKNOWLEDGEMENTS

I would like to acknowledge Professor Yishi Jin for her guidance and support as my advisor. I am appreciative of all past and present members of the Jin and Chisholm labs who have helped me so much throughout my years in the lab. In particular, I would like to thank Kate McCulloch, Wendy Knowlton, Sam Cherra, and Matt Andrusiak for helping me when I first joined the lab and teaching me about *C. elegans*, genetics, and how to survive grad school. I would like to especially thank Kyung (Kai) Won Kim for letting me work with her on the NIPI-3 project and answering my never-ending stream of questions. I thank my undergrad assistant, Hetty Zhang, for helping me with strain construction. I thank my thesis committee members for their advice and support.

I would especially like to thank my fiancé, Chris Dablio, for his loving support throughout this process. You are the hardest working person I know, and you inspire me every day. My life is full of love and happiness because of you and Maybelle.

Finally, I would like to thank my family. I am grateful that my parents are nearby and that I am able to see them often. I cannot find the words to express my gratitude for the constant love, advice and encouragement you give me. I would not have been able to survive this process without you. To my extended family, it is always a joy to be with you. Lastly, I want to dedicate this dissertation to my loving grandmothers who both passed in October 2020. Sylvia and Tita, I wish you were here to celebrate with us.

Chapter 2, in large part, is a reprint of the material as it appears in Malinow RA, Ying P, Koorman T, Boxem M, Jin Y, Kim KW. 2019. Functional Dissection of *C. elegans* bZip-Protein CEBP-1 Reveals Novel Structural Motifs Required for Axon Regeneration and Nuclear Import. *Frontiers in Cellular Neuroscience* 13:348. The

dissertation author was the primary investigator and author of the material included in this chapter.

Chapter 3 describes the work of the dissertation author in collaboration with Drs. Zhu and Kim, former postdoctoral researchers in the laboratory of Professor Jin. The dissertation author was the primary investigator and wrote the chapter in full.

VITA

2012 Bachelor of Science, Georgia Institute of Technology

2022 Doctor of Philosophy, University of California San Diego

PUBLICATIONS

Malinow RA, Ying P, Koorman T, Boxem M, Jin Y, Kim KW. 2019. Functional Dissection of *C. elegans* bZip-Protein CEBP-1 Reveals Novel Structural Motifs Required for Axon Regeneration and Nuclear Import. *Frontiers in Cellular Neuroscience* 13:348.

ABSTRACT OF THE DISSERTATION

Novel signaling mechanisms downstream of NIPI-3/Tribbles regulate development in *Caenorhabditis elegans*

by

Rose Aria Malinow

Doctor of Philosophy in Biology

University of California San Diego, 2022

Professor Yishi Jin, Chair

This dissertation explores the roles of the Tribbles pseudokinase NIPI-3 and its downstream signaling in regulating *C. elegans* development. It was previously reported that in the absence of NIPI-3, expression of the stress-response transcription factor CEBP-1 increases significantly, leading to upregulation of the PMK-1/p38 MAP kinase pathway and developmental arrest. Moreover, the developmental arrest of *nipi-3(0)* animals is rescued by loss of function in *cebp-1.* This genetic interaction formed the basis for a forward genetic screen where, through random mutagenesis, genes that are necessary for the signaling downstream of NIPI-3 can be identified, as they will rescue animal development. The genes identified from this forward genetic screen and their

signaling pathways are the subject of my dissertation. First, I isolated many alleles in two genes, CEBP-1 and MAK-2, which allowed for deeper analysis of the residues required for protein function. With further interrogation using genome-editing, I identified a novel domain that is critical for the *in vivo* function of CEBP-1. This domain is not only required for CEBP-1 function in development, but also axon regeneration. By protein structural prediction, I found that the region containing this unique domain has a predicted propensity to form alpha helices. Second, using a transcriptional reporter of *sek-1* transcription as a readout of p38 MAPK activation by CEBP-1, I found novel positive regulation from *pmk-1*/MAPK and *mak-2*/MAPKAPK to *sek-1*/MAPKK transcription. It also appears that SEK-1 activity may activate its own gene transcription, suggesting another positive possible feedback loop in this pathway. Finally, I describe a collaborative study revealing that histone deacetylation and N-terminal acetylation are involved in the regulation of development in *C. elegans*. We found that a gain of function mutation within the histone deacetylase *hda-4* prevents developmental arrest of *nipi-3(0)* animals via transcriptional regulation of *sek-1/*MAPKK. We also found that loss of function of any of the components of the N-acetyltransferase C (NatC) complex (*natc-1, natc-2,* or *natc-3)* prevents developmental arrest of *nipi-3(0)* animals, partially via regulation of the PMK-1 pathway, and partially via a parallel pathway. Altogether, my thesis work has contributed to the understanding of the intricate regulation of p38 MAPK pathway activity during *C. elegans* development.

Chapter 1: Introduction to Tribbles, C/EBPs and p38 MAPK Pathways in Innate Immunity and Animal Development

1.1 Tribbles Pseudokinases: Regulating cell signaling, innate immunity and animal development

Tribbles are highly conserved serine/threonine pseudokinases with diverse roles in physiology across metazoans (Dobens and Bouyain 2012). These proteins are defined as pseudokinases because they lack a functional ATP binding pocket, thus are unable to phosphorylate targets (Murphy et al. 2015). Tribbles pseudokinases instead are known to act as scaffolding proteins that bring target proteins into physical proximity to regulate the activity and stability of these proteins (Hegedus et al. 2007, Miyajima et al. 2015). The founding member of the Tribbles protein family was identified in *Drosophila* in a screen for genes that control cell proliferation and migration (Mata et al. 2000). Subsequently, three mammalian Tribbles family proteins were identified TRIB1, TRIB2, and TRIB3, which have diverse roles in cell cycle regulation, blood cell differentiation, and glucose and lipid metabolism (Dobens and Bouyain 2012, Johnston et al. 2015, Eyers et al. 2017, Richmond and Keeshan 2020). Because of these fundamental roles in cell and tissue homeostasis, altered Tribbles protein activity often impairs cell and tissue functions leading to a wide range of diseases (Kiss-Toth 2011, Rowan and Litherland 2015, Jadhav and Bauer 2019). Gene amplification, and therefore overexpression, of TRIB1 is often seen in AML and myelodysplastic syndromes, an umbrella term describing disrupted blood cell production and/or function (Yokoyama et al. 2010, Yokoyama and Nakamura 2011, Cunard 2013). TRIB3 expression is elevated in neurons of both Alzheimer's and Parkinson's patients and mouse and cell line models show that elevated TRIB3 causes neuronal cell death (Aime et al. 2015, Saleem and Biswas 2017, Lorenzi et al. 2018). All three human Tribbles

proteins have been associated with the development and progression of multiple cancers including leukemia, breast, thyroid, prostate, liver, and ovarian cancers (Bowers et al. 2003, Wennemers et al. 2011, Eyers et al. 2017, Richmond and Keeshan 2020). Here, I will review the role of mammalian Tribbles in animal development, immunity and metabolism, the cellular mechanisms of mammalian Tribbles, and the *C. elegans* Tribbles homolog, NIPI-3.

Mammalian tribbles in animal development and metabolic processes

Tribbles proteins play central role in animal development, through regulation of cellular differentiation, proliferation, migration, and growth (Mata et al. 2000, Rørth et al. 2000, Sakai et al. 2010, Gendelman et al. 2017). In mice, knock-out of TRIB1 causes pre-weaning lethality, likely caused by an inability to maintain body temperature due to improper development of brown adipose tissue (Zhang et al. 2021). This regulation of development is conserved in *Drosophila* as knockdown of *Tribbles* delays larval development while *Tribbles* overexpression causes precocious larval development (Seher and Leptin 2000, Das et al. 2014). The specific cellular functions of mammalian Tribbles proteins have been well-described for hematopoiesis, which is the differentiation of hematopoietic stem cells (HSCs) into red and white blood cells (Johnston et al. 2015, Stein et al. 2015, Eyers et al. 2017). Across vertebrates, there are two main lineages that differentiate from HSCs: myeloid progenitors and lymphoid progenitors (Rosental et al. 2018). Tribbles proteins are differentially expressed in these cells: TRIB1 is primarily expressed in myeloid progenitors, TRIB2 is primarily expressed in lymphoid progenitors, whereas TRIB3 is expressed in both types (Heng et al. 2008,

Salome et al. 2018). Misexpression of any of the three Tribbles proteins, either globally or specifically in the bone marrow, changes the cell fate of HSCs and leads to a disruption to the ratio of types of white blood cells (Keeshan et al. 2006, Satoh et al. 2013, Mack et al. 2019). The correct number and ratio of white blood cells is essential for the function of both the adaptive and innate immune system in mammals. Due to their central role in white blood cell differentiation, it is unsurprising that gain of function mutations in Tribbles proteins are implicated in the development of acute myeloid leukemia (AML), a cancer of white blood cells (Dedhia et al. 2010, Murphy et al. 2015, Uljon et al. 2016).

In addition to their role in the differentiation of immune cells, Tribbles proteins also regulate immune signaling, often functioning as negative regulators (Johnston et al. 2015, Stein et al. 2015). Specifically, TRIB2 negatively regulates nuclear factor kappa B (NF-κB) activity via direct binding to NF-κB2, a central transcription factor that controls many aspects of inflammatory and innate immune responses (Wei et al. 2012, Johnston et al. 2015). TRIB2 also functions as a constitutive negative regulator of production of the cytokine interleukin 8 (IL-8), via direct binding to select map kinase activated protein kinases (MAPKs) in monocytes. In general, IL-8 secretion serves to attract more white blood cells to a location of tissue damage or infection (Eder et al. 2008). In another type of immune cell, mast cells, TRIB3 negatively regulates the secretion of cytokines including IL-4 and IL-6, cytokines that stimulate the adaptive and innate immune system, respectively (Kuo et al. 2012). Also in adaptive immunity, TRIB1 negatively regulates antibody production in B lymphocytes (Simoni et al. 2018).

Tribbles proteins also play central roles in metabolism through regulating lipid and glucose homeostatic processes in the liver and adipose tissue (Qi et al. 2006, Burkhardt et al. 2010, Borsting et al. 2014). TRIB1 is a major regulator of liver function and its expression in the liver suppresses lipid metabolism (Bauer et al. 2015a, Bauer et al. 2015b, Soubeyrand et al. 2016, Soubeyrand et al. 2017). When fed a high fat diet, mice lacking hepatic TRIB1 have higher levels of triglycerides and glucose in their blood in comparison to wildtype animals fed the same diet (Satoh et al. 2013). High triglycerides can lead to stroke, heart attack, and other heart disease while high glucose levels contribute to the development of insulin resistance and diabetes. Similarly, variants of human TRIB1 are associated with the development of nonalcoholic fatty liver disease, a disease that presents as excess triglycerides stored in the liver (Kitamoto et al. 2014). Studies in human patients, rodent models of insulin resistance, and rodent cell lines expressing human TRIB3 show that TRIB3 also functions to stabilize blood glucose and lipid levels (Liu et al. 2010). In mice, when blood sugar levels drop after fasting, TRIB3 expression is upregulated in the liver and adipocytes (Lima et al. 2009). In multiple rodent models and human cell lines, TRIB3 promotes hepatic glucose production and lipid metabolism in adipose tissues (Wang et al. 2009, Prudente et al. 2012). In mouse models and human cell lines, overexpression of TRIB3 in the liver causes high blood sugar whereas overexpression of TRIB3 in adipose tissues is protective against obesity (Du et al. 2003, Qi et al. 2006). Thus, both TRIB1 and TRIB3 are required to stabilize blood glucose and lipid levels by regulating the intricate balance of glucose and lipid metabolism in the liver and adipose tissues.

Cell signaling mechanisms of mammalian tribbles

Structurally, the pseudokinase domain of Tribbles proteins resembles a canonical serine/threonine kinase domain, with two key differences: 1. The beta sheets that, in active kinases, are aligned to create a binding pocket for ATP, are disjointed and unaligned in the Tribbles pseudokinase domain. 2. The DFG motif, present in the base of the activation loop of canonical kinases which interacts with magnesium to create a conformational change to increase the affinity for ATP binding, is replaced by a SLE motif in Tribbles proteins (Taylor and Kornev 2011, Taylor et al. 2013, Murphy et al. 2015). This SLE motif locks the kinase in a conformation that is not advantageous to ATP binding, which is required for phosphorylative activity of a kinase. In addition to their pseudokinase domain, mammalian Tribbles proteins have a variable N-terminal region that determines protein localization (Kiss-Toth et al. 2006) and a unique C-terminal tail containing two binding sites, one targeting MAP2K proteins and the other ubiquitin E3 ligases, allowing Tribbles to mediate proteasomal degradation of MAP2K proteins (Keeshan et al. 2010, Eyers et al. 2017).

Mammalian tribbles proteins are able to regulate a diverse set of cellular processes by modulating the activity of CCAAT-enhancer binding protein (C/EBP) transcription factors and MAPK signaling (Naiki et al. 2007). C/EBPs are bZip transcription factors which play critical roles in many cellular processes including innate immunity, cellular proliferation, growth, and differentiation, as described further in Section 2, below. Tribbles proteins mediate the ubiquitination and proteasomal degradation of C/EBP proteins through recruitment of E3-ubiquitin ligases, primarily the E3 Ubiquitin ligase COP1 (Dedhia et al. 2010, Murphy et al. 2015). To promote nuclear

degradation of transcription factors, Tribbles prevents nuclear export of COP1, as shown in both human and mouse cell lines (Kung and Jura 2019). This regulation is generally conserved, as *Drosophila Tribbles* also negatively regulates fly C/EBP, *Slbo*, by promoting proteosome-mediated C/EBP degradation (Masoner et al. 2013).

Separately from its interactions with C/EBP proteins, Tribbles proteins also regulate MAPK signaling, which is an essential form of cellular signaling that mediates growth, differentiation, and innate immune responses, among other physiological processes. MAPK signaling is performed by three kinases that phosphorylate each other in a serial manner. MAP3Ks (MAP kinase kinase kinases) phosphorylate and activate MAP2Ks (MAP kinase kinases) which in turn phosphorylate MAPKs (MAP kinases) which directly and indirectly regulate gene expression through the activity of other kinases, transcription factors, RNA/DNA binding proteins, and structural proteins (Canovas and Nebreda 2021). MAPK signaling is discussed further, below in Section 3. Tribbles reduce MAPK signaling through two mechanisms: 1. Proteasomal degradation of MAP2Ks through processes similar to regulation of C/EBPs and 2. Inhibiting kinase activity of MAP2Ks by binding to the MAP2K and preventing MAP2K-MAPK binding (Kiss-Toth et al. 2004). All three human Tribbles can form complexes with multiple MAP2Ks and inhibit their kinase activity (Guan et al. 2016). In summary, mammalian Tribbles regulate a plethora of cellular processes through regulation of stability and activity of other proteins.

C. elegans tribbles in innate immunity and development

The *C. elegans* Tribbles homologue, NIPI-3, was first identified in a screen for genes required specifically for the induction of the innate immune response after fungal infection (Pujol et al. 2008). Here it was shown that NIPI-3 is required for the upregulation of the antimicrobial peptide NLP-29 after epidermal infection, but not after wounding of the epidermis (Pujol et al. 2008). Furthermore, NIPI-3 functions cell autonomously in distinct tissues to regulate their responses to different pathogens. In particular, epidermal, but not intestinal expression of NIPI-3 is important for immune response against the epidermal fungal pathogen *D. coniospora* (Pujol et al. 2008, Ziegler et al. 2009, Couillault et al. 2012). Conversely, intestinal, but not epidermal, NIPI-3 is required for survival after infection by the bacterial pathogen *P. aeruginosa,* which primarily infects the intestine (McEwan et al. 2016, Wu et al. 2021) **(Figure 2)**. In contrast to its cell-autonomous role in tissue-specific infection, NIPI-3 is required in multiple tissues to regulate development. *nipi-3(0)* animals arrest during larval development (Kim et al. 2016).

As with other Tribbles proteins, *C. elegans* Tribbles/NIPI-3 negatively regulates *C. elegans* C/EBP transcription factor, CEBP-1. In mammalian systems, Tribbles proteins bind directly to C/EBPs and recruit COP-1 to promote proteasomal degradation of C/EBP proteins (Keeshan et al. 2006, Dedhia et al. 2010, Keeshan et al. 2010). Interestingly, a different mechanism is utilized with the same outcome of negative regulation of CEBP-1 by NIPI-3. In *C. elegans*, NIPI-3 negatively regulates the transcription of *cebp-1* (Kim et al. 2016). *cebp-1* is required for *nipi-3* function in both development and induction of antimicrobial peptides in response to intestinal infection.

Therefore, study of the regulation of CEBP-1 and downstream pathways may lead to insights into the function of NIPI-3.

Given that Tribbles proteins function through their effects on C/EBPs in mammals, *Drosophila*, and *C. elegans*, I will next review the functions and signaling mechanisms of C/EBPs as they relate to animal development and immunity.

1.2 CCAAT-Enhancer Binding Protein (C/EBP) Transcription Factors Regulate Expression of Development and Immunity Genes

CCAAT Enhancer Binding Proteins (C/EBPs) are bZip transcription factors that play critical roles in animal development, metabolism, and immunity (Johnson 2005, Friedman 2007, Smink and Leutz 2010) and are regulated by Tribbles proteins across multiple species (Masoner et al. 2013, Bauer et al. 2015a, Kim et al. 2016). The first C/EBP protein (CEBPα) was identified in rat liver nuclei as a heat-stable factor capable of binding to the CCAAT DNA motif (Graves et al. 1986, Johnson et al. 1987) and was cloned in 1988 (Landschulz et al. 1988). This C/EBP protein was the founding member in the class of basic-leucine zipper (bZip) domain containing transcription factors. Studying this seminal C/EBP protein revealed that the bZip domain is required for transcription factor dimerization, which is essential for DNA binding (Agre et al. 1989, Landschulz et al. 1989, Vinson et al. 1989).

Humans and mice have six C/EBP genes, CEBPα, β, γ, δ, ε, ζ, and knockout mice for each gene exhibit different phenotypes, suggesting functional specialization of these homologous proteins. At the molecular level, the DNA binding bZip domain of C/EBPs is highly conserved, but they have diverse N-terminal regions, which specify their protein-protein interactions and leads to functional specialization. (Friedman and McKnight 1990, Pei and Shih 1991, Kowenz-Leutz et al. 1994). Tissue- and cell-type specific control of CEBPα-ζ also contributes to the diversity of phenotypes seen at the cellular, tissue, and organismal levels (Roman et al. 1990, Chumakov et al. 1997, Takiguchi 1998, Cassel and Nord 2003). Here, I will review mammalian C/EBPs functions in animal development and immunity, based on our interest in a potential

common signaling pathway affecting these aspects of animal physiology, followed by a discussion of molecular mechanisms governing mammalian C/EBP function, and then a review of *C. elegans* C/EBPs in regulating animal development and innate immunity.

Mammalian C/EBPs in development and immunity

CEBPα is an essential gene in development: knockout mice are unable to maintain energy homeostasis and die of hypoglycemia within hours of birth (Wang et al. 1995, Flodby et al. 1996). Additionally, knockout of both CEBPα and CEBPβ, but not CEBPβ alone, causes embryonic developmental arrest, indicating a redundant role for CEBPα and CEBPβ in early development (Begay et al. 2004). On a cellular level, C/EBPs are highly studied in their central roles in adipogenesis and hematopoiesis (i.e. differentiation of appropriate progenitor cells into adipose tissue or red and white blood cells). Coordination of four C/EBP genes, CEBPα, CEBPβ, CEBPδ, and CEBPζ is required for adipocyte differentiation (Yeh et al. 1995, Tanaka et al. 1997). As discussed in section 1, Tribbles proteins regulate both hematopoiesis and C/EBP expression. In hematopoiesis, as in many other cellular processes, C/EBP expression is regulated by TRIBs. Specifically, TRIB2 promotes the degradation of CEBPα and CEBPβ (Keeshan et al. 2006, Naiki et al. 2007). Human patient samples of hematopoietic cancers have elevated levels of TRIB1 and TRIB2 (Rucker et al. 2006, Storlazzi et al. 2006, Rothlisberger et al. 2007). These findings can be recapitulated in mice where overexpression of either TRIB1 or TRIB2 in bone marrow causes acute myeloid leukemia (AML) (Jin et al. 2007). Both TRIB1 and TRIB2 function through degradation of CEBPα to induce AML (Keeshan et al. 2006, Dedhia et al. 2010). In addition to

increased degradation of CEBPα, loss of function of CEBPα also causes AML (Pabst et al. 2001). Altogether, multiple C/EBPs have central roles in animal development and cellular differentiation.

Loss of CEBPβ or CEBPε results in severe deficiencies in innate immunity, specifically defense against bacterial infections. CEBPβ KO mice have greatly increased susceptibility to multiple bacterial pathogens including *Listeria monocytogenes*, *Salmonella typhimurium*, and *Candida albicans* (Screpanti et al. 1995, Tanaka et al. 1995, Uematsu et al. 2007). CEBPε knockout mice have very low resistance to infection and within a few months of birth succumb to bacterial infections that are easily resolved by wildtype animals (Yamanaka et al. 1997, Lekstrom-Himes and Xanthopoulos 1999). Loss of function of CEBPε causes the human disease specific granule deficiency 1 that primarily presents as frequent and severe bacterial infections (Lekstrom-Himes et al. 1999, Gombart et al. 2001, Wada et al. 2015). In addition to these severe, systemic phenotypes, C/EBPs are integral to cytokine (interleukin) expression and signaling that regulates many aspects of the mammalian adaptive and innate immune systems, such as the differentiation of specialized white blood cells. CEBPβ knockout mice phenocopy interleukin-6 (IL-6) overexpression and have reduced innate immunity and increased adaptive immunity (Screpanti et al. 1995). IL-6 cytokines induce CEBPδ activity, which in turn feedback to activate CEBPβ, reducing IL-6 expression, producing a negative regulatory feedback loop (O'Rourke et al. 1997, O'Rourke et al. 1999a, O'Rourke et al. 1999b, Sivko and DeWille 2004, Sanford and DeWille 2005). Furthermore, CEBPβ promotes the transcription of IL-4, which promotes the differentiation of white blood cells to stimulate the adaptive immune system

(Berberich-Siebelt et al. 2006). CEBPζ promotes the transcription of IL-8, a cytokine that attracts certain white blood cells and promotes angiogenesis (Caristi et al. 2005, Cucinotta et al. 2008). These examples illustrate the role of C/EBPs in the complex regulation of both adaptive and innate immunity in mammalian systems.

Cellular signaling mechanisms of mammalian C/EBPs

C/EBP proteins are regulated at multiple levels to tightly control their function in a wide variety of signal transduction pathways: 1. Dimerizing with other transcription factors to regulate activity and targets of the C/EBP, 2. Binding with other proteins that modulate the DNA affinity of the C/EBP, and 3. Post-translational modification, such as phosphorylation, regulates the transcriptional activity of the C/EBP (Tsukada et al. 2011). C/EBPs can homodimerize, dimerize with other C/EBPs, or dimerize with other transcription factors such as fos, Jun, CREB, or ATF, allowing for a greater range of control of transcriptional activity and specificity (Glover and Harrison 1995, Metallo and Schepartz 1997, Kohler et al. 1999, Newman and Keating 2003). Three C/EBPs, CEBPγ, CEBPζ, and certain isoforms of CEBPβ function as negative regulators of transcription. CEBPγ contains a bZip domain but no transactivation domain and therefore cannot bind with transcriptional machinery. When CEBPγ forms heterodimers with other C/EBP members, the complex binds DNA and blocks transcription of the target gene (Cooper et al. 1995). Heterodimers of CEBPγ with other C/EBPs are more stable than homodimers of CEBPγ, indicating the primary role of CEBPγ is to repress the of activity of other C/EBPs (Tsukada et al. 2011). CEBPζ represses C/EBP target transcription by heterodimerizing with CEBPα, CEBPβ, and CEBPδ and inhibiting DNA

binding (Ron and Habener 1992, MacDougald and Lane 1995). Activity of CEBPζ is induced and causes growth arrest in multiple cell types by cellular stresses such as DNA damage (Barone et al. 1994) and glucose starvation (Carlson et al. 1993, Fawcett et al. 1996). CEBPβ has two isoforms with opposite functions, LIP (liver inhibitory protein) and LAP (liver activating protein) (Descombes and Schibler 1991). CEBPζ preferentially associates with the inhibitory isoform of CEBPβ, functionally increasing the transcription of CEBPβ gene targets (Hattori et al. 2003). Additionally, under certain conditions, CEBPζ can promote transcription. For instance, in response to nutrient starvation, ATF4 and CEBPζ dimerize to promote transcription of TRIB3 (Ohoka et al. 2005). Interestingly, ATF4 and CEBPζ are primary targets of TRIB3 triggered COP1 degradation, indicating a negative feedback regulatory system (Ohoka et al. 2007). C/EBPs can also enhance the activity of their binding partner. For instance, CEBPδ – CEBPβ heterodimers promote transcription of CEBPβ target genes more efficiently than CEBPβ homodimers (Kinoshita et al. 1992). C/EBPs also dimerize with many other transcription factors, diversifying the target DNA sequence, leading to a wide array of transcription factor complexes that can promote or inhibit the transcription of many different genes. In addition to regulation by dimerization through the bZip domain, C/EBPs contain transactivating and regulatory domains, which control their transcriptional activity via specific protein-protein interactions (Charles et al. 2001, Duan et al. 2005, Wiper-Bergeron et al. 2007). For instance, skeletal muscle development proteins SMAD3/4 bind to and promote transcriptional activity of CEBPβ (Wang et al. 2005).

The activity of C/EBPs is highly regulated by post-translational modifications, primarily phosphorylation and acetylation. There are multiple sites within each C/EBP that can be modified, and each site has a specific effect. For example, there are multiple lysines in CEBPβ that can be acetylated and different patterns of acetylated lysines allow CEBPβ to bind to different promoters (Cesena et al. 2007). Post-translational modifications can have general regulatory or a gene specific effect. For instance, a Ras-dependent MAPK phosphorylation site in CEBPβ activates transcription of all CEBPβ targets by increasing the interaction between CEBPβ and transcriptional initiation machinery (Mo et al. 2004). Alternately, phosphorylation of the DNA binding domain of CEBPβ by PKA reduces DNA binding affinity, decreasing transcription of all CEBPβ targets (Trautwein et al. 1994). Additionally, methylation of CEBPβ also reduces the transcriptional activity of CEBPβ by reducing recruitment of transcriptional initiation machinery (Kowenz-Leutz et al. 2010). Post-translational modification of CEBPβ has been particularly well-studied, but there are many examples of other C/EBPs being regulated, both positively and negatively, by post-translational modifications (Wang and Ron 1996, Caristi et al. 2005, Wang et al. 2006, Cucinotta et al. 2008). Together, these studies indicate that the targets of C/EBP transcription and C/EBP transcriptional activity are highly regulated, at multiple levels, by binding with different transcription factors and post-translational modifications, to produce a wide variety of gene regulation.

C. elegans C/EBPs in innate immunity

C. elegans have three transcription factors in the C/EBP family: CEBP-1, CEBP-2, and ZIP-4 (Shaye and Greenwald 2011). These C/EBPs regulate three independent

innate immune pathways: 1. The response to translation elongation block, which can be caused by infection by *P. aeruginosa* (Reddy et al. 2016), 2. The Ethanol and Stress Response Element (ESRE), a gene set with an evolutionarily conserved ESRE motif that is induced after xenobiotic stresses and some pathogenic stimuli (Tjahjono and Kirienko 2017), and 3. the PMK-1/p38 MAPK pathway, a highly conserved pathway central to *C. elegans* innate immune functioning cell autonomously in multiple tissues to defend against pathogens (McEwan et al. 2016, Wu et al. 2021) **(Figure 1)**.

C. elegans C/EBPs are essential for multiple innate immune responses. One form of innate immune response, surveillance immunity, is trigged when any one of a range of normal cellular processes is interrupted by a pathogen (e.g. mRNA translation elongation, function of mitochondria, histones, or proteasomal degradation) (Beddoe et al. 2010, Dunbar et al. 2012, McEwan et al. 2012, Melo and Ruvkun 2012, Mohr and Sonenberg 2012, Lee et al. 2013, Lemaitre and Girardin 2013, Lemichez and Barbieri 2013, Liu et al. 2014). This surveillance method is more specific to detecting pathogens that cause disruption to cellular processes, in comparison to detection of microbe-associated molecular patterns (MAMPs) which only determines if molecules are foreign (for instance, non-pathogenic bacteria can activate MAMP-triggered defenses). Unlike MAMP detection, surveillance immunity doesn't require detecting a specific pathogen by its molecular structure (Spoel and Dong 2012, Stuart et al. 2013, Rajamuthiah and Mylonakis 2014, Cohen and Troemel 2015). In response to translation block induced by bacterial infection by *P. aeruginosa*, CEBP-2 functions with ZIP-2, another bZip transcription factor, to promote the transcription of infection response genes that reduce bacterial burden in the intestine including infection response gene 1 (*irg-1*), infection

response gene 2 (*irg-2*), unnamed gene involved in immune response (*F11D11.3*), and O-Acetyltransferase homolog 32 (*oac-32)* **(Figure 1)** (Reddy et al. 2016). CEBP-2 also dimerizes with ZIP-11 to regulate expression of *irg-1* after *P. aeruginosa* infection **(Figure 1)** (Zheng et al. 2021). This is an example of *C. elegans* C/EBP proteins forming different heterodimers, as is the case with mammalian C/EBPs. All three *C. elegans* C/EBPs, CEBP-1, CEBP-2, and ZIP-4 along with ZIP-2, regulate the expression of ESRE genes in response to mitochondrial damage that can be caused by *P. aeruginosa* infection **(Figure 1)** (Tjahjono and Kirienko 2017).

Interestingly, CEBP-1 has context-dependent roles in regulating the activity of PMK-1/p38 MAPK. In both development and in response to intestinal infection, the expression of CEBP-1 is negatively regulated by NIPI-3. Although during development, *nipi-3* suppresses PMK-1 activity whereas in response to intestinal infection, *nipi-3* promotes PMK-1 activity. Both of these effects on PMK-1 activity require *cebp-1*. It seems that under different circumstances, CEBP-1 promotes transcription of *sek-1*, an activator of PMK-1 activity, or *vhp-1*, a repressor of PMK-1 activity. During development, increased expression of CEBP-1 leads to an increase of *sek-1* mRNA (Kim et al. 2016). This increase in *sek-1* transcription is also seen in adult animals, in the absence of infection. In these adult uninfected animals with increased expression of CEBP-1, there is also an increase in *skn-1* mRNA, a transcription factor used as a readout of PMK-1 activity (Wu et al. 2021). This suggests that in uninfected animals, during development or adulthood, CEBP-1 activity leads to increased PMK-1 activity, via the transcription of *sek-1.* By contrast, in adult animals infected with the intestinal bacteria *E. faecalis* or *P. aeruginosa,* increased CEBP-1 leads to increased transcription of *vhp-1,* a phosphatase

that dephosphorylates and deactivates PMK-1 (Wu et al. 2021). This raises the question of how the transcriptional target of CEBP-1 is established based on the context of CEBP-1 activation.

C. elegans CEBP-1 in neuronal stress response

Much of the research on CEBP-1 has focused on its role in neuronal stress responses such as traumatic axon injury. CEBP-1 is required for regrowth of axons in the adult nervous system after laser axotomy. CEBP-1 is upregulated after axon injury by the PMK-3/p38 MAPK cascade (DLK-1/MAP3K, MKK-4/MAP2K, and PMK-3/MAPK) and downstream MAPK activated protein kinase (MK), MAK-2 (Yan et al. 2009). The nuclear import protein, IMA-3, is required for axon regeneration, likely through its function of moving CEBP-1 into the nucleus after injury (Malinow et al. 2019). After axon injury, an influx of Ca2+ increases cAMP signaling which stimulates DLK-1 activity, initiating regenerative pathways. Although these regenerative pathways usually require CEBP-1, sufficient expression of cAMP partially bypasses this requirement, indicating that CEBP-1 is not the only way DLK-1 promotes axon regeneration (Ghosh-Roy et al. 2010). After axon injury, microtubule and actin dynamics increase, shuttling molecules to and from the injury site. This increase in cytoskeletal dynamics is significantly reduced, but not fully blocked by CEBP-1 knockout (Kulkarni et al. 2021). Autophagy is another process neurons undergo after axonal injury and it is also dependent on DLK-1/MKK-4/PMK-3/MAK-2/CEBP-1 pathway (Ko et al. 2020). The growth factor SVH-1 and its cognate receptor tyrosine kinase, SVH-2, are required for axon regeneration. SVH-1 is constitutively expressed, whereas SVH-2 expression is initiated by axon injury.

svh-2 transcription requires the formation of a CEBP-1—ETS-4 transcription factor heterodimer. Both CEBP-1 and ETS-4 are upregulated in response to axon injury, each through independent pathways (Li et al. 2015, Sakai et al. 2019). Thus, CEBP-1 plays multiple roles in axon regeneration by interacting with several different signaling pathways.

Together these studies demonstrate that CEBP-1, in cooperation with other bZip transcription factors, regulate innate immune and stress responses in *C. elegans* **(Figure 1)**. CEBP-1 plays a central role in regulation of the PMK-1/p38 MAPK pathway through dual roles of transcription of the MAP2K, *sek-1*, which phosphorylates PMK-1 and transcription of *vhp-1*, which dephosphorylates PMK-1 (Kim et al. 2016, Wu et al. 2021). CEBP-1 is the functional connection between Tribbles/NIPI-3 and regulation of the PMK-1/p38 MAPK pathway. NIPI-3 negatively regulates PMK-1 activity during development by repressing the transcription of CEBP-1 (Kim et al. 2016). Other C/EBPs (CEBP-2 and ZIP-4) are not regulated by NIPI-3 and do not impact the phenotypes of *nipi-3(0)* (R.A. Malinow Unpublished work). Next, I will review the roles of p38 MAP kinases in innate immunity and animal development, both in mammalian systems and *C. elegans.*

1.3 p38 MAPK Pathways in Innate Immunity and Animal Development

Mitogen activated protein kinase (MAPK) signaling is an essential form of cellular signaling that mediates animal growth, tissue development, and innate immunity by integrating extracellular cues with internal cellular state to produce appropriate gene regulatory responses. The three-tiered phosphorylation cascade (MAP3Ks, MAP2Ks, then MAPKs) results in a phosphorylated MAP kinase that directly and indirectly regulates gene expression via phosphorylation of other kinases, RNA/DNA binding proteins, structural proteins, and transcription factors. There are three groups of MAPKs: extracellular signal-regulated kinases (ERKs), c-Jun N-terminal kinases (JNKs), and p38 mitogen activated kinases (p38s). JNK and p38s are generally grouped together because they are both activated by cellular stresses and inflammatory cytokines. Most stimuli that activate JNKs also activate p38s and vice-versa. Nevertheless, there are some unique targets of each MAPK group. For instance, JNKs specifically activate c-Jun and NFAT4, whereas p38s specifically activate MAPK activated protein kinases (MKs) MK2 and MK3. The network of MAP3Ks and MAP2Ks that regulate p38 and ERKs are highly overlapping (Kyriakis and Avruch 2012). Here, I will review the regulation of mammalian p38 MAPKs and their downstream effectors in relation to innate immunity; I will then discuss the roles of p38 MAPKs in *C. elegans* innate immunity and development.

Mammalian p38 MAPKs in innate immunity

Mammalian systems have four p38 kinase proteins: p38α, β, γ, δ (also named MAPK14, MAPK11, MAPK12, MAPK13). p38α was first discovered as a protein that

was phosphorylated after cellular exposure to signals of nearby bacteria (Han et al. 1994). It was later discovered that p38 kinases are essential in animal development: p38α and p38β are required for mouse embryogenesis, specifically development of the heart (Adams et al. 2000, Mudgett et al. 2000, Brancho et al. 2003, del Barco Barrantes et al. 2011).

p38α has a conserved role in innate immunity against bacterial and viral infection (Arthur and Ley 2013, Cho et al. 2017, Wang et al. 2018, Zhang et al. 2018). p38α has different functions under normal conditions and in response to stress, which highly activates p38s. Studies examining p38 functions under disease-related stress conditions have been particularly valuable for understanding p38 signaling. For instance, in the liver, p38α protects against tissue injury, but when injury is accompanied by inflammatory signals, p38α signaling leads to cell death (Ito et al. 2006, Jung et al. 2016, Takizawa et al. 2017, Hwang et al. 2020). p38γ and p38δ participate in tissue regeneration and immune responses (Escos et al. 2016). Excessive activation of p38 is seen in many inflammatory diseases such as IBS, asthma, and arthritis (Otsuka et al. 2010, Liang et al. 2013, Zhang et al. 2019). Upregulation of p38 MAPK pathway in intestinal epithelial cells is implicated in pathogenesis of IBS, cancer, autoimmune disorders, and immunodeficiency syndromes (Wagner and Nebreda 2009, Kyriakis and Avruch 2012, Fisk et al. 2014). Human samples of inflamed intestine from IBS patients have heightened levels of phosphorylated p38 MAPKs, but not ERK or JNK kinases (Waetzig et al. 2002). Thus, misregulation of p38 MAPK signaling is implicated in multiple human disorders, particularly those related to cellular stress.

p38 kinases play a central role in cellular stress responses, such as bacterial and microbial infection, which robustly activate p38 kinases (Gaestel et al. 2009, Kyriakis and Avruch 2012, Arthur and Ley 2013, Lee et al. 2016, Takizawa et al. 2017). Generally, the first step in the pathogen response is to block proliferation by halting cell cycle, through regulation of cyclin proteins, with subsequent redirection of resources towards clearing the infection. p38 kinases regulate both of these processes (Dolado and Nebreda 2008, Cannell et al. 2015, Canovas and Nebreda 2021).

In mammalian systems, the upstream signaling leading to p38 kinase activation is extremely complex. So far, ten MAP3Ks and three MAP2Ks have been identified as upstream activators of p38 MAPKs. p38 MAPKs are mainly phosphorylated by the MAP2Ks, MKK3 and MKK6 (Derijard et al. 1995, Han et al. 1996, Raingeaud et al. 1996, Enslen et al. 1998, Brancho et al. 2003). Another MAP2K, MKK4, usually activates JNK kinases, but can also activate p38α and p38δ in some cell types (Jiang et al. 1997). To add to the complexity, each of these upstream kinases are spatially and temporally regulated in a cell-type and cell-state specific manner (Cuadrado and Nebreda 2010). In addition to the MAP2Ks being activated by MAP3Ks, their activity is also regulated by multiple mechanisms including both post transcriptional and post translational modifications (Diao et al. 2010, Rasmussen et al. 2016).

p38 kinases directly phosphorylate more than one hundred proteins regulating transcription, chromatin remodeling, mRNA stability and translocation, protein degradation and localization, and cytoskeletal dynamics (Cuadrado and Nebreda 2010, Trempolec et al. 2013, Han et al. 2020). Each of the p38 kinases have specific downstream targets even though these kinases are ~60-75% identical to each other

(Eyers et al. 1998, Gum et al. 1998). Although diverse cell types respond to a range of cellular stresses by the activation of p38 kinases, cell-specific p38 responses to stress occur via cell-type or cell-state specific expression of different p38 protein substrates, as well as p38 kinase inactivation by phosphatases, which themselves are highly regulated (Sun et al. 1993, Nunes-Xavier et al. 2011, Cho et al. 2017, Canovas and Nebreda 2021).

C. elegans p38 MAPKs in innate immunity and development

In *C. elegans*, much like in mammalian systems, p38 MAPK signaling is essential for a wide variety of processes such as regulation of lifespan, locomotion, sleep, neuronal development, as well as responses to many cellular stressors such as oxidative stress, wounding, and infection (Kim et al. 2002, Tanaka-Hino et al. 2002, Inoue et al. 2005, Troemel et al. 2006, Pujol et al. 2008, Zugasti et al. 2016, Hoyt et al. 2017, Wu et al. 2019, Foster et al. 2020, Sinner et al. 2021). Here, I will focus on the role of p38 MAPK signaling in innate immunity and development. In *C. elegans*, most pathogens enter the animal either through the epidermis or the intestine. Decades of host-pathogen research in *C. elegans* has described the multitude of innate immune pathways functioning in these tissues in response to different pathogens. Here, I will describe a p38 MAPK pathway comprised of NSY-1/MAP3K, SEK-1/MAP2K, and PMK-1/MAPK and its role in innate immunity **(Figure 2)** and animal development **(Figure 3)**.

Producing an immune response comes at a cost to the host organism. Thus, there is a balance maintained by negative regulation of the innate immune response to allow animal development. (Fabian et al. 2021). Indeed, in *C. elegans,* upregulation of

the PMK-1/p38 MAPK pathway produces increased resistance to infection, but significantly impacts development. Depending on the level of PMK-1/p38 MAPK pathway activation, the effects range from slowed development to developmental arrest **(Figure 3)**. A constitutively active version of NSY-1 leads to modestly delayed development, dependent on PMK-1 (Cheesman et al. 2016) and extremely high activation of the PMK-1/p38 MAPK pathway by knockout of Tribbles/ NIPI-3 leads to developmental arrest (Kim et al. 2016).

The *C. elegans* PMK-1/p38 MAPK pathway is negatively regulated through multiple tissue specific and global mechanisms: 1. The caspase CED-3 directly binds to and degrades PMK-1 in the epidermis (Weaver et al. 2020). 2. Signaling from olfactory neurons suppresses TIR-1/ NSY-1/SEK-1/PMK-1 activity in the intestine (Foster et al. 2020). 3. The phosphatase VHP-1 dephosphorylates PMK-1 in multiple tissues (Richardson et al. 2010)(Wu et al. 2021). and 4. NIPI-3 negatives regulates CEBP-1 in multiple tissues, therefore reducing the activity of TIR-1/ NSY-1/ SEK-1/PMK-1, allowing animal development (Kim et al. 2016). It is interesting to note that CEBP-1 plays distinct roles in the activation and repression of PMK-1 activity, depending on the context. Two transcriptional targets of CEBP-1, *sek-1* and *vhp-1*, have opposite effects on the activity of PMK-1 and depending on the amount of each gene is transcribed, CEBP-1 activity can have a net increase or net decrease effect on PMK-1 activity (Kim et al. 2016, Wu et al. 2021).

PMK-1 regulates expression of immune response genes (Troemel et al. 2006) partially through the transcription factor ATF-7 (mammalian ATF-2/CREB5), which functions as a repressor of gene transcription unless phosphorylated by PMK-1 (Shivers

et al. 2010, Fletcher et al. 2019). PMK-1 also regulates expression of immune response genes via the transcription factor SKN-1, specifically required for intestinal pathogen defense (Hoeven et al. 2011, Wu et al. 2021) **(Figure 2)**.

Developmental delay resulting from activation of the PMK-1/p38 MAPK pathway is, at least partially, due to ER stress. ER stress activates the unfolded protein response (UPR) (Richardson et al. 2010). The UPR has three branches, each initiated by a different ER stress sensor. The IRE/XBP-1 branch of the UPR is activated by accumulation of unfolded proteins in the ER. *C. elegans* XBP-1 is activated in response to PMK-1/p38 pathway activity. Activation of PMK-1/p38 MAPK pathway upregulates around 300 genes, about half of which are predicted to be processed by the ER (Richardson et al. 2010). Simultaneous activation of the p38 MAPK pathway and disruption of the XBP branch of the UPR increases developmental delay **(Figure 3)**. Modest activation of PMK-1, by infection or knockdown of VHP-1, combined with UPR mutation causes extremely slow development (Richardson et al. 2010, Cheesman et al. 2016). Stronger hyperactivation of PMK-1 by VHP-1 knockout combined with UPR disruption causes developmental arrest (Richardson et al. 2010). Together, these results suggest that activation of PMK-1/p38 MAPK pathway results in increased protein synthesis and accumulation of unfolded proteins in the ER, thus increased ER stress, all leading to developmental delay.

It should be noted that the PMK-1/p38 MAPK pathway is not the only pathway regulating innate immune that slows development in *C. elegans* when upregulated. PALS-25 increases the expression of intracellular protein response (IPR) genes in the intestine. When this pathway is hyperactive, by knockout of the negative regulator,

PALS-22, animals have increased resistance to heat shock and certain infections but have significant developmental delay (Reddy et al. 2017, Reddy et al. 2019).

Together, the studies reviewed here highlight the role of the p38 MAPK pathway in innate immunity and animal development. There is a delicate balance where greater activity of the p38 MAPK pathway increases innate immune response but interferes with development and limiting innate immune responses are permissive for development. Regulation of the PMK-1 pathway is essential for this balance and deeper understanding of the intricate regulation of this pathway may lead to discovery of novel immune regulatory mechanisms allowing for novel therapeutics.

Figures

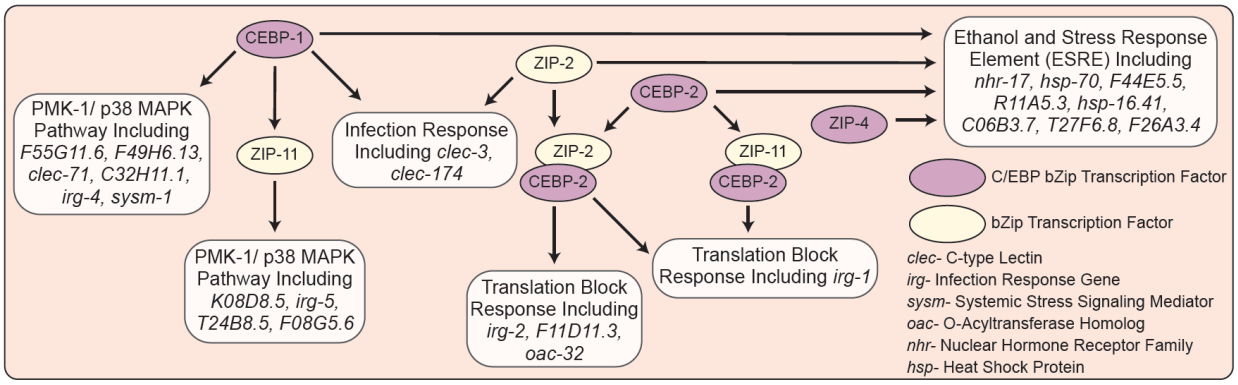

Figure 1. Transcriptional Regulation of Three Innate Immune Pathways by C/EBPs in *C. elegans*

CEBP-1, CEBP-2, ZIP-4, ZIP-2 and ZIP-11 regulate three independent innate immune pathways: 1. The response to translation elongation block, which can be caused by infection by *P. aeruginosa*, 2. The Ethanol and Stress Response Element (ESRE), a gene set with an evolutionarily conserved ESRE motif that is induced after xenobiotic stresses and some pathogenic stimuli, and 3. the PMK-1/p38 MAPK pathway, a highly conserved pathway central to *C. elegans* innate immune functioning cell autonomously in multiple tissues to defend against pathogens.

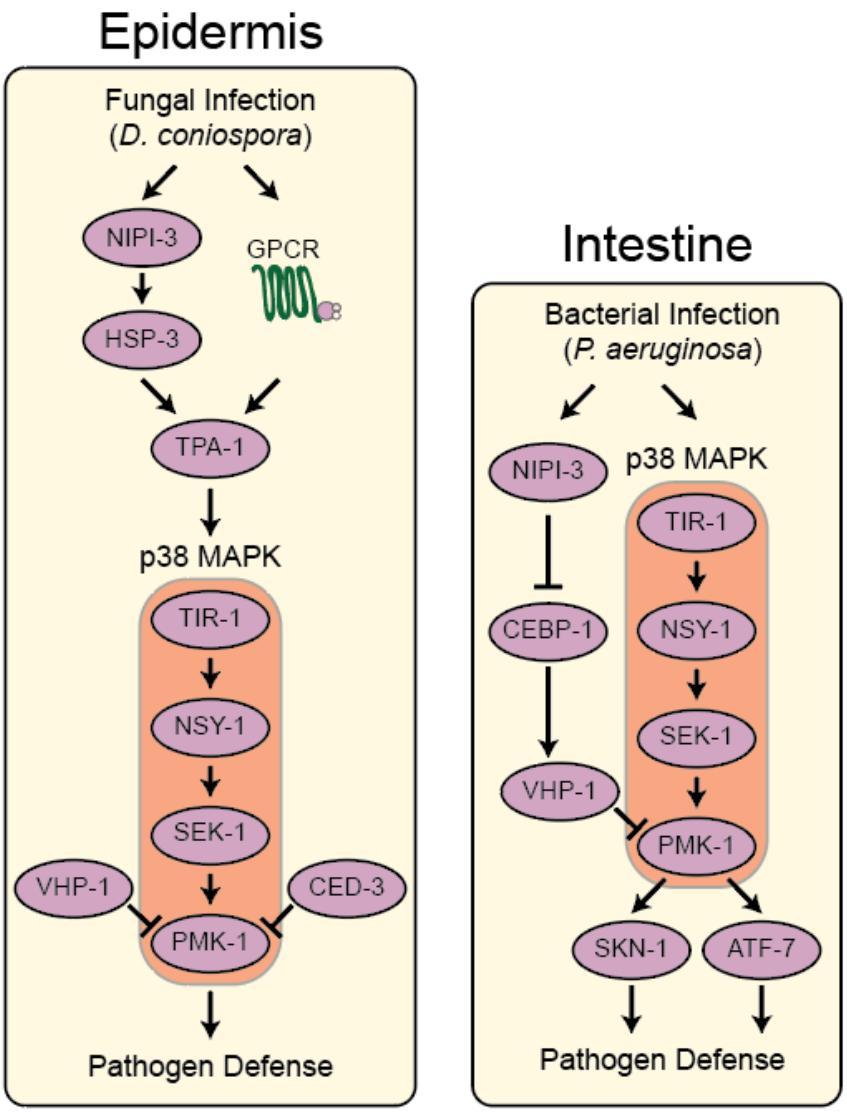

Figure 2. PMK-1/p38 MAPK pathway has cell autonomous roles in defense against fungal and bacterial infection

In the epidermis, defense against fungal infection requires NIPI-3 and p38 MAPK pathway to induce an immune response. One of the primary genes upregulated after epidermal infection is *nlp-29.* Both VHP-1 and CED-3 function cell autonomously within the epidermis to reduce PMK-1 activity, through dephosphorylation and protein degradation, respectively. In the intestine, defense against bacterial infection requires NIPI-3, CEBP-1, and the PMK-1/p38 MAPK pathway to induce an immune response. The immune response is partially regulated by the transcription factors ATF-7 and SKN-1. *vhp-1* transcription is promoted by CEBP-1, and VHP-1 functions cell autonomously within the intestine to reduce PMK-1 activity via dephosphorylation.

Figure 3. *C. elegans* development is delayed by activation of PMK-1 and the developmental delay is attenuated by the Unfolded Protein Response of the ER

A. The PMK-1/p38 MAPK pathway is activated by multiple inputs including R24, an immune-stimulating small molecule, bacterial infection by *P. aeruginosa* (PA14), and a constitutively active version of the upstream MAP3K, NSY-1. The PMK-1/p38 MAPK pathway is repressed by multiple inputs including Tribbles/NIPI-3, Caspase/ CED-3, and phosphatase/VHP-1. Activity of the PMK-1/p38 MAPK pathways leads to activation of multiple transcription factors including ATF-7 and SKN-1 which increase protein synthesis. The increased protein synthesis leads to an increase in unfolded proteins in the ER. The XBP-1 branch of the unfolded protein response (UPR) responses to the increase in unfolded proteins, reducing the negative impact of PMK-1/p38 MAPK activation on animal development. In some cases, such as NIPI-3 knockout, the stress caused by the increased PMK-1 activity is too strong to be rescued by UPR activity. **B.** There is an inverse relationship between the strength of PMK-1 activity and the speed of animal development. Animals with deficient PMK-1 activity, such as *pmk-1(0)* grow faster than wildtype animals. Animals with extremely high activation of PMK-1 pathway, such as *nipi-3(0), vhp-1(0); xbp-1(0)*, or *xbp-1(0)* animals exposed to *P. aeruginosa* infection, are unable to develop fully. Animals with varying levels of PMK-1 activation grow at different rates, commensurate with their PMK-1 activity level.

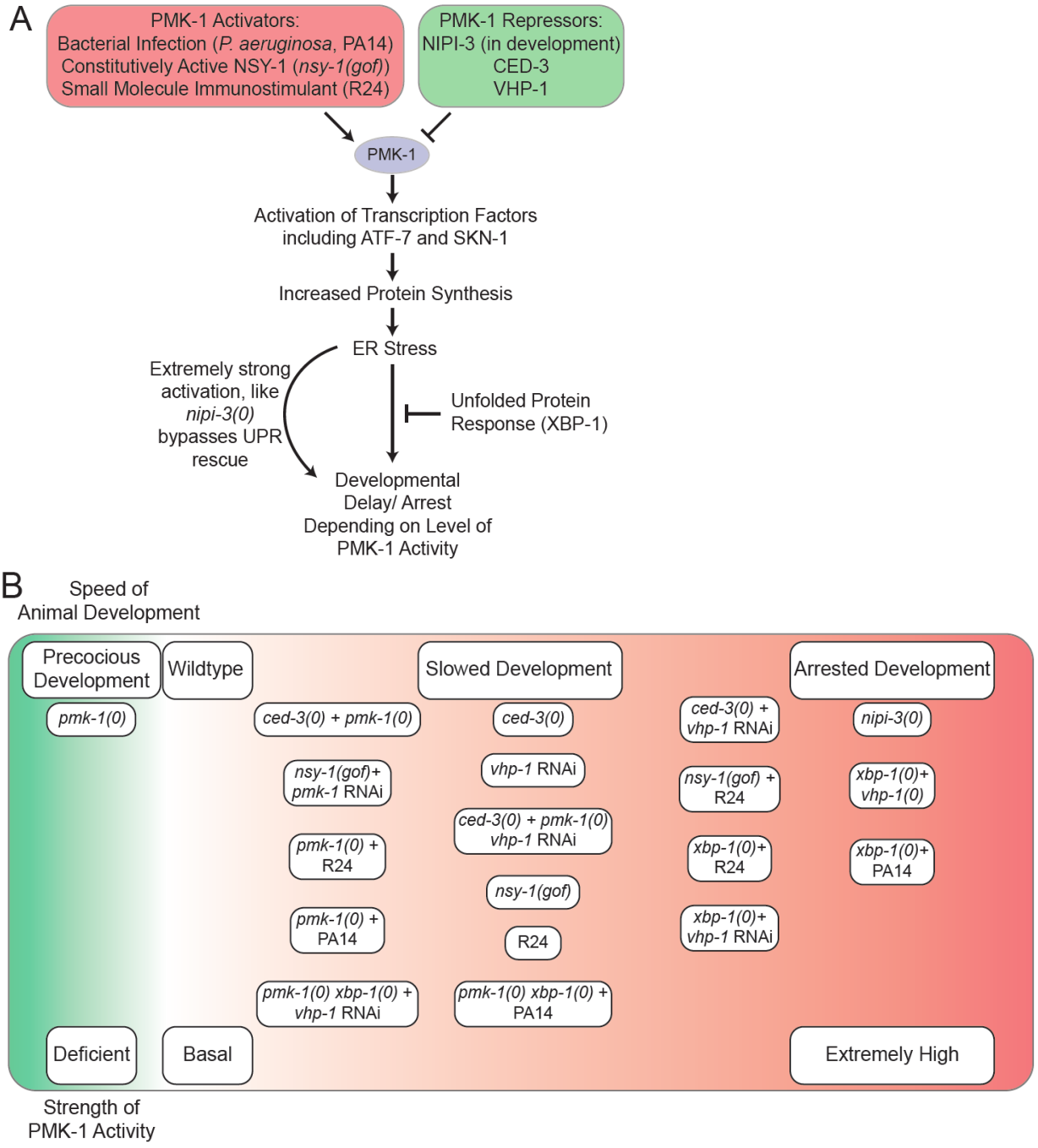
A
PMK-1 Activators:
Bacterial Infection (P. aeruginosa, PA14)
Constitutively Active NSY-1 (nsy-1(gof))
Small Molecule Immunostimulant (R24)
PMK-1 Repressors:
NIPI-3 (in development)
CED-3
VHP-1
PMK-1
Activation of Transcription Factors
including ATF-7 and SKN-1
Increased Protein Synthesis
ER Stress
Extremely strong
activation, like
nipi-3(0)
bypasses UPR
rescue
Unfolded Protein
Response (XBP-1)
Developmental
Delay/ Arrest
Depending on Level of
PMK-1 Activity
B
Speed of
Animal Development
Precocious
Development
Wildtype
Slowed Development
Arrested Development
pmk-1(0)
ced-3(0) + pmk-1(0)
ced-3(0)
ced-3(0) +
vhp-1 RNAi
nipi-3(0)
nsy-1(gof)+
pmk-1 RNAi
vhp-1 RNAi
nsy-1(gof) +
R24
xbp-1(0)+
vhp-1(0)
ced-3(0) + pmk-1(0)
vhp-1 RNAi
pmk-1(0) +
R24
xbp-1(0)+
R24
xbp-1(0)+
PA14
nsy-1(gof)
pmk-1(0) +
PA14
xbp-1(0)+
vhp-1 RNAi
R24
pmk-1(0) xbp-1(0) +
vhp-1 RNAi
pmk-1(0) xbp-1(0) +
PA14
Deficient
Basal
Extremely High
Strength of
PMK-1 Activity

References

Adams, R. H., Porras, A., Alonso, G., Jones, M., Vintersten, K., Panelli, S., Valladares, A., Perez, L., Klein, R. and Nebreda, A. R. (2000). Essential role of p38alpha MAP kinase in placental but not embryonic cardiovascular development. *Mol Cell* **6**: 109-116.

Agre, P., Johnson, P. F. and McKnight, S. L. (1989). Cognate DNA binding specificity retained after leucine zipper exchange between GCN4 and C/EBP. *Science* **246**: 922-926. doi: 10.1126/science.2530632.

Aime, P., Sun, X., Zareen, N., Rao, A., Berman, Z., Volpicelli-Daley, L., Bernd, P., Crary, J. F., Levy, O. A. and Greene, L. A. (2015). Trib3 Is Elevated in Parkinson's Disease and Mediates Death in Parkinson's Disease Models. *J Neurosci* **35**: 10731-10749. doi: 10.1523/JNEUROSCI.0614-15.2015.

Arthur, J. S. and Ley, S. C. (2013). Mitogen-activated protein kinases in innate immunity. *Nat Rev Immunol* **13**: 679-692. doi: 10.1038/nri3495.

Barone, M. V., Crozat, A., Tabaee, A., Philipson, L. and Ron, D. (1994). CHOP (GADD153) and its oncogenic variant, TLS-CHOP, have opposing effects on the induction of G1/S arrest. *Genes Dev* **8**: 453-464. doi: 10.1101/gad.8.4.453.

Bauer, R. C., Sasaki, M., Cohen, D. M., Cui, J., Smith, M. A., Yenilmez, B. O., Steger, D. J. and Rader, D. J. (2015a). Tribbles-1 regulates hepatic lipogenesis through posttranscriptional regulation of C/EBPalpha. *J Clin Invest* **125**: 3809-3818. doi: 10.1172/JCI77095.

Bauer, R. C., Yenilmez, B. O. and Rader, D. J. (2015b). Tribbles-1: a novel regulator of hepatic lipid metabolism in humans. *Biochem Soc Trans* **43**: 1079-1084. doi: 10.1042/BST20150101.

Beddoe, T., Paton, A. W., Le Nours, J., Rossjohn, J. and Paton, J. C. (2010). Structure, biological functions and applications of the AB5 toxins. *Trends Biochem Sci* **35**: 411-418. doi: 10.1016/j.tibs.2010.02.003.

Begay, V., Smink, J. and Leutz, A. (2004). Essential requirement of CCAAT/enhancer binding proteins in embryogenesis. *Mol Cell Biol* **24**: 9744-9751. doi: 10.1128/MCB.24.22.9744-9751.2004.

Berberich-Siebelt, F., Berberich, I., Andrulis, M., Santner-Nanan, B., Jha, M. K., Klein-Hessling, S., Schimpl, A. and Serfling, E. (2006). SUMOylation interferes with CCAAT/enhancer-binding protein beta-mediated c-myc repression, but not IL-4 activation in T cells. *J Immunol* **176**: 4843-4851. doi: 10.4049/jimmunol.176.8.4843.

Borsting, E., Patel, S. V., Decleves, A. E., Lee, S. J., Rahman, Q. M., Akira, S., Satriano, J., Sharma, K., Vallon, V. and Cunard, R. (2014). Tribbles homolog 3 attenuates mammalian target of rapamycin complex-2 signaling and inflammation in the diabetic kidney. *J Am Soc Nephrol* **25**: 2067-2078. doi: 10.1681/ASN.2013070811.

Bowers, A. J., Scully, S. and Boylan, J. F. (2003). SKIP3, a novel Drosophila tribbles ortholog, is overexpressed in human tumors and is regulated by hypoxia. *Oncogene* **22**: 2823-2835. doi: 10.1038/sj.onc.1206367.

Brancho, D., Tanaka, N., Jaeschke, A., Ventura, J. J., Kelkar, N., Tanaka, Y., Kyuuma, M., Takeshita, T., Flavell, R. A. and Davis, R. J. (2003). Mechanism of p38 MAP kinase activation in vivo. *Genes Dev* **17**: 1969-1978. doi: 10.1101/gad.1107303.

Burkhardt, R., Toh, S. A., Lagor, W. R., Birkeland, A., Levin, M., Li, X., Robblee, M., Fedorov, V. D., Yamamoto, M., Satoh, T., Akira, S., Kathiresan, S., Breslow, J. L. and Rader, D. J. (2010). Trib1 is a lipid- and myocardial infarction-associated gene that regulates hepatic lipogenesis and VLDL production in mice. *J Clin Invest* **120**: 4410-4414. doi: 10.1172/JCI44213.

Cannell, I. G., Merrick, K. A., Morandell, S., Zhu, C. Q., Braun, C. J., Grant, R. A., Cameron, E. R., Tsao, M. S., Hemann, M. T. and Yaffe, M. B. (2015). A Pleiotropic RNA-Binding Protein Controls Distinct Cell Cycle Checkpoints to Drive Resistance of p53-Defective Tumors to Chemotherapy. *Cancer Cell* **28**: 831. doi: 10.1016/j.ccell.2015.11.003.

Canovas, B. and Nebreda, A. R. (2021). Diversity and versatility of p38 kinase signalling in health and disease. *Nat Rev Mol Cell Biol* **22**: 346-366. doi: 10.1038/s41580-020-00322-w.

Caristi, S., Piraino, G., Cucinotta, M., Valenti, A., Loddo, S. and Teti, D. (2005). Prostaglandin E2 induces interleukin-8 gene transcription by activating C/EBP homologous protein in human T lymphocytes. *J Biol Chem* **280**: 14433-14442. doi: 10.1074/jbc.M410725200.

Carlson, S. G., Fawcett, T. W., Bartlett, J. D., Bernier, M. and Holbrook, N. J. (1993). Regulation of the C/EBP-related gene gadd153 by glucose deprivation. *Mol Cell Biol* **13**: 4736-4744. doi: 10.1128/mcb.13.8.4736-4744.1993.

Cassel, T. N. and Nord, M. (2003). C/EBP transcription factors in the lung epithelium. *Am J Physiol Lung Cell Mol Physiol* **285**: L773-781. doi: 10.1152/ajplung.00023.2003.

Cesena, T. I., Cardinaux, J. R., Kwok, R. and Schwartz, J. (2007). CCAAT/enhancer-binding protein (C/EBP) beta is acetylated at multiple lysines: acetylation of C/EBPbeta at lysine 39 modulates its ability to activate transcription. *J Biol Chem* **282**: 956-967. doi: 10.1074/jbc.M511451200.

Charles, A., Tang, X., Crouch, E., Brody, J. S. and Xiao, Z. X. (2001). Retinoblastoma protein complexes with C/EBP proteins and activates C/EBP-mediated transcription. *J Cell Biochem* **83**: 414-425. doi: 10.1002/jcb.1239.

Cheesman, H. K., Feinbaum, R. L., Thekkiniath, J., Dowen, R. H., Conery, A. L. and Pukkila-Worley, R. (2016). Aberrant Activation of p38 MAP Kinase-Dependent Innate Immune Responses Is Toxic to Caenorhabditis elegans. *G3 (Bethesda)* **6**: 541-549. doi: 10.1534/g3.115.025650.

Cho, S. S. L., Han, J., James, S. J., Png, C. W., Weerasooriya, M., Alonso, S. and Zhang, Y. (2017). Dual-Specificity Phosphatase 12 Targets p38 MAP Kinase to Regulate Macrophage Response to Intracellular Bacterial Infection. *Front Immunol* **8**: 1259. doi: 10.3389/fimmu.2017.01259.

Chumakov, A. M., Grillier, I., Chumakova, E., Chih, D., Slater, J. and Koeffler, H. P. (1997). Cloning of the novel human myeloid-cell-specific C/EBP-epsilon transcription factor. *Mol Cell Biol* **17**: 1375-1386. doi: 10.1128/MCB.17.3.1375.

Cohen, L. B. and Troemel, E. R. (2015). Microbial pathogenesis and host defense in the nematode C. elegans. *Curr Opin Microbiol* **23**: 94-101. doi: 10.1016/j.mib.2014.11.009.

Cooper, C., Henderson, A., Artandi, S., Avitahl, N. and Calame, K. (1995). Ig/EBP (C/EBP gamma) is a transdominant negative inhibitor of C/EBP family transcriptional activators. *Nucleic Acids Res* **23**: 4371-4377. doi: 10.1093/nar/23.21.4371.

Couillault, C., Fourquet, P., Pophillat, M. and Ewbank, J. J. (2012). A UPR-independent infection-specific role for a BiP/GRP78 protein in the control of antimicrobial peptide expression in C. elegans epidermis. *Virulence* **3**: 299-308. doi: 10.4161/viru.20384.

Cuadrado, A. and Nebreda, A. R. (2010). Mechanisms and functions of p38 MAPK signalling. *Biochem J* **429**: 403-417. doi: 10.1042/BJ20100323.

Cucinotta, M., Visalli, M., Aguennouz, M., Valenti, A., Loddo, S., Altucci, L. and Teti, D. (2008). Regulation of interleukin-8 gene at a distinct site of its promoter by CCAAT enhancer-binding protein homologous protein in prostaglandin E2-treated human T cells. *J Biol Chem* **283**: 29760-29769. doi: 10.1074/jbc.M803145200.

Cunard, R. (2013). Mammalian tribbles homologs at the crossroads of endoplasmic reticulum stress and Mammalian target of rapamycin pathways. *Scientifica (Cairo)* **2013**: 750871. doi: 10.1155/2013/750871.

Das, R., Sebo, Z., Pence, L. and Dobens, L. L. (2014). Drosophila tribbles antagonizes insulin signaling-mediated growth and metabolism via interactions with Akt kinase. *PLoS One* **9**: e109530. doi: 10.1371/journal.pone.0109530.

Dedhia, P. H., Keeshan, K., Uljon, S., Xu, L., Vega, M. E., Shestova, O., Zaks-Zilberman, M., Romany, C., Blacklow, S. C. and Pear, W. S. (2010). Differential ability of Tribbles family members to promote degradation of C/EBPalpha and induce acute myelogenous leukemia. *Blood* **116**: 1321-1328. doi: 10.1182/blood-2009-07-229450.

del Barco Barrantes, I., Coya, J. M., Maina, F., Arthur, J. S. and Nebreda, A. R. (2011). Genetic analysis of specific and redundant roles for p38alpha and p38beta MAPKs during mouse development. *Proc Natl Acad Sci U S A* **108**: 12764-12769. doi: 10.1073/pnas.1015013108.

Derijard, B., Raingeaud, J., Barrett, T., Wu, I. H., Han, J., Ulevitch, R. J. and Davis, R. J. (1995). Independent human MAP-kinase signal transduction pathways defined by MEK and MKK isoforms. *Science* **267**: 682-685. doi: 10.1126/science.7839144.

Descombes, P. and Schibler, U. (1991). A liver-enriched transcriptional activator protein, LAP, and a transcriptional inhibitory protein, LIP, are translated from the same mRNA. *Cell* **67**: 569-579. doi: 10.1016/0092-8674(91)90531-3.

Diao, Y., Liu, W., Wong, C. C., Wang, X., Lee, K., Cheung, P. Y., Pan, L., Xu, T., Han, J., Yates, J. R., 3rd, Zhang, M. and Wu, Z. (2010). Oxidation-induced intramolecular disulfide bond inactivates mitogen-activated protein kinase kinase 6 by inhibiting ATP binding. *Proc Natl Acad Sci U S A* **107**: 20974-20979. doi: 10.1073/pnas.1007225107.

Dobens, L. L., Jr. and Bouyain, S. (2012). Developmental roles of tribbles protein family members. *Dev Dyn* **241**: 1239-1248. doi: 10.1002/dvdy.23822.

Dolado, I. and Nebreda, A. R. (2008). AKT and oxidative stress team up to kill cancer cells. *Cancer Cell* **14**: 427-429. doi: 10.1016/j.ccr.2008.11.006.

Du, K., Herzig, S., Kulkarni, R. N. and Montminy, M. (2003). TRB3: a tribbles homolog that inhibits Akt/PKB activation by insulin in liver. *Science* **300**: 1574-1577. doi: 10.1126/science.1079817.

Duan, H., Heckman, C. A. and Boxer, L. M. (2005). Histone deacetylase inhibitors down-regulate bcl-2 expression and induce apoptosis in t(14;18) lymphomas. *Mol Cell Biol* **25**: 1608-1619. doi: 10.1128/MCB.25.5.1608-1619.2005.

Dunbar, T. L., Yan, Z., Balla, K. M., Smelkinson, M. G. and Troemel, E. R. (2012). C. elegans detects pathogen-induced translational inhibition to activate immune signaling. *Cell Host Microbe* **11**: 375-386. doi: 10.1016/j.chom.2012.02.008.

Eder, K., Guan, H., Sung, H. Y., Ward, J., Angyal, A., Janas, M., Sarmay, G., Duda, E., Turner, M., Dower, S. K., Francis, S. E., Crossman, D. C. and Kiss-Toth, E. (2008). Tribbles-2 is a novel regulator of inflammatory activation of monocytes. *Int Immunol* **20**: 1543-1550. doi: 10.1093/intimm/dxn116.

Enslen, H., Raingeaud, J. and Davis, R. J. (1998). Selective activation of p38 mitogen-activated protein (MAP) kinase isoforms by the MAP kinase kinases MKK3 and MKK6. *J Biol Chem* **273**: 1741-1748. doi: 10.1074/jbc.273.3.1741.

Escos, A., Risco, A., Alsina-Beauchamp, D. and Cuenda, A. (2016). p38gamma and p38delta Mitogen Activated Protein Kinases (MAPKs), New Stars in the MAPK Galaxy. *Front Cell Dev Biol* **4**: 31. doi: 10.3389/fcell.2016.00031.

Eyers, P. A., Craxton, M., Morrice, N., Cohen, P. and Goedert, M. (1998). Conversion of SB 203580-insensitive MAP kinase family members to drug-sensitive forms by a single amino-acid substitution. *Chem Biol* **5**: 321-328. doi: 10.1016/s1074-5521(98)90170-3.

Eyers, P. A., Keeshan, K. and Kannan, N. (2017). Tribbles in the 21st Century: The Evolving Roles of Tribbles Pseudokinases in Biology and Disease. *Trends Cell Biol* **27**: 284-298. doi: 10.1016/j.tcb.2016.11.002.

Fabian, D. K., Fuentealba, M., Donertas, H. M., Partridge, L. and Thornton, J. M. (2021). Functional conservation in genes and pathways linking ageing and immunity. *Immun Ageing* **18**: 23. doi: 10.1186/s12979-021-00232-1.

Fawcett, T. W., Eastman, H. B., Martindale, J. L. and Holbrook, N. J. (1996). Physical and functional association between GADD153 and CCAAT/enhancer-binding protein beta during cellular stress. *J Biol Chem* **271**: 14285-14289. doi: 10.1074/jbc.271.24.14285.

Fisk, M., Gajendragadkar, P. R., Maki-Petaja, K. M., Wilkinson, I. B. and Cheriyan, J. (2014). Therapeutic potential of p38 MAP kinase inhibition in the management of cardiovascular disease. *Am J Cardiovasc Drugs* **14**: 155-165. doi: 10.1007/s40256-014-0063-6.

Fletcher, M., Tillman, E. J., Butty, V. L., Levine, S. S. and Kim, D. H. (2019). Global transcriptional regulation of innate immunity by ATF-7 in C. elegans. *PLoS Genet* **15**: e1007830. doi: 10.1371/journal.pgen.1007830.

Flodby, P., Barlow, C., Kylefjord, H., Ahrlund-Richter, L. and Xanthopoulos, K. G. (1996). Increased hepatic cell proliferation and lung abnormalities in mice deficient in CCAAT/enhancer binding protein alpha. *J Biol Chem* **271**: 24753-24760. doi: 10.1074/jbc.271.40.24753.

Foster, K. J., Cheesman, H. K., Liu, P., Peterson, N. D., Anderson, S. M. and Pukkila-Worley, R. (2020). Innate Immunity in the C. elegans Intestine Is Programmed by a Neuronal Regulator of AWC Olfactory Neuron Development. *Cell Rep* **31**: 107478. doi: 10.1016/j.celrep.2020.03.042.

Friedman, A. D. (2007). Transcriptional control of granulocyte and monocyte development. *Oncogene* **26**: 6816-6828. doi: 10.1038/sj.onc.1210764.

Friedman, A. D. and McKnight, S. L. (1990). Identification of two polypeptide segments of CCAAT/enhancer-binding protein required for transcriptional activation of the serum albumin gene. *Genes Dev* **4**: 1416-1426. doi: 10.1101/gad.4.8.1416.

Gaestel, M., Kotlyarov, A. and Kracht, M. (2009). Targeting innate immunity protein kinase signalling in inflammation. *Nat Rev Drug Discov* **8**: 480-499. doi: 10.1038/nrd2829.

Gendelman, R., Xing, H., Mirzoeva, O. K., Sarde, P., Curtis, C., Feiler, H. S., McDonagh, P., Gray, J. W., Khalil, I. and Korn, W. M. (2017). Bayesian Network Inference Modeling Identifies TRIB1 as a Novel Regulator of Cell-Cycle Progression and Survival in Cancer Cells. *Cancer Res* **77**: 1575-1585. doi: 10.1158/0008-5472.CAN-16-0512.

Ghosh-Roy, A., Wu, Z., Goncharov, A., Jin, Y. and Chisholm, A. D. (2010). Calcium and cyclic AMP promote axonal regeneration in Caenorhabditis elegans and require DLK-1 kinase. *J Neurosci* **30**: 3175-3183. doi: 10.1523/JNEUROSCI.5464-09.2010.

Glover, J. N. and Harrison, S. C. (1995). Crystal structure of the heterodimeric bZIP transcription factor c-Fos-c-Jun bound to DNA. *Nature* **373**: 257-261. doi: 10.1038/373257a0.

Gombart, A. F., Shiohara, M., Kwok, S. H., Agematsu, K., Komiyama, A. and Koeffler, H. P. (2001). Neutrophil-specific granule deficiency: homozygous recessive inheritance of a frameshift mutation in the gene encoding transcription factor CCAAT/enhancer binding protein--epsilon. *Blood* **97**: 2561-2567. doi: 10.1182/blood.v97.9.2561.

Graves, B. J., Johnson, P. F. and McKnight, S. L. (1986). Homologous recognition of a promoter domain common to the MSV LTR and the HSV tk gene. *Cell* **44**: 565-576. doi: 10.1016/0092-8674(86)90266-7.

Guan, H., Shuaib, A., Leon, D. D., Angyal, A., Salazar, M., Velasco, G., Holcombe, M., Dower, S. K. and Kiss-Toth, E. (2016). Competition between members of the tribbles pseudokinase protein family shapes their interactions with mitogen activated protein kinase pathways. *Sci Rep* **6**: 32667. doi: 10.1038/srep32667.

Gum, R. J., McLaughlin, M. M., Kumar, S., Wang, Z., Bower, M. J., Lee, J. C., Adams, J. L., Livi, G. P., Goldsmith, E. J. and Young, P. R. (1998). Acquisition of sensitivity of stress-activated protein kinases to the p38 inhibitor, SB 203580, by alteration of one or more amino acids within the ATP binding pocket. *J Biol Chem* **273**: 15605-15610. doi: 10.1074/jbc.273.25.15605.

Han, J., Lee, J. D., Bibbs, L. and Ulevitch, R. J. (1994). A MAP kinase targeted by endotoxin and hyperosmolarity in mammalian cells. *Science* **265**: 808-811. doi: 10.1126/science.7914033.

Han, J., Lee, J. D., Jiang, Y., Li, Z., Feng, L. and Ulevitch, R. J. (1996). Characterization of the structure and function of a novel MAP kinase kinase (MKK6). *J Biol Chem* **271**: 2886-2891. doi: 10.1074/jbc.271.6.2886.

Han, J., Wu, J. and Silke, J. (2020). An overview of mammalian p38 mitogen-activated protein kinases, central regulators of cell stress and receptor signaling. *F1000Res* **9**. doi: 10.12688/f1000research.22092.1.

Hattori, T., Ohoka, N., Hayashi, H. and Onozaki, K. (2003). C/EBP homologous protein (CHOP) up-regulates IL-6 transcription by trapping negative regulating NF-IL6 isoform. *FEBS Lett* **541**: 33-39. doi: 10.1016/s0014-5793(03)00283-7.

Hegedus, Z., Czibula, A. and Kiss-Toth, E. (2007). Tribbles: a family of kinase-like proteins with potent signalling regulatory function. *Cell Signal* **19**: 238-250. doi: 10.1016/j.cellsig.2006.06.010.

Heng, T. S., Painter, M. W. and Immunological Genome Project, C. (2008). The Immunological Genome Project: networks of gene expression in immune cells. *Nat Immunol* **9**: 1091-1094. doi: 10.1038/ni1008-1091.

Hoeven, R., McCallum, K. C., Cruz, M. R. and Garsin, D. A. (2011). Ce-Duox1/BLI-3 generated reactive oxygen species trigger protective SKN-1 activity via p38 MAPK signaling during infection in C. elegans. *PLoS Pathog* **7**: e1002453. doi: 10.1371/journal.ppat.1002453.

Hoyt, J. M., Wilson, S. K., Kasa, M., Rise, J. S., Topalidou, I. and Ailion, M. (2017). The SEK-1 p38 MAP Kinase Pathway Modulates Gq Signaling in Caenorhabditis elegans. *G3 (Bethesda)* **7**: 2979-2989. doi: 10.1534/g3.117.043273.

Hwang, S., Wang, X., Rodrigues, R. M., Ma, J., He, Y., Seo, W., Park, S. H., Kim, S. J., Feng, D. and Gao, B. (2020). Protective and Detrimental Roles of p38alpha Mitogen-Activated Protein Kinase in Different Stages of Nonalcoholic Fatty Liver Disease. *Hepatology* **72**: 873-891. doi: 10.1002/hep.31390.

Inoue, H., Hisamoto, N., An, J. H., Oliveira, R. P., Nishida, E., Blackwell, T. K. and Matsumoto, K. (2005). The C. elegans p38 MAPK pathway regulates nuclear localization of the transcription factor SKN-1 in oxidative stress response. *Genes Dev* **19**: 2278-2283. doi: 10.1101/gad.1324805.

Ito, K., Hirao, A., Arai, F., Takubo, K., Matsuoka, S., Miyamoto, K., Ohmura, M., Naka, K., Hosokawa, K., Ikeda, Y. and Suda, T. (2006). Reactive oxygen species act through p38 MAPK to limit the lifespan of hematopoietic stem cells. *Nat Med* **12**: 446-451. doi: 10.1038/nm1388.

Jadhav, K. S. and Bauer, R. C. (2019). Trouble With Tribbles-1. *Arterioscler Thromb Vasc Biol* **39**: 998-1005. doi: 10.1161/ATVBAHA.118.311573.

Jiang, Y., Gram, H., Zhao, M., New, L., Gu, J., Feng, L., Di Padova, F., Ulevitch, R. J. and Han, J. (1997). Characterization of the structure and function of the fourth member of p38 group mitogen-activated protein kinases, p38delta. *J Biol Chem* **272**: 30122-30128. doi: 10.1074/jbc.272.48.30122.

Jin, G., Yamazaki, Y., Takuwa, M., Takahara, T., Kaneko, K., Kuwata, T., Miyata, S. and Nakamura, T. (2007). Trib1 and Evi1 cooperate with Hoxa and Meis1 in myeloid leukemogenesis. *Blood* **109**: 3998-4005. doi: 10.1182/blood-2006-08-041202.

Johnson, P. F. (2005). Molecular stop signs: regulation of cell-cycle arrest by C/EBP transcription factors. *J Cell Sci* **118**: 2545-2555. doi: 10.1242/jcs.02459.

Johnson, P. F., Landschulz, W. H., Graves, B. J. and McKnight, S. L. (1987). Identification of a rat liver nuclear protein that binds to the enhancer core element of three animal viruses. *Genes Dev* **1**: 133-146. doi: 10.1101/gad.1.2.133.

Johnston, J., Basatvat, S., Ilyas, Z., Francis, S. and Kiss-Toth, E. (2015). Tribbles in inflammation. *Biochem Soc Trans* **43**: 1069-1074. doi: 10.1042/BST20150095.

Jung, H., Kim, D. O., Byun, J. E., Kim, W. S., Kim, M. J., Song, H. Y., Kim, Y. K., Kang, D. K., Park, Y. J., Kim, T. D., Yoon, S. R., Lee, H. G., Choi, E. J., Min, S. H. and Choi, I. (2016). Thioredoxin-interacting protein regulates haematopoietic stem cell ageing and rejuvenation by inhibiting p38 kinase activity. *Nat Commun* **7**: 13674. doi: 10.1038/ncomms13674.

Keeshan, K., Bailis, W., Dedhia, P. H., Vega, M. E., Shestova, O., Xu, L., Toscano, K., Uljon, S. N., Blacklow, S. C. and Pear, W. S. (2010). Transformation by Tribbles homolog 2 (Trib2) requires both the Trib2 kinase domain and COP1 binding. *Blood* **116**: 4948-4957. doi: 10.1182/blood-2009-10-247361.

Keeshan, K., He, Y., Wouters, B. J., Shestova, O., Xu, L., Sai, H., Rodriguez, C. G., Maillard, I., Tobias, J. W., Valk, P., Carroll, M., Aster, J. C., Delwel, R. and Pear, W. S. (2006). Tribbles homolog 2 inactivates C/EBPalpha and causes acute myelogenous leukemia. *Cancer Cell* **10**: 401-411. doi: 10.1016/j.ccr.2006.09.012.

Kim, D. H., Feinbaum, R., Alloing, G., Emerson, F. E., Garsin, D. A., Inoue, H., Tanaka-Hino, M., Hisamoto, N., Matsumoto, K., Tan, M. W. and Ausubel, F. M. (2002). A

conserved p38 MAP kinase pathway in Caenorhabditis elegans innate immunity. *Science* **297**: 623-626. doi: 10.1126/science.1073759.

Kim, K. W., Thakur, N., Piggott, C. A., Omi, S., Polanowska, J., Jin, Y. and Pujol, N. (2016). Coordinated inhibition of C/EBP by Tribbles in multiple tissues is essential for Caenorhabditis elegans development. *BMC Biol* **14**: 104. doi: 10.1186/s12915-016-0320-z.

Kinoshita, S., Akira, S. and Kishimoto, T. (1992). A member of the C/EBP family, NF-IL6 beta, forms a heterodimer and transcriptionally synergizes with NF-IL6. *Proc Natl Acad Sci U S A* **89**: 1473-1476. doi: 10.1073/pnas.89.4.1473.

Kiss-Toth, E. (2011). Tribbles: 'puzzling' regulators of cell signalling. *Biochem Soc Trans* **39**: 684-687. doi: 10.1042/BST0390684.

Kiss-Toth, E., Bagstaff, S. M., Sung, H. Y., Jozsa, V., Dempsey, C., Caunt, J. C., Oxley, K. M., Wyllie, D. H., Polgar, T., Harte, M., O'Neill L, A., Qwarnstrom, E. E. and Dower, S. K. (2004). Human tribbles, a protein family controlling mitogen-activated protein kinase cascades. *J Biol Chem* **279**: 42703-42708. doi: 10.1074/jbc.M407732200.

Kiss-Toth, E., Wyllie, D. H., Holland, K., Marsden, L., Jozsa, V., Oxley, K. M., Polgar, T., Qwarnstrom, E. E. and Dower, S. K. (2006). Functional mapping and identification of novel regulators for the Toll/Interleukin-1 signalling network by transcription expression cloning. *Cell Signal* **18**: 202-214. doi: 10.1016/j.cellsig.2005.04.012.

Kitamoto, A., Kitamoto, T., Nakamura, T., Ogawa, Y., Yoneda, M., Hyogo, H., Ochi, H., Mizusawa, S., Ueno, T., Nakao, K., Sekine, A., Chayama, K., Nakajima, A. and Hotta, K. (2014). Association of polymorphisms in GCKR and TRIB1 with nonalcoholic fatty liver disease and metabolic syndrome traits. *Endocr J* **61**: 683-689. doi: 10.1507/endocrj.ej14-0052.

Ko, S. H., Apple, E. C., Liu, Z. and Chen, L. (2020). Age-dependent autophagy induction after injury promotes axon regeneration by limiting NOTCH. *Autophagy* **16**: 2052-2068. doi: 10.1080/15548627.2020.1713645.

Kohler, J. J., Metallo, S. J., Schneider, T. L. and Schepartz, A. (1999). DNA specificity enhanced by sequential binding of protein monomers. *Proc Natl Acad Sci U S A* **96**: 11735-11739. doi: 10.1073/pnas.96.21.11735.

Kowenz-Leutz, E., Pless, O., Dittmar, G., Knoblich, M. and Leutz, A. (2010). Crosstalk between C/EBPbeta phosphorylation, arginine methylation, and SWI/SNF/Mediator implies an indexing transcription factor code. *EMBO J* **29**: 1105-1115. doi: 10.1038/emboj.2010.3.

Kowenz-Leutz, E., Twamley, G., Ansieau, S. and Leutz, A. (1994). Novel mechanism of C/EBP beta (NF-M) transcriptional control: activation through derepression. *Genes Dev* **8**: 2781-2791. doi: 10.1101/gad.8.22.2781.

Kulkarni, S. S., Sabharwal, V., Sheoran, S., Basu, A., Matsumoto, K., Hisamoto, N., Ghosh-Roy, A. and Koushika, S. P. (2021). UNC-16 alters DLK-1 localization and negatively regulates actin and microtubule dynamics in Caenorhabditis elegans regenerating neurons. *Genetics* **219**. doi: 10.1093/genetics/iyab139.

Kung, J. E. and Jura, N. (2019). The pseudokinase TRIB1 toggles an intramolecular switch to regulate COP1 nuclear export. *EMBO J* **38**. doi: 10.15252/embj.201899708.

Kuo, C. H., Morohoshi, K., Aye, C. C., Garoon, R. B., Collins, A. and Ono, S. J. (2012). The role of TRB3 in mast cells sensitized with monomeric IgE. *Exp Mol Pathol* **93**: 408-415. doi: 10.1016/j.yexmp.2012.09.008.

Kyriakis, J. M. and Avruch, J. (2012). Mammalian MAPK signal transduction pathways activated by stress and inflammation: a 10-year update. *Physiol Rev* **92**: 689-737. doi: 10.1152/physrev.00028.2011.

Landschulz, W. H., Johnson, P. F., Adashi, E. Y., Graves, B. J. and McKnight, S. L. (1988). Isolation of a recombinant copy of the gene encoding C/EBP. *Genes Dev* **2**: 786-800. doi: 10.1101/gad.2.7.786.

Landschulz, W. H., Johnson, P. F. and McKnight, S. L. (1989). The DNA binding domain of the rat liver nuclear protein C/EBP is bipartite. *Science* **243**: 1681-1688. doi: 10.1126/science.2494700.

Lee, M. S., Kim, M. H. and Tesh, V. L. (2013). Shiga toxins expressed by human pathogenic bacteria induce immune responses in host cells. *J Microbiol* **51**: 724-730. doi: 10.1007/s12275-013-3429-6.

Lee, W. B., Kang, J. S., Choi, W. Y., Zhang, Q., Kim, C. H., Choi, U. Y., Kim-Ha, J. and Kim, Y. J. (2016). Mincle-mediated translational regulation is required for strong nitric

oxide production and inflammation resolution. *Nat Commun* **7**: 11322. doi: 10.1038/ncomms11322.

Lekstrom-Himes, J. and Xanthopoulos, K. G. (1999). CCAAT/enhancer binding protein epsilon is critical for effective neutrophil-mediated response to inflammatory challenge. *Blood* **93**: 3096-3105.

Lekstrom-Himes, J. A., Dorman, S. E., Kopar, P., Holland, S. M. and Gallin, J. I. (1999). Neutrophil-specific granule deficiency results from a novel mutation with loss of function of the transcription factor CCAAT/enhancer binding protein epsilon. *J Exp Med* **189**: 1847-1852. doi: 10.1084/jem.189.11.1847.

Lemaitre, B. and Girardin, S. E. (2013). Translation inhibition and metabolic stress pathways in the host response to bacterial pathogens. *Nat Rev Microbiol* **11**: 365-369. doi: 10.1038/nrmicro3029.

Lemichez, E. and Barbieri, J. T. (2013). General aspects and recent advances on bacterial protein toxins. *Cold Spring Harb Perspect Med* **3**: a013573. doi: 10.1101/cshperspect.a013573.

Li, C., Hisamoto, N. and Matsumoto, K. (2015). Axon Regeneration Is Regulated by Ets-C/EBP Transcription Complexes Generated by Activation of the cAMP/Ca2+ Signaling Pathways. *PLoS Genet* **11**: e1005603. doi: 10.1371/journal.pgen.1005603.

Liang, L., Li, F., Bao, A., Zhang, M., Chung, K. F. and Zhou, X. (2013). Activation of p38 mitogen-activated protein kinase in ovalbumin and ozone-induced mouse model of asthma. *Respirology* **18 Suppl 3**: 20-29. doi: 10.1111/resp.12189.

Lima, A. F., Ropelle, E. R., Pauli, J. R., Cintra, D. E., Frederico, M. J., Pinho, R. A., Velloso, L. A. and De Souza, C. T. (2009). Acute exercise reduces insulin resistance-induced TRB3 expression and amelioration of the hepatic production of glucose in the liver of diabetic mice. *J Cell Physiol* **221**: 92-97. doi: 10.1002/jcp.21833.

Liu, J., Wu, X., Franklin, J. L., Messina, J. L., Hill, H. S., Moellering, D. R., Walton, R. G., Martin, M. and Garvey, W. T. (2010). Mammalian Tribbles homolog 3 impairs insulin action in skeletal muscle: role in glucose-induced insulin resistance. *Am J Physiol Endocrinol Metab* **298**: E565-576. doi: 10.1152/ajpendo.00467.2009.

Liu, Y., Samuel, B. S., Breen, P. C. and Ruvkun, G. (2014). Caenorhabditis elegans pathways that surveil and defend mitochondria. *Nature* **508**: 406-410. doi: 10.1038/nature13204.

Lorenzi, M., Altmann, A., Gutman, B., Wray, S., Arber, C., Hibar, D. P., Jahanshad, N., Schott, J. M., Alexander, D. C., Thompson, P. M., Ourselin, S. and Alzheimer's Disease Neuroimaging, I. (2018). Susceptibility of brain atrophy to TRIB3 in Alzheimer's disease, evidence from functional prioritization in imaging genetics. *Proc Natl Acad Sci U S A* **115**: 3162-3167. doi: 10.1073/pnas.1706100115.

MacDougald, O. A. and Lane, M. D. (1995). Transcriptional regulation of gene expression during adipocyte differentiation. *Annu Rev Biochem* **64**: 345-373. doi: 10.1146/annurev.bi.64.070195.002021.

Mack, E. A., Stein, S. J., Rome, K. S., Xu, L., Wertheim, G. B., Melo, R. C. N. and Pear, W. S. (2019). Trib1 regulates eosinophil lineage commitment and identity by restraining the neutrophil program. *Blood* **133**: 2413-2426. doi: 10.1182/blood.2018872218.

Malinow, R. A., Ying, P., Koorman, T., Boxem, M., Jin, Y. and Kim, K. W. (2019). Functional Dissection of C. elegans bZip-Protein CEBP-1 Reveals Novel Structural Motifs Required for Axon Regeneration and Nuclear Import. *Front Cell Neurosci* **13**: 348. doi: 10.3389/fncel.2019.00348.

Masoner, V., Das, R., Pence, L., Anand, G., LaFerriere, H., Zars, T., Bouyain, S. and Dobens, L. L. (2013). The kinase domain of Drosophila Tribbles is required for turnover of fly C/EBP during cell migration. *Dev Biol* **375**: 33-44. doi: 10.1016/j.ydbio.2012.12.016.

Mata, J., Curado, S., Ephrussi, A. and Rorth, P. (2000). Tribbles coordinates mitosis and morphogenesis in Drosophila by regulating string/CDC25 proteolysis. *Cell* **101**: 511-522. doi: 10.1016/s0092-8674(00)80861-2.

McEwan, D. L., Feinbaum, R. L., Stroustrup, N., Haas, W., Conery, A. L., Anselmo, A., Sadreyev, R. and Ausubel, F. M. (2016). Tribbles ortholog NIPI-3 and bZIP transcription factor CEBP-1 regulate a Caenorhabditis elegans intestinal immune surveillance pathway. *BMC Biol* **14**: 105. doi: 10.1186/s12915-016-0334-6.

McEwan, D. L., Kirienko, N. V. and Ausubel, F. M. (2012). Host translational inhibition by Pseudomonas aeruginosa Exotoxin A Triggers an immune response in Caenorhabditis elegans. *Cell Host Microbe* **11**: 364-374. doi: 10.1016/j.chom.2012.02.007.

Melo, J. A. and Ruvkun, G. (2012). Inactivation of conserved C. elegans genes engages pathogen- and xenobiotic-associated defenses. *Cell* **149**: 452-466. doi: 10.1016/j.cell.2012.02.050.

Metallo, S. J. and Schepartz, A. (1997). Certain bZIP peptides bind DNA sequentially as monomers and dimerize on the DNA. *Nat Struct Biol* **4**: 115-117. doi: 10.1038/nsb0297-115.

Miyajima, C., Inoue, Y. and Hayashi, H. (2015). Pseudokinase Tribbles 1 (TRIB1) Negatively Regulates Tumor-Suppressor Activity of p53 through p53 Deacetylation. *Biol. Pharm. Bull.* **38**: 618-624.

Mo, X., Kowenz-Leutz, E., Xu, H. and Leutz, A. (2004). Ras induces mediator complex exchange on C/EBP beta. *Mol Cell* **13**: 241-250. doi: 10.1016/s1097-2765(03)00521-5.

Mohr, I. and Sonenberg, N. (2012). Host translation at the nexus of infection and immunity. *Cell Host Microbe* **12**: 470-483. doi: 10.1016/j.chom.2012.09.006.

Mudgett, J. S., Ding, J., Guh-Siesel, L., Chartrain, N. A., Yang, L., Gopal, S. and Shen, M. M. (2000). Essential role for p38alpha mitogen-activated protein kinase in placental angiogenesis. *Proc Natl Acad Sci U S A* **97**: 10454-10459. doi: 10.1073/pnas.180316397.

Murphy, J. M., Nakatani, Y., Jamieson, S. A., Dai, W., Lucet, I. S. and Mace, P. D. (2015). Molecular Mechanism of CCAAT-Enhancer Binding Protein Recruitment by the TRIB1 Pseudokinase. *Structure* **23**: 2111-2121. doi: 10.1016/j.str.2015.08.017.

Naiki, T., Saijou, E., Miyaoka, Y., Sekine, K. and Miyajima, A. (2007). TRB2, a mouse Tribbles ortholog, suppresses adipocyte differentiation by inhibiting AKT and C/EBPbeta. *J Biol Chem* **282**: 24075-24082. doi: 10.1074/jbc.M701409200.

Newman, J. R. and Keating, A. E. (2003). Comprehensive identification of human bZIP interactions with coiled-coil arrays. *Science* **300**: 2097-2101. doi: 10.1126/science.1084648.

Nunes-Xavier, C., Roma-Mateo, C., Rios, P., Tarrega, C., Cejudo-Marin, R., Tabernero, L. and Pulido, R. (2011). Dual-specificity MAP kinase phosphatases as targets of cancer treatment. *Anticancer Agents Med Chem* **11**: 109-132. doi: 10.2174/187152011794941190.

O'Rourke, J., Yuan, R. and DeWille, J. (1997). CCAAT/enhancer-binding protein-delta (C/EBP-delta) is induced in growth-arrested mouse mammary epithelial cells. *J Biol Chem* **272**: 6291-6296. doi: 10.1074/jbc.272.10.6291.

O'Rourke, J. P., Hutt, J. A. and DeWille, J. (1999a). Transcriptional regulation of C/EBPdelta in G(0) growth-arrested mouse mammary epithelial cells. *Biochem Biophys Res Commun* **262**: 696-701. doi: 10.1006/bbrc.1999.1256.

O'Rourke, J. P., Newbound, G. C., Hutt, J. A. and DeWille, J. (1999b). CCAAT/enhancer-binding protein delta regulates mammary epithelial cell G0 growth arrest and apoptosis. *J Biol Chem* **274**: 16582-16589. doi: 10.1074/jbc.274.23.16582.

Ohoka, N., Hattori, T., Kitagawa, M., Onozaki, K. and Hayashi, H. (2007). Critical and functional regulation of CHOP (C/EBP homologous protein) through the N-terminal portion. *J Biol Chem* **282**: 35687-35694. doi: 10.1074/jbc.M703735200.

Ohoka, N., Yoshii, S., Hattori, T., Onozaki, K. and Hayashi, H. (2005). TRB3, a novel ER stress-inducible gene, is induced via ATF4-CHOP pathway and is involved in cell death. *EMBO J* **24**: 1243-1255. doi: 10.1038/sj.emboj.7600596.

Otsuka, M., Kang, Y. J., Ren, J., Jiang, H., Wang, Y., Omata, M. and Han, J. (2010). Distinct effects of p38alpha deletion in myeloid lineage and gut epithelia in mouse models of inflammatory bowel disease. *Gastroenterology* **138**: 1255-1265, 1265 e1251-1259. doi: 10.1053/j.gastro.2010.01.005.

Pabst, T., Mueller, B. U., Zhang, P., Radomska, H. S., Narravula, S., Schnittger, S., Behre, G., Hiddemann, W. and Tenen, D. G. (2001). Dominant-negative mutations of CEBPA, encoding CCAAT/enhancer binding protein-alpha (C/EBPalpha), in acute myeloid leukemia. *Nat Genet* **27**: 263-270. doi: 10.1038/85820.

Pei, D. Q. and Shih, C. H. (1991). An "attenuator domain" is sandwiched by two distinct transactivation domains in the transcription factor C/EBP. *Mol Cell Biol* **11**: 1480-1487. doi: 10.1128/mcb.11.3.1480-1487.1991.

Prudente, S., Sesti, G., Pandolfi, A., Andreozzi, F., Consoli, A. and Trischitta, V. (2012). The mammalian tribbles homolog TRIB3, glucose homeostasis, and cardiovascular diseases. *Endocr Rev* **33**: 526-546. doi: 10.1210/er.2011-1042.

Pujol, N., Cypowyj, S., Ziegler, K., Millet, A., Astrain, A., Goncharov, A., Jin, Y., Chisholm, A. D. and Ewbank, J. J. (2008). Distinct innate immune responses to infection

and wounding in the C. elegans epidermis. *Curr Biol* **18**: 481-489. doi: 10.1016/j.cub.2008.02.079.

Qi, L., Heredia, J. E., Altarejos, J. Y., Screaton, R., Goebel, N., Niessen, S., Macleod, I. X., Liew, C. W., Kulkarni, R. N., Bain, J., Newgard, C., Nelson, M., Evans, R. M., Yates, J. and Montminy, M. (2006). TRB3 links the E3 ubiquitin ligase COP1 to lipid metabolism. *Science* **312**: 1763-1766. doi: 10.1126/science.1123374.

Raingeaud, J., Whitmarsh, A. J., Barrett, T., Derijard, B. and Davis, R. J. (1996). MKK3- and MKK6-regulated gene expression is mediated by the p38 mitogen-activated protein kinase signal transduction pathway. *Mol Cell Biol* **16**: 1247-1255. doi: 10.1128/MCB.16.3.1247.

Rajamuthiah, R. and Mylonakis, E. (2014). Effector triggered immunity. *Virulence* **5**: 697-702. doi: 10.4161/viru.29091.

Rasmussen, M. H., Lyskjaer, I., Jersie-Christensen, R. R., Tarpgaard, L. S., Primdal-Bengtson, B., Nielsen, M. M., Pedersen, J. S., Hansen, T. P., Hansen, F., Olsen, J. V., Pfeiffer, P., Orntoft, T. F. and Andersen, C. L. (2016). miR-625-3p regulates oxaliplatin resistance by targeting MAP2K6-p38 signalling in human colorectal adenocarcinoma cells. *Nat Commun* **7**: 12436. doi: 10.1038/ncomms12436.

Reddy, K. C., Dror, T., Sowa, J. N., Panek, J., Chen, K., Lim, E. S., Wang, D. and Troemel, E. R. (2017). An Intracellular Pathogen Response Pathway Promotes Proteostasis in C. elegans. *Curr Biol* **27**: 3544-3553 e3545. doi: 10.1016/j.cub.2017.10.009.

Reddy, K. C., Dror, T., Underwood, R. S., Osman, G. A., Elder, C. R., Desjardins, C. A., Cuomo, C. A., Barkoulas, M. and Troemel, E. R. (2019). Antagonistic paralogs control a switch between growth and pathogen resistance in C. elegans. *PLoS Pathog* **15**: e1007528. doi: 10.1371/journal.ppat.1007528.

Reddy, K. C., Dunbar, T. L., Nargund, A. M., Haynes, C. M. and Troemel, E. R. (2016). The C. elegans CCAAT-Enhancer-Binding Protein Gamma Is Required for Surveillance Immunity. *Cell Rep* **14**: 1581-1589. doi: 10.1016/j.celrep.2016.01.055.

Richardson, C. E., Kooistra, T. and Kim, D. H. (2010). An essential role for XBP-1 in host protection against immune activation in C. elegans. *Nature* **463**: 1092-1095. doi: 10.1038/nature08762.

Richmond, L. and Keeshan, K. (2020). Pseudokinases: a tribble-edged sword. *FEBS J* **287**: 4170-4182. doi: 10.1111/febs.15096.

Roman, C., Platero, J. S., Shuman, J. and Calame, K. (1990). Ig/EBP-1: a ubiquitously expressed immunoglobulin enhancer binding protein that is similar to C/EBP and heterodimerizes with C/EBP. *Genes Dev* **4**: 1404-1415. doi: 10.1101/gad.4.8.1404.

Ron, D. and Habener, J. F. (1992). CHOP, a novel developmentally regulated nuclear protein that dimerizes with transcription factors CEBP and LAP and functions as a dominant-negative inhibitor of gene transcription. *Genes and Development* **6**: 439-453.

Rørth, P., Szabo, K. and Texido, G. (2000). The Level of CEBP Protein Is Critical for Cell Migration during Drosophila Oogenesis and is tightly controlled by regulated degredation. *Molecular Cell* **6**: 23-30.

Rosental, B., Kowarsky, M., Seita, J., Corey, D. M., Ishizuka, K. J., Palmeri, K. J., Chen, S. Y., Sinha, R., Okamoto, J., Mantalas, G., Manni, L., Raveh, T., Clarke, D. N., Tsai, J. M., Newman, A. M., Neff, N. F., Nolan, G. P., Quake, S. R., Weissman, I. L. and Voskoboynik, A. (2018). Complex mammalian-like haematopoietic system found in a colonial chordate. *Nature* **564**: 425-429. doi: 10.1038/s41586-018-0783-x.

Rothlisberger, B., Heizmann, M., Bargetzi, M. J. and Huber, A. R. (2007). TRIB1 overexpression in acute myeloid leukemia. *Cancer Genet Cytogenet* **176**: 58-60. doi: 10.1016/j.cancergencyto.2007.03.003.

Rowan, A. D. and Litherland, G. J. (2015). Tribbles and arthritis: what are the links? *Biochem Soc Trans* **43**: 1051-1056. doi: 10.1042/BST20150076.

Rucker, F. G., Bullinger, L., Schwaenen, C., Lipka, D. B., Wessendorf, S., Frohling, S., Bentz, M., Miller, S., Scholl, C., Schlenk, R. F., Radlwimmer, B., Kestler, H. A., Pollack, J. R., Lichter, P., Dohner, K. and Dohner, H. (2006). Disclosure of candidate genes in acute myeloid leukemia with complex karyotypes using microarray-based molecular characterization. *J Clin Oncol* **24**: 3887-3894. doi: 10.1200/JCO.2005.04.5450.

Sakai, S., Ohoka, N., Onozaki, K., Kitagawa, M., Nakanishi, M. and Hayashi, H. (2010). Dual mode of regulation of cell division cycle 25 A protein by TRB3. *Biol Pharm Bull* **33**: 1112-1116. doi: 10.1248/bpb.33.1112.

Sakai, Y., Hanafusa, H., Pastuhov, S. I., Shimizu, T., Li, C., Hisamoto, N. and Matsumoto, K. (2019). TDP2 negatively regulates axon regeneration by inducing

SUMOylation of an Ets transcription factor. *EMBO Rep* **20**: e47517. doi: 10.15252/embr.201847517.

Saleem, S. and Biswas, S. C. (2017). Tribbles Pseudokinase 3 Induces Both Apoptosis and Autophagy in Amyloid-beta-induced Neuronal Death. *J Biol Chem* **292**: 2571-2585. doi: 10.1074/jbc.M116.744730.

Salome, M., Hopcroft, L. and Keeshan, K. (2018). Inverse and correlative relationships between TRIBBLES genes indicate non-redundant functions during normal and malignant hemopoiesis. *Exp Hematol* **66**: 63-78 e13. doi: 10.1016/j.exphem.2018.07.005.

Sanford, D. C. and DeWille, J. W. (2005). C/EBPdelta is a downstream mediator of IL-6 induced growth inhibition of prostate cancer cells. *Prostate* **63**: 143-154. doi: 10.1002/pros.20159.

Satoh, T., Kidoya, H., Naito, H., Yamamoto, M., Takemura, N., Nakagawa, K., Yoshioka, Y., Morii, E., Takakura, N., Takeuchi, O. and Akira, S. (2013). Critical role of Trib1 in differentiation of tissue-resident M2-like macrophages. *Nature* **495**: 524-528. doi: 10.1038/nature11930.

Screpanti, I., Romani, L., Musiani, P., Modesti, A., Fattori, E., Lazzaro, D., Sellitto, C., Scarpa, S., Bellavia, D., Lattanzio, G. and et al. (1995). Lymphoproliferative disorder and imbalanced T-helper response in C/EBP beta-deficient mice. *EMBO J* **14**: 1932-1941.

Seher, T. C. and Leptin, M. (2000). Tribbles, a cell-cycle brake that coordinates proliferation and morphogenesis during Drosophila gastrulation. *Curr Biol* **10**: 623-629. doi: 10.1016/s0960-9822(00)00502-9.

Shaye, D. D. and Greenwald, I. (2011). OrthoList: a compendium of C. elegans genes with human orthologs. *PLoS One* **6**: e20085. doi: 10.1371/journal.pone.0020085.

Shivers, R. P., Pagano, D. J., Kooistra, T., Richardson, C. E., Reddy, K. C., Whitney, J. K., Kamanzi, O., Matsumoto, K., Hisamoto, N. and Kim, D. H. (2010). Phosphorylation of the conserved transcription factor ATF-7 by PMK-1 p38 MAPK regulates innate immunity in Caenorhabditis elegans. *PLoS Genet* **6**: e1000892. doi: 10.1371/journal.pgen.1000892.

Simoni, L., Delgado, V., Ruer-Laventie, J., Bouis, D., Soley, A., Heyer, V., Robert, I., Gies, V., Martin, T., Korganow, A. S., Reina-San-Martin, B. and Soulas-Sprauel, P. (2018). Trib1 Is Overexpressed in Systemic Lupus Erythematosus, While It Regulates Immunoglobulin Production in Murine B Cells. *Front Immunol* **9**: 373. doi: 10.3389/fimmu.2018.00373.

Sinner, M. P., Masurat, F., Ewbank, J. J., Pujol, N. and Bringmann, H. (2021). Innate Immunity Promotes Sleep through Epidermal Antimicrobial Peptides. *Curr Biol* **31**: 564-577 e512. doi: 10.1016/j.cub.2020.10.076.

Sivko, G. S. and DeWille, J. W. (2004). CCAAT/Enhancer binding protein delta (c/EBPdelta) regulation and expression in human mammary epithelial cells: I. "Loss of function" alterations in the c/EBPdelta growth inhibitory pathway in breast cancer cell lines. *J Cell Biochem* **93**: 830-843. doi: 10.1002/jcb.20223.

Smink, J. J. and Leutz, A. (2010). Rapamycin and the transcription factor C/EBPβ as a switch in osteoclast differentiation: Implications for lytic bone diseases. Journal of Molecular Medicine. **88:** 227-233.

Soubeyrand, S., Martinuk, A. and McPherson, R. (2017). TRIB1 is a positive regulator of hepatocyte nuclear factor 4-alpha. *Sci Rep* **7**: 5574. doi: 10.1038/s41598-017-05768-1.

Soubeyrand, S., Martinuk, A., Naing, T., Lau, P. and McPherson, R. (2016). Role of Tribbles Pseudokinase 1 (TRIB1) in human hepatocyte metabolism. *Biochim Biophys Acta* **1862**: 223-232. doi: 10.1016/j.bbadis.2015.12.003.

Spoel, S. H. and Dong, X. (2012). How do plants achieve immunity? Defence without specialized immune cells. *Nat Rev Immunol* **12**: 89-100. doi: 10.1038/nri3141.

Stein, S. J., Mack, E. A., Rome, K. S. and Pear, W. S. (2015). Tribbles in normal and malignant haematopoiesis. *Biochem Soc Trans* **43**: 1112-1115. doi: 10.1042/BST20150117.

Storlazzi, C. T., Fioretos, T., Surace, C., Lonoce, A., Mastrorilli, A., Strombeck, B., D'Addabbo, P., Iacovelli, F., Minervini, C., Aventin, A., Dastugue, N., Fonatsch, C., Hagemeijer, A., Jotterand, M., Muhlematter, D., Lafage-Pochitaloff, M., Nguyen-Khac, F., Schoch, C., Slovak, M. L., Smith, A., Sole, F., Van Roy, N., Johansson, B. and Rocchi, M. (2006). MYC-containing double minutes in hematologic malignancies: evidence in favor of the episome model and exclusion of MYC as the target gene. *Hum Mol Genet* **15**: 933-942. doi: 10.1093/hmg/ddl010.

Stuart, L. M., Paquette, N. and Boyer, L. (2013). Effector-triggered versus pattern-triggered immunity: how animals sense pathogens. *Nat Rev Immunol* **13**: 199-206. doi: 10.1038/nri3398.

Sun, H., Charles, C. H., Lau, L. F. and Tonks, N. K. (1993). MKP-1 (3CH134), an immediate early gene product, is a dual specificity phosphatase that dephosphorylates MAP kinase in vivo. *Cell* **75**: 487-493. doi: 10.1016/0092-8674(93)90383-2.

Takiguchi, M. (1998). The C/EBP family of transcription factors in the liver and other organs. *Int J Exp Pathol* **79**: 369-391. doi: 10.1046/j.1365-2613.1998.00082.x.

Takizawa, H., Fritsch, K., Kovtonyuk, L. V., Saito, Y., Yakkala, C., Jacobs, K., Ahuja, A. K., Lopes, M., Hausmann, A., Hardt, W. D., Gomariz, A., Nombela-Arrieta, C. and Manz, M. G. (2017). Pathogen-Induced TLR4-TRIF Innate Immune Signaling in Hematopoietic Stem Cells Promotes Proliferation but Reduces Competitive Fitness. *Cell Stem Cell* **21**: 225-240 e225. doi: 10.1016/j.stem.2017.06.013.

Tanaka-Hino, M., Sagasti, A., Hisamoto, N., Kawasaki, M., Nakano, S., Ninomiya-Tsuji, J., Bargmann, C. I. and Matsumoto, K. (2002). SEK-1 MAPKK mediates Ca2+ signaling to determine neuronal asymmetric development in Caenorhabditis elegans. *EMBO Rep* **3**: 56-62. doi: 10.1093/embo-reports/kvf001.

Tanaka, T., Akira, S., Yoshida, K., Umemoto, M., Yoneda, Y., Shirafuji, N., Fujiwara, H., Suematsu, S., Yoshida, N. and Kishimoto, T. (1995). Targeted disruption of the NF-IL6 gene discloses its essential role in bacteria killing and tumor cytotoxicity by macrophages. *Cell* **80**: 353-361. doi: 10.1016/0092-8674(95)90418-2.

Tanaka, T., Yoshida, N., Kishimoto, T. and Akira, S. (1997). Defective adipocyte differentiation in mice lacking the C/EBPbeta and/or C/EBPdelta gene. *EMBO J* **16**: 7432-7443. doi: 10.1093/emboj/16.24.7432.

Taylor, S. S. and Kornev, A. P. (2011). Protein kinases: evolution of dynamic regulatory proteins. *Trends Biochem Sci* **36**: 65-77. doi: 10.1016/j.tibs.2010.09.006.

Taylor, S. S., Shaw, A., Hu, J., Meharena, H. S. and Kornev, A. (2013). Pseudokinases from a structural perspective. *Biochem Soc Trans* **41**: 981-986. doi: 10.1042/BST20130120.

Tjahjono, E. and Kirienko, N. V. (2017). A conserved mitochondrial surveillance pathway is required for defense against Pseudomonas aeruginosa. *PLoS Genet* **13**: e1006876. doi: 10.1371/journal.pgen.1006876.

Trautwein, C., van der Geer, P., Karin, M., Hunter, T. and Chojkier, M. (1994). Protein kinase A and C site-specific phosphorylations of LAP (NF-IL6) modulate its binding affinity to DNA recognition elements. *J Clin Invest* **93**: 2554-2561. doi: 10.1172/JCI117266.

Trempolec, N., Dave-Coll, N. and Nebreda, A. R. (2013). SnapShot: p38 MAPK substrates. *Cell* **152**: 924-924 e921. doi: 10.1016/j.cell.2013.01.047.

Troemel, E. R., Chu, S. W., Reinke, V., Lee, S. S., Ausubel, F. M. and Kim, D. H. (2006). p38 MAPK regulates expression of immune response genes and contributes to longevity in C. elegans. *PLoS Genet* **2**: e183. doi: 10.1371/journal.pgen.0020183.

Tsukada, J., Yoshida, Y., Kominato, Y. and Auron, P. E. (2011). The CCAAT/enhancer (C/EBP) family of basic-leucine zipper (bZIP) transcription factors is a multifaceted highly-regulated system for gene regulation. *Cytokine* **54**: 6-19. doi: 10.1016/j.cyto.2010.12.019.

Uematsu, S., Kaisho, T., Tanaka, T., Matsumoto, M., Yamakami, M., Omori, H., Yamamoto, M., Yoshimori, T. and Akira, S. (2007). The C/EBP beta isoform 34-kDa LAP is responsible for NF-IL-6-mediated gene induction in activated macrophages, but is not essential for intracellular bacteria killing. *J Immunol* **179**: 5378-5386. doi: 10.4049/jimmunol.179.8.5378.

Uljon, S., Xu, X., Durzynska, I., Stein, S., Adelmant, G., Marto, J. A., Pear, W. S. and Blacklow, S. C. (2016). Structural Basis for Substrate Selectivity of the E3 Ligase COP1. *Structure* **24**: 687-696. doi: 10.1016/j.str.2016.03.002.

Vinson, C. R., Sigler, P. B. and McKnight, S. L. (1989). Scissors-grip model for DNA recognition by a family of leucine zipper proteins. *Science* **246**: 911-916. doi: 10.1126/science.2683088.

Wada, T., Akagi, T., Muraoka, M., Toma, T., Kaji, K., Agematsu, K., Koeffler, H. P., Yokota, T. and Yachie, A. (2015). A Novel In-Frame Deletion in the Leucine Zipper Domain of C/EBPepsilon Leads to Neutrophil-Specific Granule Deficiency. *J Immunol* **195**: 80-86. doi: 10.4049/jimmunol.1402222.

Waetzig, G. H., Seegert, D., Rosenstiel, P., Nikolaus, S. and Schreiber, S. (2002). p38 mitogen-activated protein kinase is activated and linked to TNF-alpha signaling in inflammatory bowel disease. *J Immunol* **168**: 5342-5351. doi: 10.4049/jimmunol.168.10.5342.

Wagner, E. F. and Nebreda, A. R. (2009). Signal integration by JNK and p38 MAPK pathways in cancer development. *Nat Rev Cancer* **9**: 537-549. doi: 10.1038/nrc2694.

Wang, G., Long, J., Matsuura, I., He, D. and Liu, F. (2005). The Smad3 linker region contains a transcriptional activation domain. *Biochem J* **386**: 29-34. doi: 10.1042/BJ20041820.

Wang, J. M., Ko, C. Y., Chen, L. C., Wang, W. L. and Chang, W. C. (2006). Functional role of NF-IL6beta and its sumoylation and acetylation modifications in promoter activation of cyclooxygenase 2 gene. *Nucleic Acids Res* **34**: 217-231. doi: 10.1093/nar/gkj422.

Wang, N. D., Finegold, M. J., Bradley, A., Ou, C. N., Abdelsayed, S. V., Wilde, M. D., Taylor, L. R., Wilson, D. R. and Darlington, G. J. (1995). Impaired energy homeostasis in C/EBP alpha knockout mice. *Science* **269**: 1108-1112. doi: 10.1126/science.7652557.

Wang, P. Y., Hsu, P. I., Wu, D. C., Chen, T. C., Jarman, A. P., Powell, L. M. and Chen, A. (2018). SUMOs Mediate the Nuclear Transfer of p38 and p-p38 during Helicobacter Pylori Infection. *Int J Mol Sci* **19**. doi: 10.3390/ijms19092482.

Wang, X. Z. and Ron, D. (1996). Stress-induced phosphorylation and activation of the transcription factor CHOP (GADD153) by p38 MAP Kinase. *Science* **272**: 1347-1349. doi: 10.1126/science.272.5266.1347.

Wang, Y. G., Shi, M., Wang, T., Shi, T., Wei, J., Wang, N. and Chen, X. M. (2009). Signal transduction mechanism of TRB3 in rats with non-alcoholic fatty liver disease. *World J Gastroenterol* **15**: 2329-2335. doi: 10.3748/wjg.15.2329.

Weaver, B. P., Weaver, Y. M., Omi, S., Yuan, W., Ewbank, J. J. and Han, M. (2020). Non-Canonical Caspase Activity Antagonizes p38 MAPK Stress-Priming Function to Support Development. *Dev Cell* **53**: 358-369 e356. doi: 10.1016/j.devcel.2020.03.015.

Wei, S. C., Rosenberg, I. M., Cao, Z., Huett, A. S., Xavier, R. J. and Podolsky, D. K. (2012). Tribbles 2 (Trib2) is a novel regulator of toll-like receptor 5 signaling. *Inflamm Bowel Dis* **18**: 877-888. doi: 10.1002/ibd.22883.

Wennemers, M., Bussink, J., Scheijen, B., Nagtegaal, I. D., van Laarhoven, H. W., Raleigh, J. A., Varia, M. A., Heuvel, J. J., Rouschop, K. M., Sweep, F. C. and Span, P. N. (2011). Tribbles homolog 3 denotes a poor prognosis in breast cancer and is involved in hypoxia response. *Breast Cancer Res* **13**: R82. doi: 10.1186/bcr2934.

Wiper-Bergeron, N., Salem, H. A., Tomlinson, J. J., Wu, D. and Hache, R. J. (2007). Glucocorticoid-stimulated preadipocyte differentiation is mediated through acetylation of C/EBPbeta by GCN5. *Proc Natl Acad Sci U S A* **104**: 2703-2708. doi: 10.1073/pnas.0607378104.

Wu, C., Karakuzu, O. and Garsin, D. A. (2021). Tribbles pseudokinase NIPI-3 regulates intestinal immunity in Caenorhabditis elegans by controlling SKN-1/Nrf activity. *Cell Rep* **36**: 109529. doi: 10.1016/j.celrep.2021.109529.

Wu, Z., Isik, M., Moroz, N., Steinbaugh, M. J., Zhang, P. and Blackwell, T. K. (2019). Dietary Restriction Extends Lifespan through Metabolic Regulation of Innate Immunity. *Cell Metab* **29**: 1192-1205 e1198. doi: 10.1016/j.cmet.2019.02.013.

Yamanaka, R., Barlow, C., Lekstrom-Himes, J., Castilla, L. H., Liu, P. P., Eckhaus, M., Decker, T., Wynshaw-Boris, A. and Xanthopoulos, K. G. (1997). Impaired granulopoiesis, myelodysplasia, and early lethality in CCAAT/enhancer binding protein epsilon-deficient mice. *Proc Natl Acad Sci U S A* **94**: 13187-13192. doi: 10.1073/pnas.94.24.13187.

Yan, D., Wu, Z., Chisholm, A. D. and Jin, Y. (2009). The DLK-1 kinase promotes mRNA stability and local translation in C. elegans synapses and axon regeneration. *Cell* **138**: 1005-1018. doi: 10.1016/j.cell.2009.06.023.

Yeh, W. C., Cao, Z., Classon, M. and McKnight, S. L. (1995). Cascade regulation of terminal adipocyte differentiation by three members of the C/EBP family of leucine zipper proteins. *Genes Dev* **9**: 168-181. doi: 10.1101/gad.9.2.168.

Yokoyama, T., Kanno, Y., Yamazaki, Y., Takahara, T., Miyata, S. and Nakamura, T. (2010). Trib1 links the MEK1/ERK pathway in myeloid leukemogenesis. *Blood* **116**: 2768-2775. doi: 10.1182/blood-2009-10-246264.

Yokoyama, T. and Nakamura, T. (2011). Tribbles in disease: Signaling pathways important for cellular function and neoplastic transformation. *Cancer Sci* **102**: 1115-1122. doi: 10.1111/j.1349-7006.2011.01914.x.

Zhang, F., Zhao, Q., Tian, J., Chang, Y. F., Wen, X., Huang, X., Wu, R., Wen, Y., Yan, Q., Huang, Y., Ma, X., Han, X., Miao, C. and Cao, S. (2018). Effective Pro-Inflammatory Induced Activity of GALT, a Conserved Antigen in A. Pleuropneumoniae, Improves the Cytokines Secretion of Macrophage via p38, ERK1/2 and JNK MAPKs Signal Pathway. *Front Cell Infect Microbiol* **8**: 337. doi: 10.3389/fcimb.2018.00337.

Zhang, X., Fan, L., Wu, J., Xu, H., Leung, W. Y., Fu, K., Wu, J., Liu, K., Man, K., Yang, X., Han, J., Ren, J. and Yu, J. (2019). Macrophage p38alpha promotes nutritional steatohepatitis through M1 polarization. *J Hepatol* **71**: 163-174. doi: 10.1016/j.jhep.2019.03.014.

Zhang, X., Zhang, B., Zhang, C., Sun, G. and Sun, X. (2021). Trib1 deficiency causes brown adipose respiratory chain depletion and mitochondrial disorder. *Cell Death Dis* **12**: 1098. doi: 10.1038/s41419-021-04389-x.

Zheng, Z., Aihemaiti, Y., Liu, J., Afridi, M. I., Yang, S., Zhang, X., Xu, Y., Chen, C. and Tu, H. (2021). The bZIP Transcription Factor ZIP-11 Is Required for the Innate Immune Regulation in Caenorhabditis elegans. *Front Immunol* **12**: 744454. doi: 10.3389/fimmu.2021.744454.

Ziegler, K., Kurz, C. L., Cypowyj, S., Couillault, C., Pophillat, M., Pujol, N. and Ewbank, J. J. (2009). Antifungal innate immunity in C. elegans: PKCdelta links G protein signaling and a conserved p38 MAPK cascade. *Cell Host Microbe* **5**: 341-352. doi: 10.1016/j.chom.2009.03.006.

Zugasti, O., Thakur, N., Belougne, J., Squiban, B., Kurz, C. L., Soule, J., Omi, S., Tichit, L., Pujol, N. and Ewbank, J. J. (2016). A quantitative genome-wide RNAi screen in C. elegans for antifungal innate immunity genes. *BMC Biol* **14**: 35. doi: 10.1186/s12915-016-0256-3.

Chapter 2: Identification of novel structural motif in *C. elegans* bZip- transcription factor CEBP-1 required for axon regeneration

Abstract

The basic leucine-zipper (bZIP) domain transcription factors CCAAT/enhancer-binding proteins (C/EBP) have a variety of roles in cell proliferation, differentiation, and stress response. In the nervous system, several isoforms of C/EBP function in learning and memory, neuronal plasticity, neuroinflammation and axon regeneration. We previously reported that the *C. elegans* C/EBP homolog, CEBP-1, is essential for axon regeneration. CEBP-1 consists of 319 amino acids, with its bZIP domain at the C-terminus and a long N-terminal fragment with no known protein motifs. Here, using forward genetic screening with targeted genome editing, we have identified a unique domain in the N-terminus that is critical for its *in vivo* function.

Introduction

CCAAT/enhancer-binding proteins (C/EBP) are conserved basic leucine zipper (bZIP) domain transcription factors that are widely expressed and have a variety of roles in cell proliferation, differentiation, and stress response (Ramji and Foka 2002, Yang et al. 2017). In neurons, C/EBPs have been linked to learning and memory (Alberini et al. 1994, Lee et al. 2012) as well as neuronal repair after injury (Nadeau et al. 2005, Yan et al. 2009, Aleksic and Feng 2012, Lopez de Heredia and Magoulas 2013). Expression and function of C/EBPs are regulated at multiple levels. For example, humans and mice have six C/EBP genes, CEBPα–ζ, and each C/EBP shows temporally regulated activity during development and in different tissue types (Ramji and Foka 2002). While the bZIP domain of C/EBPs plays essential roles in DNA binding and transcriptional function, a variety of regulatory domains residing within the N- or C-terminus modulate the transcriptional activity and contribute to distinct functional outcomes.

In this paper, we investigate the regulation of CEBP-1, the *C. elegans* homolog of C/EBP transcription factors, which is essential for axon regeneration (Yan et al. 2009). CEBP-1 consists of a canonical bZIP domain at the C-terminus, with a long N-terminal region having no known protein motifs. Here, through forward genetic analyses, we have identified a stretch of 15 amino acids at the N-terminus of CEBP-1 that is critical for its *in vivo* function and axon regeneration. The region containing this unique domain has a predicted propensity to form alpha helices.

Materials and Methods

C. elegans culture

Strains were maintained on NGM plates at 20°C as described previously (Brenner 1974). Alleles and genotypes of strains are summarized in Table 1. We followed standard procedures to generate new transgenes. Plasmid and transgene information is in Table 2. Transgenes were introduced into mutants by genetic crossing or by microinjection, and genotypes for all mutations were confirmed by PCR or sequencing.

Isolation of novel *cebp-1* mutations in a suppressor screen of *nipi-3(0)* mutants

We previously reported that loss of function mutations of *cebp-1* suppress larval lethality of the Tribbles kinase *nipi-3(ju1293)* null mutant (Kim et al. 2016). We performed a large-scale suppressor screen using an efficient selection scheme. Briefly, we mutagenized L4 animals of the genotype: *nipi-3(ju1293); juEx7152[nipi-3(+); Pmyo-2::gfp; Phsp::peel-1]* using ethyl methane sulphonate (EMS), following standard procedures (Brenner 1974). F2 progeny were subjected to heat shock at 37°C for 1 hour, which induced the expression of the toxic protein PEEL-1 to kill any animals whose survival depended on the expression of *nipi-3(+)* from the *juEx7152* transgene. Those lived to fertile adults without *juEx7152* likely contained a mutation that suppressed *nipi-3(ju1293)* lethality. We then performed Sanger sequencing for *cebp-1* and identified mutations within *cebp-1* for 15 independent suppressor alleles (*ju1518* – *ju1532*).

CRISPR/Cas9-mediated editing to generate new alleles affecting the N' domain of CEBP-1

We generated missense, insertion and deletion alleles in the N' domain of *cebp-1 (ju1586, ju1587, ju1588, ju1589, ju1590, ju1591, ju1592, ju1685, ju1686)* using the co-CRISPR method (Friedland et al. 2013). We designed one single guide RNA (sgRNA; 5'-GCAACGUGACCGCGAACGCC-3') to target CCA for Glu61 in the N' domain of the *cebp-1* gene. A mixture of *cebp-1* crRNA (0.3µL of 200µM), *dpy-10* crRNA (0.3µL of 200µM), tracrRNA (0.9µL of 100µM), Cas9 protein (3.5µL of 40µM) was injected into CZ24853 (*nipi-3(ju1293); juEx7152[nipi-3(+); Pmyo-2::gfp; Phsp::peel-1]*). F1 animals displaying dumpy and/or normal animal growth reaching adulthood without *juEx7152* transgene were propagated to the F2 generation. A total of 139 independent F2 isolates that were confirmed for suppression of *nipi-3(ju1293)* larval lethality were then analyzed by PCR and Sanger sequencing to identify changes in *cebp-1.* The animals containing large deletions based on size of PCR amplification products were not analyzed further, because they most likely altered protein translation affecting the downstream bZIP domain. We focused only on those having missense or small in-frame deletions and insertions within N' domain.

Laser axotomy

We cut mechanosensory PLM axons using *muIs32[Pmec-7::gfp]* or *zdIs5[Pmec-4::gfp]* and GABAergic motor neuron commissures (VD3, DD2, and VD4) using *juIs76[Punc-25::gfp]* in anesthetized L4 larvae as previously described (Wu et al. 2007).

Images of regrowing axons after 24 hours were collected using LSM510 confocal microscope (Zeiss), and the axon regrowth length was quantified as described.

Quantification and Statistical Analysis

Statistical analysis was performed using GraphPad Prism 5. Significance was determined using unpaired *t*-tests for two samples, one-way ANOVA followed by Tukey multiple comparison tests for multiple samples. For two nominal variables, Fisher's exact test (two-tailed) was used. $P < 0.05$ (*) was considered statistically significant. * $P < 0.05$; ** $P < 0.01$; *** $P < 0.001$. Data are shown as mean ± SEM. "n" represents the number of animals and is shown in graphs.

Results

In previous genetic suppressor screens for loss of function mutations in *rpm-1,* a conserved E3 ubiquitin ligase, we isolated a missense mutation of *cebp-1*, *ju634,* that changes Arg63 to Pro in the N-terminus of CEBP-1 (Noma et al. 2014) **(Figure 1A, #3)**. *cebp-1(ju634)* behaved as a genetic null, based on its effects to restore the synapse and axon developmental defects in *rpm-1* to normal (Noma et al. 2014). Moreover, in laser axotomy assay, we found that *cebp-1(ju634)* blocked injury-induced axon regrowth **(Figure 1B)**, similarly to *cebp-1* null (Yan et al. 2009).

In a parallel investigation, we identified *cebp-1* to be negatively regulated by the Tribbles pseudokinase *nipi-3* in larval development (Kim et al. 2016). Loss of *nipi-3* results in larval lethality, which is fully suppressed by loss of *cebp-1.* We performed a large-scale genetic suppressor screen of *nipi-3(ju1293)* mediated developmental arrest (Methods), and isolated four new missense mutations affecting amino acids adjacent to Arg63 **(Figure 1A, #1,2,4,5)**. As all these point mutants phenocopied the *cebp-1(tm2807)* null, we hypothesized that this region may define a domain of functional significance.

To test this hypothesis, we designed genome-editing using a CRISPR/Cas9 directed mutagenesis with a sgRNA designed to target amino acid Glu61 **(Figure 1A, black arrow)**. Following microinjection of sgRNA and Cas9 mixture into *nipi-3(ju1293)* mutants expressing a transgene, *juEx7152[nipi-3(+); myo-2p::gfp; Phsp::peel-1]*, we isolated > 100 animals that were able to reach adulthood without the *juEx7152* rescue array (Methods). Using PCR and Sanger sequencing, we then identified multiple alleles that contained missense mutations, as well as a single amino acid deletion or in-frame

insertion of one or more amino acids **(Figure 1A, #6–14)**. These new alleles all behaved similarly to each other and to *cebp-1* null, based on the suppression of *nipi-3(ju1293)* lethality. Together, these results strongly support that this stretch of 15 amino acids within the N-terminus of CEBP-1 defines a functional domain, named as N' domain.

While this N' domain is highly conserved among nematode homologs of *cebp-1,* we did not find homologous regions among C/EBPs in other species by BLAST search (Altschul et al. 1990). We next asked whether the N' domain may form any secondary structure. Using RaptorX (http://raptorx.uchicago.edu; an online predictor of protein structure) (Wang et al. 2016), we found that amino acids 55-106 in CEBP-1 N-terminus region has high propensity to form alpha helices **(Figure 1C)**. Several missense mutations and amino acid insertion and deletion within the N' domain are also predicted to alter the propensity of this region to form alpha helices **(Figure 1C)**. Thus, this analysis suggests that the N' region of CEBP-1 may form a highly structured domain to mediate interactions with other proteins.

Discussion

While previous work on CEBP-1 has shown it is essential for axon regeneration, the only defined functional domain has been the highly conserved bZIP domain (Yan et al. 2009). In this study, through forward genetic screenings and a site-directed mutagenesis screening, we have identified a unique functional domain in the N' terminus of CEBP-1. We showed that this domain is required for the function of CEBP-1 in the NIPI-3-mediated development pathway as well as the function in adult axon regeneration. Furthermore, analysis from protein structural and modeling prediction suggests that this domain resides within a highly structured region, and that this structure can be altered by the mutations isolated in our screens. A majority of CEBP homologues in other species contain regulatory domains in their N' terminus that contribute to the proteins' function (Hunter and Karin 1992, Tsukada et al. 2011). For example, the transactivating domains in the N' terminus of mouse CEBPα can bind directly to CDKs and a chromatin remodeling complex, and mediate specific functional outcomes in cell cycle progression and epigenetic regulation (Nerlov 2007). Thus, we propose that this newly identified domain in CEBP-1 likely impacts the transcriptional activity of CEBP-1 via binding to other unidentified factors. The interaction that involves this N' domain likely leads to transcriptional activation as mutations in this domain phenocopy null mutations of CEBP-1. Further, it is worthy commenting on the CRISPR/Cas9-mediating genome editing technology. The sgRNA we designed showed high efficiency to guide Cas9 to the PAM sequence, as we observed all editing occurred 3' downstream from the PAM site. As we were able to obtain a large number of editing mutants because of the efficient functional assay for *cebp-1* loss of function, our

findings reveal a surprising degree of imprecise repair, ranging from a few nucleotide modification, insertion, deletion, to large deletion of several hundred nucleotides. Thus, this analysis raises caution for medical intervention, and urges deep studies of genome editing technology.

Acknowledgements

I thank my lab members for valuable discussions, Zilu Wu for technical support in laser axotomy, and Hetty Zhang for assistance in strain construction. I thank Dr. S Mitani and National Bioresource Project of Japan, and the *Caenorhabditis* Genetics Center (funded by NIH Office of Research Infrastructure Programs P40 OD010440) for strains. This work was supported by National Research Foundation of Korea (NRF-2019R1A2C1003329) to KWK, Hallym University Research Fund (HRF-201809-014) to KWK, and National Institutes of Health (R01-0395588S1) to RAM.

Chapter 2, in large part, is a reprint of the material as it appears in Malinow RA, Ying P, Koorman T, Boxem M, Jin Y, Kim KW. 2019. Functional Dissection of C. elegans bZip-Protein CEBP-1 Reveals Novel Structural Motifs Required for Axon Regeneration and Nuclear Import. *Frontiers in Cellular Neuroscience* 13:348. The dissertation author was the primary investigator and author of the material included in this chapter.

Figures

Figure 4. N' functional domain in CEBP-1 is required for proper axon regeneration and protein structure formation

A. CEBP-1 N' domain mutants isolated in several forward genetic screens. Mutations 1-5 are missense mutations isolated in forward genetic screens utilizing EMS as a chemical mutagen. #1, *ju1518* S53F; #2, *ju1519* L54F; #3, *ju634* R63P; #4/5, *ju1520/ju1521* D64N. Mutations 6-14 were isolated in a forward genetic screen utilizing targeted CRISPR/Cas9 mutagenesis. The site targeted for double stranded DNA breakage is marked with a black arrow. These mutations do not cause a shift in frame, only add and/or delete amino acids adjacent to the cut site. #6, *ju1588* Δ(L60,Q61); #7, *ju1587* Δ(Q61, Q62, R63, D64) +HH; #8, *ju1592* L60[HSTRS]Q61; #9, *ju1590* ΔQ62; #10, *ju1685* ΔQ62 +HE; #11, *ju1686* ΔQ62 +HRG; #12, *ju1591* Δ(Q62, R63) +RPVTS; 13, *ju1586* Δ(Q62,R63)+H Δ(E66, R67); 14, *ju1589* Δ(Q62, R63, D64)+H.
B. PLM axon regrowth 24 hr post-axotomy in *cebp-1(ju634), cebp-1(ju1521),* and *cebp-1(ju1590)* mutants in PLM mechanosensory neurons. Length of regrowth was quantified by subtracting the initial length of the axon at 0 hours from the length of the axon 24 hours after injury. Data are shown as mean ± SEM. Student's t-test. ***p<0.001. Right: representative images of PLM axons 24 hr post-axotomy. Red arrowhead, site of axotomy.
C. Alteration of predicted alpha helices structure upon *cebp-1* N' mutations based on RaptorX. The S53F mutation (#1) makes a predicted break in α-2, producing two helices. The L54F mutation (#2) makes lengthening of α-1 and α-2, and the R63P mutation (#3) makes lengthening of α-2. The D64N mutation (#4/5) is predicted to cause the additional turn in the C' end of α-2.

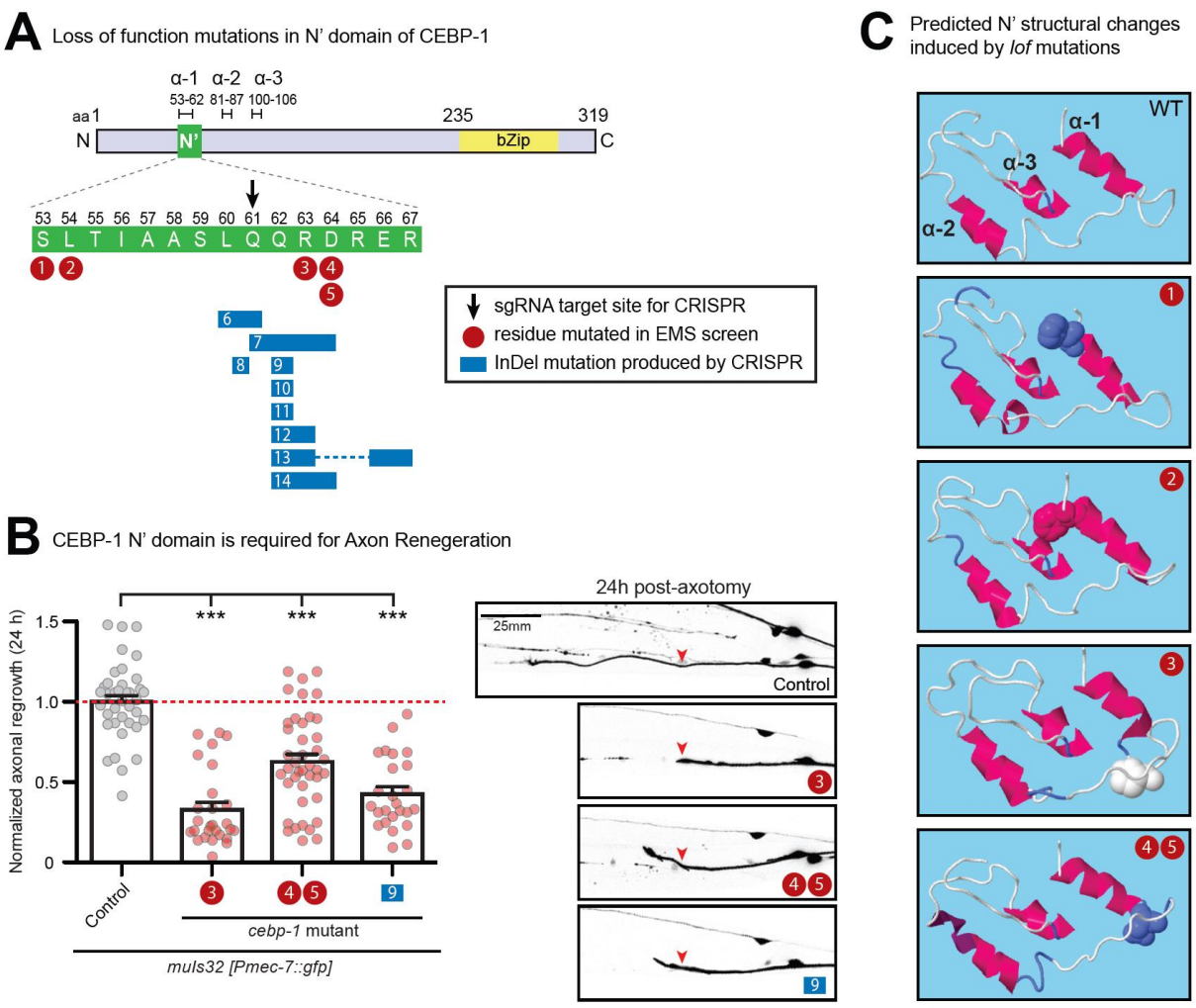
A
Loss of function mutations in N' domain of CEBP-1
α-1 α-2 α-3
53-62 81-87 100-106
aa 1
235
319
N
N'
bZip
C
53 54 55 56 57 58 59 60 61 62 63 64 65 66 67
S L T I A A S L Q Q R D R E R
sgRNA target site for CRISPR
residue mutated in EMS screen
InDel mutation produced by CRISPR
B
CEBP-1 N' domain is required for Axon Renegeration
Normalized axonal regrowth (24 h)
1.5
1.0
0.5
0
***
***
***
Control
cebp-1 mutant
muIs32 [Pmec-7::gfp]
24h post-axotomy
25mm
Control
C
Predicted N' structural changes
induced by lof mutations
WT
α-1
α-3
α-2

Tables

Table 1. Chapter 2 Strains and Genotypes

Strain name	Genotype
CZ24853	*nipi-3(ju1293); juEx7152[nipi-3(+); Pmyo-2::gfp; Phsp::peel-1]*
CZ25378	*cebp-1(ju1518) nipi-3(ju1293) X*
CZ25379	*cebp-1(ju1519) nipi-3(ju1293) X*
CZ25380	*cebp-1(ju1520) nipi-3(ju1293) X*
CZ25381	*cebp-1(ju1521) nipi-3(ju1293) X*
CZ25382	*cebp-1(ju1522) nipi-3(ju1293) X*
CZ25383	*cebp-1(ju1523) nipi-3(ju1293) X*
CZ25384	*cebp-1(ju1524) nipi-3(ju1293) X*
CZ25385	*cebp-1(ju1525) nipi-3(ju1293) X*
CZ25386	*cebp-1(ju1526) nipi-3(ju1293) X*
CZ25387	*cebp-1(ju1527) nipi-3(ju1293) X*
CZ25388	*cebp-1(ju1528) nipi-3(ju1293) X*
CZ25389	*cebp-1(ju1529) nipi-3(ju1293) X*
CZ25390	*cebp-1(ju1530) nipi-3(ju1293) X*
CZ25391	*cebp-1(ju1531) nipi-3(ju1293) X*
CZ25392	*cebp-1(ju1532) nipi-3(ju1293) X*
CZ26013	*cebp-1(ju1586) nipi-3(ju1293) X*
CZ26014	*cebp-1(ju1587) nipi-3(ju1293) X*
CZ26015	*cebp-1(ju1588) nipi-3(ju1293) X*
CZ26016	*cebp-1(ju1589) nipi-3(ju1293) X*
CZ26017	*cebp-1(ju1590) nipi-3(ju1293) X*
CZ26018	*cebp-1(ju1591) nipi-3(ju1293) X*
CZ26019	*cebp-1(ju1592) nipi-3(ju1293) X*
CZ10969	*Pmec-7::gfp(muIs32) II*
CZ16489	*Pmec-7::gfp(muIs32) II; cebp-1(ju634) X*
CZ27204	*Pmec-7::gfp(muIs32) II; cebp-1(ju1521) X*
CZ27464	*Pmec-7::gfp(muIs32) II; cebp-1(ju1590) X*

Table 2. Chapter 2 Plasmids and Transgenes

Plasmid name	Description	Transgene
pMA122[#]	*Phsp::peel-1*	*juEx7152*
pCZGY1095	*Pmyo-2::gfp*	*juEx7152*
pCZGY3044	*nipi-3 gDNA*	*juEx7152*

[#] pMA122 **(Seidel et al. 2011)**

References

Alberini, C. M., Ghirardi, M., Metz, R. and Kandel, E. R. (1994). C/EBP is an immediate-early gene required for the consolidation of long-term facilitation in Aplysia. *Cell* **76**: 1099-1114. doi: 10.1016/0092-8674(94)90386-7.

Aleksic, M. and Feng, Z. P. (2012). Identification of the role of C/EBP in neurite regeneration following microarray analysis of a L. stagnalis CNS injury model. *BMC Neurosci* **13**: 2. doi: 10.1186/1471-2202-13-2.

Altschul, S. F., Gish, W., Miller, W., Myers, E. W. and Lipman, D. J. (1990). Basic local alignment search tool. *J Mol Biol* **215**: 403-410. doi: 10.1016/S0022-2836(05)80360-2.

Brenner, S. (1974). The genetics of Caenorhabditis elegans. *Genetics* **77**: 71-94. doi: 10.1093/genetics/77.1.71.

Friedland, A. E., Tzur, Y. B., Esvelt, K. M., Colaiacovo, M. P., Church, G. M. and Calarco, J. A. (2013). Heritable genome editing in C. elegans via a CRISPR-Cas9 system. *Nat Methods* **10**: 741-743. doi: 10.1038/nmeth.2532.

Hunter, T. and Karin, M. (1992). The regulation of transcription by phosphorylation. *Cell* **70**: 375-387. doi: 10.1016/0092-8674(92)90162-6.

Kim, K. W., Thakur, N., Piggott, C. A., Omi, S., Polanowska, J., Jin, Y. and Pujol, N. (2016). Coordinated inhibition of C/EBP by Tribbles in multiple tissues is essential for Caenorhabditis elegans development. *BMC Biol* **14**: 104. doi: 10.1186/s12915-016-0320-z.

Lee, Y. S., Choi, S. L., Jun, H., Yim, S. J., Lee, J. A., Kim, H. F., Lee, S. H., Shim, J., Lee, K., Jang, D. J. and Kaang, B. K. (2012). AU-rich element-binding protein negatively regulates CCAAT enhancer-binding protein mRNA stability during long-term synaptic plasticity in Aplysia. *Proc Natl Acad Sci U S A* **109**: 15520-15525. doi: 10.1073/pnas.1116224109.

Lopez de Heredia, L. and Magoulas, C. (2013). Lack of the transcription factor C/EBPdelta impairs the intrinsic capacity of peripheral neurons for regeneration. *Exp Neurol* **239**: 148-157. doi: 10.1016/j.expneurol.2012.10.012.

Nadeau, S., Hein, P., Fernandes, K. J., Peterson, A. C. and Miller, F. D. (2005). A transcriptional role for C/EBP beta in the neuronal response to axonal injury. *Mol Cell Neurosci* **29**: 525-535. doi: 10.1016/j.mcn.2005.04.004.

Nerlov, C. (2007). The C/EBP family of transcription factors: a paradigm for interaction between gene expression and proliferation control. *Trends Cell Biol* **17**: 318-324. doi: 10.1016/j.tcb.2007.07.004.

Noma, K., Goncharov, A. and Jin, Y. (2014). Systematic analyses of rpm-1 suppressors reveal roles for ESS-2 in mRNA splicing in Caenorhabditis elegans. *Genetics* **198**: 1101-1115. doi: 10.1534/genetics.114.167841.

Ramji, D. P. and Foka, P. (2002). CCAAT/enhancer-binding proteins: structure, function and regulation. *Biochem J* **365**: 561-575. doi: 10.1042/BJ20020508.

Seidel, H. S., Ailion, M., Li, J., van Oudenaarden, A., Rockman, M. V. and Kruglyak, L. (2011). A novel sperm-delivered toxin causes late-stage embryo lethality and transmission ratio distortion in *C. elegans*. *PLoS Biol* **9**: e1001115. doi: 10.1371/journal.pbio.1001115.

Tsukada, J., Yoshida, Y., Kominato, Y. and Auron, P. E. (2011). The CCAAT/enhancer (C/EBP) family of basic-leucine zipper (bZIP) transcription factors is a multifaceted highly-regulated system for gene regulation. *Cytokine* **54**: 6-19. doi: 10.1016/j.cyto.2010.12.019.

Wang, S., Li, W., Liu, S. and Xu, J. (2016). RaptorX-Property: a web server for protein structure property prediction. *Nucleic Acids Res* **44**: W430-435. doi: 10.1093/nar/gkw306.

Wu, Z., Ghosh-Roy, A., Yanik, M. F., Zhang, J. Z., Jin, Y. and Chisholm, A. D. (2007). Caenorhabditis elegans neuronal regeneration is influenced by life stage, ephrin signaling, and synaptic branching. *Proc Natl Acad Sci U S A* **104**: 15132-15137. doi: 10.1073/pnas.0707001104.

Yan, D., Wu, Z., Chisholm, A. D. and Jin, Y. (2009). The DLK-1 kinase promotes mRNA stability and local translation in C. elegans synapses and axon regeneration. *Cell* **138**: 1005-1018. doi: 10.1016/j.cell.2009.06.023.

Yang, Y., Liu, L., Naik, I., Braunstein, Z., Zhong, J. and Ren, B. (2017). Transcription Factor C/EBP Homologous Protein in Health and Diseases. *Front Immunol* **8**: 1612. doi: 10.3389/fimmu.2017.01612.

Chapter 3: Novel signaling downstream of NIPI-3/Tribbles regulates development in *Caenorhabditis elegans*

Abstract

Cellular response to external and internal cues is essential for organismal survival. MAP kinase signaling pathways are one means of transmitting these signals to the nucleus to produce adaptive transcriptional responses. Although these pathways have been well studied, questions remain regarding possible feedback mechanisms within MAPK pathways. Here, we utilize a genetically sensitized background in *C. elegans* that highly upregulates the stress response transcription factor CEBP-1 to characterize how this leads to upregulated p38 MAPK gene expression. We show the activation of MAP2K/*sek-1* through imaging of a transcriptional reporter in *C. elegans* and find unexpected positive feedback from MAPK signaling molecules, p38 MAPK/*pmk-1* and MAPKAPK/*mak-2* as well as from its own, MAP2K/*sek-1*, activity. Thus, our study suggests a novel feedback mechanism within this highly conserved MAPK pathway. This positive feedback mechanism could amplify MAPK signaling responses and, if dysregulated, could become unstable and deleterious in pathological conditions. Additionally, from a forward genetic screen, we identify novel genetic interactions between histone deacetylase/*hda-4*, N-terminal acetyltransferases/*natc-1, natc-2,* and *natc-3*, and regulation of p38 MAPK signaling downstream of CEBP-1 in *C. elegans* development.

Introduction

Cellular signaling is a fundamental function of all cells to be able to sense their environment and produce expression changes appropriate to the situation. One such signaling system involves mitogen activated protein kinases (MAPKs) that form a kinase cascade and transmit signals through phosphorylation. p38 MAPKs are a subfamily of MAPKs that are activated by environmental or intracellular signals pertaining to healthy physiological processes or stress related signals such as DNA damage, bacterial toxins, oxidative stress, or osmotic stress (Glise et al. 1995, Kockel et al. 1997, Yang et al. 1997, Dolado et al. 2007). p38 MAPKs are also activated by intercellular signaling molecules such as cytokines, to coordinate cross-tissue responses (Freshney et al. 1994, Sapkota 2013, Sabio and Davis 2014, Tzavlaki and Moustakas 2020). p38 MAPK signaling results in the phosphorylation and activation of transcription factors, regulatory proteins, and DNA/RNA binding proteins, culminating in changes in gene expression and protein activity (Wang and Ron 1996, Williamson et al. 2005, Joshi and Platanias 2014, Reyskens and Arthur 2016). p38 MAPK signaling regulates a wide variety of cellular processes such as cell cycle regulation, DNA repair, autophagy, cytokine production, apoptosis, differentiation, and RNA metabolism (Dolado and Nebreda 2008, Phong et al. 2010, Cannell et al. 2015, Lin et al. 2015). As p38 MAPKs regulate many cellular processes, dysfunction of this signaling results in many pathological outcomes such as cancers, autoimmune diseases, and neurological diseases (Hensley et al. 1999, Sun et al. 2003, Wagner and Nebreda 2009, Gupta and Nebreda 2015, Gubern et al. 2016, Muranen et al. 2016, Chen et al. 2018, Youssif et al. 2018, Zheng et al. 2018).

Different facets of p38 MAPK signaling have been studied using a range of model systems. The biochemistry of p38 MAPK signaling was initially studied in pathological contexts in cell lines which allows direct activation of these pathways by adjusting media conditions to contain various stressful stimuli (Rouse et al. 1994, Sapkota 2013, Sabio and Davis 2014, Lin et al. 2015, Tzavlaki and Moustakas 2020). Tissue culture studies also revealed cell-type specific regulation of MAPK signaling (Engelman et al. 1998, Qiao et al. 2006, Pillai et al. 2011, Hayakawa et al. 2017). Genetic mouse models have been used to study the systemic phenotypes of p38 MAPK signaling including development, aging, and immune responses (Warr et al. 2012, Gupta and Nebreda 2015, Colie et al. 2017, Growcott et al. 2018, Grimes and Grimes 2020). A disadvantage of mouse models is the challenge of recording real-time readouts of p38 MAPK function which help demonstrate the spatial and temporal dimensions of signaling in the intact animal. The ground-dwelling nematode *Caenorhabditis elegans* provides a genetically tractable model system where conserved elements of the p38 MAPK signaling pathway can be studied. In *C. elegans,* p38 MAPK signaling is required for development, aging, and responses to multiple perturbations such as infection, wounding, or oxidative stress (Troemel et al. 2006, Shivers et al. 2010, Andrusiak and Jin 2016, Garcia-Sanchez et al. 2021, Harding and Ewbank 2021). Many studies have taken advantage of transcriptional and translational reporters of MAPK activity that can be visualized in living animals (Pujol et al. 2008, Ziegler et al. 2009, Couillault et al. 2012, Weaver et al. 2020, Wu et al. 2021).

NIPI-3 is a regulator of p38 MAPK signaling in *C. elegans* and its function is required for animal development (Kim et al. 2016). NIPI-3 also functions cell-autonomously following infection of the epidermis or intestine to mediate pathogen defense by positively regulating a PMK-1/p38 MAPK pathway (Pujol et al. 2008, Ziegler et al. 2009, Couillault et al. 2012, McEwan et al. 2016, Wu et al. 2021). Interestingly, the transcription factor CEBP-1 is required for the function of NIPI-3 in response to intestinal infection and during animal development, but not in response to epidermal infection. Furthermore, during intestinal infection, CEBP-1 functions cell autonomously as a negative regulator of PMK-1/p38 MAPK activity by increasing expression of the phosphatase VHP-1 which dephosphorylates and deactivates PMK-1 (Wu et al. 2021). During development in young larval animals, CEBP-1 functions in multiple tissues as a positive regulator of PMK-1/p38 MAPK activity by increasing the expression of the MAPKK SEK-1 which phosphorylates and activates PMK-1 (Kim et al. 2016). This temporal and cell-type specific regulation is typical of MAPK signaling and is seen in different physiological and pathological conditions in a variety of experimental systems (Canovas and Nebreda 2021).

Here, I describe collaborative studies that examine the role of NIPI-3 and PMK-1/p38 MAPK signaling during *C. elegans* development. In the absence of NIPI-3, *C. elegans* larva arrest mid-development via upregulation of the transcription factor CEBP-1 and hyperactivation of a PMK-1/p38 MAPK pathway (Kim et al. 2016). Using a transcriptional reporter as a readout of p38 MAPK activation by CEBP-1, we find novel positive regulation from *pmk-1*/MAPK and *mak-2*/MAPKAPK to *sek-1*/MAPKK

transcription. It appears that SEK-1 activity unexpectedly activates its own gene transcription, suggesting another positive feedback loop in this pathway. Additionally, we have leveraged the developmental arrest phenotype of *nipi-3(0)* as a genetically sensitized background to perform a forward genetic screen to identify novel regulators of the signaling downstream of NIPI-3. An unexpected finding from this screen is that histone deacetylation and N-terminal acetylation are involved in the regulation of development in *C. elegans*. We found that a gain of function mutation within the histone deacetylase *hda-4* prevents developmental arrest of *nipi-3(0)* animals via transcriptional regulation of *sek-1/*MAPKK. We also found that loss of function of any of the components of the N-acetyltransferase C (NatC) complex (*natc-1, natc-2,* or *natc-3)* prevents developmental arrest of *nipi-3(0)* animals.

Materials and Methods

C. elegans Strains and Genetics

Strains were maintained on NGM plates at 20ºC as described previously (Brenner 1974). Genetic crosses were performed using standard methods and genotypes for all mutations were confirmed using PCR or standard sequencing. Genotypes of strains are summarized in **Table 3**, alleles are summarized in **Table 4**, and genotyping primers are summarized in **Table 7**. Transgenes were made by microinjection following standard protocol (Mello et al. 1991) and are summarized in **Table 5**. The *juIs559* integrated transcriptional reporter of *sek-1* was produced from CZ24469: *juEx7488* following standard UV/TMP mutagenesis (Yandell et al. 1994) and was twice outcrossed with N2 animals.

Fluorescence microscopy and Imaging

Images were taken on a Zeiss LSM 800 confocal or a Zeiss Axioplan compound microscope. Microscope, laser power, pinhole size, and objective settings are summarized in **Table 9**. Unless otherwise indicated, animals were mounted on 2% agarose pads and anesthetized with 2.5 mM levamisole for imaging. All strains were maintained at 20ºC under well-fed conditions for at least three generations before imaging.

For quantification of *Psek-1::GFP* intensity, animals with *juIs559* reporter were synchronized by placing 20-40 gravid adults on a seeded NGM plate and allowing them to lay eggs for 2 hours. For all strains containing the *nipi-3* rescue array (*juEx6807)*, the

gravid adults were array positive, to minimize any trans-generation effects. Ten animals of a single genotype, 36 hours post egg-laying, were aligned on 2% agarose pads anesthetized in 25 mM sodium azide. Images were acquired on a Zeiss Axioplan compound microscope using 10x objective and 850 ms exposure time across all genotypes. Microscope settings were such that no pixels were saturated in any images. This protocol was repeated over three days to collect images of 30 animals. Quantification of expression of *juIs559* (*Psek-1::GFP)* reporter was done using ImageJ software (National Institutes of Health, Bethesda, MD, USA). Although I saw a drastic change in GFP intensity throughout the animal **(Figure 5D and E)**, I chose to quantify the head to avoid the auto-fluorescence from the intestine. The nerve ring was not included in the analysis ROI because there was very high expression in the nerve ring in all genetic backgrounds. Images were analyzed by drawing an elliptical ROI in the head of each animal, anterior to the nerve ring, and measuring mean intensity **(Figure 5H)**. The image in 5H is a single slice from a confocal microscope to show a high magnification of the region analyzed. For the quantification, a compound image was used, which shows the GFP from all tissues in the head. The background was subtracted from each of these readings. The background was quantified by the average of the mean intensity of four elliptical ROIs, each placed near the heads of the animals, where no animals are present. Both the imaging and quantification of the *Psek-1::GFP* strains was done under genotype-blind conditions.

For imaging strains with *wgIs563* (*Pcebp-1::cebp-1::gfp*) (Sarov et al. 2006) or *mak-2::*GFP KI, animals were synchronized by moving eggs to an NGM plate and

picking just-hatched animals to a fresh seeded NGM plate. The plates with eggs were checked every 30 minutes to 2 hours for freshly hatched animals. These animals were imaged on 10% agar pads anesthetized with 2.5uM levamisole, 24 hours post hatch. These animals were synchronized using hatch timing. I chose this strategy because I observed that some of the strains with overexpression of CEBP-1 (*wgIs563* transgene) retain their eggs and therefore all animals with *wgIs563* were prepared similarly.

Body length measurement and animal staging

For quantification of body length, animals were synchronized by placing 20-40 gravid adults on a seeded NGM plate and allowing them to lay eggs for 2 hours. Animals were imaged 72 hours after egg-laying. Images were acquired on a Zeiss Axioplan compound microscope on 2% agarose pads anesthetized with 2.5mM levamisole. At least 30 animals were imaged of each genotype. For all strains containing the *nipi-3* rescue array (*nipi-3 gDNA juEx6807)*, the gravid adults were array positive. Quantification of body length was done using Image J by manually drawing a segmented line along the length of the animal and the developmental stage of the animal was recorded. Both the imaging and quantification was done under genotype-blind conditions. All strains were maintained at 20ºC under well-fed conditions for at least three generations before imaging.

CRISPR-Cas9-mediated genome editing

We generated *hda-4(ju1403), natc-2(ju1797), natc-2(ju1866), natc-3(ju1837)* deletion alleles using the co-CRISPR method (Friedland et al. 2013, Paix et al. 2015). CRISPR RNAs (crRNA) sequences are summarized in **Table 8** and were ordered from Integrated DNA Technologies. For each gene, two crRNAs were used, one targeting the 5' region of the gene and one targeting the 3' region. A mixture of gene specific crRNA (for *hda-4*, *natc-2,* or *natc-3,* respectively, at 0.3µL of 200µM), *dpy-10* crRNA (0.3µL of 200µM), tracrRNA (0.9µL of 100µM), and Cas9 protein from MacroLabs, University of California, Berkeley (3.5µL of 40µM) was injected into N2 for *ju1403* and *ju1837,* WU1036: *natc-1(am138)* for *ju1797,* or CZ27728: *nipi-3(0); juIs559(Psek-1::GFP); Tg[nipi-3(+)]* for *ju1866*. F1 animals displaying dumpy and/or roller phenotype were single housed on NGM plates and propagated to the F2 generation. Approximately 10 F2s were used for lysis for PCR analysis. Animals containing large deletions based on the size of the PCR of the targeted gene (*hda-4 natc-2,* or *natc-3)* were isolated and subsequent generations were tracked to confirm homozygosity. Sanger sequencing was used to identify the bounds of the deletion. Strains were outcrossed with N2 to remove dumpy phenotype and maintain desired deletion.

GFP KI at the *natc-1, natc-2,* and *mak-2* loci were produced by standard methods (Dickinson et al. 2015). Primers used to produce the subgenomic RNA (sgRNA) and repair template plasmids are summarized in **Table 6**. We designed sgRNAs: agctttacgggtccaatgcc for *natc-1,* ttgccataatgaaagagtac for *natc-2*, and aaagccataatttcgtccgg for *mak-2*. A mixture of 20 ng/µl of sgRNA, 80 ng/µl of homology

arm repair template, and 2.5 ng/µl of pCFJ90 *Pmyo-2::mCherry* (Addgene plasmid 19327) was injected into N2 animals. 3 days after injection, hygromycin was added to the plates to kill the untransformed F1 animals. On day 6 post-injection, we looked for candidate GFP knock-in animals which were L4/adult roller, survived hygromycin selection and without the mCherry extrachromosomal array marker. These animals were genotyped to confirm genomic insertion of GFP and saved as candidate transcriptional reporters. We then heat shocked 20 L1/L2 animals at 34°C for 4 hours to remove the self-excising cassette. Non-roller animals were checked for GFP expression using compound microscopy and GFP genomic insertion was again confirmed by genotyping PCR and sequencing. The sequence of the bounds of the GFP insertion are in **Figures 15, 16** and **17.**

Outcrossing of *nipi-3(0)* suppressors isolated from EMS screen

For *ju1369*, the first two outcrosses were done using CZ10175: *zdIs5 (Pmec-4::GFP)* I, which helped identify cross-progeny. The next two outcrosses were done with N2 males and cross progeny were selected for WT phenotype, whereas *nipi-3(ju1293); ju1369* was visibly dumpy and egg laying defective.

For *ju1371,* the first outcross was done with CZ10969: *muIs32 (Pmec-7::GFP) II,* which helped to identify cross progeny. The second outcross was done with CZ10175: *zdIs5 (Pmec-4::GFP)* I. The next two outcrosses were done with N2 males and cross progeny were selected for WT phenotype, whereas *nipi-3(ju1293); ju1371* was visibly dumpy and egg laying defective.

Whole-genome sequencing analysis

Genomic DNA was prepared using the Puregene Cell and Tissue Kit (Qiagen) according to the manufacturer's instructions and 20x coverage of sequences was obtained using a 90bp paired-end Illumina HiSeq 2000 at Beijing Genomics Institute. The raw sequence reads were mapped to the *C. elegans* reference genome (ce10) using Burrows-Wheeler Aligner (Li and Durbin 2009) in the Galaxy platform (http://use-galaxy.org) (Afgan et al. 2016) followed by a custom workflow incorporating tools including SAMtools (Li et al. 2009), Genome Analysis Toolkit (GATK), SnpSift, and SnpEff.

The whole genome sequence data set of CZ23399: *nipi-3(ju1293); ju1369* (0x outcross from EMS isolate) was compared to the whole genome sequencing data obtained of the parental strain CZ22446: *nipi-3(ju1293); juEx6807[nipi-3(+)]* and the whole genome sequencing data from the other strains isolated in this screen. Candidate SNPs were identified by being unique to only the data from CZ23399 and predicted to alter the function of the protein. A SNP is predicted to alter the function of the protein if there is a missense mutation within the coding region of the gene or a mutation located at a splice site. Candidate SNPs were verified by Sanger sequencing, and used to track chromosomal recombinants over the course of four outcrosses as previously described (Sarin et al. 2008). This analysis placed *ju1369* on Chromosome V between -8 and +6mu. Inspection of mutagenesis induced SNPs in this region revealed a missense mutation (449 g>a, G150E) in the N-Acetyltransferase domain of *natc-2.*

Whole genome sequencing data for CZ23401: *nipi-3(ju1293); ju1371* (0x outcross from EMS isolate) and CZ23692: *nipi-3(ju1293) ; ju1371* (2x outcross from EMS isolate) was analyzed to guide further mapping as previously described (Sarin et al. 2008). The whole genome sequence data set of CZ23401 and CZ23692 was compared to the whole genome sequencing data obtained of the parental strain, CZ22446: *nipi-3(ju1293); juEx6807[nipi-3(+)]*. Candidate SNPs were identified by present in both the non-outcrossed and two times outcrossed isolates of *ju1371* and not present in the parental strain. Candidate SNPs were tracked by Sanger sequencing over the course of two additional outcrosses, a total of four times outcrossed from the original EMS isolate. During this outcrossing, the *nipi-3(0)* phenotype was never re-isolated, indicating that the suppressor was likely linked to *nipi-3.* Mapping of candidate SNPs and the likely linkage to *nipi-3* placed *ju1371* on Chromosome X to the right of +12mu. Inspection of mutagenesis induced SNPs in this region revealed a missense mutation (1817 g>a, G606D) in *hda-4.*

Statistical Analysis

We used JMP for all statistical analyses. For the *juIs559* dataset, the two microscopes used to collect the images differed in their general intensities. Thus, data points for each microscope were converted to percent of mean wildtype intensity of that microscope. Then, a one-way ANOVA was applied with genotype as the independent variable and %WT as the dependent variable. A plot of residuals revealed heteroscedasticity across genotypes and their distribution was highly leptokurtotic.

Consequently, a Box-Cox transformation was applied to these data (Sakia 1992). After applying a one-way ANOVA again with genotype as the independent variable and Transformed %WT as the dependent variable, the residuals appeared homoscedastic. While the distribution of transformed residuals still was slightly leptokurtotic, it was "near-normal". Generally, ANOVAs remain robust with near-normal distributions (Lix et al. 1996, Glass et al. 2016, Harwell et al. 2016). After ANOVA, all pairs of genotypes were compared using Tukey-Kramer HSD, which adjusts critical P values from multiple comparisons. *** $p<0.001$, ** $p<0.01$, * $p<0.05$, "ns" not significant $p>0.05$.

For the body length data set, a one-way ANOVA was applied with genotype as the independent variable and body length as the dependent variable. A plot of residuals revealed homoscedasticity across genotypes and with a normal distribution. After ANOVA, all pairs of genotypes were compared using Tukey-Kramer HSD, which adjusts critical P values from multiple comparisons. *** $p<0.001$, ** $p<0.01$, * $p<0.05$, "ns" not significant $p>0.05$.

Results and Discussion

Transcriptional reporter of *sek-1* is a functional readout of CEBP-1 activity downstream of NIPI-3

A previous study reported CEBP-1 ChIP-seq analyses to identify putative transcriptional targets (Kim et al. 2016). Among them, the promoter of *sek-1,* encoding a MAP2K, contains two CEBP-1 binding sites 1.3 kb upstream from the start codon **(Figure 5A)**. To verify that transcription of *sek-1* is under the control of CEBP-1, Dr. Kim constructed a transgenic *Psek-1::GFP* reporter using 4.9 kb upstream sequences of *sek-1* to drive expression of GFP. Since NIPI-3 represses CEBP-1 expression (Kim et al. 2016), Dr. Kim tested if *Psek-1* transcription is regulated by NIPI-3. With the non-integrated reporter in *nipi-3(0)* background (CZ24961), her qualitative observations suggested that *Psek-1::GFP* transcription is regulated by NIPI-3 via the transcription factor CEBP-1. Dr. Kim also validated these results with qRT-PCR analysis of sek-1 mRNA transcripts in wildtype, *nipi-3(0)* and *cebp-1(0) nipi-3(0)* animals (Kim et al. 2016). I then generated an integrated *Psek-1::GFP* transgene, *juIs559,* which has more stable GFP expression than a non-integrated strain and allowed me to quantify GFP expression in different genetic backgrounds. In wild type animals expressing *Psek-1::GFP (juIs559)*, I observed a pattern of low levels of diffuse GFP fluorescence in all developmental stages and in multiple tissues including nervous system, intestine, and uterine muscles, but not body wall muscles or pharyngeal muscles **(**L4 stage, **Figure 5B)**. Within the nervous system, GFP was expressed in many neurons in ganglia in the head and tail, and touch receptor neurons. In *nipi-3(0)* larvae 36 hours after egg laying

expressing *Psek-1::GFP (juIs559)*, I observed GFP expression was much greater throughout the animal compared to wild type animals **(Figure 5E)**. I quantified the expression of *Psek-1::GFP* in the head of the animal to avoid autofluorescence from the intestine. A caveat of this quantification is that I do not have tissue or cell-type specific measurements (Methods). In addition, quantification of the GFP reporter expression may not necessarily reflect the endogenous *sek-1* RNA levels and therefore qRT-PCR experiments would provide direct confirmation of these observations. My quantification of *Psek-1::GFP* in *cebp-1(0) nipi-3(0)* animals confirmed Dr. Kim's qualitative observation that CEBP-1 is required for this upregulation, as *cebp-1(0) nipi-3(0)* animals have wildtype level expression of *Psek-1::GFP* **(Figure 5F, G)**. This regulation is due to the direct binding of CEBP-1 to the promoter of *sek-1* because another reporter, *juEx7617[Psek-1(del)::GFP*] made by Dr. Kim, in which the CEBP-1 binding sites were deleted from *Psek-1::GFP,* displayed no increase in the expression of *Psek-1(del)::GFP* in *nipi-3(0)* animals **(Figure 5E')**. The deletion of these binding sites did not change the expression level and pattern (expression still seen in nerve ring, intestine, and vulval muscles) of GFP in wildtype background **(Figure 5C, D')**. Combined with the ChIP-seq analyses, these results show that upregulation of *Psek-1::GFP* in *nipi-3(0)* is mediated by CEBP-1 binding to the *sek-1* promoter. Thus, CEBP-1 activity levels in this NIPI-3 regulated pathway can be measured with the *Psek-1* transcriptional reporter, which I used to examine the complexity of the signaling downstream of NIPI-3 and CEBP-1.

Transcriptional reporter of *sek-1* suggests *pmk-1*/p38 MAPK and *mak-2*/MAPKAPK feedback regulation of transcription of *sek-1*

A previous genetic screen performed by Dr. Kim identified a highly conserved p38 MAPK pathway (TIR-1/NSY-1/SEK-1/PMK-1/MAK-2) as essential for developmental arrest caused by *nipi-3(0)* (Kim et al. 2016). I used the *Psek-1::GFP* reporter to characterize signaling linking NIPI-3 to this PMK-1/p38 MAPK pathway. As described above, transcription of *sek-1* is strongly upregulated in *nipi-3(0)* animals. TIR-1 and NSY-1 increase SEK-1 activity (Sagasti et al. 2001, Tanaka-Hino et al. 2002, Chuang and Bargmann 2005) and I found that *tir-1(0)* or *nsy-1(0)* significantly reduces the transcriptional upregulation of *sek-1* in *nipi-3(0)*. This suggests that decreasing SEK-1 activity decreases the transcription of *sek-1*. I also found that *sek-1(0)* significantly reduces *Psek-1::GFP* expression in *nipi-3(0)* animals further supporting the idea that SEK-1 activity positively regulates *sek-1* transcription **(Figure 6A;** additional data examining *Psek-1::GFP* in other genetic backgrounds in **Figures 18,19;** statistical comparisons in **Table 10)**. Thus, *sek-1, tir-1* and *nsy-1* contribute to the upregulation of *sek-1* transcription in the context of *nipi-3(0)*. *pmk-1(0)* also reduce the high levels of *Psek-1::GFP* observed in *nipi-3(0)* (although not as much as *sek-1(0)*) **(Figure 6A)**, indicating that *pmk-1* also positively regulates *sek-1* transcription. This feedback loop was unexpected because in the context of innate immunity, many studies have placed SEK-1 function upstream of PMK-1 (Troemel et al. 2006, Pujol et al. 2008, Ziegler et al. 2009, Shivers et al. 2010, Ermolaeva and Schumacher 2014, Cheesman et al. 2016, Foster et al. 2020, Wu et al. 2021). Dr. Kim's previous studies also show that *sek-1* is

required for PMK-1 phosphorylation, placing *pmk-1* downstream of *sek-1* (Kim et al. 2016). The fact that knocking out *pmk-1* has a significantly weaker effect on *sek-1* transcription than knockout of *sek-1* suggests that SEK-1 regulates its own transcription, at least in part, independently from *pmk-1*. In neuronal development and signaling, another p38 MAPK homologue, *pmk-2*, functions redundantly with *pmk-1* downstream of *sek-1* (Pagano et al. 2015). *pmk-2* is almost exclusively expressed in neurons and therefore doesn't function with *pmk-1* in cell autonomous innate immunity in the intestine or epidermis. As *nipi-3* and *cebp-1* expression is required in the neurons (and other tissues) to regulate animal development (Kim et al. 2016), it is possible that *pmk-2* is functioning redundantly with *pmk-1* in neurons and a *pmk-2(0) pmk-1(0)* double mutant would have the same phenotype as *sek-1(0).*

I also found that removing *mak-2* produced similar *Psek-1::GFP* levels as removing *tir-1, nsy-1*, or *sek-1* **(Figure 6A)**, suggesting that *mak-2* also provides positive feedback to *sek-1* transcription. Notably, removing *mak-2* has stronger effects than removal of *pmk-1*. This was also unexpected since knockout of *mak-2* should phenocopy knockout of *pmk-1*, based on models of MAPK signaling (Gaestel 2006). That is, in other systems, MAPK activated protein kinases (i.e. MAK-2) are downstream of p38 MAPK kinases (i.e. PMK-1) (Roux and Blenis 2004). In *C. elegans,* this has been demonstrated that *mak-2* functions downstream of *pmk-3*/p38 MAPK in axon regeneration, synapse formation, muscle extension, cell fate patterning, and lifespan extension after mitochondrial disruption (Yan et al. 2009, D'Souza et al. 2016, Munkacsy et al. 2016, Shin et al. 2018). My data suggests that MAK-2 activity in this

pathway is regulated, at least in part, through signaling that does not depend on *pmk-1*. These findings suggest that the MAPK signaling participating in *C. elegans* development is not the linear pathway previously described, but rather a network containing numerous unexpected positive feedback loops with SEK-1 playing a central role **(Figure 7)**.

mak-2*/MAPKAPK regulates transcription of *sek-1*/MAP2K in *nipi-3* development pathway, independently of *cebp-1

Although MAP Kinase activated protein kinases (MAPKAPKs) are generally known to act downstream of p38 MAPK (PMK-1, PMK-2, and PMK-3 in *C. elegans)*, my *Psek-1::GFP* data described above suggest that this simple linear signaling is not the case in *nipi-3* dependent development. Previous studies by Dr. Kim with *nipi-3(0)* animals support this view as knocking out *mak-2* reduces the level of phosphorylated PMK-1 (Kim et al. 2016), suggesting MAK-2 acts at least in part upstream of PMK-1 or as part of a feedback loop regulating SEK-1 activity . Since I found that *mak-2* appears to promote *sek-1* transcription, I tested if *mak-2* acts in parallel with *nsy-1* or *pmk-1.* I found that neither *nsy-1(0); mak-2(0); nipi-3(0)* nor *pmk-1(0); mak-2(0); nipi-3(0)* have significantly different *Psek-1::GFP* from the levels in *mak-2(0); nipi-3(0)* **(Figure 6B)** suggesting that these genes are not functioning in parallel in this pathway. If they were functioning in parallel, I would expect to see an additive effect on *Psek-1::GFP* expression, where the double mutant (i.e. *nsy-1(0); mak-2(0); nipi-3(0)* or *pmk-1(0);*

mak-2(0); nipi-3(0)) has a statistically significantly different expression than either of the respective single mutants (*nsy-1(0); nipi-3(0)*, *pmk-1(0); nipi-3(0)*, or *mak-2(0); nipi-3(0)*).

I also tested if *mak-2* or *nsy-1* act in parallel with *cebp-1,* by producing triple mutants of *mak-2(0); cebp-1(0) nipi-3(0)* and *nsy-1(0); cebp-1(0) nipi-3(0)* and quantifying *Psek-1::GFP*. I did find a statistical (albeit small) difference between *Psek-1::GFP* expression in *mak-2(0); cebp-1(0) nipi-3(0)* and *cebp-1(0) nipi-3(0)* animals **(Figure 6C)** suggesting *mak-2* can have effects on *sek-1* transcription independent of *cebp-1*. In contrast, removing *nsy-1* and *cebp-1* did not show an additive effect **(Figure 6C)**, suggesting that *nsy-1* does not have effects on *sek-1* transcription independent of *cebp-1*. Of note, removing *cebp-1* almost completely blocks the effect of *nipi-3(0)* on *Psek-1::GFP* expression, which could limit meaningful results from these types of experiments. That is, in *nipi-3(0)* animals, *cebp-1(0)* may have a maximal effect on reducing *Psek-1::GFP.* Therefore, in *cebp-1(0) nipi-3(0)* background, removing an additional gene acting in parallel to CEBP-1 may only produce small and possibly undetectable effects on *Psek-1::GFP* expression.

I next tested if *mak-2* regulates the expression of CEBP-1 in the context of *nipi-3(0).* We reasoned this might be the case because in motor and touch neurons, MAK-2 acts upstream of CEBP-1*,* increasing CEBP-1 expression by binding to the *cebp-1* 3'UTR and thereby stabilizing its mRNA (Yan et al. 2009). Using a strain expressing the translational reporter of *cebp-1* (*wgIs563)* (Sarov et al. 2006), I tested the effect of loss of *mak-2* on CEBP-1 expression. As previously described, the expression of *wgIs563* is seen within nuclei throughout the body in all tissues. *nipi-3(0)* animals have very high

levels of the CEBP-1 reporter in all tissues. *mak-2(0); nipi-3(0)* animals also have very high expression of CEBP-1::GFP, comparable to *nipi-3(0)* **(Figure 8A, B, C)**. Thus, *mak-2* is not required for the upregulation of CEBP-1 in *nipi-3(0)* animals.

Next, I examined if MAK-2 is regulated by *cebp-1* in the context of *nipi-3(0)*. To test this, I took advantage of the fact that the localization of MAPK activated protein kinases (i.e. MAK-2) is controlled by their phosphorylation state. In mammalian systems, when phosphorylated and active, the protein localizes to the cytoplasm and when unphosphorylated and inactive, it is sequestered in the nucleus (Gurgis et al. 2014). Indeed, such regulation of localization has been shown in *C. elegans* neurons using transgenic constructs overexpressing phospho-mimetic or phospho-dead variants of MAK-2 driven by a neuronal specific promoter (Yan et al. 2009). To visualize MAK-2 localization, I produced a strain in which the endogenous MAK-2 protein was tagged with GFP using standard knock in methods (Methods) (Dickinson et al. 2015). I observed expression of GFP::MAK-2 in multiple tissues including epidermis, muscle, intestine, and neuronal cells **(Figure 8D)**. High levels of CEBP-1 in *nipi-3(0)* animals, did not cause any obvious changes in GFP::MAK-2 abundance or localization **(Figure 8E)**, suggesting that MAK-2 activity is not, as is the case in homologous systems, downstream of PMK-1 (p38 MAPK). This result is in striking contrast to the effect of high levels of CEBP-1 on *sek-1* transcription **(Figure 6C)**. Thus, if *mak-2* were downstream of *sek-1* via *pmk-1*, upregulating CEBP-1 should have produced a strong effect on MAK-2 activity. This raises the possibility that MAK-2 is not a downstream output of NSY-1/SEK-1/PMK-1 signaling, suggesting a role for a MAPKAPK (MAK-2) acting

differently from canonically upstream MAPK signaling. Together, these data suggest that MAK-2 regulates the transcription of *sek-1* in response to *nipi-3(0)* in a pathway that does not include CEBP-1.

A gain-of-function mutation in HDAC *hda-4* suppresses *nipi-3(0)*

In the previously reported screen to identify mutations that suppress *nipi-3(0)* lethality, Dr. Kim isolated *ju1371* and has since identified that it contains a missense mutation in the histone deacetylase (HDAC) *hda-4* (Methods). *hda-4* has the highest homology to human class IIa HDACs, HDAC4 and HDAC7. HDACs are enzymatic proteins that are most highly studied in their role in chromatin regulation, removing acetyl groups from histones, producing a closed chromatin state where transcription is less active (Porter and Christianson 2019). HDACs also have non-enzymatic functions as transcriptional regulators via direct binding to transcription factors, corepressors, and protein-modifying enzymes (Haberland et al. 2009, Seo et al. 2009). Of the four classes of mammalian HDACs, IIa HDACs are unique because they have extremely low deacetylase activity in biochemical assays due to a variation in a highly conserved motif in the deacetylase catalytic domain (Fischle et al. 2002). The LEGGY catalytic motif, present in zinc dependent active deacetylate domains HDACs, is replaced by a LEGGH motif in mammalian class IIa HDACs. The tyrosine of the LEGGY motif is necessary and sufficient to produce deacetylase activity (Lahm et al. 2007).

ju1371 changes a conserved glycine into an aspartic acid (G606D) within the HDAC domain of HDA-4 **(Figure 9A)**. This residue change is just two amino acids away

from the zinc binding site and structurally adjacent to the catalytic LEGGY motif within the HDAC domain, suggesting this mutation may affect the enzymatic function of the protein. Although the closest human homologues of HDA-4 are class IIa HDAC7 (70% similar HDAC domain) and HDAC4 (65% similar HDAC domain), HDA-4 contains the active catalytic motif (LEGGY) unlike HDAC7/4 which contain both the inactive motif (LEGGH). This suggests that HDA-4 may be an active deacetylase, but biochemical studies must be performed with this *C. elegans* protein to experimentally determine its catalytic activity.

Overexpression of wildtype HDA-4, with the *oyIs73* transgene (van der Linden et al. 2007), reverses the suppression phenotype of *ju1371* **(Figure 9B)**. In order to address whether *hda-4(ju1371)* is a gain or loss of function allele, Dr. Kim produced a deletion mutant *hda-4(ju1403)* by CRISPR/Cas9 which removes most of the coding region of *hda-4* and is referred to as *hda-4(0)* hereafter **(**Methods, **Figure 9A)**. I observed that both *hda-4(ju1371)* and *hda-4(0)* showed WT-like development, although *hda-4(0)* animals were noticeably thin **(Figure 9C, D)**. Dr. Zhu, another post-doctoral fellow in the Jin Lab, constructed the *nipi-3(0) hda-4(0)* double mutant and observed that this strain is larval lethal, resembling *nipi-3(0)* **(Figure 9E)**, indicating that *hda-4(ju1371)* does not behave as a null allele. Furthermore, *hda-4(ju1371/+)* is able to partially suppress *nipi-3(0)* lethality **(Figure 9F)**. *nipi-3(0) hda-4(ju1371/+)* animals are able to reach adulthood **(Figure 9G)**, but are sterile, indicating *hda-4(ju1371)* dosage is relevant in rescue of larval arrest of *nipi-3(0)*. On the other hand, one copy of *hda-4(ju1371)* is not able to suppress *nipi-3(0)* in the absence of wildtype *hda-4* as *hda-*

4(ju1371/0) animals arrest in early larval stage **(Figure 9H)**, much like *hda-4(0)*. Thus, we conclude that *ju1371* is a semi-dominant gain of function allele.

To further investigate the mechanism of *hda-4(ju1371)* suppression of *nipi-3(0)* larval lethality, we wanted to determine if this phenotype requires the transcription factor *mef-2*. In mammalian systems, HDACs and MEF2 form a protein complex that binds to DNA and represses transcription of MEF2 targets (Miska et al. 1999, Wang et al. 1999, Lu et al. 2000). The HDAC and MEF2 interaction is conserved in C. elegans, where HDA-4 and MEF-2 form a phosphorylation-dependent complex that can bind to DNA and inhibit the transcription of targeted genes (van der Linden et al. 2007, van der Linden et al. 2008). In C. elegans, MEF-2 and HDA-4 cooperate to regulate lifespan, lethargus (a sleep-like state), and dauer (a stress-induced developmental stage) entry (van der Linden et al. 2008, Grubbs et al. 2020, Nikooei et al. 2020). Dr. Zhu found that *mef-2(0)* does not suppress *nipi-3(0)* lethality **(Figure 9H)**, but interestingly mef-*2(0); nipi-3(0) hda-4(ju1371)* mutants arrest in larval stage **(Figure 9I)**, indicating that *hda-4(ju1371)* requires *mef-2* to suppress *nipi-3(0).* This suggests that *hda-4* may act through its role as a transcriptional repressor with *mef-2*.

We next asked if the suppression of *nipi-3(0)* by *hda-4(ju1371)* involves regulation of the p38 MAPK pathway. I found that the upregulation of *Psek-1::GFP* expression in *nipi-3(0)* background was dramatically reduced by *hda-4(ju1371),* but not *hda-4(0)* **(Figure 9J)**. Thus, *hda-4(ju1371),* but not *hda-4(0),* reduces the transcription of *sek-1* in response to *nipi-3(0)*. I next tested if *hda-4(ju1371)* regulates the expression of CEBP-1. I found that the upregulation of CEBP-1 in response to *nipi-3(0)* is not

blocked by *hda-4(ju1371)* **(Figure 9K, L, M)**. These results suggest that *hda-4(ju1371)* likely functions through the PMK-1/p38 MAPK pathway by a mechanism independent of CEBP-1 expression level to regulate *nipi-3* dependent development.

The HDA-4/MEF-2 repressor complex has been previously described to regulate lifespan, chemoreceptor expression, and transition to dauer stage in *C. elegans* (van der Linden et al. 2007, van der Linden et al. 2008). We find that both *hda-4(ju1371)* and *mef-2* are required for suppression of *nipi-3(0)* developmental arrest. We also find a dose-dependent rescue where one copy of WT *hda-4* and one copy of *hda-4(ju1371)* is able to partially rescue *nipi-3(0)*. One possibility is that the gain of function mutation in *hda-4*, *ju1371*, may increase the repressive activity of the HDA-4/MEF-2 protein complex. In mammalian systems, the binding between MEF2 and HDAC4 is independent of the histone deacetylase domain (Miska et al. 1999). Since *ju1371* is a mutation in the histone deacetylase domain, it seems unlikely this mutation would affect the interaction with MEF-2 (Aude-Garcia et al. 2010, Mathias et al. 2015). If this were the case, the transcriptional targets of the HDA-4/MEF-2 protein complex could provide insight into understanding this phenotype and a ChIP-seq experiment may provide this information. It is possible the HDA-4/MEF-2 complex binds to the promoter of *sek-1* to repress its expression, although we cannot rule out the possibility that the regulation of *sek-1* transcription is indirect.

Another possibility is that HDA-4 normally has a dual function in the nucleus, both as an active deacetylase and through direct transcriptional regulation by binding with MEF-2. In this case, the *ju1371* mutation may inhibit the deacetylase activity, but

leave the function of the HDA-4/MEF-2 protein complex intact. While it would be interesting to further test this idea using an engineered HDA-4 (LEGGY->LEGGH) mutant, technical limitations prevented this experiment. Thus, at this time we are unable to determine the mechanism by which *ju1371* changes the activity of HDA-4. Here, we report that HDA-4, the homolog of human HDAC4/7 (class IIa HDAC), genetically interacts with *mef-2* and *nipi-3* to regulate development in *C. elegans* through a highly conserved PMK-1/p38 MAPK pathway. Thus, we have found a new link between MEF-2/HDA-4 gene regulation and the PMK-1/p38 MAPK pathway. Considering that numerous previous genetic screens for regulators of the PMK-1/p38 MAPK pathway haven't identified this genetic interaction, our findings indicate that there is still value in designing different forward genetic screens to find novel regulators of highly studied pathways.

N-terminal acetyltransferase C complex mediates *nipi-3(0)* induced lethality partially via the *pmk-1*/p38 MAPK pathway

In our previously reported *nipi-3(0)* suppressor screen (Kim et al. 2016), Dr. Kim also isolated *ju1369* and has since identified that it contains a missense mutation in *natc-2* (Methods). *natc-2* encodes a homolog of human Naa30, the catalytic subunit of the N-terminal acetyltransferase C (NatC) complex. Homologues of Naa30 are defined by a N-acetyltransferase domain that is 76% similar and 62% identical between the *C. elegans* (*natc-2*) and human homologues. Protein N-terminal acetylation is one of the most common protein modifications, occurring on more than 80% of mammalian

proteins (Arnesen et al. 2009). This protein modification can regulate the subcellular localization, structure, and stability of the target protein (Jornvall 1975, Brown 1979, Persson et al. 1985, Murthi and Hopper 2005, Hwang et al. 2010, Forte et al. 2011, Scott et al. 2011, Holmes et al. 2014).

ju1369 changes glycine 150 to glutamic acid **(Figure 10A)** in the N-acetyltransferase domain. Based on the crystal structure model of Naa30, this SNP (G150E in *C. elegans* NATC-2 / G266E in hNaa30) is adjacent to the acetyl-CoA binding pocket of the protein **(Figure 11)** suggesting this mutation may affect the enzymatic activity of the protein. To determine if *natc-2(ju1369)* is a loss of function mutation, I generated an independent deletion allele (*ju1866)* in *natc-2* using CRISPR/Cas9 which deletes a large portion of the coding region of *natc-2* and will referred to as *natc-2(0)* hereafter **(**Methods, **Figure 10A**). *natc-2(ju1866); nipi-3(0)* animals were viable and fertile indicating that *natc-2(0)* suppresses *nipi-3(0)* lethality and that *ju1369* is likely a loss of function mutation **(Figure 10D)**. I found that the missense mutation *natc-2(ju1369)* rescues body length significantly better than of *natc-2(0)* **(Figure 10D)**. This may be because in animals containing *ju1369*, the NatC complex likely forms, but is not functional. Whereas when one of the proteins in the complex is not produced, the NatC complex likely doesn't form, possibly signaling compensatory N' acetylation by other Nat complexes (Gao et al. 2016).

The N-terminal acetyltransferase protein complex has at least two proteins: one that binds to the ribosome and one that binds to acetyl-CoA and catalyzes the transfer of the acetyl group to the substrate protein. In mammalian NatA, NatC, and NatE, there

is also an auxiliary subunit, and the function of these auxiliary proteins is less well understood (Aksnes et al. 2019). The mammalian NatC complex is comprised of Naa30, the catalytic subunit, Naa35, the anchoring subunit, and Naa38, the auxiliary subunit (Aksnes et al. 2016). The *C. elegans* orthologues of Naa30 and Naa35 are NATC-2 and NATC-1, respectively. I found that like *natc-2(0),* two independent deletion alleles of *natc-1, am138* (Bruinsma et al. 2008) and *ok2062* (Consortium 2012) show suppression of *nipi-3(0)* lethality **(Figure 10B, D, Figure 20)**. Furthermore, I created *natc-2(0) natc-1(0)* double mutants using CRISPR/Cas9 (Methods). I produced *natc-2(ju1797) natc-1(am138); nipi-3(0)* and found that these double mutants do not show enhanced suppression over each of the single mutants **(Figure 20)** suggesting that these proteins function together in their role as a protein complex. Based on sequence homology, we suspected that Y48G1C.9 encodes the third subunit (Naa38) of NatC **(Figure 12)**. To begin testing this, Dr. Zhu produced a deletion allele using CRISPR/Cas9 **(**Methods, **Figure 10C)** and generated *natc-3(ju1837); nipi-3(0)*, which was viable and fertile **(Figure 10D)**. This suggests that this protein is likely functioning as a necessary component in a protein complex with NATC-1 and NATC-2. We therefore rename this gene *natc-3* based on sequence homology to Naa38 and phenotype in *nipi-3(0)* mediated development.

Next, we asked if *natc-1*, *natc-2,* and *natc-3* function through the PMK-1/p38 MAPK pathway to regulate *nipi-3* developmental arrest using *Psek-1::GFP* as a functional readout. I found that in *natc-1(0); nipi-3(0), natc-2(0) natc-1(0); nipi-3(0),* and *natc-3(0); nipi-3(0)* animals, the expression level of *Psek-1::GFP* was reduced in

comparison to *nipi-3(0)*, but still significantly higher than that seen in *sek-1(0) nipi-3(0)* animals **(Figure 10E, 18)**. This suggests that the NatC complex has a minor contribution to the transcription of *sek-1.* Furthermore, I produced *natc-3(0); pmk-1(0); nipi-3(0)* and found that almost all (96%) of animals contained eggs after 3 days of development (Methods). This is in stark contrast to the developmental delay seen in *natc-3(0); nipi-3(0)* (0% with eggs) and *pmk-1(0); nipi-3(0)* (53% with eggs) **(Figure 10G)**. Taken together, these results suggest that the *C. elegans* NatC complex acts partially through the PMK-1/p38 MAPK pathway and partially parallel to the PMK-1/p38 MAPK pathway in *nipi-3* dependent development.

We considered that NIPI-3 may repress expression of NATC-1/2 during development. To test this, Dr. Zhu and I generated N-terminal GFP knock-in alleles *ju1801* and *ju1803* for *natc-1* and *natc-2*, respectively (Methods). Endogenous NATC-1 is broadly expressed in intestine, hypodermis, and gonad, and localized in cytoplasm **(Figure 13A-F)**. Endogenous NATC-2 has the same expression pattern as NATC-1 **(Figure 13G-L)**. The endogenous expression pattern of NATC-1 is consistent with a transgene overexpressing GFP tagged *natc-1* genomic sequence (Warnhoff et al. 2014). To test if NIPI-3 regulates the expression of NATC-1 and NATC-2, Dr. Zhu produced double mutants of *nipi-3(0)* and *natc-1(ju1801)* or *natc-2(ju1803)*. These animals remain arrested as larvae, indicating *ju1801* and *ju1803* do not disrupt the function of either gene. Dr. Zhu found that the endogenous expression of NATC-1 and NATC-2 is unchanged in *nipi-3(0)* animals in comparison to wildtype background **(Figure 14A, B)**.

In *C. elegans*, homologues of NatA, NatB, and NatC have been identified to play a role in the regulation of animal development and stress tolerance (Warnhoff and Kornfeld 2015). Specifically, both NatA and NatC regulate *C. elegans* entry into the stress-resistant dauer developmental stage (Warnhoff and Kornfeld 2015). Under conditions of starvation or other stressful conditions, *C. elegans* temporarily enter the dauer stage that allows them to be more likely to survive the stressful conditions. When food is again readily available, the dauer animals return to the normal developmental cycle and become fertile adults (Riddle and Albert 1997). Mutations within NatA cause the animals to develop into an abnormal “dauer-like” stage, where they exhibit some characteristics of dauer animals, but are unable to exit this stage and reach adulthood. Even under well-fed conditions, these animals enter an abnormal “dauer-like” stage and die during larval development (Chen et al. 2014). Mutations within NatC on their own do not confer phenotypic abnormalities in dauer formation, but these mutations greatly enhance the abnormal entry of *daf-2(0)* animals into dauer stage (Warnhoff et al. 2014). *daf-2(0)* animals will become dauer even in the presence of food, in a temperature sensitive manner (Malone and Thomas 1994). Double mutants of *natc-2(0); daf-2(0)* transition to dauer stage at a significantly lower temperature than *daf-2(0)* single mutants. Additionally, NatC negatively regulates cellular stress responses to oxidative stress, heat shock, and heavy metal toxicity. NatB is essential for proper pairing of chromatin during meiosis, allowing for the development of viable embryos (Gao et al. 2015, Gao et al. 2016). Thus, N-terminal acetylation modulates growth, development,

stress tolerance, and entry into stress resistant developmental stages in *C. elegans* (Warnhoff and Kornfeld 2015).

As N-terminal acetylation can have such a variety of effects on protein function, from regulating proteins stability, to protein complex formation, to subcellular localization, it is difficult to theorize how the NatC complex is contributing to the larval arrest caused by *nipi-3(0)*. Additionally, the NatC complex targets hundreds of individual proteins for modification, so it is likely modification of many different proteins that contribute to the *nipi-3(0)* phenotype.

Caveats of the study

I have not yet identified the mechanistic link between NIPI-3 and regulation of the transcription of *cebp-1*. Both *mak-2* and *hda-4(ju1371)* regulate the transcription of *sek-1*, likely through the regulation of CEBP-1 activity, as neither change the expression of CEBP-1. In mammalian systems, the regulation of C/EBP activity occurs primarily at the post-translational level, either through post-translational modifications or binding with different transcription factors. Therefore, it is unsurprising that I found these proteins regulate the activity of CEBP-1, but not the expression of CEBP-1. It is also possible that *mak-2* and/or *hda-4(ju1371)* regulate the activity of SEK-1, as I found that SEK-1 activity is possibly required for the increase in *sek-1* transcription in response to *nipi-3(0)*. To more directly test the effect of SEK-1 activity on *sek-1* transcription, it would be best to observe *sek-1* transcription in a *sek-1* mutant that encodes a kinase dead version of SEK-1.

Another caveat is the quantification of the *sek-1* transcriptional reporter may not be representative of the actual *sek-1* mRNA levels. For instance, any post transcriptional regulation of *sek-1* mRNA would not be represented by changes in *Psek-1::GFP.* mRNA stability can be regulated via intronic regions of the gene or by the 3' UTR (Pagano et al. 2015, Mishra and Thakran 2018), neither of which are present in *Psek-1::GFP.* There is also always the possibility of transgene silencing when working with multi-copy arrays. qRT-PCR is a way to directly measure mRNA levels and smFISH would allow for interrogation of tissue specific mRNA expression.

Although this study examined the role of p38 MAPK in larval development, it would be interesting to test whether or not these same feedback loops that I identified are present in the PMK-1 pathway in other processes such as infection response.

As I have found multiple positive feedback loops to the transcription of *sek-1*, there likely negative regulation present to balance this. Recent studies have found that in the context of innate immune signaling in the intestine, CEBP-1 promotes the transcription of *vhp-1*, a phosphatase that dephosphorylates and deactivates PMK-1. I have not tested if *vhp-1* is involved in regulating development. It would be interesting to measure *vhp-1* mRNA levels in *nipi-3(0)* and *cebp-1(0) nipi-3(0)* animals during development.

Conclusion

p38 MAPK signaling is essential for a multitude of cellular processes across many forms of life. Although decades of studies have revealed much about these signaling pathways, the intricacies of feedback regulation within the pathway are poorly understood. Here, we used a genetically sensitized background that simulates overactive p38 MAPK signaling to identify novel regulators of this pathway in *C. elegans* development. From a forward genetic screen, we identified novel genetic interactions between histone deacetylase *hda-4*, N-terminal acetyltransferase C complex *natc-1/2/3*, and regulation of animal development downstream of NIPI-3/Tribbles and CEBP-1. Additionally, we identified the gene encoding the third subunit of the N-terminal acetyltransferase C complex in *C. elegans* using the phenotype of this sensitized background. Many forward genetic screens have been performed to identify genes required for innate immune response in *C. elegans* using bacterial, viral, and fungal infections as well as xenobiotic activators of the innate immune system (Pujol et al. 2008, Fuhrman et al. 2009, Ziegler et al. 2009, Pukkila-Worley et al. 2012, Iatsenko et al. 2013, De Arras et al. 2014, Sinha and Rae 2014, Cheesman et al. 2016, Zugasti et al. 2016, Tanguy et al. 2017), but none have identified HDA-4 or NATC-1/2/3 as regulators of the PMK-1/p38 MAPK pathway. Thus, using this unique sensitized background, we were able to identify previously unknown regulation of a highly studied p38 MAPK pathway.

nipi-3(0) produces extremely high levels of the transcription factor CEBP-1, which binds a conserved DNA motif in many genes regulating development and stress

response in *C. elegans* (Kim et al. 2016). The overexpression of CEBP-1 leads to developmental arrest, likely as an effect of the upregulation of genes downstream of CEBP-1 such as *sek-1.* Since *sek-1(0)* prevents the larval arrest of *nipi-3(0)* animals, *sek-1* expression is likely essential to the developmental arrest of the animals. Therefore, we produced a transcriptional reporter of *sek-1,* which allowed us to identify novel feedback regulation from *pmk-1* and *mak-2*. Although these genes (*tir-1, nsy-1, sek-1, pmk-1*) have been studied extensively in their role in innate immunity, to my knowledge, no previous studies have identified feedback regulation from *pmk-1* or *mak-2* to *sek-1* transcription. Many screens are designed to evaluate the transcriptional output of this complex signaling pathway and therefore are not able to identify complexities of regulation within the pathway. We were able to identify feedback by virtue of a reporter of activity within the p38 pathway. Similarly, Wu et al was able to identify feedback by interrogating expression of members within the PMK-1 signaling pathway in response to intestinal infection (Wu et al. 2021). We have found these regulatory feedback loops to be so interconnected that it will be challenging to design experiments to further dissect this pathway. Indeed, it is inherently challenging to resolve feedback loops within signaling pathway (Harris and Levine 2005).

Acknowledgements

I thank my lab members for valuable discussions and Hetty Zhang for assistance in strain construction. I thank Dr. S Mitani and National Bioresource Project of Japan, and the *Caenorhabditis* Genetics Center (funded by NIH Office of Research Infrastructure Programs P40 OD010440) for strains. This work was supported by National Research Foundation of Korea (NRF-2019R1A2C1003329) to KWK, Hallym University Research Fund (HRF-201809-014) to KWK, and National Institutes of Health (5F31GM131677-03) to RAM.

Chapter 3 describes the work of the dissertation author in collaboration with Drs. Zhu and Kim, former postdoctoral researchers in the laboratory of Professor Jin. The dissertation author was the primary investigator and wrote the chapter in full.

Figures

Figure 5. Transcriptional reporter of *sek-1* is a functional readout of CEBP-1 activity in the NIPI-3 dependent signaling network

(A) Illustration of the promoter and coding region of *sek-1.* The promoter region includes two identified CEBP-1 binding motifs (red triangles in illustration and red letters in sequence) Exons are purple boxes, introns are angled black lines connecting exons, and the 5'UTR is the black horizontal line. **(B)** Single plane confocal image of GFP expression driven by 4870bp upstream sequence of *sek-1* as a multi-copy integrated reporter (*juIs559)* in L4 stage animal. Scale bar 100µm. **(C)** Single plane confocal image of GFP expression driven by 4870bp upstream sequence of *sek-1,* with two identified CEBP-1 binding motifs deleted, called *Psek-1(del)::GFP*, as a multi-copy extrachromosomal array (*juEx7617)* in L4 stage animal. Expression pattern is not altered by the deletion of the two CEBP-1 binding sites. Scale bar 100 µm. **(D-F)** Single plane confocal images of *Psek-1::GFP* in wildtype (WT), *nipi-3(0)* and *cebp-1(0) nipi-3(0)* backgrounds. Scale bars 50 µm. **(D)** Expression level is low in WT animals. **(E)** Expression level is upregulated >40x by knockout of *nipi-3.* **(F)** CEBP-1 is required for upregulation of *Psek-1::GFP* in response to knockout of *nipi-3*. **(D'-E')** Single plane confocal images of *Psek-1(del)::GFP* in wildtype (WT) and *nipi-3(0)* backgrounds. Scale bars 50 µm. **(D')** Expression level is low in WT animals. **(E')** Expression level is unchanged by knockout of *nipi-3.* **(G)** Quantification of *Psek-1::GFP* expression in animals 36 hours post egg laid. In wildtype background, *cebp-1(0)* does not have an effect on *Psek-1::GFP* expression. Knockout of *nipi-3* substantially increases *Psek-1::GFP* expression, which is rescued by knockout of *cebp-1.* Each dot represents a single animal, each red line represents the mean value. Statistics: See Methods. *ns* not significant, ****P* < 0.001. **(H)** Single plane confocal image of *juIs559* in the head of a L4 stage animal. ROI used for quantification in **(G)** is marked with white dashed circle (see Methods for details). Scale bar 20µm. Dr. Kim made panel **(A)** Dr. Zhu collected images in **(D-F, D'-E')**.

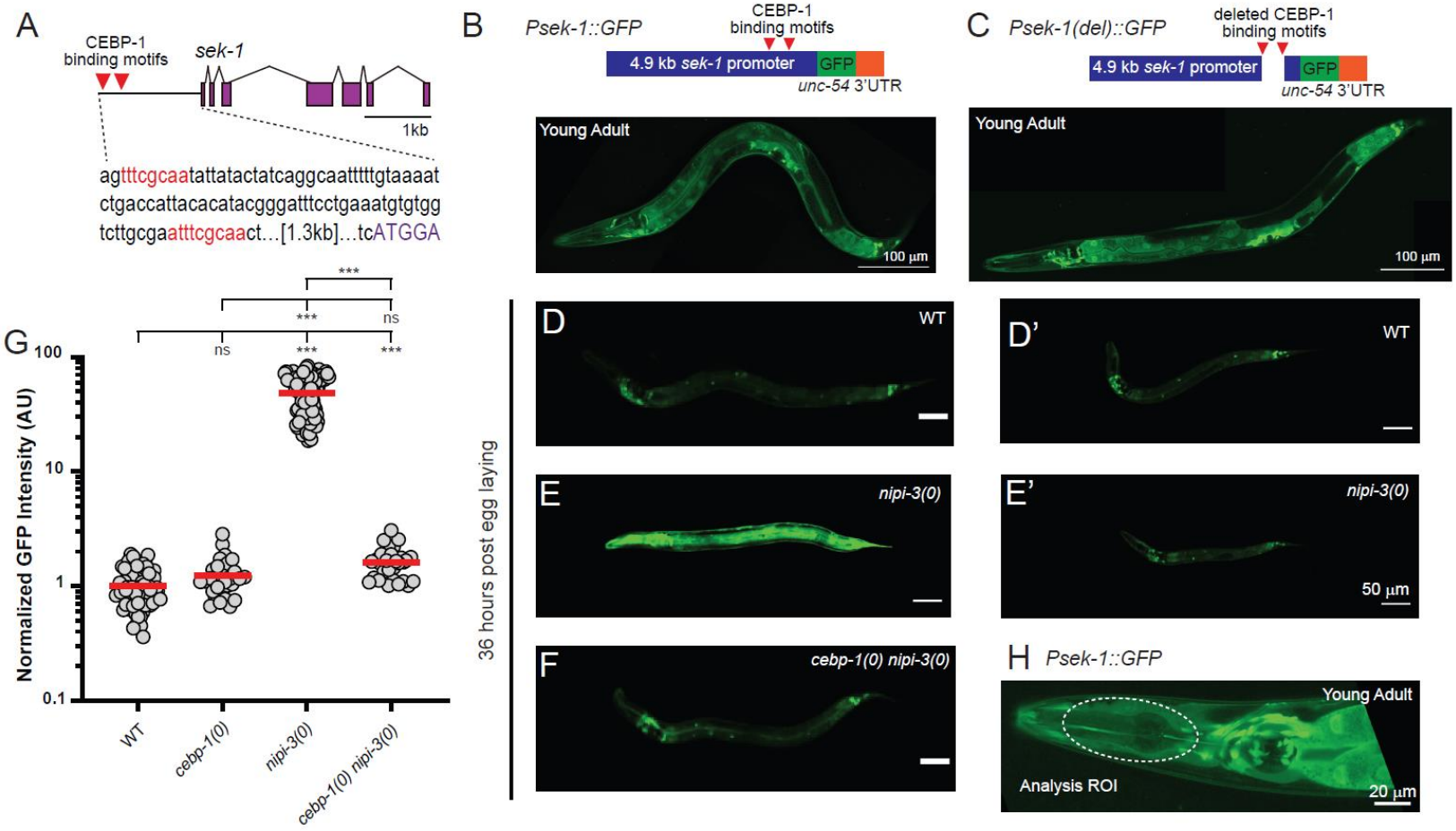
A
CEBP-1 binding motifs
sek-1
1kb
agtttcgcaatattatactatcaggcaatttttgtaaaat
ctgaccattacacatacgggatttcctgaaatgtgtgg
tcttgcgaatttcgcaact...[1.3kb]...tcATGGA
B
Psek-1::GFP
CEBP-1 binding motifs
4.9 kb sek-1 promoter
GFP
unc-54 3'UTR
Young Adult
100 µm
C
Psek-1(del)::GFP
deleted CEBP-1 binding motifs
4.9 kb sek-1 promoter
GFP
unc-54 3'UTR
Young Adult
100 µm
36 hours post egg laying
D
WT
D'
WT
E
nipi-3(0)
E'
nipi-3(0)
50 µm
F
cebp-1(0) nipi-3(0)
G
Normalized GFP Intensity (AU)
100
10
1
0.1
***
***
ns
ns
***
***
WT
cebp-1(0)
nipi-3(0)
cebp-1(0) nipi-3(0)
H
Psek-1::GFP
Young Adult
Analysis ROI
20 µm

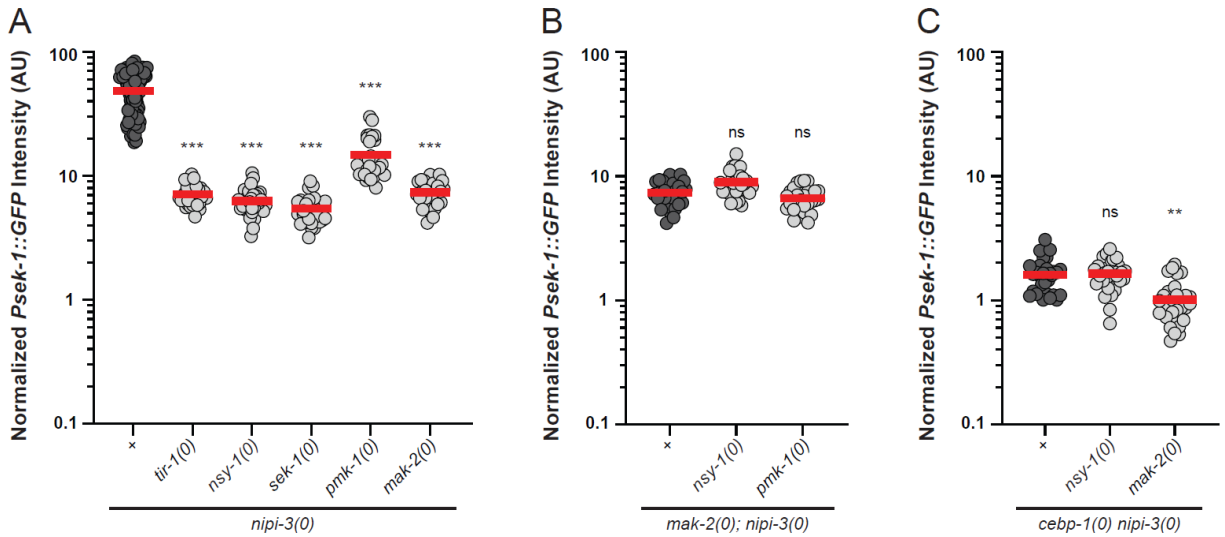

Figure 6. Transcriptional reporter of *sek-1* suggests *pmk-1*/p38 MAPK and *mak-2*/MAPKAPK cause feedback regulation of transcription of *sek-1*

(A-C) Quantification of *Psek-1::GFP* expression in animals 36 hours post egg laid. Each dot represents a single animal; each red line represents the mean value. Some data are replicated from Figure 5 shown in darker grey dots. Null alleles in this figure are *nipi-3(ju1293)*, *cebp-1(tm2807), tir-1(qd4), nsy-1(ok593), sek-1(km4), pmk-1(km25),* and *mak-2(ok2394)*. Statistics: One-Way ANOVA with Tukey's post hoc test, see Methods. *ns* not significant, ***P*<0.01, ****P*<0.001. For more statistical comparisons, see **Table 10**. For additional data examining *Psek-1::GFP* in other genetic backgrounds see **Figures 18** and **19. (A)** Knockout of *nipi-3* substantially increases *Psek-1::GFP* expression, which is significantly reduced by null mutations to any member of this MAPK pathway. *pmk-1(0)* is significantly weaker at suppressing *Psek-1::GFP* expression in comparison to all other knockouts. *Psek-1::GFP* expression in *mak-2(0); nipi-3(0)* is not significantly different than *nsy-1(0), tir-1(0),* or *sek-1(0)* with *nipi-3(0),* indicating that it is likely not downstream of *pmk-1* in this pathway regulating *sek-1* expression. Significance in graph is in comparison to *nipi-3(0)*. **(B)** Compound mutants of *mak-2(0); nipi-3(0)* with *nsy-1(0)* or *pmk-1(0)* do not confer greater *Psek-1::GFP* suppression than each of the single mutants. Significance is in comparison to *mak-2(0); nipi-3(0)*. **(C)** Compound mutants of *cebp-1(0) nipi-3(0)* with *nsy-1(0)* or *mak-2(0)* do not confer greater *Psek-1::GFP* suppression than each of the single mutants. Significance is in comparison to *cebp-1(0) nipi-3(0).*

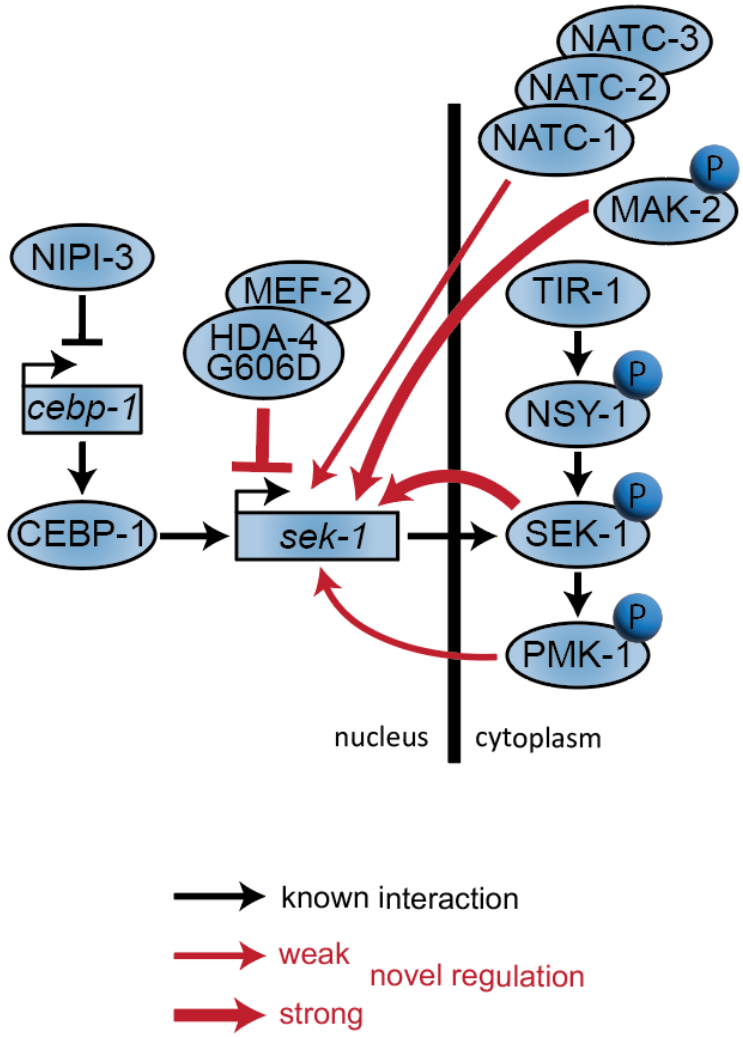

Figure 7. Model of signaling downstream of NIPI-3/Tribbles

The regulation of transcription of *sek-1* has multiple inputs. See main text for details.

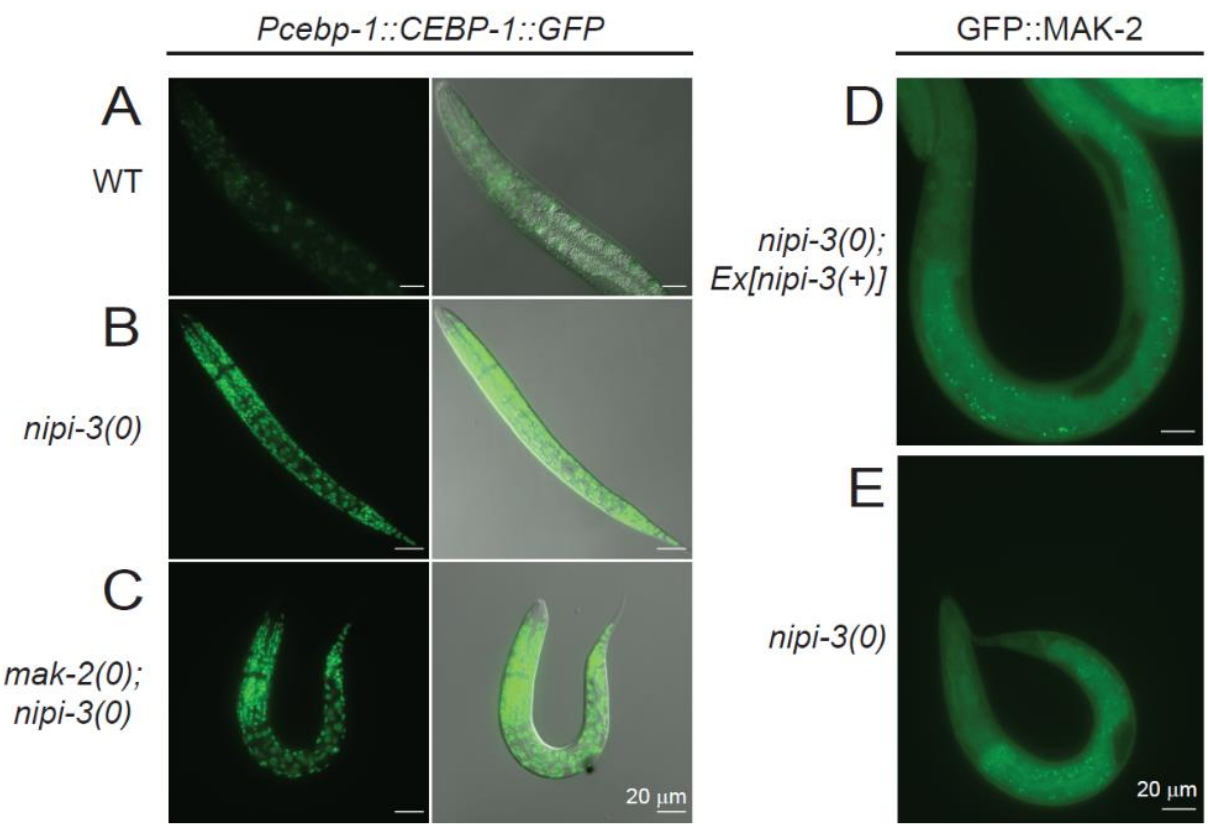

Figure 8. *mak-2* is not required for upregulation of CEBP-1 in response to *nipi-3(0)* and MAK-2 localization isn't changed by *nipi-3(0)*

(A-C) Fluorescent and DIC images of CEBP-1::GFP under the *cebp-1* promoter as a multicopy integrated reporter (*wgIs593*) in animals 24 hours post hatch. Scale bar = 20 µm. **(A)** CEBP-1::GFP is expressed at low levels in wildtype background **(B)** CEBP-1::GFP is highly upregulated in *nipi-3(ju1293)* **(C)** *mak-2(tm2927)* does not change CEBP-1::GFP expression. **(D-E)** Fluorescence images of MAK-2 translational reporter. GFP inserted into the endogenous locus of *mak-2* using standard CRISPR knock-in methods (*ju1851)* in animals 24 hours post hatch. Scale bar = 20 µm. **(D)** GFP is expressed throughout the animal but is noticeably absent from the gonad. **(E)** GFP expression is not changed by *nipi-3(ju1293)*.

Figure 9. A gain of function mutation in histone deacetylase HDA-4 suppresses *nipi-3(0)* larval lethality through PMK-1/p38 MAPK pathway

(A) Illustration of gene structure, missense allele, and deletion allele. Exons are purple boxes, introns are angled black lines connecting exons, and the UTRs are black horizonal lines. There is a 10,113 bp first intron that is not illustrated to scale. Protein motif is illustrated in green. Blue dots illustrate zinc binding sites. The blue bar within the HDAC domain illustrates the LEGGY motif. Deletion allele is indicated as red horizonal line showing the region of DNA that is deleted. *ju1403* is a 3064 bp deletion. The missense mutation is indicated as a red dot in the exon where the mutation exists, allele name and amino acid substitution are labeled above the red dot. Missense mutation *ju1371* was isolated in EMS screen for suppressors of *nipi-3(0)* larval arrest. **(B)** Quantification of body length of animals 3 days post egg laid. *nipi-3(0)* mutants have a short body length. This phenotype is rescued by *ju1371*. Overexpression of either HDA-4 or CEBP-1 can reverse the phenotype of *hda-4(ju1371).* Significance is in comparison to *nipi-3(0)*. Each dot represents a single animal, each red line represents the mean value. Statistics: One-Way ANOVA with Tukey's post hoc test. *ns* not significant, ****P*<0.001. For more details about statistics, see Methods. For more statistical comparisons, see **Table 13**. **(C-J)** Bright-field or DIC images of animals at 3 days post egg laid. Scale bar = 100 µm. **(C)** *hda-4(ju1371)* does not confer any gross developmental defects. **(D)** *hda-4(0)* animals are skinnier than wildtype but have no developmental delay. **(E)** Developmental arrest phenotype of *nipi-3(0)* is rescued by *hda-4(ju1371)*. **(F)** The developmental arrest phenotype of *nipi-3(0)* is not rescued by *hda-4(0)*. **(G)** Animal size, but not fertility is rescued by one copy of ju1371 and one copy of wild type *hda-4*. **(H)** *ju1371* suppression is not dominant to *hda-4* null **(I)** *mef-2(0)* does not suppress *nipi-3(0)* **(J)** *mef-2* is required for *ju1371* suppression of *nipi-3(0)*. **(K)** Quantification of *Psek-1::GFP* expression in animals 36 hours post egg laid. Knockout of *nipi-3* substantially increases *Psek-1::GFP* expression. Expression of *Psek-1::GFP* is significantly lower in rescued animals, *nipi-3(0) hda-4(ju1371),* in comparison to the animals that arrest during development, *nipi-3(0) hda-4(0).* Each dot represents a single animal, each red line represents the mean value. Some data are replicated from Figure 5, shown in darker grey dots. The statistics are in comparison to *nipi-3(0)*. Statistics: One-Way ANOVA with Tukey's post hoc test, see Methods. ****P*<0.001. For more statistical comparisons, see **Table 11**. **(L-N)** Fluorescent and DIC images of CEBP-1::GFP under the *cebp-1* promoter as a multicopy integrated reporter (*wgIs593*) in animals 24 hours post hatch. Scale bar = 20 µm. Images K and L are previously presented in Figure 8. **(L)** CEBP-1::GFP is expressed at low levels in wildtype background **(M)** CEBP-1::GFP is highly upregulated in *nipi-3(0)* **(N)** *hda-4(ju1371)* does not change CEBP-1::GFP expression. Dr. Zhu collected images in **(C-I)**.

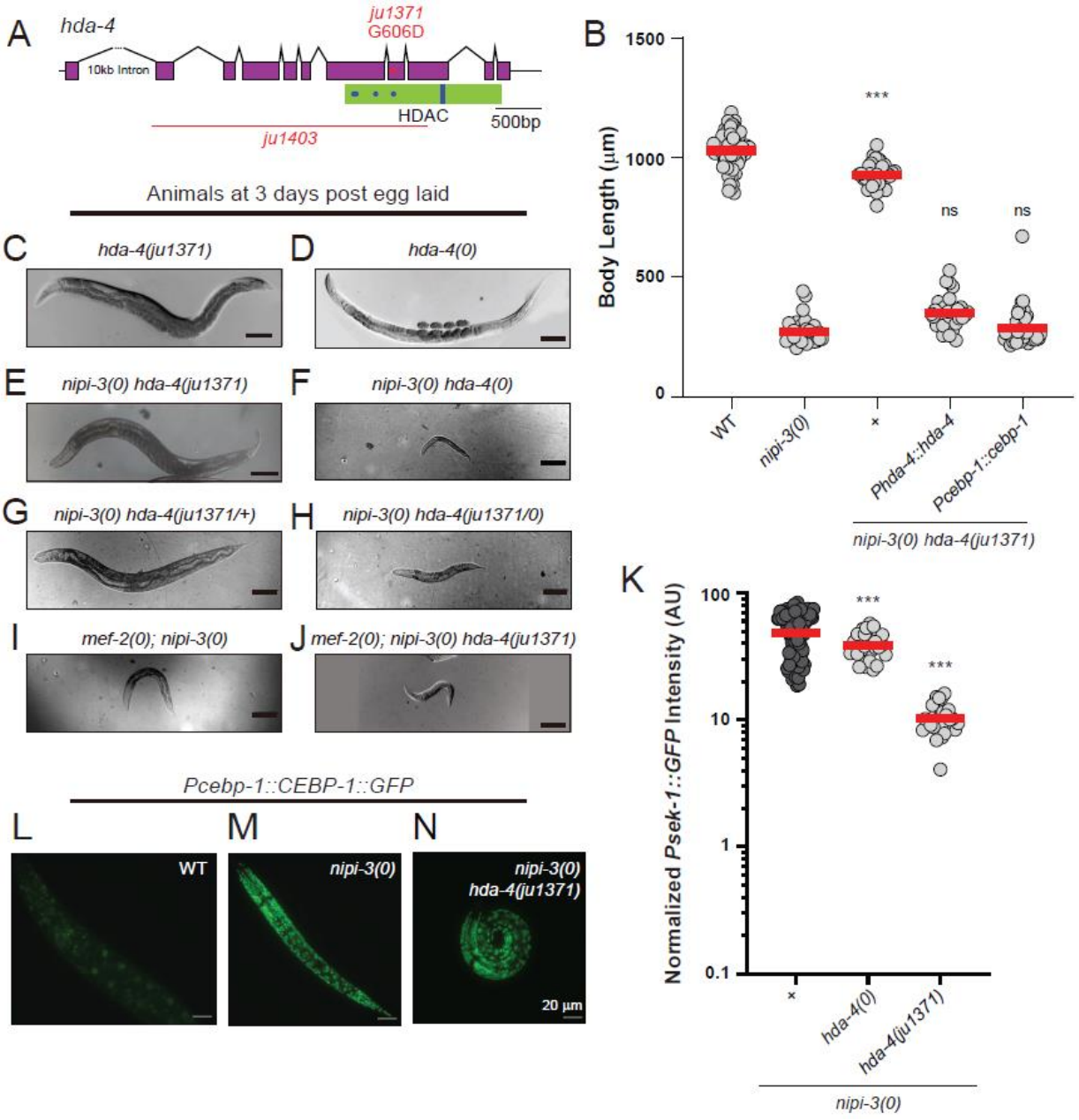
A
hda-4
ju1371
G606D
10kb Intron
HDAC
500bp
ju1403
Animals at 3 days post egg laid
C
hda-4(ju1371)
D
hda-4(0)
E
nipi-3(0) hda-4(ju1371)
F
nipi-3(0) hda-4(0)
G
nipi-3(0) hda-4(ju1371/+)
H
nipi-3(0) hda-4(ju1371/0)
I
mef-2(0); nipi-3(0)
J
mef-2(0); nipi-3(0) hda-4(ju1371)
Pcebp-1::CEBP-1::GFP
L
M
N
WT
nipi-3(0)
nipi-3(0)
hda-4(ju1371)
20 µm
B
Body Length (µm)
1500
1000
500
0
***
ns
ns
WT
nipi-3(0)
*
Phda-4::hda-4
Pcebp-1::cebp-1
nipi-3(0) hda-4(ju1371)
K
Normalized Psek-1::GFP Intensity (AU)
100
10
1
0.1
***
***
*
hda-4(0)
hda-4(ju1371)
nipi-3(0)

Figure 10. Loss of N-terminal acetyltransferase C complex suppresses *nipi-3(0)* larval lethality

(A-C) Illustrations of gene structure, missense allele, and deletion alleles. Exons are purple boxes, introns are angled black lines connecting exons, and the UTRs are black horizonal lines. Protein motifs are illustrated in green. Deletion alleles are indicated as red horizonal lines showing the region of DNA that is deleted. The missense mutation is indicated as a red dot in the exon where the mutation exists, allele name and amino acid substitution are labeled above the red dot. **(A)** Operon CEOP5527 containing *B0238.11.1* and *natc-2.* There are 3331 bp between the 3' UTR of *B0238.11.1* and the 5' UTR of *natc-2* that is not illustrated to scale*.* Missense mutation *ju1369* was isolated in EMS screen for suppressors of *nipi-3(0)* larval arrest. *ju1797* is a 721 bp deletion covering the N-Acetyltransferase domain. *ju1866* is a 1219 bp deletion covering exons 3-4 and the 3'UTR of *natc-2*. **(B)** *natc-1. am138* is a 186 bp deletion and *ok2062* is a 1108 bp deletion. **(C)** *natc-3,* previously named *Y48G1C.9. ju1837* is a 1086 bp deletion with a 57 bp insertion. **(D, F)** Quantification of body length of animals 3 days post egg laid. Each dot represents a single animal, each red line represents the mean value. Some data are replicated from Figure 9, shown in darker grey dots. Statistics: One-Way ANOVA with Tukey's post hoc test. ***P<0.001. For more details about statistics, see Methods. For more statistical comparisons, see **Table 14. (D)** *nipi-3(0)* mutants have a short body length after 3 days of development post egg laid. This phenotype is rescued by *ju1369* missense mutation in *natc-2* or *natc-1(ok2062), natc-2(ju1866)* or *natc-3(ju1837).* Compound knockout of *natc-1, natc-2* and *natc-3* does not rescue body length significantly more than each knockout on their own. Statistics are in comparison to *nipi-3(0)*. **(E)** Quantification of *Psek-1::GFP* expression in animals 36 hours post egg laid. Knockout of *nipi-3* substantially increases *Psek-1::GFP* expression, which is significantly reduced, but not brought to wildtype expression levels by knockout of *natc-1(ok2394), natc-2(ju1797* or *natc-3(ju1837).* Statistics are in comparison to *nipi-3(0).* Each dot represents a single animal, each red line represents the mean value. Some data are replicated from Figure 5, shown in darker grey dots. Statistics: One-Way ANOVA with Tukey's post hoc test, see Methods. ***P<0.001. For more statistical comparisons, see **Table 12. (F)** Double knockout of *natc-3* and *pmk-1* rescues body length significantly more than each knockout on its own suggesting these two genes are functioning in parallel. Statistics are in comparison to *natc-3(0); pmk-10); nipi-3(0)*. **(G)** Quantification of % of animals, measured for body length in (F), that contain eggs after 3 days of development post egg laying. Double knockout of *natc-3* and *pmk-1* rescues developmental delay defect of *nipi-3(0)* to almost wildtype levels.

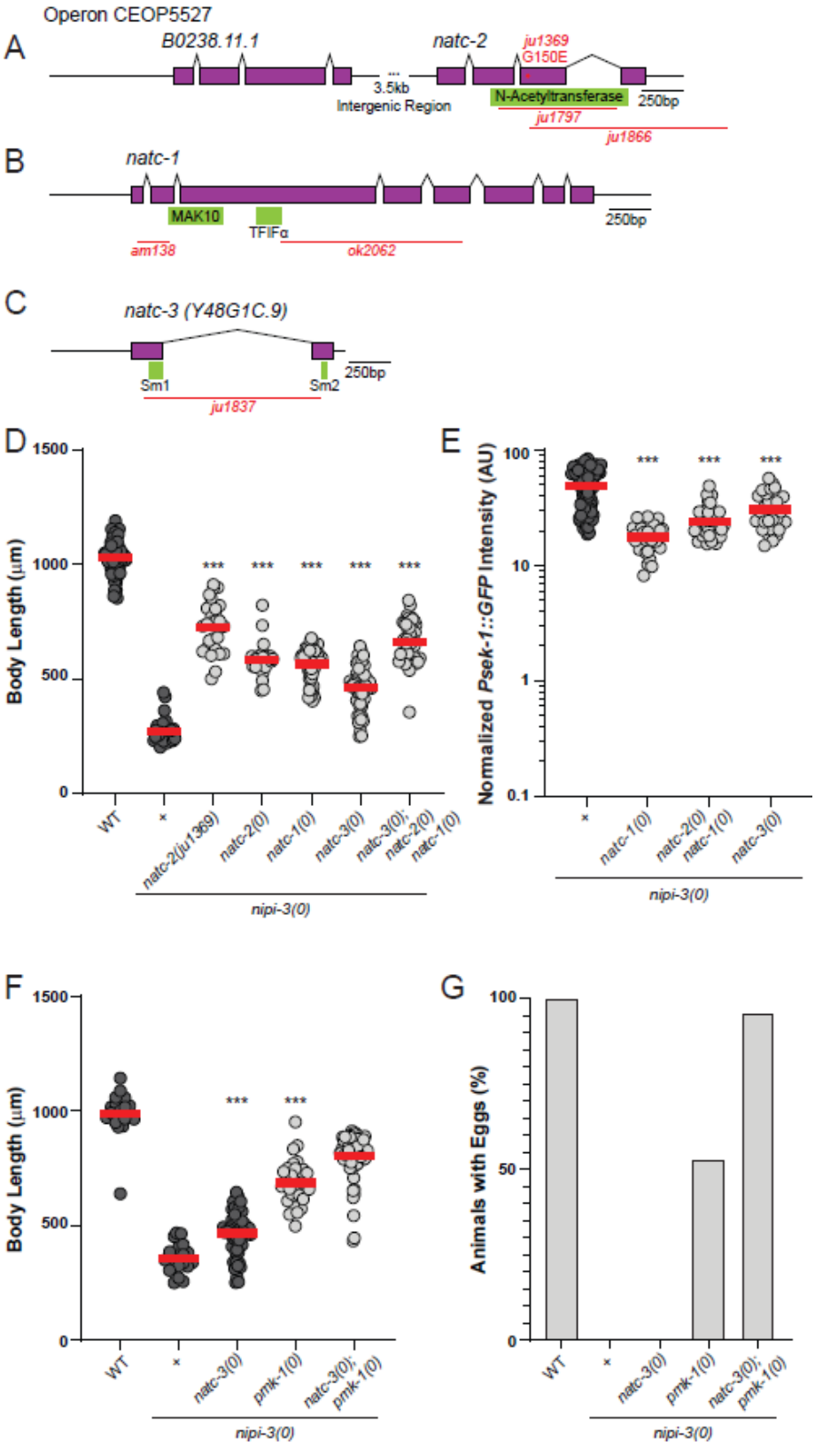
Operon CEOP5527
A
B0238.11.1
natc-2
ju1369
G150E
3.5kb
Intergenic Region
N-Acetyltransferase
250bp
ju1797
ju1866
B
natc-1
MAK10
TFIIFα
250bp
am138
ok2062
C
natc-3 (Y48G1C.9)
Sm1
Sm2
250bp
ju1837
D
Body Length (µm)
1500
1000
500
0
***
WT
*
natc-2(ju1369)
natc-2(0)
natc-1(0)
natc-3(0)
natc-3(0);
natc-2(0)
natc-1(0)
nipi-3(0)
E
Normalized Psek-1::GFP Intensity (AU)
100
10
1
0.1
***
*
natc-1(0)
natc-2(0)
natc-1(0)
natc-3(0)
nipi-3(0)
F
Body Length (µm)
1500
1000
500
0
***
WT
*
natc-3(0)
pmk-1(0)
natc-3(0);
pmk-1(0)
nipi-3(0)
G
Animals with Eggs (%)
100
50
0
WT
*
natc-3(0)
pmk-1(0)
natc-3(0);
pmk-1(0)
nipi-3(0)

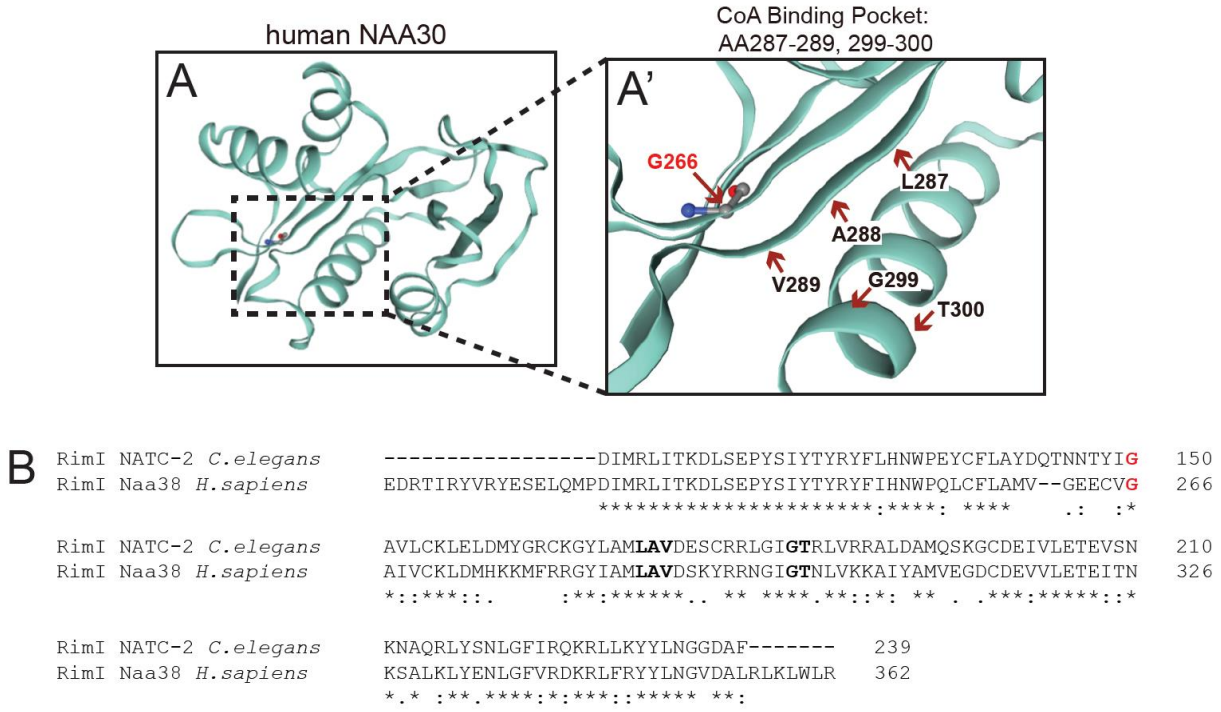

Figure 11. *natc-2(ju1369)* is predicted to be adjacent to CoA binding pocket

(A) Crystal structure of human NAA30, homologue of NATC-2 **(A')** Inset shows CoA binding pocket and the location of the mutated residue in *ju1369*. *C. elegans* G150 is homologous to human G266. **(B)** Protein alignment of the functional domain (RimI) of *C. elegans* NATC-2 and human NAA30. The domain is 62% identical and 76% similar and spans AA209-362 in hNAA30 and AA108-239 in NATC-2. The CoA binding pocket, indicated in bold, has 100% identity between the human and *C. elegans* proteins. The mutated residue in *ju1369* is indicated in red text.

A

```
NATC-3 C.elegans      ---------------MCDDQSTDL--IQLKGH-ENAKKSEAHLKVLEYIGKRYEIRMTDG     42
Naa38 H.sapiens       MAGAGPTMLLREENGCCSRRQSSSSAGDSDGEREDSAAERARQQLEALLNKTMRIRMTDG     60
                                    *. :.:.    : .*. *::  ..*: ::   :.*  .******

NATC-3 C.elegans      RYIRGTMIATDKDANMVFNKADERWDKDPQL--KGVRFLGQAMISKKHVESMHALPDPKE     100
Naa38 H.sapiens       RTLVGCFLCTDRDCNVILGSAQEFLKPSDSFSAGEPRVLGLAMVPGHHIVSIEVQRESLT     120
                      * : * ::.**:*.*:::..*:*  . . .:     *.** **:  :*: *:..  :

NATC-3 C.elegans      TEI--      103
Naa38 H.sapiens       GPPYL      125
```

Figure 12. NATC-3 is homologous to hNaa38

(A) Protein alignment of *C. elegans* NATC-3 (formerly named Y38G1C.9) and human Naa38, the auxiliary subunit of the human NatC complex. The proteins are 25% identical and 41% similar. The functional domains (Sm1, Sm2), indicated in bold, have 41% identity and 80% similarity between the human and *C. elegans* proteins.

Figure 13. NATC-1 and NATC-2 are expressed in many tissues in *C. elegans*

(A) Single plane confocal image of GFP inserted into the endogenous locus of *natc-1* using standard CRISPR knock-in (Methods, *ju1801)* in young adult animals. This reporter shows N' tagged NATC-1 protein is expressed throughout the animals including **(B)** head neurons, **(C)** intestine, **(D)** hypodermis, **(E)** gonad, and **(F)** vulva. This tagged protein is functional, based on phenotype when combined with *nipi-3(0)*. Scale bar A = 100µm, Scale Bar B-F = 10µm **(G)** Single plane confocal images of GFP inserted into the endogenous locus of *natc-2* using standard CRISPR knock-in (Methods, *ju1803)* in young adult animals. This reporter shows N' tagged NATC-2 protein is expressed throughout the animals including **(H)** head neurons, **(I)** intestine, **(J)** hypodermis, **(K)** gonad, and **(L)** vulva. This tagged protein is functional, based on phenotype when combined with *nipi-3(0)*. Scale bar G = 100µm, Scale Bar H-L = 10µm. Dr. Zhu collected all of the images in this Figure.

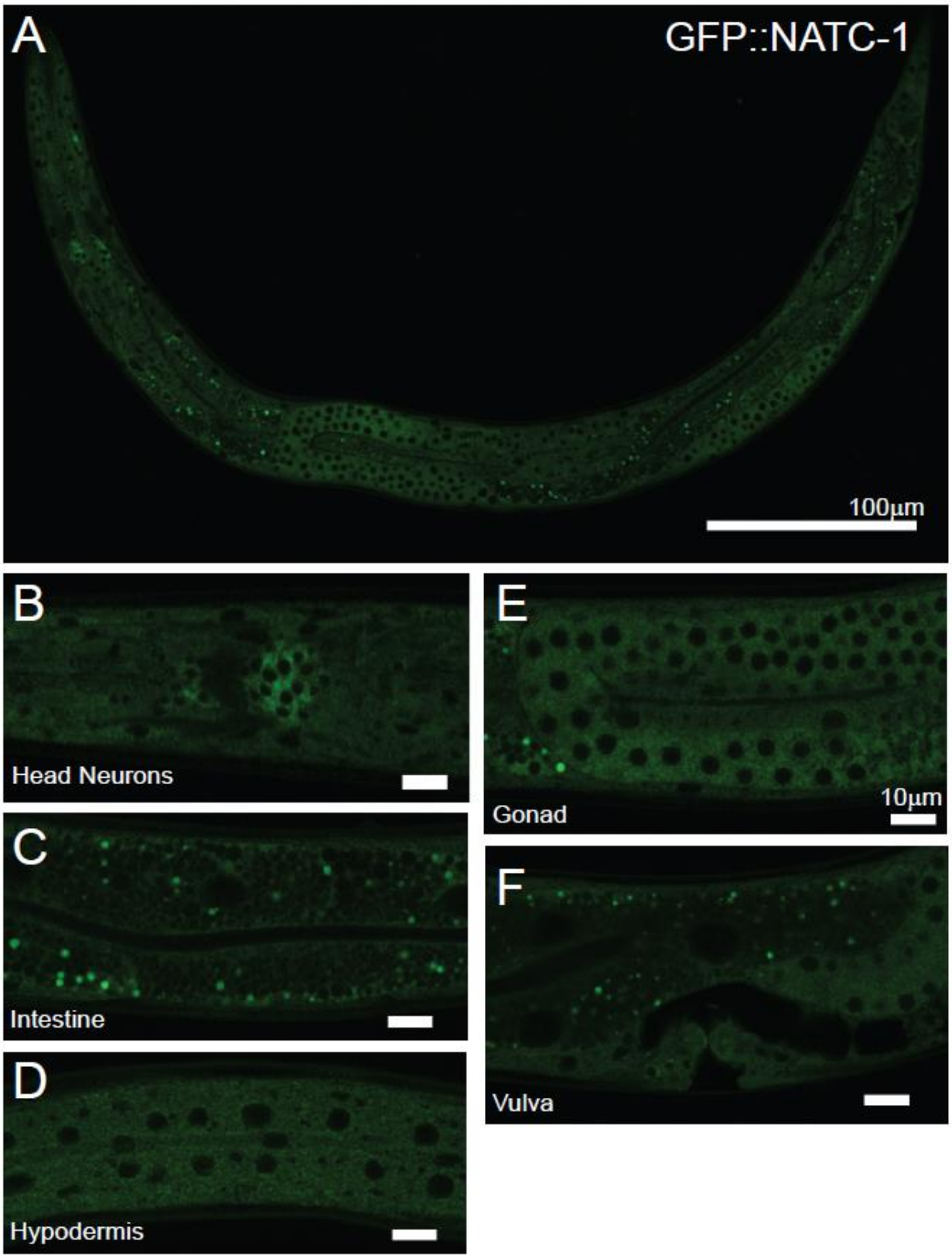
A
GFP::NATC-1
100µm
B
Head Neurons
C
Intestine
D
Hypodermis
E
Gonad
10µm
F
Vulva

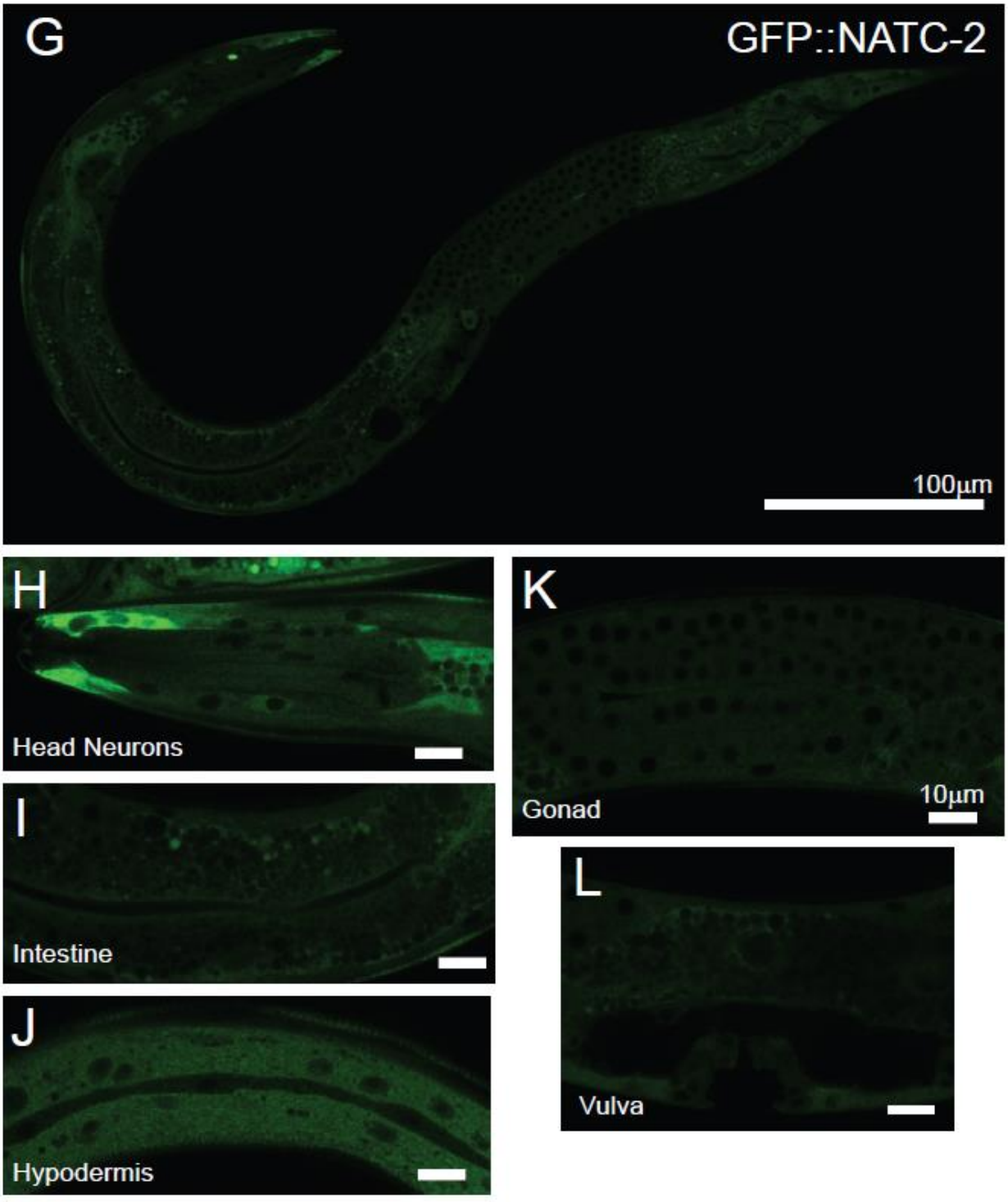

Figure 13. NATC-1 and NATC-2 are expressed in many tissues in *C. elegans*, continued.

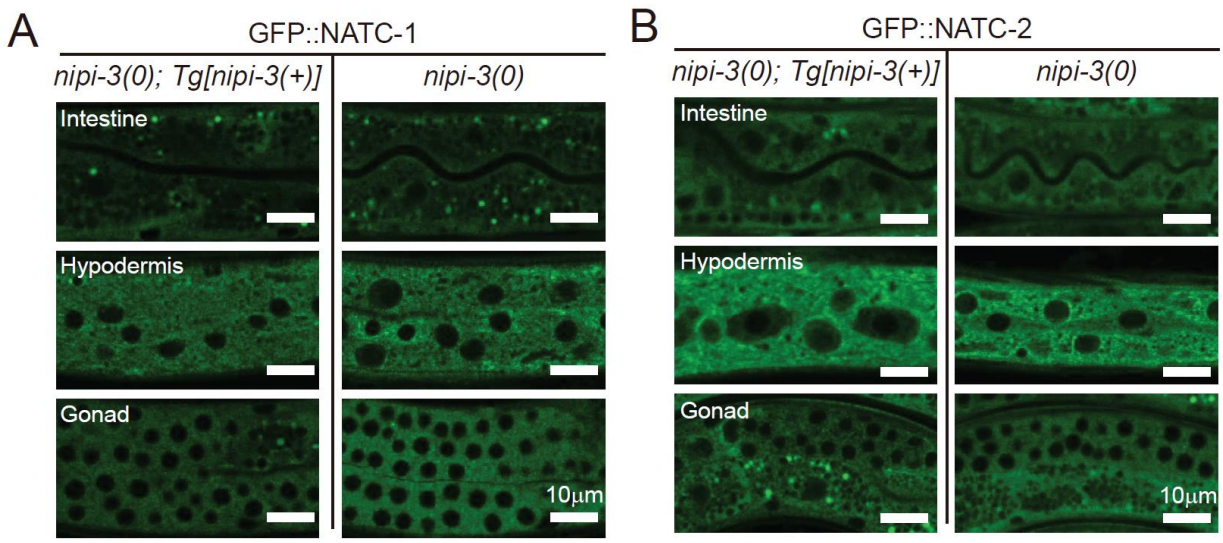

Figure 14. Expression of NATC-1 and NATC-2 is unchanged by *nipi-3(0)*

(A) Single plane confocal images of GFP inserted into the endogenous locus of *natc-1* using standard CRISPR knock-in (Methods, *ju1801)* in L3 animals. The left column of images is in the background of *nipi-3(0); Tg[nipi-3(+)]*, which has expression of wildtype *nipi-3*, rescuing the larval arrest phenotype. There is no obvious change in localization or intensity of GFP::NATC-1 in the sibling animals without the transgene (Tg) expressing wildtype *nipi-3.* Scale bar = 10μm. **(B)** Single plane confocal images of GFP inserted into the endogenous locus of *natc-2* using standard CRISPR knock-in (Methods, *ju1803)* in L3 animals. The left column of images is in the background of *nipi-3(0); Tg[nipi-3(+)]*, which has expression of wildtype *nipi-3*, rescuing the larval arrest phenotype. There is no obvious change in localization or intensity of GFP::NATC-2 in the sibling animals without the transgene (Tg) expressing wildtype *nipi-3.* Scale bar = 10μm. Dr. Zhu collected all of the images in this figure.

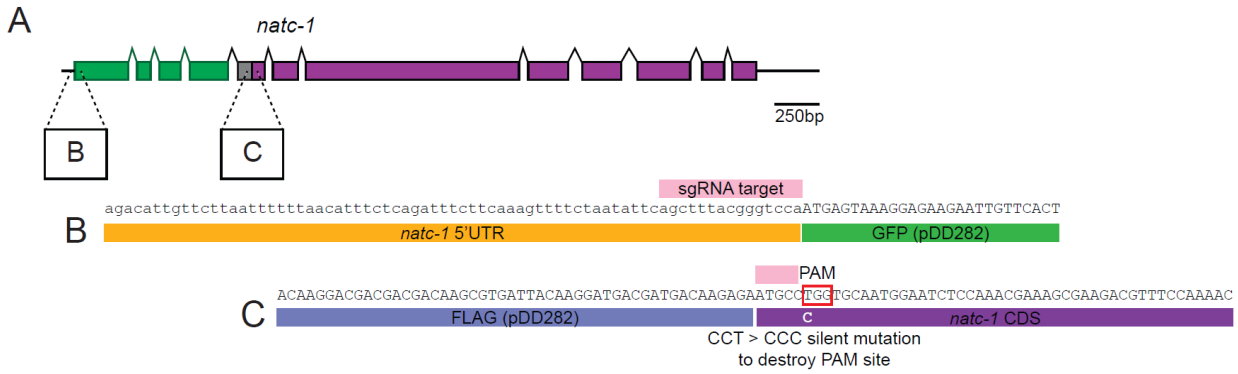

Figure 15. *natc-1* GFP knock-in sequence

(A) Illustration of gene structure and GFP::3xFLAG insertion after removal of self-excision cassette ((Dickinson et al. 2015), Methods). Exons are purple boxes (*natc-1)* and green boxes (GFP), introns are angled black or green lines connecting exons. **(B)** Sequence of *natc-1* 5'UTR and the beginning of the GFP::3xFLAG insertion from pDD282. The targeting sequence for the sgRNA is illustrated in pink. **(C)** Sequence of the end of the GFP::3xFLAG insertion and the beginning of the coding sequence for *natc-1.* The targeting sequence for the sgRNA is illustrated in pink and the PAM site is outlined in red. In the primer used to amplify the 5' arm for the repair template plasmid, a silent mutation was introduced to mutate the PAM site and prevent Cas9 cutting again after the insertion of the GFP construct. I designed the constructs and performed cloning to produce the plasmids for injection. Dr. Zhu performed the injections and screening to isolate the knock-in strain.

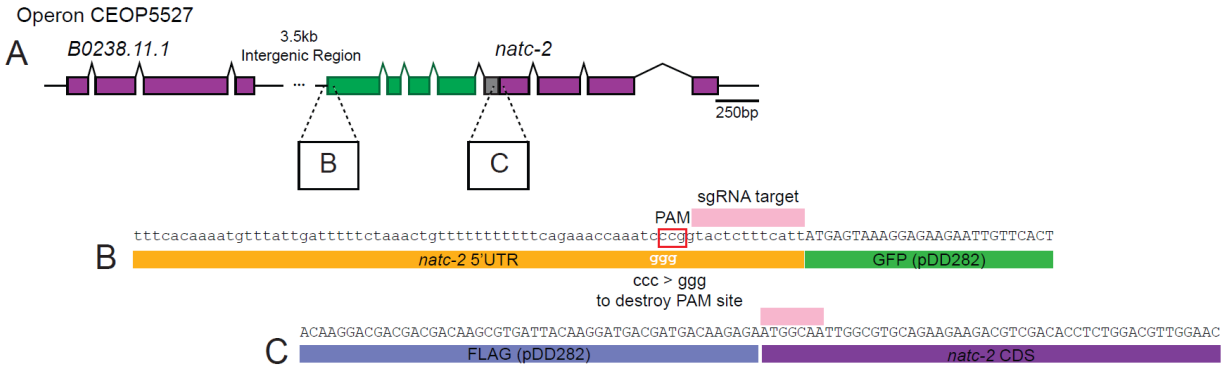

Figure 16. *natc-2* GFP knock-in sequence

(A) Illustration of gene structure and GFP::3xFLAG insertion after removal of self-excision cassette ((Dickinson et al. 2015), Methods). Exons are purple boxes (*natc-2)* and green boxes (GFP), introns are angled black or green lines connecting exons. **(B)** Sequence of *natc-2* 5'UTR and the beginning of the GFP::3xFLAG insertion from pDD282. The targeting sequence for the sgRNA is illustrated in pink and the PAM site is outlined in red. In the primer used to amplify the 3' arm for the repair template plasmid, a mutation was introduced to mutate the PAM site and prevent Cas9 cutting again after the insertion of the GFP construct. **(C)** Sequence of the end of the GFP::3xFLAG insertion and the beginning of the coding sequence for *natc-2.* The targeting sequence for the sgRNA is illustrated in pink. I designed the constructs and performed cloning to produce the plasmids for injection. Dr. Zhu performed the injections and screening to isolate the knock-in strain.

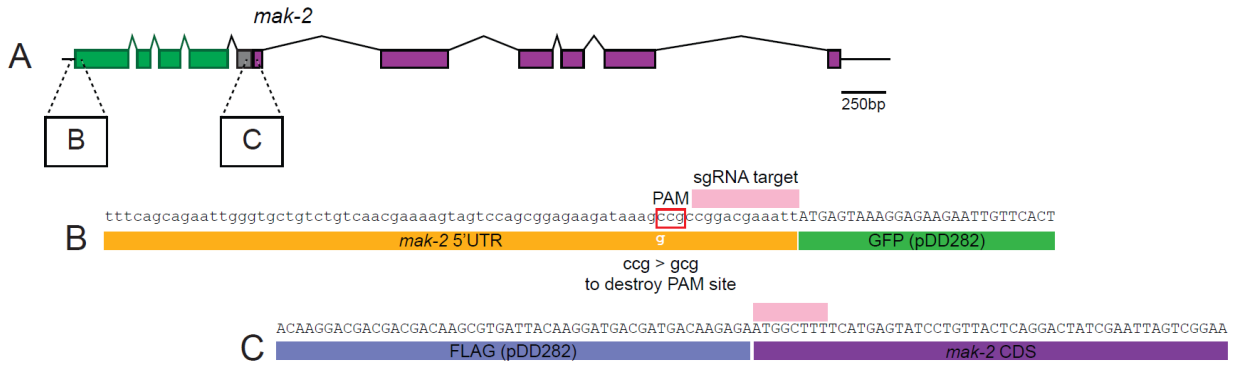

Figure 17. *mak-2* GFP knock-in sequence

(A) Illustration of gene structure and GFP::3xFLAG insertion after removal of self-excision cassette ((Dickinson et al. 2015), Methods). Exons are purple boxes (*mak-2)* and green boxes (GFP), introns are angled black or green lines connecting exons. **(B)** Sequence of *mak-2* 5'UTR and the beginning of the GFP::3xFLAG insertion from pDD282. The targeting sequence for the sgRNA is illustrated in pink and the PAM site is outlined in red. In the primer used to amplify the 3' arm for the repair template plasmid, a mutation was introduced to mutate the PAM site and prevent Cas9 cutting again after the insertion of the GFP construct. **(C)** Sequence of the end of the GFP::3xFLAG insertion and the beginning of the coding sequence for *mak-2.* The targeting sequence for the sgRNA is illustrated in pink. I designed the constructs, cloned the injection plasmids, and performed the injections and screening to isolate the knock-in strain.

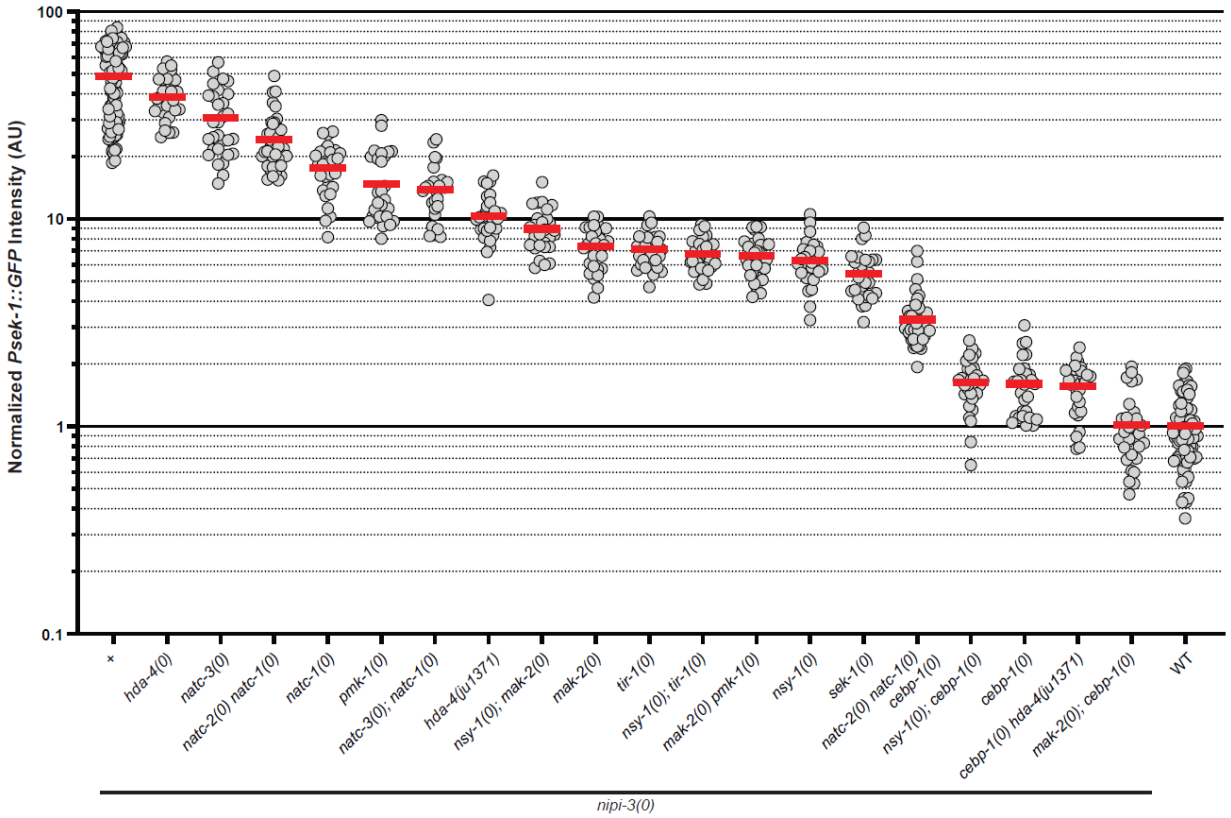

Figure 18. Normalized *Psek-1::GFP* Intensity for all strains containing *nipi-3(0)*

Quantification of *Psek-1::GFP* expression in animals 36 hours post egg laid. Each dot represents a single animal, each red line represents the mean value. Null alleles in this graph are: *hda-4(ju1403)*, *natc-3(ju1837)*, *natc-2(ju1797)*, *natc-1(am138)*, *pmk-1(km25)*, *nsy-1(ok593)*, *mak-2(ok2394)*, *tir-1(qd4)*, *sek-1(km4)*, *cebp-1(tm2807)*, *nipi-3(ju1293)*. For statistical comparisons, see **Tables 10-12**.

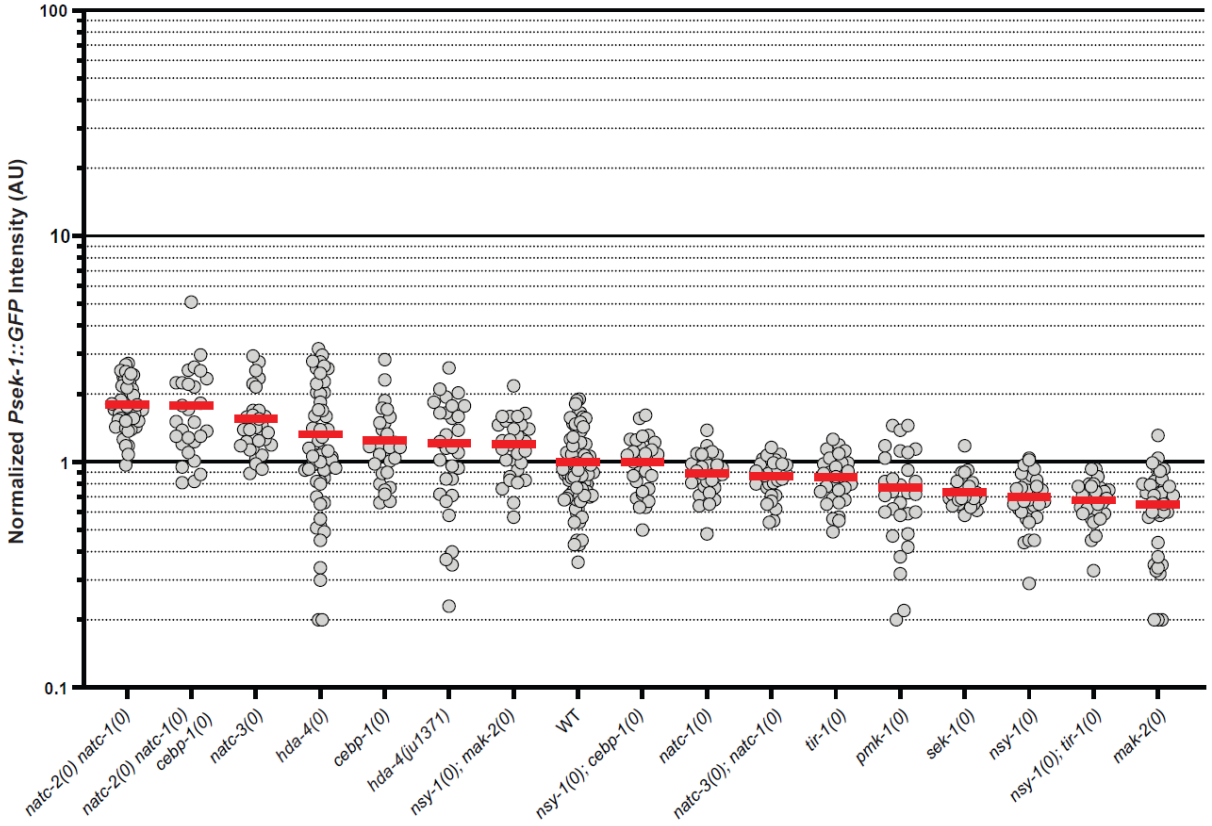

Figure 19. Normalized *Psek-1::GFP* Intensity for all strains without *nipi-3(0)*

Quantification of *Psek-1::GFP* expression in animals 36 hours post egg laid. Each dot represents a single animal, each red line represents the mean value. Null alleles in this graph are: *natc-2(ju1797), natc-1(am138), cebp-1(tm2807), natc-3(ju1837), hda-4(ju1403), nsy-1(ok593), mak-2(ok2394), tir-1(qd4), pmk-1(km25), sek-1(km4).* For statistical comparisons, see **Tables 10-12**.

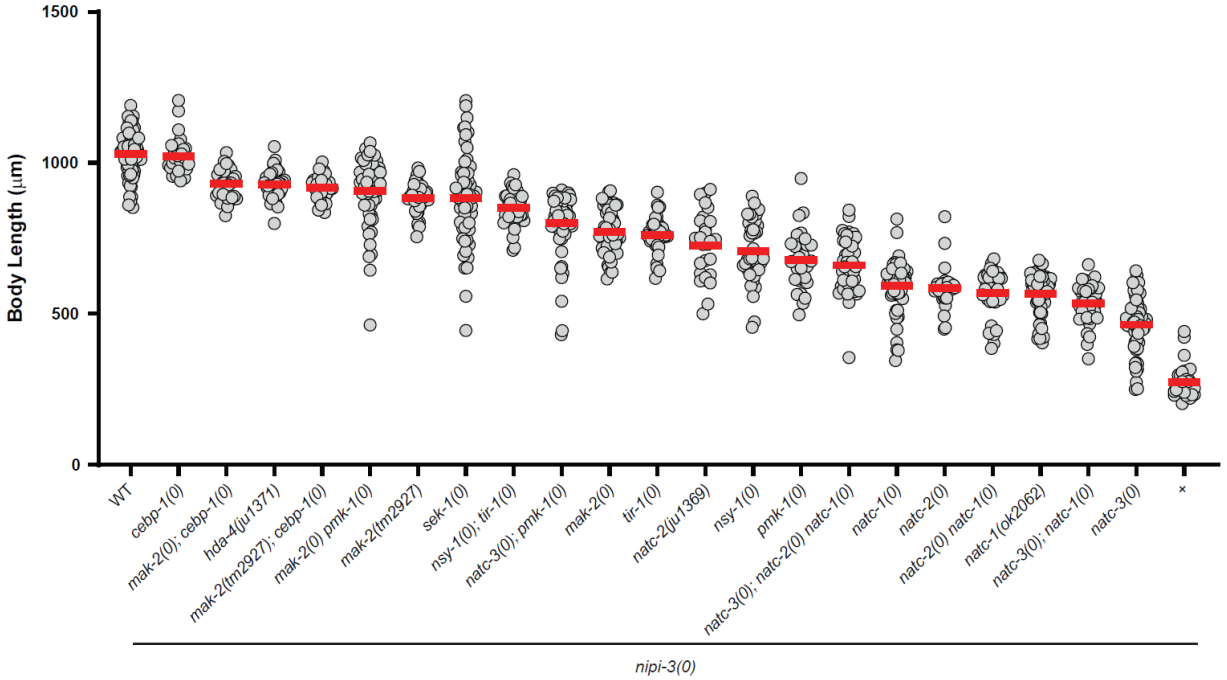

Figure 20. Body length, 3 days post hatch for all strains containing *nipi-3(0)*

Quantification of body length of animals 3 days post egg laid. Each dot represents a single animal, each red line represents the mean value. Null alleles in this graph are: *cebp-1(tm2807), mak-2(ok2394), pmk-1(km25), sek-1(km4), nsy-1(ok593), tir-1(qd4), natc-3(ju1837), natc-2(ju1797), natc-1(am138), nipi-3(ju1293).* Statistics: One-Way ANOVA with Tukey's post hoc test. For more details about statistics, see Methods. For statistical comparisons, see **Tables 13-15**.

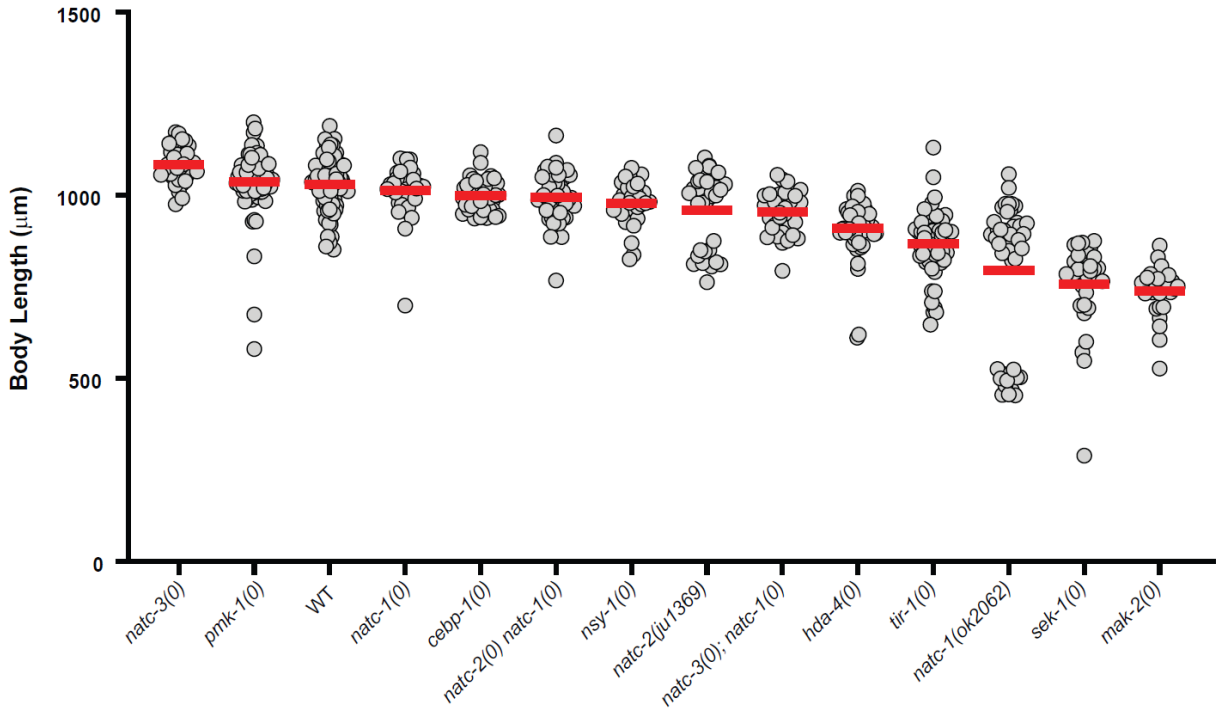

Figure 21. Body length, 3 days post hatch for all strains without *nipi-3(0)*

Quantification of body length of animals 3 days post egg laid. Each dot represents a single animal, each red line represents the mean value. Null alleles in this graph are: *natc-3(ju1837), pmk-1(km25), natc-1(am138), cebp-1(tm2807), natc-2(ju1797), nsy-1(ok593), hda-4(ju1403), tir-1(qd4), sek-1(km4), mak-2(ok2394).* Statistics: One-Way ANOVA with Tukey's post hoc test. For more details about statistics, see Methods. For statistical comparisons, see **Table 16**.

Tables

Table 3. Chapter 3 Strains and Genotypes

Strain	Genotype	Figure
CZ27584	*Psek-1::GFP(juIs559)*	Figure 5A
CZ27585	*Psek-1::GFP(juIs559)*	Figure 5B, D, G, 9B, 10D, 18, 19, 20, 21
CZ24959	*Psek-1(∆CEBP-1 binding sites)::gfp(juEx7617)*	Figure 5C, D’
CZ27728	*nipi-3(ju1293) X; Psek-1::GFP(juIs559); nipi-3 gDNA(juEx6807)*	Figure 5E, G, 6A, 9B, J, 10D, E, 18, 20
CZ24961	*nipi-3(ju1293) X; nipi-3 gDNA(juEx6807); Psek-1(∆CEBP-1 binding sites)::gfp(juEx7617)*	Figure 5E’
CZ27864	*cebp-1(tm2807) X nipi-3(ju1293) X; Psek-1::GFP(juIs559); nipi-3 gDNA(juEx6807)*	Figure 5F, 18, 20
CZ27809	*cebp-1(tm2807) X; Psek-1::GFP(juIs559)*	Figure 5G, 19, 21
CZ28370	*sek-1(km4) nipi-3(ju1293); Psek-1::GFP(juIs559)*	Figure 6A, 18
CZ27136	*pmk-1(km25) IV; nipi-3(ju1293) X; Psek-1::GFP(juIs559); nipi-3 gDNA(juEx6807)*	Figure 6A, 18, 20
CZ28037	*nsy-1(ok593) II; nipi-3(ju1293) X; Psek-1::GFP(juIs559); nipi-3 gDNA(juEx6807)*	Figure 6A, 18, 20
CZ28038	*tir-1(qd4) III; nipi-3(ju1293) X; Psek-1::GFP(juIs559); nipi-3 gDNA(juEx6807)*	Figure 6A, 18, 20
CZ27918	*mak-2(ok2394) IV; nipi-3(ju1293) X; Psek-1::GFP(juIs559); nipi-3 gDNA(juEx6807)*	Figure 6A, B, 18, 20
CZ28036	*mak-2(ok2394) IV pmk-1(km25) IV; nipi-3(ju1293) X; Psek-1::GFP(juIs559); nipi-3 gDNA(juEx6807)*	Figure 6B, 18, 20
CZ28160	*nsy-1(ok593) II; mak-2(ok2394) IV; Psek-1::GFP(juIs559)*	Figure 6B, 19
CZ28371	*nsy-1(ok593) II; cebp-1(tm2807) X nipi-3(ju1293) X; Psek-1::GFP(juIs559)*	Figure 6C, 18
CZ28035	*mak-2(ok2394) IV; cebp-1(tm2807) X nipi-3(ju1293) X; Psek-1::GFP(juIs559); nipi-3 gDNA(juEx6807)*	Figure 6C, 18, 20
CZ25830	*cebp-1::GFP(wgIs563)*	Figure 8A, 9K
CZ24854	*nipi-3(ju1293) X; cebp-1::GFP(wgIs563); nipi-3 gDNA(juEx6807)*	Figure 8B, 9L
CZ28459	*mak-2(tm2927) IV; nipi-3(ju1293) X; cebp-1::GFP(wgIs563); nipi-3 gDNA(juEx6807)*	Figure 8C
CZ28605	*GFP::mak-2(ju1851) IV; nipi-3(ju1293) X; nipi-3 gDNA(juEx6807)*	Figure 8D, E, 17
CZ23401[#]	*nipi-3(ju1293) X hda-4(ju1371) X (EMS isolate)*	Figure 9A
CZ23692[#]	*nipi-3(ju1293) X hda-4(ju1371) X (2x O.C.)*	Figure 9A
CZ22446[#]	*nipi-3(ju1293) X; nipi-3 gDNA(juEx6807) (pre-mutagenized strain)*	Figure 9A, 10A
CZ24455	*nipi-3(ju1293) X hda-4(ju1371) X; Phda-4::hda-4(genomic)::gfp(oyIs73); nipi-3 gDNA(juEx6807)*	Figure 9B
CZ24911	*nipi-3(ju1293) X hda-4(ju1371) X Pcebp-1(2.2kb): flag::cebp-1:: cebp-1 3'UTR(juIs418) X ; nipi-3 gDNA(juEx7233)*	Figure 9B
N2	wild type	Figure 9B, 10D, 20, 21

Table 3. Chapter 3 Strains and Genotypes, continued

Strain	Genotype	Figure
CZ24195	*nipi-3(ju1293) X hda-4(ju1371) X*	Figure 9B, 20
CZ28249	*hda-4(ju1371) X; Psek-1::GFP(juIs559)*	Figure 9C, 19
CZ27919	*hda-4(ju1403) X; Psek-1::GFP(juIs559)*	Figure 9D, 19, 21
CZ28181	*nipi-3(ju1293) X hda-4(ju1403) X; Psek-1::GFP(juIs559)*	Figure 9E, 9J, 18
CZ22882	*mef-2(gv1) I; nipi-3(ju1293) X; nipi-3 gDNA(juEx6807)*	Figure 9H
CZ28030	*mef-2(gv1) I; nipi-3(ju1293) X hda-4(ju1371) X; nipi-3 gDNA(juEx6807)*	Figure 9I
CZ28142	*nipi-3(ju1293) X hda-4(ju1371) X; Psek-1::GFP(juIs559); nipi-3 gDNA(juEx6807)*	Figure 9J, 18
CZ28606	*nipi-3(ju1293) X hda-4(ju1371) X; cebp-1::GFP(wgIs563); nipi-3 gDNA(juEx6807)*	Figure 9M
CZ23399[#]	*natc-2(ju1369) V; nipi-3(ju1293) X (EMS isolate)*	Figure 10A
CZ24194	*natc-2(ju1369) V; nipi-3(ju1293) X*	Figure 10D, 20
CZ27143	*natc-1(ok2062) V; nipi-3(ju1293) X; nipi-3 gDNA(juEx6807)*	Figure 10D, 20
CZ28553	*natc-3(ju1837) I; natc-2(ju1797) V natc-1(am138) V; nipi-3(ju1293) X; nipi-3 gDNA(juEx6807)*	Figure 10D, 20
CZ28664	*natc-2(ju1866) V; nipi-3(ju1371) X; Psek-1::GFP(juIs559) ; nipi-3 gDNA(juEx6807)*	Figure 10D, 20
CZ28337	*natc-3(ju1837) I; nipi-3(ju1293) X; Psek-1::GFP(juIs559); nipi-3 gDNA(juEx6807)*	Figure 10D, E, 18, 20
CZ28362	*natc-1(ok2062) V; nipi-3(ju1293) X; Psek-1::GFP(juIs559); nipi-3 gDNA(juEx6807)*	Figure 10E, 18
CZ27861	*natc-2(ju1797) V natc-1(am138) V; nipi-3(ju1293) X; Psek-1::GFP(juIs559); nipi-3 gDNA(juEx6807)*	Figure 10E, 18, 20
CZ27898	*GFP::natc-1(ju1801) V*	Figure 13A-F, 15
CZ27900	*GFP::natc-2(ju1803) V*	Figure 13G-L, 16
CZ28028	*GFP::natc-1(ju1801) V; nipi-3(ju1293) X; nipi-3 gDNA(juEx6807)*	Figure 14A, 15
CZ28029	*GFP::natc-2(ju1803) V; nipi-3(ju1293) X; nipi-3 gDNA(juEx6807)*	Figure 14B, 16
CZ28637	*GFP::SEC::mak-2(ju1850) IV*	Figure 17
CZ28638	*GFP::mak-2(ju1851) IV*	Figure 17
CZ27862	*natc-2(ju1797) V natc-1(am138) V; cebp-1(tm2807) X nipi-3(ju1293) X; Psek-1::GFP(juIs559); nipi-3 gDNA(juEx6807)*	Figure 18
CZ28161	*nsy-1(ok593) II; mak-2(ok2394) IV; nipi-3(ju1293) X; Psek-1::GFP(juIs559) ; nipi-3 gDNA(juEx6807)*	Figure 18
CZ28140	*cebp-1(tm2807) X nipi-3(ju1293) X hda-4(ju1371) X; nipi-3 gDNA(juEx6807)*	Figure 18
CZ28039	*nsy-1(ok593) II; tir-1(qd4) III; nipi-3(ju1293) X; Psek-1::GFP(juIs559); nipi-3 gDNA(juEx6807)*	Figure 18, 20
CZ28364	*natc-3(ju1837) I; natc-1(am138) V; nipi-3(ju1293) X; Psek-1::GFP(juIs559); nipi-3 gDNA(juEx6807)*	Figure 18, 20
CZ27863	*natc-2(ju1797) V natc-1(am138) V; cebp-1(tm2807) X; Psek-1::GFP(juIs559)*	Figure 19
CZ27917	*mak-2(ok2394) IV; Psek-1::GFP(juIs559)*	Figure 19
CZ28373	*tir-1(qd4) III; Psek-1::GFP(juIs559)*	Figure 19

Table 3. Chapter 3 Strains and Genotypes, continued

Strain	Genotype	Figure
CZ28374	*nsy-1(ok593) II; tir-1(qd4) III; Psek-1::GFP(juIs559)*	Figure 19
CZ28369	*sek-1(km4) X; Psek-1::GFP(juIs559)*	Figure 19
CZ28159	*nsy-1(ok593) II; cebp-1(tm2807) X; Psek-1::GFP(juIs559)*	Figure 19
CZ27727	*natc-2(ju1797) V natc-1(am138) V; Psek-1::GFP(juIs559)*	Figure 19, 21
CZ27135	*pmk-1(km25) IV; Psek-1::GFP(juIs559)*	Figure 19, 21
CZ28354	*natc-3(ju1837) I; Psek-1::GFP(juIs559)*	Figure 19, 21
CZ28361	*natc-1(ok2062) V; Psek-1::GFP(juIs559)*	Figure 19, 21
CZ28372	*nsy-1(ok593) II; Psek-1::GFP(juIs559)*	Figure 19, 21
CZ28363	*natc-3(ju1837) I; natc-1(am138) V; Psek-1::GFP(juIs559)*	Figure 19, 21
CZ23578	*sek-1(km4) X nipi-3(ju1293) X*	Figure 20
CZ27142	*natc-1(am138) V; nipi-3(ju1293) X; nipi-3 gDNA(juEx6807)*	Figure 20
CZ28458	*mak-2(tm2927) IV; nipi-3(ju1293) X; Psek-1::GFP(juIs559); nipi-3 gDNA(juEx6807)*	Figure 20
CZ28552	*mak-2(tm2927) IV; cebp-1(tm2807) X nipi-3(ju1293) X; Psek-1::GFP(juIs559); nipi-3 gDNA(juEx6807)*	Figure 20
WU1036	*natc-1(am138) V*	Figure 21
CZ21653	*sek-1(km4) X*	Figure 21
CZ21739	*tir-1(qd4) III*	Figure 21
CZ8762	*mak-2(ok2394) IV*	Figure 21
CZ28341	*natc-2(ju1369) V*	Figure 21

[#] - strains analyzed by whole genome sequencing

Table 4. Chapter 3 Alleles

Allele	Gene	Effect	Flanking Sequence	Detection
ju1293	*nipi-3*	Deletion	ttatctcatttgctt/ /atccagctccgcacc	PCR with Platinum II 2xMM Taq: YJ11161 + YJ12708 WT: 990 mut: 400
ju1369	*natc-2*	G150E	acctacatcgAagctgttttg	PCR: YJ12701 + YJ12715 Sequence: YJ12701
ju1371	*hda-4*	G606D	cggccgccagAtcatcatgca	PCR: YJ12700 +YJ12709 Sequence: YJ12700
ju1403	*hda-4*	Deletion	ctcgccctgcccctg/ /aaccgttattgagcc	PCR: YJ12707 +YJ12700 +YJ12709 WT: 670 mut: 390
ju1797	*natc-2*	Deletion	caacgatattatgcg/ /aatataattttcaag	PCR: YJ12705 + YJ12701 +YJ12715 WT: 883 mut: 719
ju1801	*natc-1*	GFP KI	agctttacgggtcca/ /atgcctggtgcaatg	fluorescence microscope
ju1803	*natc-2*	GFP KI	cggtactctttcatt/ /atggcaattggcgtg	fluorescence microscope
ju1837	*natc-3*	Deletion	gaagcccatctgaaa/ /agggcaagcgatgat	PCR: YJ12722 + YJ12723 WT: 1799 mut: 751

Table 4. Chapter 3 Alleles, continued

Allele	Gene	Effect	Flanking Sequence	Detection
ju1850	*mak-2*	GFP KI	ccgccggacgaaatt/ /atggcttttcatgag	fluorescence microscope
ju1851	*mak-2*	GFP KI	ccgccggacgaaatt/ /atggcttttcatgag	fluorescence microscope
ju1866	*natc-2*	Deletion	gatatgtatggacgg/ /ggaggaaggaactta	PCR: YJ12701F + YJ12706 WT: 1408 mut: 736
am138	*natc-1*	Deletion	ccaaacgaaagcgaa/ /acacattaaaacatt	PCR: YJ12710 + YJ12711 WT: 429 mut: 243
km25	*pmk-1*	Deletion	atattggttttacgt/ /cgttgtatgtgtcat	PCR: AC2408+ YJ12697 +YJ12698 WT: 725 mut: 900
km4	*sek-1*	Deletion	acactagaataagtg/ /ctatgctagatttgc	PCR: YJ9980F + YJ12717 + YJ12718 WT: 508 mut: 830
ok2062	*natc-1*	Deletion	aagcaaaatcggaaa/ /aactttggaacggag	PCR: YJ12712 + YJ12713 + YJ12714 WT: 515 mut: 292
ok2394	*mak-2*	Deletion	gaagattgaaagaat/ /tccagatactccatt	PCR: YJ12693 + YJ12692 + YJ12694 WT: 435 mut: 784
ok593	*nsy-1*	Deletion	gtcaattattccttt/ /atcacttcagccgtt	PCR: AC2396 + AC2397 + AC2398 WT: 851 mut: 587
qd4	*tir-1*	Deletion	ctaccaaatgctcac/ /tttccaacaaaaaac	PCR: YJ10840 + YJ10841 + YJ10842 WT: 296 mut: 708
tm2807	*cebp-1*	Deletion	tccagcaatccgagg/ /ttatgacgattacca	PCR: YJ9850 + YJ8980 WT: 924 mut: 445
tm2927	*mak-2*	Deletion	acttggctaggaaaa/ /cataaaaatcatata	PCR: YJ12690 + YJ12691 + YJ12692 WT: 320 mut: 730

Table 5. Chapter 3 Transgenes and Plasmids

Transgene	Description	Plasmid(s)
juEx7488	Transcriptional reporter of *sek-1*	5 ng/ul of pKK279 [*Psek-1(4870bp upstream)-gfp*] 90 ng/ul pCZGY [*Pgcy-8-mCherry*]
juEx7617	Transcriptional reporter of *sek-1* without CEBP-1 binding sites	5 ng/ul of pKK285 [*Psek-1(4870bp upstream – deletion of 120bp containing two CEBP-1 binding sites)-gfp*] 90 ng/ul pCZGY [*Pgcy-8-mCherry*]
juEx6807	genomic rescue of *nipi-3*	5ng/ul of pCZGY3044 [*nipi-3 gDNA*] 2ng/ul of pCFJ90[*Pmyo-2-mCherry*]
juIs559	TMP/UV multicopy integration	pKK279 [*Psek-1(4870bp upstream)-gfp*] pCZGY [*Pgcy-8-mCherry*]
wgIs563[#]	Bombardment integration	[*cebp-1::TY1::EGFP::3xFLAG*] [*unc-119(+)*]
oyIs73[##]	Multicopy integration	[*Phda-4::hda-4(genomic)::gfp*] [*Punc-122::RFP*]
juIs418	TMP/UV multicopy integration	pCZGY2508 [*Pcebp-1(2.2kb)::flag::cebp-1::cebp-1 3'UTR*] pCFJ90 [*Pmyo-2-mCherry*]

[#] - source is (Sarov et al. 2006)
[##] - source is (van der Linden et al. 2007)

Table 6. Chapter 3 Cloning Primers

Primer	Sequence	Description
YJ12724	acgttgtaaaacgacggccagtcgccggcaatggtgttcctgagccattc	*natc-1* N' GFP KI 5' HA
YJ12725	TCCAGTGAACAATTCTTCTCCTTTACTCATtggacccgtaaagctgaata	
YJ12726	CGTGATTACAAGGATGACGATGACAAGAGAATGCCcGGTGCAATGGAATC	*natc-1* N' GFP KI 3' HA
YJ12727	tcacacaggaaacagctatgaccatgttatGCATGAGCATTTCGAATGAA	
YJ12728	agctttacgggtccaatgccGTTTTAGAGCTAGAAATAGCAAGT	*natc-1* sgRNA into pDD162
YJ12729	acgttgtaaaacgacggccagtcgccggcatcttcgcatttgttgagacg	*natc-2* N' GFP KI 5' HA
YJ12730	TCCAGTGAACAATTCTTCTCCTTTACTCATaatgaaagagtacccccatttgg	
YJ12731	CGTGATTACAAGGATGACGATGACAAGAGAATGGCAATTGGCGTGCAG	*natc-2* N' GFP KI 3' HA
YJ12732	tcacacaggaaacagctatgaccatgttatGCCAACATGGCAAGATAACC	

Table 6. Chapter 3 Cloning Primers, continued

Primer	Sequence	Description
YJ12733	TTGCCATaatgaaagagtacGTTTTAGAGCTAGAAATAGCAAGT	*natc-2* sgRNA into pDD162
YJ12734	cccagtcacgacgttgtaaaacgacggccagtcgccggcaactctgtgccaccaaaaacc	*mak-2* N' GFP KI 5' HA
YJ12735	GGGACAACTCCAGTGAACAATTCTTCTCCTTTACTCATaatttcgtcc ggcgCctttatc	
YJ12736	CGACGACAAGCGTGATTACAAGGATGACGATGACAAGAGAATG GCTTTTCATGAGTATCC	*mak-2* N' GFP KI 3' HA
YJ12737	gataacaatttcacacaggaaacagctatgaccatgttataaaagaagcgaaaggtaggc	
YJ12738	AAAGCCATAATTTCGTCCGGGTTTTAGAGCTAGAAATAGCAAGT	*mak-2* sgRNA into pDD162
YJ12739	CCGGACGAAATTATGGCTTTCaagacatctcgcaatagg	
YJ12740	atccattttgctccgatgag	pKK279: *sek-1* promoter
YJ12741	TCGCTCCATgatgtaagactc	
YJ12742	aatgtgtttggtcacaaaaacg	pKK285: remove CEBP-1 binding sites from pKK279
YJ12743	atttagacggtgtgggttcg	

HA = Homology arm to make repair template from pDD282 for GFP knock-in. pDD162 is plasmid encoding Cas9 and sgRNA target. (Dickinson et al. 2015).

Table 7. Chapter 3 Genotyping Primers

Primer	Sequence	Target Gene
YJ12690	tttgaggtcaggcaggtagg	*mak-2*
YJ12691	cttacgcttaggctgggaac	*mak-2*
YJ9850	ATGACGTCATCATTTCACTTTTC	*cebp-1*
YJ8980	TTAGGTCGGCTCAGCCTTCTCC	*cebp-1*
YJ11161	ctctcttccgattcctctcg	*nipi-3*
YJ12693	tattgaggcgagagctaggc	*mak-2*
YJ12692	acCGGACTAGCTCCACCTTT	*mak-2*
YJ12694	CGAATGGGATTGTGTTTCTG	*mak-2*
YJ12695	GCATCCGGCTTGTACAGTct	*sek-1*
YJ12697	CCGACTCCACGAGAAGGATA	*pmk-1*
YJ12698	acGATCAGATCCAGGGAACA	*pmk-1*
YJ12699	CGGGAGATAGAAGGCATctg	*tir-1*
YJ12700	CGGGGTTGATTCAGACACTT	*hda-4*
YJ12701	CGCTTGATCACCAAGGATCT	*natc-2*
YJ12702	TGAAACCGTCGAACATTCTG	*sek-1*
YJ12703	CTCATGCACATCTTCCAATGA	*nsy-1*

Table 7. Chapter 3 Genotyping Primers, continued

Primer	Sequence	Target Gene
YJ12704	CGGCGTGTCTACAACTTTCA	*nsy-1*
YJ12705	tcgctgcgagatattttgtg	*natc-2*
YJ12706	acgattctcgtttcccacac	*natc-2*
YJ12707	tcatggccttattggaggag	*hda-4*
YJ12708	caaacagcgcgagtaacaag	*nipi-3*
YJ12709	acttcatatccgccaagtgc	*hda-4*
YJ12710	cgaggtgcatgttgtttacc	*natc-1*
YJ12711	TAATCGTCGGCGTAGAGTCC	*natc-1*
YJ12712	AGGAGCCGAAGAGAATTCTGAC	*natc-1*
YJ12713	GACCGAAAGTTCTCGCAAAG	*natc-1*
YJ12714	CACGACGTTTCAACTCTTCTCC	*natc-1*
YJ12715	CCTCCTCATCCGGAGTATCA	*natc-2*
YJ12716	gtctcgaagcttccacttgc	*natc-2*
YJ12717	cgatttgcttaagtctcggttc	*sek-1*
YJ12718	tgacatcgaaaatggcactg	*sek-1*
YJ12719	tttcagGAAATCGGTGCAAT	*tir-1*
YJ12720	tctggaaaacagccaacaga	*nsy-1*
YJ12721	catcaacggttgtacttcctca	*nsy-1*
YJ12722	ggcgggaacctacttcactt	*natc-3*
YJ12723	cacggggacttcgtttacca	*natc-3*
YJ9980	acgcaggtcactcgtttc	*sek-1*
AC2396	gcagtgactgaatcgaaacga	*nsy-1*
AC2397	acacggaactcgtagtgactg	*nsy-1*
AC2398	atccacgtagccaactgacaa	*nsy-1*
AC2408	ctgtacggatacggaagaaga	*pmk-1*
YJ12609	tcggattcaggagcgaggtcag	*mak-2*
YJ10840	gggcattgggtaaatgagg	*tir-1*
YJ10841	AGCCTTCTGCATCCACAACT	*tir-1*
YJ10842	gccagctgtcaataccgttt	*tir-1*

Table 8. Chapter 3 CRISPR crRNA sequences

crRNA Target	Sequence
hda-4 5'	3'-GGATGAGTAGGAATAAGGCA-5'
hda-4 3'	5'-GGACACCCGAACGCACTTGG-3'
natc-2 5'	3'-GGCAAGTTCATCGTTGCGTG-5'
natc-2 3'	5'-GGATGATACTCCGGATGAGG-3'
natc-3 5'	3'-GGAAGCCCATCTGAAAGTGCA-5'
natc-3 3'	5'-TGAAAGGAGTCCGATTTCTA-3'

Table 9. Chapter 3 Microscope Settings

Figure	Microscope	Objective	Laser Power (%)	Gain (V)	Exposure Time (ms)
5B, 5C	confocal	63x	3	600	-
5D-5F, 5D'-E'	confocal	10x	1	600	-
8A-C	compound	40x	-	-	500
8D-E	compound	40x	-	-	500
9C-I	compound	10x	-	-	-
9K-M	compound	40x	-	-	500
13A-F,H	confocal	63x	2	650	-
13G,I-L	confocal	63x	1.2	620	-
14A,B	confocal	63x	2	650	-

confocal = Zeiss LSM 800 confocal microscope
compound = Zeiss Axioplan compound microscope

Table 10. Chapter 3 Statistics for Psek-1::GFP Intensity – related to Figure 6

Strain	vs Strain	Difference (AU)	p-Value
cebp-1(0)	WT	0.6	0.92
cebp-1(0) nipi-3(0)	*mak-2(0); cebp-1(0) nipi-3(0)*	1.4	0.01
cebp-1(0) nipi-3(0)	WT	1.4	<.0001
mak-2(0) pmk-1(0); nipi-3(0)	WT	6.1	<.0001
mak-2(0); cebp-1(0) nipi-3(0)	WT	0.0	1.00
mak-2(0); nipi-3(0)	*cebp-1(0) nipi-3(0)*	5.1	<.0001
mak-2(0); nipi-3(0)	*mak-2(0) pmk-1(0); nipi-3(0)*	0.4	1.00
mak-2(0); nipi-3(0)	*mak-2(0); cebp-1(0) nipi-3(0)*	6.4	<.0001
mak-2(0); nipi-3(0)	*nsy-1(0); nipi-3(0)*	0.6	1.00
mak-2(0); nipi-3(0)	*sek-1(0) nipi-3(0)*	0.8	0.77
mak-2(0); nipi-3(0)	*tir-1(0); nipi-3(0)*	0.1	1.00
mak-2(0); nipi-3(0)	WT	6.5	<.0001
nipi-3(0)	*cebp-1(0) nipi-3(0)*	12.7	<.0001
nipi-3(0)	*mak-2(0) pmk-1(0); nipi-3(0)*	8.0	<.0001
nipi-3(0)	*mak-2(0); cebp-1(0) nipi-3(0)*	14.1	<.0001
nipi-3(0)	*mak-2(0); nipi-3(0)*	7.6	<.0001
nipi-3(0)	*nsy-1(0); cebp-1(0) nipi-3(0)*	12.5	<.0001
nipi-3(0)	*nsy-1(0); mak-2(0); nipi-3(0)*	6.6	<.0001
nipi-3(0)	*nsy-1(0); nipi-3(0)*	8.2	<.0001
nipi-3(0)	*nsy-1(0); tir-1(0); nipi-3(0)*	7.9	<.0001
nipi-3(0)	*pmk-1(0); nipi-3(0)*	5.2	<.0001
nipi-3(0)	*sek-1(0) nipi-3(0)*	8.5	<.0001
nipi-3(0)	*tir-1(0); nipi-3(0)*	7.7	<.0001
nipi-3(0)	WT	14.1	<.0001
nsy-1(0); cebp-1(0)	WT	0.1	1.00
nsy-1(0); cebp-1(0) nipi-3(0)	*cebp-1(0) nipi-3(0)*	0.2	1.00
nsy-1(0); cebp-1(0) nipi-3(0)	WT	1.6	<.0001
nsy-1(0); mak-2(0)	WT	0.6	0.97
nsy-1(0); mak-2(0); nipi-3(0)	*mak-2(0); nipi-3(0)*	1.0	0.34
nsy-1(0); mak-2(0); nipi-3(0)	*nsy-1(0); nipi-3(0)*	1.6	0.0004
nsy-1(0); mak-2(0); nipi-3(0)	WT	7.5	<.0001
nsy-1(0); nipi-3(0)	*cebp-1(0) nipi-3(0)*	4.5	<.0001
nsy-1(0); nipi-3(0)	*nsy-1(0); cebp-1(0) nipi-3(0)*	4.3	<.0001
nsy-1(0); nipi-3(0)	*sek-1(0) nipi-3(0)*	0.3	1.00

Table 10. Chapter 3 Statistics for Psek-1::GFP Intensity – related to Figure 6, continued

Strain	vs Strain	Difference (AU)	p-Value
nsy-1(0); nipi-3(0)	WT	5.9	<.0001
nsy-1(0); tir-1(0); nipi-3(0)	*nsy-1(0); cebp-1(0) nipi-3(0)*	4.6	<.0001
nsy-1(0); tir-1(0); nipi-3(0)	*nsy-1(0); nipi-3(0)*	0.3	1.00
nsy-1(0); tir-1(0); nipi-3(0)	WT	6.2	<.0001
pmk-1(0); nipi-3(0)	*cebp-1(0) nipi-3(0)*	7.5	<.0001
pmk-1(0); nipi-3(0)	*mak-2(0) pmk-1(0); nipi-3(0)*	2.8	<.0001
pmk-1(0); nipi-3(0)	*mak-2(0); nipi-3(0)*	2.4	<.0001
pmk-1(0); nipi-3(0)	*nsy-1(0); nipi-3(0)*	3.0	<.0001
pmk-1(0); nipi-3(0)	*sek-1(0) nipi-3(0)*	3.3	<.0001
pmk-1(0); nipi-3(0)	*tir-1(0); nipi-3(0)*	2.5	<.0001
pmk-1(0); nipi-3(0)	WT	8.9	<.0001
sek-1(0) nipi-3(0)	*cebp-1(0) nipi-3(0)*	4.2	<.0001
sek-1(0) nipi-3(0)	WT	5.6	<.0001
tir-1(0); nipi-3(0)	*cebp-1(0) nipi-3(0)*	5.0	<.0001
tir-1(0); nipi-3(0)	*nsy-1(0); nipi-3(0)*	0.5	1.00
tir-1(0); nipi-3(0)	*nsy-1(0); tir-1(0); nipi-3(0)*	0.2	1.00
tir-1(0); nipi-3(0)	*sek-1(0) nipi-3(0)*	0.7	0.93
tir-1(0); nipi-3(0)	WT	6.4	<.0001
WT	*mak-2(0)*	1.5	<.0001
WT	*nsy-1(0)*	1.0	0.05
WT	*nsy-1(0); tir-1(0)*	1.1	0.02
WT	*pmk-1(0)*	1.0	0.03
WT	*sek-1(0)*	0.8	0.39
WT	*tir-1(0)*	0.4	1.00

Table 11. Chapter 3 Statistics for Psek-1::GFP Intensity – related to Figure 9

Strain	vs Strain	Difference (AU)	p-Value
cebp-1(0) nipi-3(0) hda-4(ju1371)	*cebp-1(0) nipi-3(0)*	0.0	1.00
cebp-1(0) nipi-3(0) hda-4(ju1371)	WT	1.4	<.0001
hda-4(0)	*hda-4(ju1371)*	0.1	1.00
hda-4(0)	WT	0.5	0.97
hda-4(ju1371)	WT	0.4	1.00
nipi-3(0)	*cebp-1(0) nipi-3(0) hda-4(ju1371)*	12.7	<.0001
nipi-3(0)	*nipi-3(0) hda-4(0)*	1.8	<.0001
nipi-3(0)	*nipi-3(0) hda-4(ju1371)*	7.0	<.0001
nipi-3(0) hda-4(0)	*hda-4(0)*	11.9	<.0001
nipi-3(0) hda-4(0)	*nipi-3(0) hda-4(ju1371)*	5.2	<.0001
nipi-3(0) hda-4(0)	WT	12.3	<.0001
nipi-3(0) hda-4(ju1371)	*cebp-1(0) nipi-3(0) hda-4(ju1371)*	5.7	<.0001
nipi-3(0) hda-4(ju1371)	*hda-4(ju1371)*	6.8	<.0001
nipi-3(0) hda-4(ju1371)	WT	7.1	<.0001

Table 12. Chapter 3 Statistics for Psek-1::GFP Intensity – related to Figure 10

Strain	vs Strain	Difference (AU)	p-Value
natc-1(0); natc-3(0); nipi-3(0)	*natc-2(0) natc-1(0); cebp-1(0) nipi-3(0)*	5.3	<.0001
natc-1(0); natc-3(0); nipi-3(0)	WT	9.1	<.0001
natc-1(0); nipi-3(0)	*natc-1(0); natc-3(0); nipi-3(0)*	1.0	0.54
natc-1(0); nipi-3(0)	*natc-2(0) natc-1(0); cebp-1(0) nipi-3(0)*	6.2	<.0001
natc-1(0); nipi-3(0)	WT	10.0	<.0001
natc-2(0) natc-1(0)	WT	1.9	<.0001
natc-2(0) natc-1(0); cebp-1(0)	WT	1.6	<.0001
natc-2(0) natc-1(0); cebp-1(0) nipi-3(0)	WT	3.8	<.0001
natc-2(0) natc-1(0); nipi-3(0)	*natc-1(0); natc-3(0); nipi-3(0)*	2.1	<.0001
natc-2(0) natc-1(0); nipi-3(0)	*natc-1(0); nipi-3(0)*	1.2	0.03
natc-2(0) natc-1(0); nipi-3(0)	*natc-2(0) natc-1(0); cebp-1(0) nipi-3(0)*	7.4	<.0001
natc-2(0) natc-1(0); nipi-3(0)	WT	11.2	<.0001
natc-3(0)	WT	1.4	0.0001
natc-3(0); nipi-3(0)	*natc-1(0); natc-3(0); nipi-3(0)*	3.1	<.0001
natc-3(0); nipi-3(0)	*natc-1(0); nipi-3(0)*	2.2	<.0001
natc-3(0); nipi-3(0)	*natc-2(0) natc-1(0); cebp-1(0) nipi-3(0)*	8.4	<.0001
natc-3(0); nipi-3(0)	*natc-2(0) natc-1(0); nipi-3(0)*	1.0	0.21
natc-3(0); nipi-3(0)	WT	12.2	<.0001
nipi-3(0)	*natc-1(0); natc-3(0); nipi-3(0)*	5.0	<.0001
nipi-3(0)	*natc-1(0); nipi-3(0)*	4.1	<.0001
nipi-3(0)	*natc-2(0) natc-1(0); cebp-1(0) nipi-3(0)*	10.3	<.0001
nipi-3(0)	*natc-2(0) natc-1(0); nipi-3(0)*	2.9	<.0001
nipi-3(0)	*natc-3(0); nipi-3(0)*	1.9	<.0001
WT	*natc-1(0)*	0.3	1.00
WT	*natc-1(0); natc-3(0)*	0.3	1.00

Table 13. Chapter 3 Statistics for Body Length – related to Figure 20, p38 pathway

Strain	vs Strain	Difference (µm)	p-Value
cebp-1(0) nipi-3(0)	*mak-2(0); cebp-1(0) nipi-3(0)*	91	0.02
cebp-1(0) nipi-3(0)	*mak-2(0); nipi-3(0)*	251	<.0001
cebp-1(0) nipi-3(0)	*mak-2(tm2927); cebp-1(0) nipi-3(0)*	104	0.001
cebp-1(0) nipi-3(0)	*mak-2(tm2927); nipi-3(0)*	138	<.0001
cebp-1(0) nipi-3(0)	*nipi-3(0)*	749	<.0001
cebp-1(0) nipi-3(0)	*nsy-1(0); nipi-3(0)*	314	<.0001
cebp-1(0) nipi-3(0)	*pmk-1(0); nipi-3(0)*	343	<.0001
cebp-1(0) nipi-3(0)	*sek-1(0) nipi-3(0)*	142	<.0001
cebp-1(0) nipi-3(0)	*tir-1(0); nipi-3(0)*	261	<.0001
mak-2(0) pmk-1(0); nipi-3(0)	*mak-2(0); nipi-3(0)*	136	<.0001
mak-2(0) pmk-1(0); nipi-3(0)	*nipi-3(0)*	634	<.0001
mak-2(0) pmk-1(0); nipi-3(0)	*pmk-1(0); nipi-3(0)*	228	<.0001
mak-2(0); cebp-1(0) nipi-3(0)	*mak-2(0); nipi-3(0)*	159	<.0001
mak-2(0); cebp-1(0) nipi-3(0)	*nipi-3(0)*	658	<.0001
mak-2(0); nipi-3(0)	*nsy-1(0); nipi-3(0)*	63	0.20
mak-2(0); nipi-3(0)	*tir-1(0); nipi-3(0)*	11	1.00
mak-2(0); nipi-3(0)	*nipi-3(0)*	498	<.0001
mak-2(0); nipi-3(0)	*pmk-1(0); nipi-3(0)*	92	0.002
mak-2(tm2927); cebp-1(0) nipi-3(0)	*mak-2(tm2927); nipi-3(0)*	35	1.00
mak-2(tm2927); cebp-1(0) nipi-3(0)	*nipi-3(0)*	645	<.0001
mak-2(tm2927); nipi-3(0)	*nsy-1(0); nipi-3(0)*	176	<.0001
mak-2(tm2927); nipi-3(0)	*sek-1(0) nipi-3(0)*	4	1.00
mak-2(tm2927); nipi-3(0)	*tir-1(0); nipi-3(0)*	123	<.0001
mak-2(tm2927); nipi-3(0)	*mak-2(0); nipi-3(0)*	112	<.0001
mak-2(tm2927); nipi-3(0)	*nipi-3(0)*	611	<.0001
mak-2(tm2927); nipi-3(0)	*pmk-1(0); nipi-3(0)*	205	<.0001
nsy-1(0); nipi-3(0)	*nipi-3(0)*	435	<.0001
nsy-1(0); nipi-3(0)	*pmk-1(0); nipi-3(0)*	29	1.00
nsy-1(0); tir-1(0); nipi-3(0)	*nipi-3(0)*	577	<.0001
nsy-1(0); tir-1(0); nipi-3(0)	*nsy-1(0); nipi-3(0)*	142	<.0001
nsy-1(0); tir-1(0); nipi-3(0)	*tir-1(0); nipi-3(0)*	90	0.003
pmk-1(0); nipi-3(0)	*nipi-3(0)*	406	<.0001
sek-1(0) nipi-3(0)	*mak-2(0); nipi-3(0)*	108	<.0001
sek-1(0) nipi-3(0)	*nipi-3(0)*	607	<.0001
sek-1(0) nipi-3(0)	*nsy-1(0); nipi-3(0)*	172	<.0001
sek-1(0) nipi-3(0)	*pmk-1(0); nipi-3(0)*	201	<.0001

Table 13. Chapter 3 Statistics for Body Length – related to Figure 20, p38 pathway, continued

Strain	vs Strain	Difference (µm)	p-Value
sek-1(0) nipi-3(0)	*tir-1(0); nipi-3(0)*	119	<.0001
tir-1(0); nipi-3(0)	*nipi-3(0)*	488	<.0001
tir-1(0); nipi-3(0)	*pmk-1(0); nipi-3(0)*	82	0.07
tir-1(0); nipi-3(0)	*nsy-1(0); nipi-3(0)*	53	0.83
WT	*cebp-1(0) nipi-3(0)*	9	1.00
WT	*mak-2(0) pmk-1(0); nipi-3(0)*	124	<.0001
WT	*mak-2(0); cebp-1(0) nipi-3(0)*	100	<.0001
WT	*mak-2(0); nipi-3(0)*	259	<.0001
WT	*mak-2(tm2927); cebp-1(0) nipi-3(0)*	112	<.0001
WT	*mak-2(tm2927); nipi-3(0)*	147	<.0001
WT	*nipi-3(0)*	758	<.0001
WT	*nsy-1(0); nipi-3(0)*	323	<.0001
WT	*nsy-1(0); tir-1(0); nipi-3(0)*	180	<.0001
WT	*pmk-1(0); nipi-3(0)*	352	<.0001
WT	*sek-1(0) nipi-3(0)*	151	<.0001
WT	*tir-1(0); nipi-3(0)*	270	<.0001

Table 14. Chapter 3 Statistics for Body Length – related to Figure 20, HDA-4

Strain	vs Strain	Difference (µm)	p-Value
nipi-3(0) hda-4(ju1371)	*nipi-3(0)*	656	<.0001
nipi-3(0) hda-4(ju1371)	*nipi-3(0) hda-4(ju1371); Phda-4::hda-4*	579	<.0001
nipi-3(0) hda-4(ju1371)	*Pcebp-1::cebp-1 nipi-3(0) hda-4(ju1371)*	641	<.0001
nipi-3(0) hda-4(ju1371); Phda-4::hda-4	*nipi-3(0)*	77	0.17
nipi-3(0) hda-4(ju1371); Phda-4::hda-4	*Pcebp-1::cebp-1 nipi-3(0) hda-4(ju1371)*	62	0.48
Pcebp-1::cebp-1 nipi-3(0) hda-4(ju1371)	*nipi-3(0)*	15	1.00
WT	*nipi-3(0)*	758	<.0001
WT	*nipi-3(0) hda-4(ju1371)*	102	<.0001
WT	*nipi-3(0) hda-4(ju1371); Phda-4::hda-4*	681	<.0001
WT	*Pcebp-1::cebp-1 nipi-3(0) hda-4(ju1371)*	743	<.0001

Table 15. Chapter 3 Statistics for Body Length – related to Figure 20, NATC

Strain	vs Strain	Difference (µm)	p-Value
natc-1(0); nipi-3(0)	*natc-3(0); natc-1(0); nipi-3(0)*	58	0.48
natc-1(0); nipi-3(0)	*natc-1(ok2062); nipi-3(0)*	26	1.00
natc-1(0); nipi-3(0)	*natc-2(0) natc-1(0); nipi-3(0)*	23	1.00
natc-1(0); nipi-3(0)	*natc-2(0); nipi-3(0)*	8	1.00
natc-1(0); nipi-3(0)	*nipi-3(0)*	287	<.0001
natc-1(0); nipi-3(0)	*natc-3(0); nipi-3(0)*	129	<.0001
natc-1(ok2062); nipi-3(0)	*natc-3(0); natc-1(0); nipi-3(0)*	32	1.00
natc-1(ok2062); nipi-3(0)	*nipi-3(0)*	262	<.0001
natc-1(ok2062); nipi-3(0)	*natc-3(0); nipi-3(0)*	103	<.0001
natc-2(0) natc-1(0); nipi-3(0)	*natc-3(0); natc-1(0); nipi-3(0)*	35	1.00
natc-2(0) natc-1(0); nipi-3(0)	*nipi-3(0)*	265	<.0001
natc-2(0) natc-1(0); nipi-3(0)	*natc-3(0); nipi-3(0)*	106	<.0001
natc-2(ju1369); nipi-3(0)	*natc-3(0); natc-2(0) natc-1(0); nipi-3(0)*	66	0.48
natc-2(ju1369); nipi-3(0)	*nipi-3(0)*	422	<.0001
natc-2(ju1369); nipi-3(0)	*natc-3(0); nipi-3(0)*	263	<.0001
natc-2(ju1369); nipi-3(0)	*natc-3(0); natc-1(0); nipi-3(0)*	192	<.0001
natc-2(ju1369); nipi-3(0)	*natc-1(ok2062); nipi-3(0)*	160	<.0001
natc-2(ju1369); nipi-3(0)	*natc-2(0) natc-1(0); nipi-3(0)*	157	<.0001
natc-2(ju1369); nipi-3(0)	*natc-2(0); nipi-3(0)*	142	<.0001
natc-2(ju1369); nipi-3(0)	*natc-1(0); nipi-3(0)*	134	<.0001
natc-2(0); nipi-3(0)	*natc-3(0); natc-1(0); nipi-3(0)*	50	0.98
natc-2(0); nipi-3(0)	*natc-1(ok2062); nipi-3(0)*	18	1.00
natc-2(0); nipi-3(0)	*natc-2(0) natc-1(0); nipi-3(0)*	15	1.00
natc-2(0); nipi-3(0)	*nipi-3(0)*	280	<.0001
natc-2(0); nipi-3(0)	*natc-3(0); nipi-3(0)*	121	<.0001
natc-3(0); natc-1(0); nipi-3(0)	*natc-3(0); nipi-3(0)*	71	0.07
natc-3(0); natc-1(0); nipi-3(0)	*nipi-3(0)*	229	<.0001
natc-3(0); natc-2(0) natc-1(0); nipi-3(0)	*natc-2(0) natc-1(0); nipi-3(0)*	91	0.00
natc-3(0); natc-2(0) natc-1(0); nipi-3(0)	*natc-1(0); nipi-3(0)*	68	0.06
natc-3(0); natc-2(0) natc-1(0); nipi-3(0)	*natc-2(0); nipi-3(0)*	76	0.14
natc-3(0); natc-2(0) natc-1(0); nipi-3(0)	*nipi-3(0)*	356	<.0001
natc-3(0); natc-2(0) natc-1(0); nipi-3(0)	*natc-3(0); nipi-3(0)*	197	<.0001
natc-3(0); natc-2(0) natc-1(0); nipi-3(0)	*natc-3(0); natc-1(0); nipi-3(0)*	126	<.0001
natc-3(0); natc-2(0) natc-1(0); nipi-3(0)	*natc-1(ok2062); nipi-3(0)*	94	<.0001
natc-3(0); nipi-3(0)	*nipi-3(0)*	158	<.0001

Table 15. Chapter 3 Statistics for Body Length – related to Figure 20, NATC, continued

Strain	vs Strain	Difference (µm)	p-Value
natc-3(0); pmk-1(0); nipi-3(0)	*nipi-3(0)*	496	<.0001
natc-3(0); pmk-1(0); nipi-3(0)	*natc-3(0); nipi-3(0)*	338	<.0001
WT	*nipi-3(0)*	716	<.0001
WT	*natc-3(0); nipi-3(0)*	557	<.0001
WT	*natc-3(0); natc-1(0); nipi-3(0)*	486	<.0001
WT	*natc-1(ok2062); nipi-3(0)*	454	<.0001
WT	*natc-2(0) natc-1(0); nipi-3(0)*	451	<.0001
WT	*natc-2(0); nipi-3(0)*	436	<.0001
WT	*natc-1(0); nipi-3(0)*	428	<.0001
WT	*natc-3(0); natc-2(0) natc-1(0); nipi-3(0)*	360	<.0001
WT	*natc-2(ju1369); nipi-3(0)*	294	<.0001
WT	*natc-3(0); pmk-1(0); nipi-3(0)*	219	<.0001

Table 16. Chapter 3 Statistics for Body Length – related to Figure 21

Strain	vs Strain	Difference (μm)	p-Value
cebp-1(0)	*mak-2(0)*	261	<.0001
cebp-1(0)	*nsy-1(0)*	22	1.00
cebp-1(0)	*sek-1(0)*	242	<.0001
cebp-1(0)	*tir-1(0)*	131	<.0001
natc-1(0)	*natc-1(ok2062)*	218	<.0001
natc-1(0)	*natc-2(0) natc-1(0)*	19	1.00
natc-1(0)	*natc-2(ju1369)*	54	0.87
natc-1(0)	*natc-3(0); natc-1(0)*	59	0.69
natc-2(0) natc-1(0)	*natc-1(ok2062)*	199	<.0001
natc-2(0) natc-1(0)	*natc-2(ju1369)*	35	1.00
natc-2(0) natc-1(0)	*natc-3(0); natc-1(0)*	41	1.00
natc-2(ju1369)	*natc-1(ok2062)*	164	<.0001
natc-2(ju1369)	*natc-3(0); natc-1(0)*	5	1.00
natc-3(0)	*natc-1(0)*	70	0.28
natc-3(0)	*natc-1(ok2062)*	288	<.0001
natc-3(0)	*natc-2(0) natc-1(0)*	89	0.01
natc-3(0)	*natc-2(ju1369)*	124	<.0001
natc-3(0)	*natc-3(0); natc-1(0)*	130	<.0001
natc-3(0)	WT	53	0.65
nsy-1(0)	*mak-2(0)*	238	<.0001
nsy-1(0)	*sek-1(0)*	220	<.0001
nsy-1(0)	*tir-1(0)*	109	<.0001
pmk-1(0)	*cebp-1(0)*	37	0.99
pmk-1(0)	*mak-2(0)*	298	<.0001
pmk-1(0)	*nsy-1(0)*	59	0.41
pmk-1(0)	*sek-1(0)*	279	<.0001
pmk-1(0)	*tir-1(0)*	168	<.0001
pmk-1(0)	WT	7	1.00
sek-1(0)	*mak-2(0)*	19	1.00
tir-1(0)	*mak-2(0)*	130	<.0001
tir-1(0)	*sek-1(0)*	111	<.0001
WT	*cebp-1(0)*	30	1.00
WT	*hda-4(0)*	121	<.0001
WT	*mak-2(0)*	291	<.0001
WT	*natc-1(0)*	17	1.00

Table 16. Chapter 3 Statistics for Body Length – related to Figure 21, continued

Strain	vs Strain	Difference (µm)	p-Value
WT	*natc-1(ok2062)*	235	<.0001
WT	*natc-2(0) natc-1(0)*	36	0.99
WT	*natc-2(ju1369)*	71	0.05
WT	*natc-3(0); natc-1(0)*	77	0.02
WT	*nsy-1(0)*	53	0.72
WT	*sek-1(0)*	272	<.0001
WT	*tir-1(0)*	162	<.0001

References

Afgan, E., Baker, D., van den Beek, M., Blankenberg, D., Bouvier, D., Cech, M., Chilton, J., Clements, D., Coraor, N., Eberhard, C., Gruning, B., Guerler, A., Hillman-Jackson, J., Von Kuster, G., Rasche, E., Soranzo, N., Turaga, N., Taylor, J., Nekrutenko, A. and Goecks, J. (2016). The Galaxy platform for accessible, reproducible and collaborative biomedical analyses: 2016 update. *Nucleic Acids Res* **44**: W3-W10. doi: 10.1093/nar/gkw343.

Aksnes, H., Drazic, A., Marie, M. and Arnesen, T. (2016). First Things First: Vital Protein Marks by N-Terminal Acetyltransferases. *Trends Biochem Sci* **41**: 746-760. doi: 10.1016/j.tibs.2016.07.005.

Aksnes, H., Ree, R. and Arnesen, T. (2019). Co-translational, Post-translational, and Non-catalytic Roles of N-Terminal Acetyltransferases. *Mol Cell* **73**: 1097-1114. doi: 10.1016/j.molcel.2019.02.007.

Andrusiak, M. G. and Jin, Y. (2016). Context Specificity of Stress-activated Mitogen-activated Protein (MAP) Kinase Signaling: The Story as Told by Caenorhabditis elegans. *J Biol Chem* **291**: 7796-7804. doi: 10.1074/jbc.R115.711101.

Arnesen, T., Van Damme, P., Polevoda, B., Helsens, K., Evjenth, R., Colaert, N., Varhaug, J. E., Vandekerckhove, J., Lillehaug, J. R., Sherman, F. and Gevaert, K. (2009). Proteomics analyses reveal the evolutionary conservation and divergence of N-terminal acetyltransferases from yeast and humans. *Proc Natl Acad Sci U S A* **106**: 8157-8162. doi: 10.1073/pnas.0901931106.

Aude-Garcia, C., Collin-Faure, V., Bausinger, H., Hanau, D., Rabilloud, T. and Lemercier, C. (2010). Dual roles for MEF2A and MEF2D during human macrophage terminal differentiation and c-Jun expression. *Biochem J* **430**: 237-244. doi: 10.1042/BJ20100131.

Brenner, S. (1974). The genetics of Caenorhabditis elegans. *Genetics* **77**: 71-94. doi: 10.1093/genetics/77.1.71.

Brown, J. L. (1979). A comparison of the turnover of alpha-N-acetylated and nonacetylated mouse L-cell proteins. *J Biol Chem* **254**: 1447-1449.

Bruinsma, J. J., Schneider, D. L., Davis, D. E. and Kornfeld, K. (2008). Identification of mutations in Caenorhabditis elegans that cause resistance to high levels of dietary zinc and analysis using a genomewide map of single nucleotide polymorphisms scored by pyrosequencing. *Genetics* **179**: 811-828. doi: 10.1534/genetics.107.084384.

Cannell, I. G., Merrick, K. A., Morandell, S., Zhu, C. Q., Braun, C. J., Grant, R. A., Cameron, E. R., Tsao, M. S., Hemann, M. T. and Yaffe, M. B. (2015). A Pleiotropic RNA-Binding Protein Controls Distinct Cell Cycle Checkpoints to Drive Resistance of p53-Defective Tumors to Chemotherapy. *Cancer Cell* **28**: 831. doi: 10.1016/j.ccell.2015.11.003.

Canovas, B. and Nebreda, A. R. (2021). Diversity and versatility of p38 kinase signalling in health and disease. *Nat Rev Mol Cell Biol* **22**: 346-366. doi: 10.1038/s41580-020-00322-w.

Cheesman, H. K., Feinbaum, R. L., Thekkiniath, J., Dowen, R. H., Conery, A. L. and Pukkila-Worley, R. (2016). Aberrant Activation of p38 MAP Kinase-Dependent Innate Immune Responses Is Toxic to Caenorhabditis elegans. *G3 (Bethesda)* **6**: 541-549. doi: 10.1534/g3.115.025650.

Chen, D., Zhang, J., Minnerly, J., Kaul, T., Riddle, D. L. and Jia, K. (2014). daf-31 encodes the catalytic subunit of N alpha-acetyltransferase that regulates Caenorhabditis elegans development, metabolism and adult lifespan. *PLoS Genet* **10**: e1004699. doi: 10.1371/journal.pgen.1004699.

Chen, J., Ren, Y., Gui, C., Zhao, M., Wu, X., Mao, K., Li, W. and Zou, F. (2018). Phosphorylation of Parkin at serine 131 by p38 MAPK promotes mitochondrial dysfunction and neuronal death in mutant A53T alpha-synuclein model of Parkinson's disease. *Cell Death Dis* **9**: 700. doi: 10.1038/s41419-018-0722-7.

Chuang, C. F. and Bargmann, C. I. (2005). A Toll-interleukin 1 repeat protein at the synapse specifies asymmetric odorant receptor expression via ASK1 MAPKKK signaling. *Genes Dev* **19**: 270-281. doi: 10.1101/gad.1276505.

Colie, S., Sarroca, S., Palenzuela, R., Garcia, I., Matheu, A., Corpas, R., Dotti, C. G., Esteban, J. A., Sanfeliu, C. and Nebreda, A. R. (2017). Neuronal p38alpha mediates synaptic and cognitive dysfunction in an Alzheimer's mouse model by controlling beta-amyloid production. *Sci Rep* **7**: 45306. doi: 10.1038/srep45306.

Consortium, C. e. D. M. (2012). large-scale screening for targeted knockouts in the Caenorhabditis elegans genome. *G3 (Bethesda)* **2**: 1415-1425. doi: 10.1534/g3.112.003830.

Couillault, C., Fourquet, P., Pophillat, M. and Ewbank, J. J. (2012). A UPR-independent infection-specific role for a BiP/GRP78 protein in the control of antimicrobial peptide expression in C. elegans epidermis. *Virulence* **3**: 299-308. doi: 10.4161/viru.20384.

D'Souza, S. A., Rajendran, L., Bagg, R., Barbier, L., van Pel, D. M., Moshiri, H. and Roy, P. J. (2016). The MADD-3 LAMMER Kinase Interacts with a p38 MAP Kinase Pathway to Regulate the Display of the EVA-1 Guidance Receptor in Caenorhabditis elegans. *PLoS Genet* **12**: e1006010. doi: 10.1371/journal.pgen.1006010.

De Arras, L., Laws, R., Leach, S. M., Pontis, K., Freedman, J. H., Schwartz, D. A. and Alper, S. (2014). Comparative genomics RNAi screen identifies Eftud2 as a novel regulator of innate immunity. *Genetics* **197**: 485-496. doi: 10.1534/genetics.113.160499.

Dickinson, D. J., Pani, A. M., Heppert, J. K., Higgins, C. D. and Goldstein, B. (2015). Streamlined Genome Engineering with a Self-Excising Drug Selection Cassette. *Genetics* **200**: 1035-1049. doi: 10.1534/genetics.115.178335.

Dolado, I. and Nebreda, A. R. (2008). AKT and oxidative stress team up to kill cancer cells. *Cancer Cell* **14**: 427-429. doi: 10.1016/j.ccr.2008.11.006.

Dolado, I., Swat, A., Ajenjo, N., De Vita, G., Cuadrado, A. and Nebreda, A. R. (2007). p38alpha MAP kinase as a sensor of reactive oxygen species in tumorigenesis. *Cancer Cell* **11**: 191-205. doi: 10.1016/j.ccr.2006.12.013.

Engelman, J. A., Lisanti, M. P. and Scherer, P. E. (1998). Specific inhibitors of p38 mitogen-activated protein kinase block 3T3-L1 adipogenesis. *J Biol Chem* **273**: 32111-32120. doi: 10.1074/jbc.273.48.32111.

Ermolaeva, M. A. and Schumacher, B. (2014). Insights from the worm: the C. elegans model for innate immunity. *Semin Immunol* **26**: 303-309. doi: 10.1016/j.smim.2014.04.005.

Fischle, W., Dequiedt, F., Hendzel, M. J., Guenther, M. G., Lazar, M. A., Voelter, W. and Verdin, E. (2002). Enzymatic activity associated with class II HDACs is dependent on a multiprotein complex containing HDAC3 and SMRT/N-CoR. *Mol Cell* **9**: 45-57. doi: 10.1016/s1097-2765(01)00429-4.

Forte, G. M., Pool, M. R. and Stirling, C. J. (2011). N-terminal acetylation inhibits protein targeting to the endoplasmic reticulum. *PLoS Biol* **9**: e1001073. doi: 10.1371/journal.pbio.1001073.

Foster, K. J., Cheesman, H. K., Liu, P., Peterson, N. D., Anderson, S. M. and Pukkila-Worley, R. (2020). Innate Immunity in the C. elegans Intestine Is Programmed by a Neuronal Regulator of AWC Olfactory Neuron Development. *Cell Rep* **31**: 107478. doi: 10.1016/j.celrep.2020.03.042.

Freshney, N. W., Rawlinson, L., Guesdon, F., Jones, E., Cowley, S., Hsuan, J. and Saklatvala, J. (1994). Interleukin-1 activates a novel protein kinase cascade that results in the phosphorylation of Hsp27. *Cell* **78**: 1039-1049. doi: 10.1016/0092-8674(94)90278-x.

Friedland, A. E., Tzur, Y. B., Esvelt, K. M., Colaiacovo, M. P., Church, G. M. and Calarco, J. A. (2013). Heritable genome editing in C. elegans via a CRISPR-Cas9 system. *Nat Methods* **10**: 741-743. doi: 10.1038/nmeth.2532.

Fuhrman, L. E., Goel, A. K., Smith, J., Shianna, K. V. and Aballay, A. (2009). Nucleolar proteins suppress Caenorhabditis elegans innate immunity by inhibiting p53/CEP-1. *PLoS Genet* **5**: e1000657. doi: 10.1371/journal.pgen.1000657.

Gaestel, M. (2006). MAPKAP kinases - MKs - two's company, three's a crowd. *Nat Rev Mol Cell Biol* **7**: 120-130. doi: 10.1038/nrm1834.

Gao, J., Barroso, C., Zhang, P., Kim, H. M., Li, S., Labrador, L., Lightfoot, J., Gerashchenko, M. V., Labunskyy, V. M., Dong, M. Q., Martinez-Perez, E. and Colaiacovo, M. P. (2016). N-terminal acetylation promotes synaptonemal complex assembly in C. elegans. *Genes Dev* **30**: 2404-2416. doi: 10.1101/gad.277350.116.

Gao, J., Kim, H. M., Elia, A. E., Elledge, S. J. and Colaiacovo, M. P. (2015). NatB domain-containing CRA-1 antagonizes hydrolase ACER-1 linking acetyl-CoA

metabolism to the initiation of recombination during C. elegans meiosis. *PLoS Genet* **11**: e1005029. doi: 10.1371/journal.pgen.1005029.

Garcia-Sanchez, J. A., Ewbank, J. J. and Visvikis, O. (2021). Ubiquitin-related processes and innate immunity in C. elegans. *Cell Mol Life Sci* **78**: 4305-4333. doi: 10.1007/s00018-021-03787-w.

Glass, G. V., Peckham, P. D. and Sanders, J. R. (2016). Consequences of Failure to Meet Assumptions Underlying the Fixed Effects Analyses of Variance and Covariance. *Review of Educational Research* **42**: 237-288. doi: 10.3102/00346543042003237.

Glise, B., Bourbon, H. and Noselli, S. (1995). hemipterous encodes a novel Drosophila MAP kinase kinase, required for epithelial cell sheet movement. *Cell* **83**: 451-461. doi: 10.1016/0092-8674(95)90123-x.

Grimes, J. M. and Grimes, K. V. (2020). p38 MAPK inhibition: A promising therapeutic approach for COVID-19. *J Mol Cell Cardiol* **144**: 63-65. doi: 10.1016/j.yjmcc.2020.05.007.

Growcott, E. J., Bamba, D., Galarneau, J. R., Leonard, V. H. J., Schul, W., Stein, D. and Osborne, C. S. (2018). The effect of P38 MAP kinase inhibition in a mouse model of influenza. *J Med Microbiol* **67**: 452-462. doi: 10.1099/jmm.0.000684.

Grubbs, J. J., Lopes, L. E., van der Linden, A. M. and Raizen, D. M. (2020). A salt-induced kinase is required for the metabolic regulation of sleep. *PLoS Biol* **18**: e3000220. doi: 10.1371/journal.pbio.3000220.

Gubern, A., Joaquin, M., Marques, M., Maseres, P., Garcia-Garcia, J., Amat, R., Gonzalez-Nunez, D., Oliva, B., Real, F. X., de Nadal, E. and Posas, F. (2016). The N-Terminal Phosphorylation of RB by p38 Bypasses Its Inactivation by CDKs and Prevents Proliferation in Cancer Cells. *Mol Cell* **64**: 25-36. doi: 10.1016/j.molcel.2016.08.015.

Gupta, J. and Nebreda, A. R. (2015). Roles of p38alpha mitogen-activated protein kinase in mouse models of inflammatory diseases and cancer. *FEBS J* **282**: 1841-1857. doi: 10.1111/febs.13250.

Gurgis, F. M., Ziaziaris, W. and Munoz, L. (2014). Mitogen-activated protein kinase-activated protein kinase 2 in neuroinflammation, heat shock protein 27 phosphorylation, and cell cycle: role and targeting. *Mol Pharmacol* **85**: 345-356. doi: 10.1124/mol.113.090365.

Haberland, M., Montgomery, R. L. and Olson, E. N. (2009). The many roles of histone deacetylases in development and physiology: implications for disease and therapy. *Nat Rev Genet* **10**: 32-42. doi: 10.1038/nrg2485.

Harding, B. W. and Ewbank, J. J. (2021). An integrated view of innate immune mechanisms in C. elegans. *Biochem Soc Trans* **49**: 2307-2317. doi: 10.1042/BST20210399.

Harris, S. L. and Levine, A. J. (2005). The p53 pathway: positive and negative feedback loops. *Oncogene* **24**: 2899-2908. doi: 10.1038/sj.onc.1208615.

Harwell, M. R., Rubinstein, E. N., Hayes, W. S. and Olds, C. C. (2016). Summarizing Monte Carlo Results in Methodological Research: The One- and Two-Factor Fixed Effects ANOVA Cases. *Journal of Educational Statistics* **17**: 315-339. doi: 10.3102/10769986017004315.

Hayakawa, M., Hayakawa, H., Petrova, T., Ritprajak, P., Sutavani, R. V., Jimenez-Andrade, G. Y., Sano, Y., Choo, M. K., Seavitt, J., Venigalla, R. K. C., Otsu, K., Georgopoulos, K., Arthur, J. S. C. and Park, J. M. (2017). Loss of Functionally Redundant p38 Isoforms in T Cells Enhances Regulatory T Cell Induction. *J Biol Chem* **292**: 1762-1772. doi: 10.1074/jbc.M116.764548.

Hensley, K., Floyd, R. A., Zheng, N. Y., Nael, R., Robinson, K. A., Nguyen, X., Pye, Q. N., Stewart, C. A., Geddes, J., Markesbery, W. R., Patel, E., Johnson, G. V. and Bing, G. (1999). p38 kinase is activated in the Alzheimer's disease brain. *J Neurochem* **72**: 2053-2058. doi: 10.1046/j.1471-4159.1999.0722053.x.

Holmes, W. M., Mannakee, B. K., Gutenkunst, R. N. and Serio, T. R. (2014). Loss of amino-terminal acetylation suppresses a prion phenotype by modulating global protein folding. *Nat Commun* **5**: 4383. doi: 10.1038/ncomms5383.

Hwang, C. S., Shemorry, A. and Varshavsky, A. (2010). N-terminal acetylation of cellular proteins creates specific degradation signals. *Science* **327**: 973-977. doi: 10.1126/science.1183147.

Iatsenko, I., Sinha, A., Rodelsperger, C. and Sommer, R. J. (2013). New role for DCR-1/dicer in Caenorhabditis elegans innate immunity against the highly virulent bacterium Bacillus thuringiensis DB27. *Infect Immun* **81**: 3942-3957. doi: 10.1128/IAI.00700-13.

Jornvall, H. (1975). Acetylation of Protein N-terminal amino groups structural observations on alpha-amino acetylated proteins. *J Theor Biol* **55**: 1-12. doi: 10.1016/s0022-5193(75)80105-6.

Joshi, S. and Platanias, L. C. (2014). Mnk kinase pathway: Cellular functions and biological outcomes. *World J Biol Chem* **5**: 321-333. doi: 10.4331/wjbc.v5.i3.321.

Kim, K. W., Thakur, N., Piggott, C. A., Omi, S., Polanowska, J., Jin, Y. and Pujol, N. (2016). Coordinated inhibition of C/EBP by Tribbles in multiple tissues is essential for Caenorhabditis elegans development. *BMC Biol* **14**: 104. doi: 10.1186/s12915-016-0320-z.

Kockel, L., Zeitlinger, J., Staszewski, L. M., Mlodzik, M. and Bohmann, D. (1997). Jun in Drosophila development: redundant and nonredundant functions and regulation by two MAPK signal transduction pathways. *Genes Dev* **11**: 1748-1758. doi: 10.1101/gad.11.13.1748.

Lahm, A., Paolini, C., Pallaoro, M., Nardi, M. C., Jones, P., Neddermann, P., Sambucini, S., Bottomley, M. J., Lo Surdo, P., Carfi, A., Koch, U., De Francesco, R., Steinkuhler, C. and Gallinari, P. (2007). Unraveling the hidden catalytic activity of vertebrate class IIa histone deacetylases. *Proc Natl Acad Sci U S A* **104**: 17335-17340. doi: 10.1073/pnas.0706487104.

Li, H. and Durbin, R. (2009). Fast and accurate short read alignment with Burrows-Wheeler transform. *Bioinformatics* **25**: 1754-1760. doi: 10.1093/bioinformatics/btp324.

Li, H., Handsaker, B., Wysoker, A., Fennell, T., Ruan, J., Homer, N., Marth, G., Abecasis, G., Durbin, R. and Genome Project Data Processing, S. (2009). The Sequence Alignment/Map format and SAMtools. *Bioinformatics* **25**: 2078-2079. doi: 10.1093/bioinformatics/btp352.

Lin, J., Lee, D., Choi, Y. and Lee, S. Y. (2015). The scaffold protein RACK1 mediates the RANKL-dependent activation of p38 MAPK in osteoclast precursors. *Sci Signal* **8**: ra54. doi: 10.1126/scisignal.2005867.

Lix, L. M., Keselman, J. C. and Keselman, H. J. (1996). Consequences of Assumption Violations Revisited: A Quantitative Review of Alternatives to the One-Way Analysis of Variance "F" Test. *Review of Educational Research* **66**: 579-619. doi: 10.2307/1170654.

Lu, J., McKinsey, T. A., Nicol, R. L. and Olson, E. N. (2000). Signal-dependent activation of the MEF2 transcription factor by dissociation from histone deacetylases. *Proc Natl Acad Sci U S A* **97**: 4070-4075. doi: 10.1073/pnas.080064097.

Malone, E. A. and Thomas, J. H. (1994). A screen for nonconditional dauer-constitutive mutations in Caenorhabditis elegans. *Genetics* **136**: 879-886. doi: 10.1093/genetics/136.3.879.

Mathias, R. A., Guise, A. J. and Cristea, I. M. (2015). Post-translational modifications regulate class IIa histone deacetylase (HDAC) function in health and disease. *Mol Cell Proteomics* **14**: 456-470. doi: 10.1074/mcp.O114.046565.

McEwan, D. L., Feinbaum, R. L., Stroustrup, N., Haas, W., Conery, A. L., Anselmo, A., Sadreyev, R. and Ausubel, F. M. (2016). Tribbles ortholog NIPI-3 and bZIP transcription factor CEBP-1 regulate a Caenorhabditis elegans intestinal immune surveillance pathway. *BMC Biol* **14**: 105. doi: 10.1186/s12915-016-0334-6.

Mello, C. C., Kramer, J. M., Stinchcomb, D. and Ambros, V. (1991). Efficient gene transfer in C.elegans: extrachromosomal maintenance and integration of transforming sequences. *EMBO J* **10**: 3959-3970.

Mishra, S. K. and Thakran, P. (2018). Intron specificity in pre-mRNA splicing. *Curr Genet* **64**: 777-784. doi: 10.1007/s00294-017-0802-8.

Miska, E. A., Karlsson, C., Langley, E., Nielsen, S. J., Pines, J. and Kouzarides, T. (1999). HDAC4 deacetylase associates with and represses the MEF2 transcription factor. *EMBO J* **18**: 5099-5107. doi: 10.1093/emboj/18.18.5099.

Munkacsy, E., Khan, M. H., Lane, R. K., Borror, M. B., Park, J. H., Bokov, A. F., Fisher, A. L., Link, C. D. and Rea, S. L. (2016). DLK-1, SEK-3 and PMK-3 Are Required for the Life Extension Induced by Mitochondrial Bioenergetic Disruption in C. elegans. *PLoS Genet* **12**: e1006133. doi: 10.1371/journal.pgen.1006133.

Muranen, T., Selfors, L. M., Hwang, J., Gallegos, L. L., Coloff, J. L., Thoreen, C. C., Kang, S. A., Sabatini, D. M., Mills, G. B. and Brugge, J. S. (2016). ERK and p38 MAPK Activities Determine Sensitivity to PI3K/mTOR Inhibition via Regulation of MYC and YAP. *Cancer Res* **76**: 7168-7180. doi: 10.1158/0008-5472.CAN-16-0155.

Murthi, A. and Hopper, A. K. (2005). Genome-wide screen for inner nuclear membrane protein targeting in Saccharomyces cerevisiae: roles for N-acetylation and an integral membrane protein. *Genetics* **170**: 1553-1560. doi: 10.1534/genetics.105.043620.

Nikooei, T., McDonagh, A. and A, M. v. d. L. (2020). The salt-inducible kinase KIN-29 regulates lifespan via the class II histone-deacetylase HDA-4. *MicroPubl Biol* **2020**. doi: 10.17912/micropub.biology.000289.

Pagano, D. J., Kingston, E. R. and Kim, D. H. (2015). Tissue expression pattern of PMK-2 p38 MAPK is established by the miR-58 family in C. elegans. *PLoS Genet* **11**: e1004997. doi: 10.1371/journal.pgen.1004997.

Paix, A., Folkmann, A., Rasoloson, D. and Seydoux, G. (2015). High Efficiency, Homology-Directed Genome Editing in Caenorhabditis elegans Using CRISPR-Cas9 Ribonucleoprotein Complexes. *Genetics* **201**: 47-54. doi: 10.1534/genetics.115.179382.

Persson, B., Flinta, C., von Heijne, G. and Jornvall, H. (1985). Structures of N-terminally acetylated proteins. *Eur J Biochem* **152**: 523-527. doi: 10.1111/j.1432-1033.1985.tb09227.x.

Phong, M. S., Van Horn, R. D., Li, S., Tucker-Kellogg, G., Surana, U. and Ye, X. S. (2010). p38 mitogen-activated protein kinase promotes cell survival in response to DNA damage but is not required for the G(2) DNA damage checkpoint in human cancer cells. *Mol Cell Biol* **30**: 3816-3826. doi: 10.1128/MCB.00949-09.

Pillai, V. B., Sundaresan, N. R., Samant, S. A., Wolfgeher, D., Trivedi, C. M. and Gupta, M. P. (2011). Acetylation of a conserved lysine residue in the ATP binding pocket of p38

augments its kinase activity during hypertrophy of cardiomyocytes. *Mol Cell Biol* **31**: 2349-2363. doi: 10.1128/MCB.01205-10.

Porter, N. J. and Christianson, D. W. (2019). Structure, mechanism, and inhibition of the zinc-dependent histone deacetylases. *Curr Opin Struct Biol* **59**: 9-18. doi: 10.1016/j.sbi.2019.01.004.

Pujol, N., Cypowyj, S., Ziegler, K., Millet, A., Astrain, A., Goncharov, A., Jin, Y., Chisholm, A. D. and Ewbank, J. J. (2008). Distinct innate immune responses to infection and wounding in the C. elegans epidermis. *Curr Biol* **18**: 481-489. doi: 10.1016/j.cub.2008.02.079.

Pukkila-Worley, R., Feinbaum, R., Kirienko, N. V., Larkins-Ford, J., Conery, A. L. and Ausubel, F. M. (2012). Stimulation of host immune defenses by a small molecule protects C. elegans from bacterial infection. *PLoS Genet* **8**: e1002733. doi: 10.1371/journal.pgen.1002733.

Qiao, L., MacDougald, O. A. and Shao, J. (2006). CCAAT/enhancer-binding protein alpha mediates induction of hepatic phosphoenolpyruvate carboxykinase by p38 mitogen-activated protein kinase. *J Biol Chem* **281**: 24390-24397. doi: 10.1074/jbc.M603038200.

Reyskens, K. M. and Arthur, J. S. (2016). Emerging Roles of the Mitogen and Stress Activated Kinases MSK1 and MSK2. *Front Cell Dev Biol* **4**: 56. doi: 10.3389/fcell.2016.00056.

Riddle, D. L. and Albert, P. S. (1997). Genetic and Environmental Regulation of Dauer Larva Development. C. elegans II. nd, D. L. Riddle, T. Blumenthal, B. J. Meyer and J. R. Priess. Cold Spring Harbor (NY).

Rouse, J., Cohen, P., Trigon, S., Morange, M., Alonso-Llamazares, A., Zamanillo, D., Hunt, T. and Nebreda, A. R. (1994). A novel kinase cascade triggered by stress and heat shock that stimulates MAPKAP kinase-2 and phosphorylation of the small heat shock proteins. *Cell* **78**: 1027-1037. doi: 10.1016/0092-8674(94)90277-1.

Roux, P. P. and Blenis, J. (2004). ERK and p38 MAPK-activated protein kinases: a family of protein kinases with diverse biological functions. *Microbiol Mol Biol Rev* **68**: 320-344. doi: 10.1128/MMBR.68.2.320-344.2004.

Sabio, G. and Davis, R. J. (2014). TNF and MAP kinase signalling pathways. *Semin Immunol* **26**: 237-245. doi: 10.1016/j.smim.2014.02.009.

Sagasti, A., Hisamoto, N., Hyodo, J., Tanaka-Hino, M., Matsumoto, K. and Bargmann, C. I. (2001). The CaMKII UNC-43 activates the MAPKKK NSY-1 to execute a lateral signaling decision required for asymmetric olfactory neuron fates. *Cell* **105**: 221-232. doi: 10.1016/s0092-8674(01)00313-0.

Sakia, R. M. (1992). The Box-Cox Transformation Technique A Review. *Journal of the Royal Statistical Society* **41**: 169-178.

Sapkota, G. P. (2013). The TGFbeta-induced phosphorylation and activation of p38 mitogen-activated protein kinase is mediated by MAP3K4 and MAP3K10 but not TAK1. *Open Biol* **3**: 130067. doi: 10.1098/rsob.130067.

Sarin, S., Prabhu, S., O'Meara, M. M., Pe'er, I. and Hobert, O. (2008). Caenorhabditis elegans mutant allele identification by whole-genome sequencing. *Nat Methods* **5**: 865-867. doi: 10.1038/nmeth.1249.

Sarov, M., Schneider, S., Pozniakovski, A., Roguev, A., Ernst, S., Zhang, Y., Hyman, A. A. and Stewart, A. F. (2006). A recombineering pipeline for functional genomics applied to Caenorhabditis elegans. *Nat Methods* **3**: 839-844. doi: 10.1038/nmeth933.

Scott, D. C., Monda, J. K., Bennett, E. J., Harper, J. W. and Schulman, B. A. (2011). N-terminal acetylation acts as an avidity enhancer within an interconnected multiprotein complex. *Science* **334**: 674-678. doi: 10.1126/science.1209307.

Seo, H. W., Kim, E. J., Na, H. and Lee, M. O. (2009). Transcriptional activation of hypoxia-inducible factor-1alpha by HDAC4 and HDAC5 involves differential recruitment of p300 and FIH-1. *FEBS Lett* **583**: 55-60. doi: 10.1016/j.febslet.2008.11.044.

Shin, H., Kaplan, R. E. W., Duong, T., Fakieh, R. and Reiner, D. J. (2018). Ral Signals through a MAP4 Kinase-p38 MAP Kinase Cascade in C. elegans Cell Fate Patterning. *Cell Rep* **24**: 2669-2681 e2665. doi: 10.1016/j.celrep.2018.08.011.

Shivers, R. P., Pagano, D. J., Kooistra, T., Richardson, C. E., Reddy, K. C., Whitney, J. K., Kamanzi, O., Matsumoto, K., Hisamoto, N. and Kim, D. H. (2010). Phosphorylation

of the conserved transcription factor ATF-7 by PMK-1 p38 MAPK regulates innate immunity in Caenorhabditis elegans. *PLoS Genet* **6**: e1000892. doi: 10.1371/journal.pgen.1000892.

Sinha, A. and Rae, R. (2014). A functional genomic screen for evolutionarily conserved genes required for lifespan and immunity in germline-deficient C. elegans. *PLoS One* **9**: e101970. doi: 10.1371/journal.pone.0101970.

Sun, A., Liu, M., Nguyen, X. V. and Bing, G. (2003). P38 MAP kinase is activated at early stages in Alzheimer's disease brain. *Exp Neurol* **183**: 394-405. doi: 10.1016/s0014-4886(03)00180-8.

Tanaka-Hino, M., Sagasti, A., Hisamoto, N., Kawasaki, M., Nakano, S., Ninomiya-Tsuji, J., Bargmann, C. I. and Matsumoto, K. (2002). SEK-1 MAPKK mediates Ca2+ signaling to determine neuronal asymmetric development in Caenorhabditis elegans. *EMBO Rep* **3**: 56-62. doi: 10.1093/embo-reports/kvf001.

Tanguy, M., Veron, L., Stempor, P., Ahringer, J., Sarkies, P. and Miska, E. A. (2017). An Alternative STAT Signaling Pathway Acts in Viral Immunity in Caenorhabditis elegans. *mBio* **8**. doi: 10.1128/mBio.00924-17.

Troemel, E. R., Chu, S. W., Reinke, V., Lee, S. S., Ausubel, F. M. and Kim, D. H. (2006). p38 MAPK regulates expression of immune response genes and contributes to longevity in C. elegans. *PLoS Genet* **2**: e183. doi: 10.1371/journal.pgen.0020183.

Tzavlaki, K. and Moustakas, A. (2020). TGF-beta Signaling. *Biomoleculles* **10**. doi: 10.3390/biom10030487.

van der Linden, A. M., Nolan, K. M. and Sengupta, P. (2007). KIN-29 SIK regulates chemoreceptor gene expression via an MEF2 transcription factor and a class II HDAC. *EMBO J* **26**: 358-370. doi: 10.1038/sj.emboj.7601479.

van der Linden, A. M., Wiener, S., You, Y. J., Kim, K., Avery, L. and Sengupta, P. (2008). The EGL-4 PKG acts with KIN-29 salt-inducible kinase and protein kinase A to regulate chemoreceptor gene expression and sensory behaviors in Caenorhabditis elegans. *Genetics* **180**: 1475-1491. doi: 10.1534/genetics.108.094771.

Wagner, E. F. and Nebreda, A. R. (2009). Signal integration by JNK and p38 MAPK pathways in cancer development. *Nat Rev Cancer* **9**: 537-549. doi: 10.1038/nrc2694.

Wang, A. H., Bertos, N. R., Vezmar, M., Pelletier, N., Crosato, M., Heng, H. H., Th'ng, J., Han, J. and Yang, X. J. (1999). HDAC4, a human histone deacetylase related to yeast HDA1, is a transcriptional corepressor. *Mol Cell Biol* **19**: 7816-7827. doi: 10.1128/MCB.19.11.7816.

Wang, X. Z. and Ron, D. (1996). Stress-induced phosphorylation and activation of the transcription factor CHOP (GADD153) by p38 MAP Kinase. *Science* **272**: 1347-1349. doi: 10.1126/science.272.5266.1347.

Warnhoff, K. and Kornfeld, K. (2015). New links between protein N-terminal acetylation, dauer diapause, and the insulin/IGF-1 signaling pathway in Caenorhabditis elegans. *Worm* **4**: e1023498. doi: 10.1080/21624054.2015.1023498.

Warnhoff, K., Murphy, J. T., Kumar, S., Schneider, D. L., Peterson, M., Hsu, S., Guthrie, J., Robertson, J. D. and Kornfeld, K. (2014). The DAF-16 FOXO transcription factor regulates natc-1 to modulate stress resistance in Caenorhabditis elegans, linking insulin/IGF-1 signaling to protein N-terminal acetylation. *PLoS Genet* **10**: e1004703. doi: 10.1371/journal.pgen.1004703.

Warr, N., Carre, G. A., Siggers, P., Faleato, J. V., Brixey, R., Pope, M., Bogani, D., Childers, M., Wells, S., Scudamore, C. L., Tedesco, M., del Barco Barrantes, I., Nebreda, A. R., Trainor, P. A. and Greenfield, A. (2012). Gadd45gamma and Map3k4 interactions regulate mouse testis determination via p38 MAPK-mediated control of Sry expression. *Dev Cell* **23**: 1020-1031. doi: 10.1016/j.devcel.2012.09.016.

Weaver, B. P., Weaver, Y. M., Omi, S., Yuan, W., Ewbank, J. J. and Han, M. (2020). Non-Canonical Caspase Activity Antagonizes p38 MAPK Stress-Priming Function to Support Development. *Dev Cell* **53**: 358-369 e356. doi: 10.1016/j.devcel.2020.03.015.

Williamson, E. A., Williamson, I. K., Chumakov, A. M., Friedman, A. D. and Koeffler, H. P. (2005). CCAAT/enhancer binding protein epsilon: changes in function upon phosphorylation by p38 MAP kinase. *Blood* **105**: 3841-3847. doi: 10.1182/blood-2004-09-3708.

Wu, C., Karakuzu, O. and Garsin, D. A. (2021). Tribbles pseudokinase NIPI-3 regulates intestinal immunity in Caenorhabditis elegans by controlling SKN-1/Nrf activity. *Cell Rep* **36**: 109529. doi: 10.1016/j.celrep.2021.109529.

Yan, D., Wu, Z., Chisholm, A. D. and Jin, Y. (2009). The DLK-1 kinase promotes mRNA stability and local translation in C. elegans synapses and axon regeneration. *Cell* **138**: 1005-1018. doi: 10.1016/j.cell.2009.06.023.

Yandell, M. D., Edgar, L. G. and Wood, W. B. (1994). Trimethylpsoralen induces small deletion mutations in Caenorhabditis elegans. *Proc Natl Acad Sci U S A* **91**: 1381-1385. doi: 10.1073/pnas.91.4.1381.

Yang, D., Tournier, C., Wysk, M., Lu, H. T., Xu, J., Davis, R. J. and Flavell, R. A. (1997). Targeted disruption of the MKK4 gene causes embryonic death, inhibition of c-Jun NH2-terminal kinase activation, and defects in AP-1 transcriptional activity. *Proc Natl Acad Sci U S A* **94**: 3004-3009. doi: 10.1073/pnas.94.7.3004.

Youssif, C., Cubillos-Rojas, M., Comalada, M., Llonch, E., Perna, C., Djouder, N. and Nebreda, A. R. (2018). Myeloid p38alpha signaling promotes intestinal IGF-1 production and inflammation-associated tumorigenesis. *EMBO Mol Med* **10**. doi: 10.15252/emmm.201708403.

Zheng, T., Zhang, B., Chen, C., Ma, J., Meng, D., Huang, J., Hu, R., Liu, X., Otsu, K., Liu, A. C., Li, H., Yin, Z. and Huang, G. (2018). Protein kinase p38alpha signaling in dendritic cells regulates colon inflammation and tumorigenesis. *Proc Natl Acad Sci U S A* **115**: E12313-E12322. doi: 10.1073/pnas.1814705115.

Ziegler, K., Kurz, C. L., Cypowyj, S., Couillault, C., Pophillat, M., Pujol, N. and Ewbank, J. J. (2009). Antifungal innate immunity in C. elegans: PKCdelta links G protein signaling and a conserved p38 MAPK cascade. *Cell Host Microbe* **5**: 341-352. doi: 10.1016/j.chom.2009.03.006.

Zugasti, O., Thakur, N., Belougne, J., Squiban, B., Kurz, C. L., Soule, J., Omi, S., Tichit, L., Pujol, N. and Ewbank, J. J. (2016). A quantitative genome-wide RNAi screen in C. elegans for antifungal innate immunity genes. *BMC Biol* **14**: 35. doi: 10.1186/s12915-016-0256-3.

Chapter 4: Discussion and Future Directions

The work presented in this dissertation examines the fine balance between development and activation of MAPK signaling by an organism. In this chapter, I discuss my results and identify future directions that can expand on the data presented in this dissertation to build our knowledge about the interactions between MAPK signaling regulation and development.

Forward genetic screening with selection improves screen efficiency

We have previously shown that the *C. elegans* Tribbles homologue, NIPI-3, is a regulator of PMK-1 activity and required for animal development (Kim et al. 2016). A previous forward genetic screen identified CEBP-1 and a highly conserved p38 MAPK cascade (TIR-1/NSY-1/SEK-1/PMK-1/MAK-2) as mediators of animal development downstream of NIPI-3 (Kim et al. 2016). To further explore the signaling downstream of Tribbles in *C. elegans*, I performed a forward genetic screen utilizing a genetically-encoded heat-shock induced toxin as a counter-selection method (screen details described in the Appendix). The counter-selection method of this screen ensured that only animals containing a suppressor of *nipi-3(0)* developmental arrest survived screening. Whereas the original screen, done without counter-selection, isolated 9 independent alleles, my screen utilizing counter-selection isolated 35 independent alleles and didn't require any screening of animals by fluorescence microscope. From my screen I found many new alleles of previously identified suppressors of *nipi-3(0)*, including a cluster of missense mutations in the N' of CEBP-1, in a region that had not been previously identified as a functional domain (these mutations are discussed further below). I isolated one allele that is not in a previously identified suppressor of *nipi-3(0)*

and despite extensive outcrossing and mapping, I was unable to identify the causative mutation in this strain (mapping of this allele detailed in the Appendix). In the process of performing this screen, some of the plates of animals grew faster than I anticipated and became starved. *C. elegans* can generally recover without issue even after months of starvation. There were at least seven plates that contained suppressed animals but could not recover after starvation. I later observed this phenotype in some strains with weak suppression of *nipi-3(0)*, specifically in some *sek-1(lf) nipi-3(0)* and *nsy-1(lf); nipi-3(0)* strains.

An alternate genetic screen design, to isolate more alleles of the weaker suppressors of *nipi-3(0)*, would involve a secondary screen for alleles that do not rescue recovery after starvation. Specifically, the EMS screen would be performed as described in the Appendix, then each isolate would be split into two conditions: one that was maintained to prevent starvation, and another designed to test recovery after starvation. The isolates that recovered after starvation likely contain mutations within the stronger suppressors (*cebp-1* or *mak-2*) and would be frozen and saved for future examination. Many of these strains are likely to overlap with those identified in my screen. Of interest are the isolates that were unable to recover after starvation, as they likely contain mutations in genes that are weaker suppressors of *nipi-3(0)* and were lost during my screen. Standard sequencing and mapping procedures would follow to map the causative mutations in these isolates, possibly identifying novel downstream regulators of NIPI-3 mediated development. The forward genetic screen with counter-selection that I performed identified many alleles of strong suppressors with much less effort than the previous version of the screen performed by Dr. Kim. The screen strategy

proposed above would specifically identify weak suppressors, that were missed in my screen. These tools would allow for in depth analysis of the interactions between the regulation of innate immunity and development.

Genetic screen identifies a novel functional domain in *C. elegans* C/EBP

We have previously reported the roles of CEBP-1 in neuronal stress responses and development (Nakata et al. 2005, Yan et al. 2009, Trujillo et al. 2010, Kurup et al. 2015, Kim et al. 2016, Sharifnia et al. 2017). From the forward genetic screen I performed, I found a cluster of missense mutations in the N' region of CEBP-1. This pattern of mutations indicates that the identity of each individual amino acid is essential for the function of the protein. Dr. Kim confirmed protein expression of one of the missense mutations by expressing a GFP tagged fusion protein. As presented in Chapter 2, I found that these missense mutations not only affect the activity of CEBP-1 downstream of NIPI-3 in development, but also in CEBP-1's essential role in axon regeneration (Zilu Wu performed the axotomy experiments). Under normal circumstances, when the axon of a neuron is severed in *C. elegans*, a certain amount of regrowth occurs within 24 hours after the injury. In animals lacking CEBP-1, this regrowth does not occur. This phenotype does not lend itself well to screening, as the assay is technically difficult and time intensive. On the other hand, rescue of a lethal phenotype (developmental arrest caused by *nipi-3(0)*) is relatively easy to screen for. Thus, to further investigate the functionality of this N' region of CEBP-1, I designed crRNAs to make targeted mutations to this area of CEBP-1. I performed the CRIPSR injections in the background of *nipi-3(0)*, to readily screen for animals that have loss of

function in CEBP-1. Of interest were the mutations that did not cause a frame shift, thus maintaining the functionality of the downstream DNA binding domain, but still cause loss of function. The isolated mutants, detailed in Chapter 2, showed that this N' region is indeed functionally significant as deletion or insertion of single amino acids in this region is sufficient to abrogate the function of the protein.

Next steps in this project would be to determine the functional significance of this N' region of CEBP-1. Mammalian C/EBPs have diverse N-terminal sequences with different functional domains, specifying protein-protein interactions and functional specialization of the different C/EBP genes (Friedman and McKnight 1990, Pei and Shih 1991, Kowenz-Leutz et al. 1994). Based on studies of the varied N' domains of mammalian C/EBPs, I hypothesize that this region mediates protein-protein interactions, possibly interacting with transcriptional machinery. An experiment to address this hypothesis would be to perform differential Immunoprecipitation - Mass spectrometry (IP-MS) to compare *in-vivo* binding partners of WT CEBP-1 and CEBP-1 containing N' domain mutations. This experiment would allow us to determine if the N' mutations prevent binding with key transcriptional proteins.

Genetic screen identifies novel link between innate immunity and HDAC

Dr. Kim isolated *ju1371* as a suppressor of *nipi-3(0)* in her forward genetic screen. She found that overexpression of wildtype HDA-4 reverted the phenotype of *ju1371*, indicating that the mutation within *hda-4* was very likely causative of the suppression of *nipi-3(0)*. Dr. Kim produced a deletion mutant of *hda-4,* that removes most of the coding region of *hda-4*, using CRISPR deletion. Dr. Zhu subsequently crossed this *hda-4*

deletion mutant into *nipi-3(0)* background and found that deletion of *hda-4* does not produce the same phenotype as *ju1371*, indicating that *ju1371* is not a null mutation. Dr. Zhu also found that the phenotype of *ju1371* requires a previously identified binding partner of HDA-4, MEF-2. To test whether this suppression occurs via the regulation of the PMK-1/p38 MAPK pathway, I crossed *Psek-1::GFP* reporter into both *nipi-3(0) hda-4(ju1371)* and *nipi-3(0) hda-4(0).* In Chapter 3, I show that *hda-4(ju1371)* reduces *Psek-1::GFP* in *nipi-3(0)* background whereas *hda-4(0)* does not. Furthermore, I show that *ju1371* does not change the level of CEBP-1 protein level. These data indicate that *hda-4(ju1371)* requires the activity of the transcription factor MEF-2 and reduces the transcription of *sek-1*, not through regulating the expression of the upstream transcription factor CEBP-1.

The next steps for this project are to determine how the *ju1371* mutation changes the function of HDA-4, specifically in relation to the function of MEF-2. Here, I propose possible scenarios and experiments to test their validity. The *ju1371* mutation occurs adjacent to the active site in the deacetylase domain of HDA-4, suggesting that this mutation may influence the enzymatic activity of the protein. One way to test this would be by purifying the mutant HDA-4 and performing biochemical assays to quantify the deacetylase activity of the wildtype vs mutant HDA-4 protein. An alternate technique more aligned with the genetic specialties of the Jin lab would be to test if a new mutation in HDA-4, that is predicted to inhibit its enzymatic activity, has the same phenotype as *ju1371*. Based on mammalian homology, mutating the LEGGY motif of HDA-4 to LEGGH should fully inhibit any enzymatic activity of the protein. Dr. Zhu attempted this experiment using CRISPR and homology directed repair but was

unsuccessful. It seems likely that the crRNA designed to target Cas9 to the location to cause a double stranded break in *hda-4* was not efficient. The next step in producing this mutant would be to design a new crRNA and repair template and do CRISPR injections to test the efficiency of mutations within *hda-4*.

The subcellular localization of class IIa HDACs is tightly correlated to their function: HDACs are only active in the nucleus and are shuttled from the nucleus to the cytoplasm based on their phosphorylative state. Dr. Zhu produced some preliminary data suggesting that cytoplasmic HDA-4 is higher in *nipi-3(0)* animals, suggesting that *nipi-3(0)* may alter the phosphorylation state of HDA-4. From the data collected, it is not clear if the overall level of HDA-4 is changed and/or if there is a reduction in the nuclear expression of HDA-4, which could suggest a change in the nucleo-cytoplasmic shuttling of HDA-4. Dr. Zhu used overexpression of HDA-4::GFP for this experiment and it would be better to observe the endogenous localization of HDA-4 without overexpression of HDA-4. The localization of both wildtype and *ju1371* can be visualized by insertion of GFP at the endogenous locus of *hda-4* using standard methods (Dickinson et al. 2015). It will be clear if the GFP tagging inhibits the function of HDA-4, as *hda-4(0)* animals are noticeably thin in comparison to wildtype. It may be the case that *nipi-3(0)* increases the cytoplasmic fraction of wildtype HDA-4, but not HDA-4(G606D) (the theoretical protein translated from *hda-4(ju1371)).* This would suggest that HDA-4(G606D) somehow affects the phosphorylation of HDA-4 and would indicate follow-up IP-MS to identify any differences in post-translational modifications between wildtype and HDA-4(G606D). This localization data may provide clues to the mechanism of *ju1371* suppression of *nipi-3(0)* and why *hda-4(0)* does not have the same phenotype.

Although *ju1371* is not at the predicted binding interface between MEF-2 and HDA-4, it is still possible that this mutation changes the binding affinity between these two proteins. I propose to immunoprecipitate (IP) GFP::HDA-4(WT) and GFP::HDA-4(G606D) and then perform western blots to test if there is any difference in the amount of MEF-2 pulled down with the HDA-4. This experiment would require tagging MEF-2, as antibodies against this *C. elegans* protein are not available. This tagging can be done using standard methods of inserting mKate::Myc into the endogenous locus of *mef-2*.

It is possible that *ju1371* changes the transcriptional targets of the MEF-2—HDA-4 protein complex. To address this possibility, I propose ChIP-seq to identify DNA binding locations of MEF-2 in wildtype, *nipi-3(0)*, *nipi-3(0) hda-4(ju1371)*, and *nipi-3(0) hda-4(0)*. I expect that the transcriptional targets of interest would be differentially bound in the *nipi-3(0) hda-4(ju1371)* animals vs *nipi-3(0)* and *nipi-3(0) hda-4(0)* animals. For a more general look at changes in transcription, RNAseq of these same four strains would provide crucial information about transcriptional aberrations in animals displaying developmental arrest (*nipi-3(0)* and *nipi-3(0) hda-4(0))* in comparison to wildtype, and if any of these transcripts are returned to wildtype levels in *nipi-3(0) hda-4(ju1371)* animals.

Together, the experiments proposed above would provide further characterization of the effect of *ju1371* on the enzymatic activity and subcellular localization of HDA-4 and on the binding and activity of the HDA-4—MEF-2 protein complex. This would provide mechanistic insight into the connection between HDA-4 and the regulation of development in *C. elegans*.

Genetic screen identifies novel link between innate immunity and NATC

Dr. Kim isolated *ju1369* as a suppressor of *nipi-3(0)* in her forward genetic screen. Although she had suspicions that the mutation in *natc-2* was causative of suppression, she never produced the double mutant of *natc-2(0); nipi-3(0)* to directly test the hypothesis. In Chapter 3, I show that deletion allele of *natc-2* is able to suppress *nipi-3(0)*, indicating that *ju1369* encodes a loss of function mutation in *natc-2.* Furthermore, deletion of *natc-1* is also able to suppress *nipi-3(0)*. Dr. Zhu produced a deletion mutant of *Y48G1C.9* that showed a phenotype similar to *natc-1(0)* or *natc-2(0)*, therefore we rename this gene *natc-3.* I then crossed *Psek-1::GFP* reporter to *natc-1/2/3(0); nipi-3(0)* and show that NatC knockout reduces *Psek-1::GFP* in *nipi-3(0)* background, but not to the same level as knockout of MAPK. This suggests that NatC functions both through the PMK-1/p38 MAPK pathway and other pathways to regulate development in *C. elegans*.

The next steps for this project are to determine how mutation of NatC changes the protein modification landscape. This could be identified by comparing N' modifications between wildtype, *natc-2(ju1369)* and *nipi-3(0) natc-2(ju1369)* proteomes. A recently developed method of purifying proteins for mass spectrometry is particularly designed to enrich for N' peptides to detect the N' modifications of proteins (Chang et al. 2021). I propose using the *ju1369* mutation for the MS experiment because it has the strongest phenotype in suppressing *nipi-3(0)*. Among the candidates that are differentially modified in the NatC mutant condition, one or a few key proteins may regulate development. A first step in assessing the potential function of these candidates is to test if genetic knockout of the gene is able to suppress the *nipi-3(0)*

larval arrest phenotype. If this were the case, it would suggest that the candidate protein is non-functional without N' acetylation. However, it is possible that knockout of the gene does not have the same phenotype as the condition in which the protein is produced, but not N' acetylated. A way to test this is to produce a mutant that changes the 2nd amino acid to a proline which would specifically prevent the N' acetylation of the protein. Together, these experiments would identify regulators of development in *C. elegans* that require N' acetylation by NatC.

Transcriptional reporter of *sek-1* identifies novel feedback loop in MAPK signaling downstream of NIPI-3/CEBP-1

We have previously shown that CEBP-1 and a highly conserved p38 MAPK cascade (TIR-1/NSY-1/SEK-1/PMK-1/MAK-2) function downstream of NIPI-3 to mediate animal development. To further investigate this pathway, I produced an integrated reporter of *Psek-1::GFP* that is a functional readout of CEBP-1 activity. In Chapter 3, I show that SEK-1 activity regulates its own transcription and that both PMK-1 and MAK-2 also regulates the transcription of *sek-1.* The future directions for the project involve providing further understanding of the connection between NIPI-3 and the PMK-1/p38 MAPK pathways and determining how the upregulation of this pathway causes developmental arrest.

One of the major discrepancies between the data for the null mutant *nipi-3(ju1293)* and the partial loss of function mutant *nipi-3(fr4)* is the level of phosphorylated p38 MAPK PMK-1. In McEwan et al. 2016 and Wu et al. 2021, they observed lower p-PMK-1 in *nipi-3(fr4)* in comparison to wildtype whereas Dr. Kim saw a much higher level

of p-PMK-1 in *nipi-3(ju1293)* in comparison to wildtype (Kim et al. 2016, McEwan et al. 2016, Wu et al. 2021). Other than the different genotypes, the main difference between these experiments is the age of the animals. In the McEwan and Wu papers, they used L4 stage animals, whereas *ju1293* animals never reach L4 stage, so they were analyzed in their arrested L2/L3 stage. I propose measuring p-PMK-1 levels in age-matched *ju1293* and *fr4* animals for a valid side-by-side comparison. For a more general look at the differences between these two genotypes, I also propose RNAseq on age-matched animals of WT, *nipi-3(fr4)*, *nipi-3(ju1293).* RNAseq for *cebp-1(0) nipi-3(ju1293)* is also of interest to see which genes are differentially expressed in these rescued animals vs *nipi-3(ju1293)* on its own. These experiments may provide insight into the different observations seen in *nipi-3(fr4)* animals vs *nipi-3(ju1293)* animals.

Wu et al propose a model for the regulation of PMK-1-mediated intestinal immunity regulated by NIPI-3 and CEBP-1. In this model, increased levels of CEBP-1, due to the knockout of NIPI-3, increases the transcription of *cebp-1* and *vhp-1*. VHP-1 is a phosphatase that dephosphorylates PMK-1 thus reducing the activity of the transcription factor SKN-1. SKN-1 in turn, is then unable to promote the transcription of protective genes in response to intestinal infection. In support of this model, they find that NIPI-3 is required for the upregulation of phosphorylated PMK-1 and transcription of SKN-1 targets in response to intestinal infection (Wu et al. 2021). For the experiments in this paper, they either used the partial loss of function *nipi-3(fr4)* allele or RNAi to knockdown levels of *nipi-3* in adult animals. Neither of these conditions replicate our experimental condition of complete knockout of *nipi-3* during development. If the model presented in Wu et al 2021 applies to animal development, *vhp-1(lf)* would increase

PMK-1 activity and exacerbate the effects of *nipi-3(lf).* Indeed, Dr. Kim has observed that *vhp-1(lf); nipi-3(fr4)* animals are larval lethal. It would be interesting to test if VHP-1 overexpression is able to suppress *nipi-3(0)* developmental arrest. Such an outcome would support our model for animal development where overexpression of CEBP-1 increases the transcription of *sek-1*, leading to more activation of PMK-1, leading to developmental arrest. It is interesting that CEBP-1 promotes transcription of both *sek-1*, an activator of PMK-1 activity, and *vhp-1*, a repressor of PMK-1 activity. Heightened levels of CEBP-1 during development led to a net increase in activated PMK-1, possibly by promoting the transcription of *sek-1* more than *vhp-1*, but heightened levels of CEBP-1 during infection in the adult animal led to a net decrease in activated PMK-1. Interestingly, Wu et al. also found an increase in *sek-1* and *skn-1* mRNA in *nipi-3(fr4)* adult animals in the absence of infection, but not in infected animals. SKN-1 is a transcription factor that they used as a readout of PMK-1 pathway activity. Although when they directly measure p-PMK-1 in *nipi-3(fr4)* adult animals in the absence of infection, they see lower p-PMK-1 in comparison to uninfected N2 adults. These two pieces of data seem contradictory, so I propose measuring *sek-1, skn-1,* and *vhp-1* transcription and p-PMK-1 levels at different developmental stages in *nipi-3(0), cebp-1(0), cebp-1(0) nipi-3(0),* and WT animals. This would provide insight into transcriptional changes occurring during development and if they are dependent on *cebp-1.* Specifically interesting would be the ratio of *sek-1* to *vhp-1* transcripts and if that correlates to the levels of p-PMK-1, changes over time, or requires *cebp-1.* I would expect that when there are more transcripts of *sek-1* than *vhp-1*, that would correlate to an increase in p-PMK-1. One possibility is that p-PMK-1 levels are high in *nipi-3(fr4)*

during larval development and decrease as the animal reaches L4 stage. I propose that this would be the effect of CEBP-1 switching from more *sek-1* transcription to more *vhp-1* transcription. This would lead to many more interesting questions to study the regulation of the targets of CEBP-1 transcription.

NIPI-3 and the PMK-1/p38 MAPK pathway function cell autonomously in the intestine and epidermis in infection response. In development, Dr. Kim found that *nipi-3* and *cebp-1* expression in the intestine, epidermis, and neurons all contribute to animal development, but expression in these three tissues is not sufficient to regulate development. In my *sek-1* transcriptional reporter, I see the most striking upregulation in the epidermis in *nipi-3(0).* The expression in the neurons is also markedly higher, but intestinal expression isn't affected much by *nipi-3(0).* My project did not address tissue-specific regulation of the PMK-1 pathway during development. To determine the tissue -specific requirement of *sek-1,* one could do tissue-specific rescue of *sek-1* (using tissue specific promoters to drive expression of *sek-1* in *sek-1(0) nipi-3(0)* animals).

Based on the findings that the developmental delay resulting from the activation of PMK-1/p38 MAPK is exacerbated by loss of function of the IRE/XBP-1 branch of the unfolded protein response to ER stress, I propose that *nipi-3(0)* is causing ER stress and activating the UPR. To test this, I propose using a common reporter of UPR activity (*Phsp-4::GFP)*. If this reporter is upregulated in *nipi-3(0)* animals, it would be interesting to test if its expression is rescued in suppressed animals. This would provide some insight into the mechanism of larval arrest in *nipi-3(0)* animals.

The work presented in my dissertation demonstrates that there is a balance between the activation of the PMK-1/ p38 MAPK pathway and animal development in *C.*

elegans. In addition, I characterized two novel regulators of the PMK-1/ p38 MAPK pathway and animal development in *C. elegans.* Mammalian systems have a much more complex network of TRIBs, C/EBPs, and p38 MAPKs that function together to regulate metabolism, immunity, and development, among many other systemic and cellular processes. Perturbations to this signaling network can cause a wide array of human diseases, from neurological disfunction in Parkinson's and Alzheimer's to autoimmune and metabolic disorders. *C. elegans* provide a model where we can observe the interactions between these protein families with fewer protein homologues while still maintaining a conserved function in regulating innate immune signaling and development. These findings may help identify novel regulators of immune signaling in humans allowing for the development of new therapeutics for autoimmune disorders.

References

Chang, C. H., Chang, H. Y., Rappsilber, J. and Ishihama, Y. (2021). Isolation of Acetylated and Unmodified Protein N-Terminal Peptides by Strong Cation Exchange Chromatographic Separation of TrypN-Digested Peptides. *Mol Cell Proteomics* **20**: 100003. doi: 10.1074/mcp.TIR120.002148.

Dickinson, D. J., Pani, A. M., Heppert, J. K., Higgins, C. D. and Goldstein, B. (2015). Streamlined Genome Engineering with a Self-Excising Drug Selection Cassette. *Genetics* **200**: 1035-1049. doi: 10.1534/genetics.115.178335.

Friedman, A. D. and McKnight, S. L. (1990). Identification of two polypeptide segments of CCAAT/enhancer-binding protein required for transcriptional activation of the serum albumin gene. *Genes Dev* **4**: 1416-1426. doi: 10.1101/gad.4.8.1416.

Kim, K. W., Thakur, N., Piggott, C. A., Omi, S., Polanowska, J., Jin, Y. and Pujol, N. (2016). Coordinated inhibition of C/EBP by Tribbles in multiple tissues is essential for Caenorhabditis elegans development. *BMC Biol* **14**: 104. doi: 10.1186/s12915-016-0320-z.

Kowenz-Leutz, E., Twamley, G., Ansieau, S. and Leutz, A. (1994). Novel mechanism of C/EBP beta (NF-M) transcriptional control: activation through derepression. *Genes Dev* **8**: 2781-2791. doi: 10.1101/gad.8.22.2781.

Kurup, N., Yan, D., Goncharov, A. and Jin, Y. (2015). Dynamic microtubules drive circuit rewiring in the absence of neurite remodeling. *Curr Biol* **25**: 1594-1605. doi: 10.1016/j.cub.2015.04.061.

McEwan, D. L., Feinbaum, R. L., Stroustrup, N., Haas, W., Conery, A. L., Anselmo, A., Sadreyev, R. and Ausubel, F. M. (2016). Tribbles ortholog NIPI-3 and bZIP transcription factor CEBP-1 regulate a Caenorhabditis elegans intestinal immune surveillance pathway. *BMC Biol* **14**: 105. doi: 10.1186/s12915-016-0334-6.

Nakata, K., Abrams, B., Grill, B., Goncharov, A., Huang, X., Chisholm, A. D. and Jin, Y. (2005). Regulation of a DLK-1 and p38 MAP kinase pathway by the ubiquitin ligase RPM-1 is required for presynaptic development. *Cell* **120**: 407-420. doi: 10.1016/j.cell.2004.12.017.

Pei, D. Q. and Shih, C. H. (1991). An "attenuator domain" is sandwiched by two distinct transactivation domains in the transcription factor C/EBP. *Mol Cell Biol* **11**: 1480-1487. doi: 10.1128/mcb.11.3.1480-1487.1991.

Sharifnia, P., Kim, K. W., Wu, Z. and Jin, Y. (2017). Distinct cis elements in the 3' UTR of the C. elegans cebp-1 mRNA mediate its regulation in neuronal development. *Dev Biol* **429**: 240-248. doi: 10.1016/j.ydbio.2017.06.022.

Trujillo, G., Nakata, K., Yan, D., Maruyama, I. N. and Jin, Y. (2010). A ubiquitin E2 variant protein acts in axon termination and synaptogenesis in Caenorhabditis elegans. *Genetics* **186**: 135-145. doi: 10.1534/genetics.110.117341.

Wu, C., Karakuzu, O. and Garsin, D. A. (2021). Tribbles pseudokinase NIPI-3 regulates intestinal immunity in Caenorhabditis elegans by controlling SKN-1/Nrf activity. *Cell Rep* **36**: 109529. doi: 10.1016/j.celrep.2021.109529.

Yan, D., Wu, Z., Chisholm, A. D. and Jin, Y. (2009). The DLK-1 kinase promotes mRNA stability and local translation in C. elegans synapses and axon regeneration. *Cell* **138**: 1005-1018. doi: 10.1016/j.cell.2009.06.023.

Appendix

EMS Screen and *ju1541* Mapping

A forward genetic screen identifies 34 additional alleles that suppress *nipi-3(0)* lethality

A previous genetic screen, designed to identify genes that participate in innate immune signaling and larval development (using *nipi-3(0)* to create a sensitized background) isolated nine alleles covering seven genes (Kim et al. 2016) (two unpublished alleles). I performed a follow-up screen that relied on selection against peel-induced toxicity (Described in Chapter 2 material and methods, **Figure 22A)**. I mutagenized L4 animals of CZ24853: nipi-3(ju1293); *juEx7152 [nipi-3(+); Phsp::peel-1; Pmyo-2::GFP]* using ethyl methane sulphonate (EMS, three rounds of mutagenesis with concentration between 25-40mM) following standard protocol (Brenner 1974). After mutagenesis, L4 animals were placed on seeded 60mm plates, approximately 1000 P0s were screened. The F2 progeny were subjected to a two-hour heat shock at 37ºC to induce expression of the toxic protein PEEL-1 from Phsp::peel-1, which results in killing animals expressing juEx7152 **(Figure 22A)**. I define suppressor mutations as those that can reverse the developmental arrest phenotype of *nipi-3(0)* such that the homozygous suppressor mutations with *nipi-3(0)* propagate for generations, in the absence of *juEx7152*. To ensure independent isolation of suppressor mutations, I kept only one suppressor per P0 plate.

For the first round of screening, 100 L4 animals were isolated on individual seeded NGM plates. Of these 100 P0 plates, seven had animals that survived selection.

For the next two rounds of mutagenesis, to increase the coverage of my screen and to minimize the efforts to set up the screen, I no longer singled individual P0s onto their own plates. Instead, a mixed population of about 20-30 animals, containing mostly L4s, was placed together on a seeded 60mm plate. I found that this protocol biased the screen towards isolation of suppressors that have a large brood size and can recover from starvation. Loss of CEBP-1 or MAK-2 strongly suppresses *nipi-3(0)*, and 90% of the alleles isolated in the second and third rounds of mutagenesis were located within *cebp-1* or *mak-2* **(Figure 22B)**.

In this follow-up screen, I expanded the mutagenized genome and isolated 35 independent suppressor mutations. I sequenced *cebp-1* and *mak-2* in each of the 35 isolated strains. The remaining 7 strains were outcrossed using CZ10175: *zdIs5 (Pmec-4::GFP)* and genomic DNA from the one-time outcrossed strains was prepared and analyzed by whole genome sequencing (Methods in Chapter 3). Reads from these 7 strains: CZ25728, CZ25730, CZ25732, CZ25734, CZ25738, CZ25740, and CZ25742 were searched for mutations within previously identified suppressors of *nipi-3(0)*. All strains except CZ25730 contain nonsense, missense, or splice site mutations in tir-1, nsy-1, or sek-1, which are all previously identified suppressors of nipi-3(0) (Figure 22C). These newly isolated alleles show that different alleles of the same gene can have different effects on suppressing the short body length of *nipi-3(0)* animals **(Figure 22D)**.

One allele, *ju1541*, did not contain any mutations in previously identified suppressors of *nipi-3(0).* I outcrossed this strain using CZ22446: *nipi-3(ju1293) X; juEx6807[nipi-3(+); Pmyo-2::mCherry]*, which allowed for replacement of the X chromosome. Whole genome sequencing data for CZ25730: *nipi-3(ju1293); ju1541* (1x

outcross from EMS isolate) and CZ27062: *nipi-3(ju1293) ; ju1541* (2x outcross from EMS isolate) were analyzed to guide further mapping as previously described (Sarin et al. 2008). The whole genome sequence data set of CZ25730 and CZ27062 was compared to the whole genome sequencing data obtained from the other strains isolated in this screen, CZ25728, CZ25732, CZ25734, CZ25738, CZ25740, and CZ25742 and the strain used for the second outcross, CZ22446: *nipi-3(ju1293); juEx6807[nipi-3(+)]*. Candidate SNPs were identified by their presence in both the one time and two times outcrossed isolates of *ju1541* and their absence from any of the other WGS datasets **(Figure 23A)**. The SNPs were grouped by likeliness to influence protein expression or function, Non-synonymous mutations being most likely to change protein function, Synonymous, intronic, or UTR mutations being less likely, and mutations that are up or downstream of a gene (outside of the UTR) being least likely to change protein function.

The majority of SNPs unique to *ju1541* were on Chromosome I, V, and X. Using recombinants, produced by crossing CZ25730 with CZ22446, I calculated the recombination rate at locations along chromosomes I, V, and X. The lower the recombination rate, the more likely that the causative SNP is located nearby on the chromosome. Very low recombination rates were detected near the middle of Chromosome X **(Figure 23B)**. I further investigated this region by producing an additional 91 recombinant strains by crossing CZ27062 with CZ22446. At ChX +0.27 mu there was 15% recombination and at ChX -1.8mu there was 3% recombination **(Figure 23C)**. This suggests that the SNP causative of the suppression of *nipi-3(0)* in

ju1541 is present on Chromosome X, between -9.98 and -1.8 mu. The mutations in this region are listed in **Figure 23C*.***

I note that the screen was designed to identify only strong suppressors. Specifically, to increase the efficiency of the screen, mutagenized animals were housed at a higher density than standard protocol. This created a competitive environment for resources. Thus, alleles with strong suppressor activity would produce animals with the highest fitness (i.e. greatest brood size) and would therefore be more likely to be detected in the screen. Consequently, this screen likely identified all genes with strong suppression of *nipi-3(0)* lethality.

Figure 22. Forward Genetic Screening with Selection identifies additional alleles of *cebp-1* and genes in p38 MAPK pathway

(A) Schematic overview of the forward genetic screen designed to identify suppressors of *nipi-3(0)* larval arrest using selection with heat shock activated expression of PEEL-1, a protein toxic to *C. elegans.* Mutagenized animals contain a transgene (*Tg*) containing wildtype *nipi-3*, the gene encoding a toxic protein, PEEL-1, under a heat shock (*hsp)* promoter, and a fluorescent co-injection marker that expresses GFP under the pharyngeal muscle (*myo-2)* promoter. The mutagenized P0 animals were grown on seeded NGM plates to F2 generation without transferring any animals to fresh plates. The plates were subjected to 1 hour heat shock at 37ºC (illustrated by red box) to induce expression of PEEL-1, effectively killing all animals containing the transgene. The only surviving animals contain a mutation that suppresses the larval arrest of *nipi-3(0).* **(B-C)** Illustrations of gene structures, missense alleles, and deletion alleles. Exons are purple boxes, introns are angled black lines connecting exons, and the UTRs are black horizonal lines. Protein motifs are illustrated in green. Missense alleles isolated in EMS screen for suppressors of *nipi-3(0)* larval arrest are indicated as a dot in the exon where the mutation exists, allele name and amino acid substitution are labeled above the dot. Blue dots indicate the allele was isolated and previously published in Kim et al, 2016 and red dots indicate novel alleles from this screen. Deletion alleles are indicated as black or red horizonal lines showing the region of DNA that is deleted. **(C)** *tir-1* contains a 8377 bp intron between the first two coding exons and a 8481 bp intron between the 7^{th} and 8^{th} coding exons which are not illustrated to scale. **(D)** Quantification of body length of animals 3 days post egg laid. *nipi-3(0)* mutants have a short body length. This phenotype is rescued by loss of function or deletion mutations of *tir-1, nsy-1,* and *sek-1.* Different alleles within the same gene can have significantly different suppression of *nipi-3(0)* body length. This may be caused by different effects on the expression and function of the protein. mRNA was not collected to confirm expression of these mutant proteins. Each dot represents a single animal, each red line represents the mean value. Statistics: One-Way ANOVA with Tukey's post hoc test. *ns* not significant, **P*<0.05, ***P*<0.01, ****P*<0.001.

A

Forward genetic screen with heat shock selection isolates 35 independent suppressor alleles

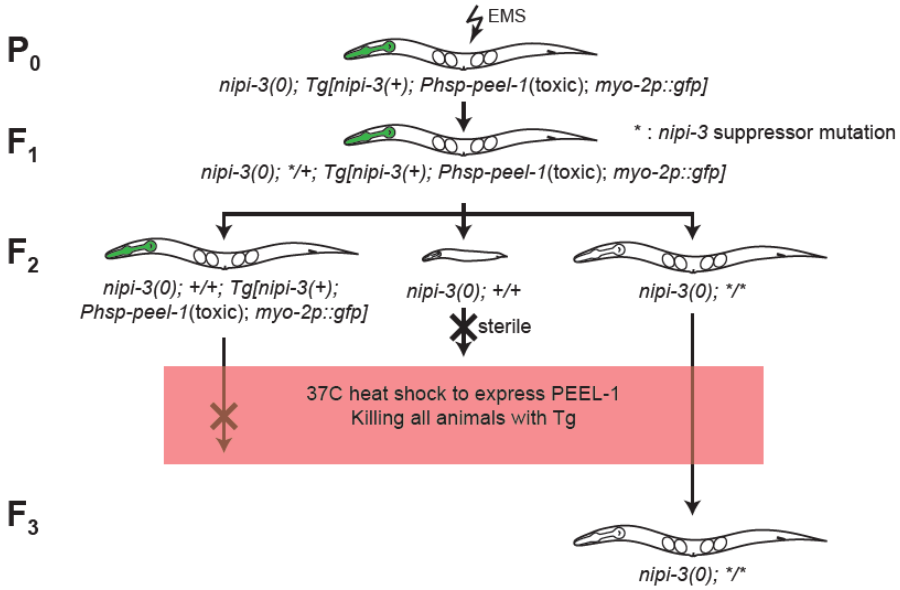

B

Sanger sequencing reveals 28 of 35 isolated alleles are mutations within *cebp-1* or *mak-2*

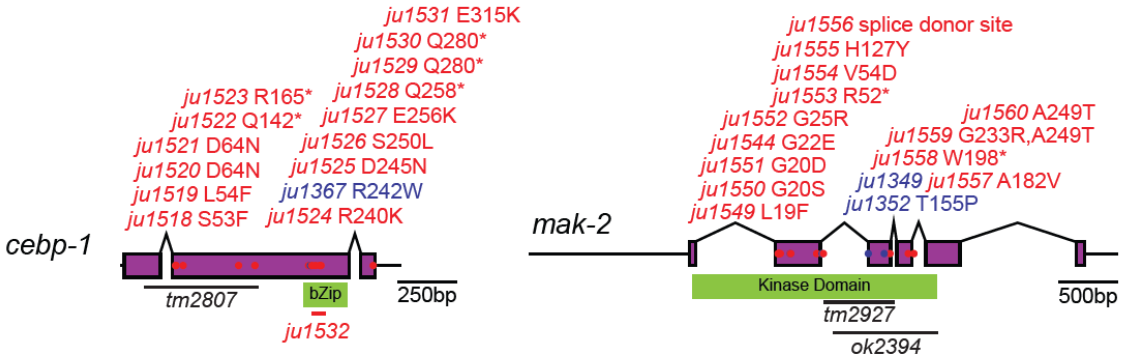

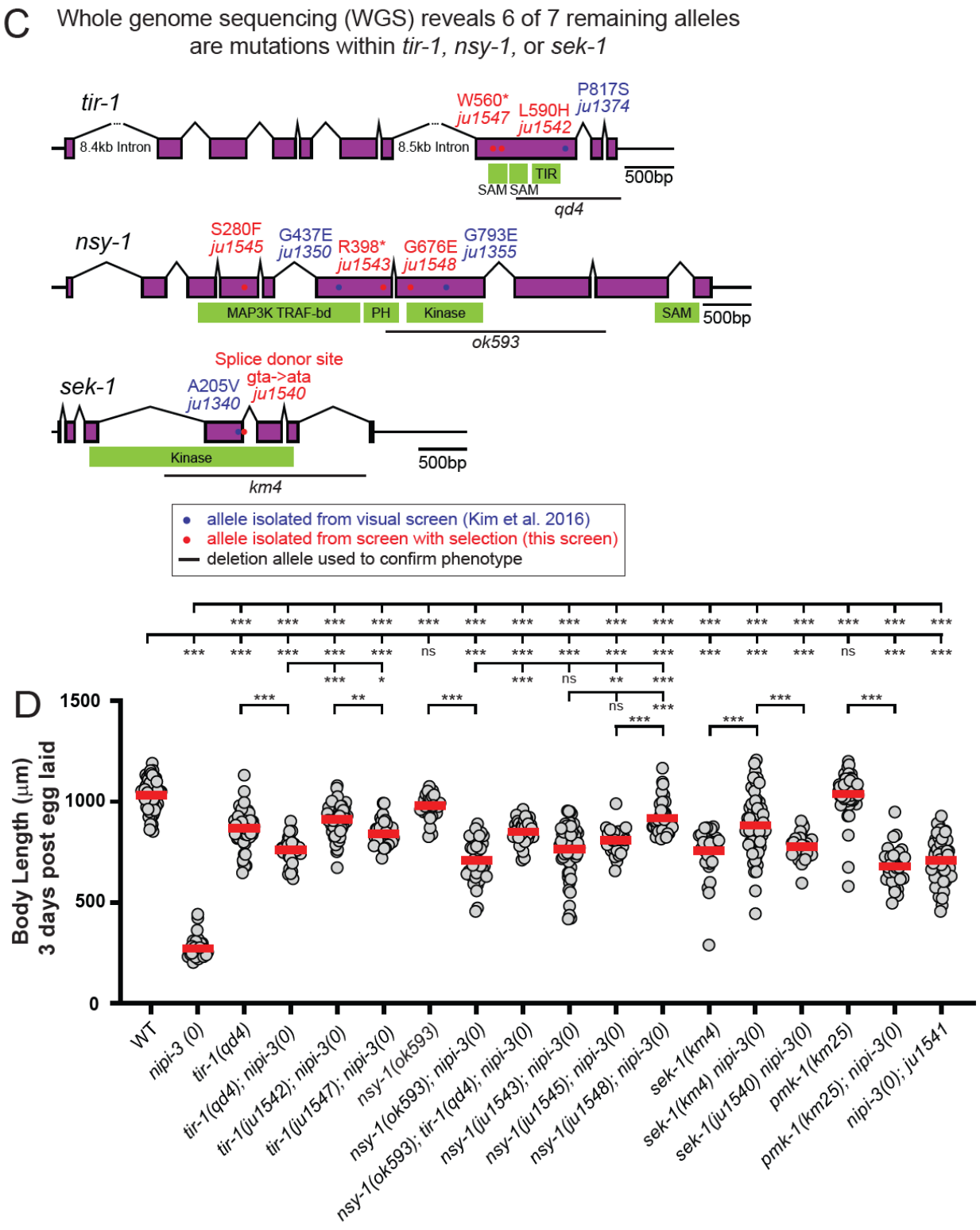

Figure 22. Forward Genetic Screening with Selection identifies additional alleles of *cebp-1* and genes in p38 MAPK pathway, continued

Figure 23. Mapping of *ju1541*, a suppressor of nipi-3(0)
(A) Venn diagram showing the overlapping single nucleotide polymorphisms (SNPs) present in two strains containing the unknown allele *ju1541*, the unmutagenized *nipi-3(0)* strain used for outcrossing, and the pooled SNPs present in strains containing identified alleles *ju1540, ju1542-ju1548*. The mutation causative for the phenotype is going to be present only in the two strains containing *ju1541,* but none of the other data sets. The black circle indicates the region of the Venn diagram which will contain the causative mutation. This analysis was performed for each chromosome. For more details, see Methods. **(B)** Unique alleles from Venn diagram, visualized on the chromosomes and recombination rates at locations tested on Chromosome I, V, and X. **(C)** Recombinant mapping shows *ju1541* is likely on Ch X between -9.17 mu and -2.92 mu. A list of genetic mutations in this region of the X chromosome, from whole genome sequencing data.

A

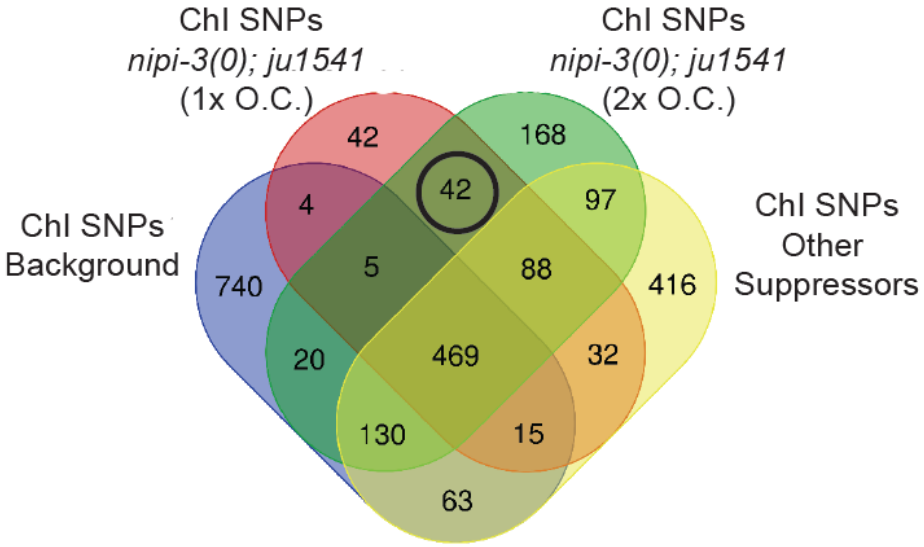

Venn Diagram of # of SNPs present on Chromosome I
in whole genome sequenced strains

Background = *nipi-3(0)* strain used for outcrossing
O.C. = outcrossed with *nipi-3(0)*
Other Suppressors = combined WGS data of strains containing *ju1540, ju1542-ju1548*

B

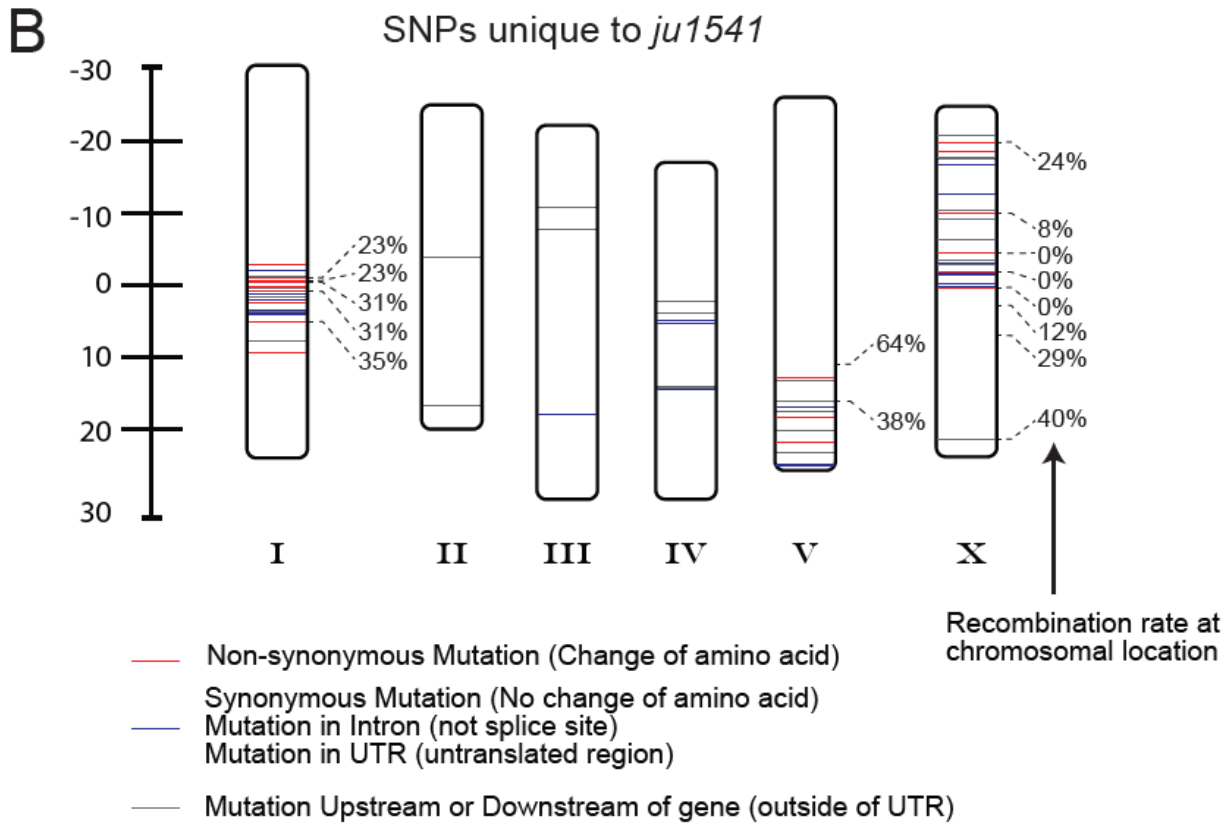

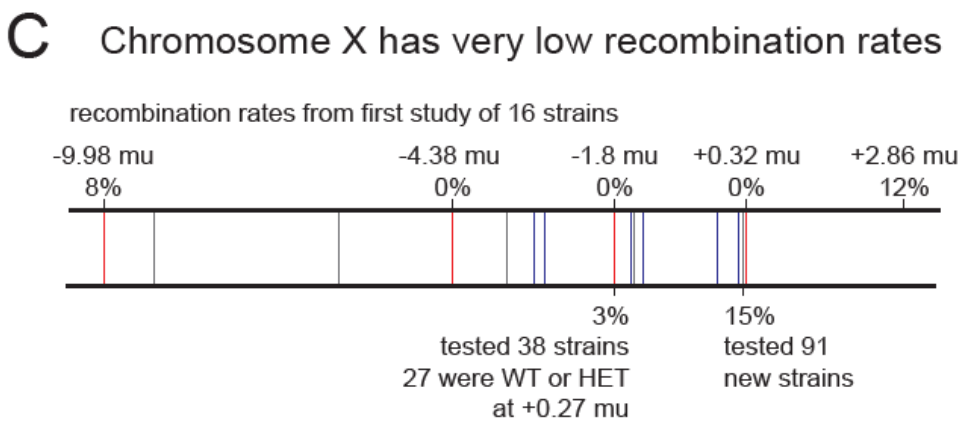

-9.98	C18B2.5	protein_coding	NON_SYNONYMOUS_CODING
-9.17	T22B2.8	ncRNA	DOWNSTREAM: 236 bases
-6.22	K05B2.9	ncRNA	UPSTREAM: 399 bases
-4.38	rgs-6	protein_coding	NON_SYNONYMOUS_CODING
-4.38	rgs-6	protein_coding	STOP_GAINED
-3.51	T25B2.4	protein_coding	DOWNSTREAM: 111 bases
-3.08	T10E10.9	ncRNA	TRANSCRIPT: T10E10.9
-2.92	T22E5.14	ncRNA	UPSTREAM: 939 bases
-2.92	mup-2	protein_coding	UTR_3_PRIME: 111 bases from CDS
-1.79	F46H5.2	protein_coding	NON_SYNONYMOUS_CODING

Figure 23. Mapping of ju1541, a suppressor of *nipi-3(0)*, continued

Table 17. Appendix Strains and Genotypes

Strain	Genotype
CZ24853	*nipi-3(ju1293) X; nipi-3 gDNA + Phsp-peel-1(juEx7152)*
CZ25591	*sek-1(ju1540) X nipi-3(ju1293) X*
CZ25592	*nipi-3(ju1293) X; ju1541*
CZ25593	*tir-1(ju1542) III; nipi-3(ju1293) X*
CZ25594	*nsy-1(ju1543) II; nipi-3(ju1293) X*
CZ25595	*mak-2(ju1544) IV; nipi-3(ju1293) X*
CZ25596	*nsy-1(ju1545) II; nipi-3(ju1293) X*
CZ25598	*tir-1(ju1547) III; nipi-3(ju1293) X*
CZ25599	*nsy-1(ju1548) II; nipi-3(ju1293) X*
CZ25600	*mak-2(ju1549) IV; nipi-3(ju1293) X*
CZ25601	*mak-2(ju1550) IV; nipi-3(ju1293) X*
CZ25602	*mak-2(ju1551) IV; nipi-3(ju1293) X*
CZ25603	*mak-2(ju1552) IV; nipi-3(ju1293) X*
CZ25604	*mak-2(ju1553) IV; nipi-3(ju1293) X*
CZ25605	*mak-2(ju1554) IV; nipi-3(ju1293) X*
CZ25606	*mak-2(ju1555) IV; nipi-3(ju1293) X*
CZ25607	*mak-2(ju1556) IV; nipi-3(ju1293) X*
CZ25608	*mak-2(ju1557) IV; nipi-3(ju1293) X*
CZ25609	*mak-2(ju1558) IV; nipi-3(ju1293) X*
CZ25610	*mak-2(ju1559) IV; nipi-3(ju1293) X*
CZ25611	*mak-2(ju1560) IV; nipi-3(ju1293) X*
CZ25728[#]	*sek-1(ju1540) X nipi-3(ju1293) X*
CZ25729	*mec-4-GFP(zdIs5) I; sek-1(ju1540) X nipi-3(ju1293) X*
CZ25730[#]	*nipi-3(ju1293) X; ju1541*
CZ25731	*mec-4-GFP(zdIs5) I; nipi-3(ju1293) X; ju1541*
CZ25732[#]	*tir-1(ju1542) III; nipi-3(ju1293) X;*
CZ25733	*mec-4-GFP(zdIs5) I; tir-1(ju1542) III; nipi-3(ju1293) X*
CZ25734[#]	*nsy-1(ju1543) II; nipi-3(ju1293) X*
CZ25735	*mec-4-GFP(zdIs5) I; nsy-1(ju1543) II; nipi-3(ju1293) X*
CZ25736	*mak-2(ju1544) IV; nipi-3(ju1293) X*
CZ25737	*mec-4-GFP(zdIs5) I; mak-2(ju1544) IV; nipi-3(ju1293) X*
CZ25738[#]	*nsy-1(ju1545) II; nipi-3(ju1293) X*
CZ25739	*mec-4-GFP(zdIs5) I; nsy-1(ju1545) II; nipi-3(ju1293) X*
CZ25740[#]	*tir-1(ju1547) III; nipi-3(ju1293) X*
CZ25741	*mec-4-GFP(zdIs5) I; tir-1(ju1547) III; nipi-3(ju1293) X*
CZ25742[#]	*nsy-1(ju1548) II; nipi-3(ju1293) X*
CZ25743	*mec-4-GFP(zdIs5) I; nsy-1(ju1548) II; nipi-3(ju1293) X*
CZ27062	*nipi-3(ju1293) X; ju1541*
CZ27860	*nipi-3(ju1293) X; ju1541 ; Psek-1::GFP(juIs559)*

[#] - strains analyzed by whole genome sequencing

Table 18. Appendix Alleles

Allele	Gene	Effect	Source	Flanking Sequence	Detection
ju1540	*sek-1*	splice site	EMS	catggccaagAtacggaaaat	PCR: YJ12702 +YJ12695 Digest: StyI WT: 174/87 mut: 261
ju1542	*tir-1*	L590H	EMS	gatggagatcAtttacttcaa	PCR: YJ12719 + YJ12699R Sequence: YJ12719
ju1543	*nsy-1*	R598*	EMS	tgaatcgaaaTgagatgatcg	PCR: YJ12720 + YJ12721 Sequence: YJ12720
ju1544	*mak-2*	G22E	EMS	ctcggcgtagAaatcaacgga	PCR: YJ12690 + YJ12691 Sequence: YJ12690
ju1545	*nsy-1*	S280F	EMS	gataccgtatTccttatgatg	PCR: YJ12703 + YJ12704 Sequence: YJ12703
ju1547	*tir-1*	W560*	EMS	gtacctggctAgacatgcgca	PCR: YJ12719 + YJ12699R Sequence: YJ12719
ju1548	*nsy-1*	G676E	EMS	ggaacctatgAaactgtgtac	PCR: YJ12720 + YJ12721 Sequence: YJ12720
ju1549	*mak-2*	L19F	EMS	tttacaggttTtcggcgtagg	PCR: YJ12690 + YJ12691 Sequence: YJ12690
ju1550	*mak-2*	G20S	EMS	acaggttctcAgcgtaggaat	PCR: YJ12690 + YJ12691 Sequence: YJ12690
ju1551	*mak-2*	G20D	EMS	caggttctcgAcgtaggaatc	PCR: YJ12690 + YJ12691 Sequence: YJ12690
ju1552	*mak-2*	G25R	EMS	aggaatcaacAgaaaagttgtg	PCR: YJ12690 + YJ12691 Sequence: YJ12690
ju1553	*mak-2*	R52*	EMS	gaaagctcgtTgagaagtcga	PCR: YJ12690 + YJ12691 Sequence: YJ12690
ju1554	*mak-2*	V54D	EMS	cgtcgagaagAcgaacttcac	PCR: YJ12690 + YJ12691 Sequence: YJ12690
ju1555	*mak-2*	H127Y	EMS	tgctcatttgTatcgaatgag	PCR: YJ12690 + YJ12691 Sequence: YJ12690
ju1556	*mak-2*	splice site	EMS	ttatgtgtgaAttttttagaa	PCR: YJ12690 + YJ12691 Sequence: YJ12690
ju1557	*mak-2*	A182V	EMS	tactattgtgTtccggaagtg	PCR: YJ9306 + YJ9307 Sequence: YJ9306
ju1558	*mak-2*	W198*	EMS	gtgatttatgAtcgatcggag	PCR: YJ9306 + YJ9307 Sequence: YJ9306
ju1559	*mak-2*	G233R, A249T	EMS	aatcaagtcaAgacagtacac, ttctgaagcaAgtaagagtta	PCR: YJ9306 + YJ9307 Sequence: YJ9306
ju1560	*mak-2*	A249T	EMS	ttctgaagcaAgtaagagtta	PCR: YJ9306 + YJ9307 Sequence: YJ9306
ju1406	*natc-2*	Deletion	Cas9	ccaaaacatgcgaaa/ /aaaaattgtgtggga	PCR: YJ12701 +YJ12715 +YJ12716 WT: 883 mut: 1176
ju1407	*natc-2*	Deletion	Cas9	cgaggatgatactcc/ /agaaaaaattgtgtg	PCR: YJ12701 +YJ12715 +YJ12716 WT: 883 mut: 1460

Statistical Analysis of *Psek-1::GFP* and Body Length (Chapter 3)

I used JMP for all statistical analyses. For the *juIs559* dataset, the two microscopes used to collect the images differed in their general intensities. Thus, data points for each microscope were converted to percent of wildtype intensity. Then, a one-way ANOVA was applied with genotype as the independent variable and %WT as the dependent variable. A plot of residuals revealed heteroscedasticity across genotypes **(Figure 24A)** and their distribution was highly leptokurtotic **(Figure 24B)**. Consequently, a Box-Cox transformation was applied to these data (Sakia 1992) **(Figure 24C)**. After applying a one-way ANOVA again with genotype as the independent variable and Transformed %WT as the dependent variable, the residuals appeared homoscedastic **(Figure 24D)**. While the distribution of transformed residuals still was slightly leptokurtotic, it was "near-normal" **(Figure 24E)**. Generally, ANOVAs remain robust with near-normal distributions (Lix et al. 1996, Glass et al. 2016, Harwell et al. 2016). After ANOVA, all pairs of genotypes were compared using Tukey-Kramer HSD, which adjusts critical P values from multiple comparisons. *** $p<0.001$, ** $p<0.01$, * $p<0.05$, "ns" not significant $p>0.05$.

For the body length data set, a one-way ANOVA was applied with genotype as the independent variable and body length as the dependent variable. A plot of residuals revealed homoscedasticity across genotypes **(Figure 25A)** and with a normal distribution **(Figure 25B)**. After ANOVA, all pairs of genotypes were compared using Tukey-Kramer HSD, which adjusts critical P values from multiple comparisons. *** $p<0.001$, ** $p<0.01$, * $p<0.05$, "ns" not significant $p>0.05$.

Figure 24. Plots for statistical analysis of Psek-1::GFP dataset
(A) The plot of the residuals from a one-way ANOVA with genotype as the independent variable and %WT as the dependent variable showed a wedge shape, where the variance increases as the intensity value increases. This is called heteroskedastic distribution and indicates this dataset does not have a homogeneity of variance. Statistical tests of significance that assume a homogeneity of variance, like ANOVA, are invalid on this data. A heteroskedastic distribution of residuals is typical for a multiplicative scale of measurement (such as GFP intensity). **(B)** The distribution of the residuals from (A). The bars represent the residuals, and the green line represents the theoretical normal distribution. This dataset is not normally distributed, as there are many more values at the center rather than the edges. This is called a leptokurtotic distribution. **(C)** In order to use a parametric statistical test, such as an ANOVA, a transformation is applied to transform a non-normal data set into a normal shape. The goal of a transformation is to minimize the discrepancy between the data and a normal distribution. One test that can be used is a Box-Cox transformation method. This method calculates the SSE (sum of squares error, just another way of measuring the discrepancy between the data and a normal distribution model) for thousands of transformations changing a single variable, λ, between -2 and +2. The optimal λ is calculated to be 0.096, so the Box-Cox formula is applied each data point with λ=0.096, and the output is Transformed %WT. **(D)** The plot of the residuals from a one-way ANOVA with genotype as the independent variable and Transformed %WT as the dependent variable now shows a homoscedastic distribution after transformation. **(E)** The distribution of the residuals from (D). The bars represent the residuals, and the green line represents the theoretical normal distribution. This dataset is still slightly leptokurtotic but is considered to be “near normal. It is clear when comparing the plots **(Figure 15 A vs D and B vs E)** that the transformation successfully improved the normality of the dataset.

A Residuals of %WT have a heteroskedastic distribution

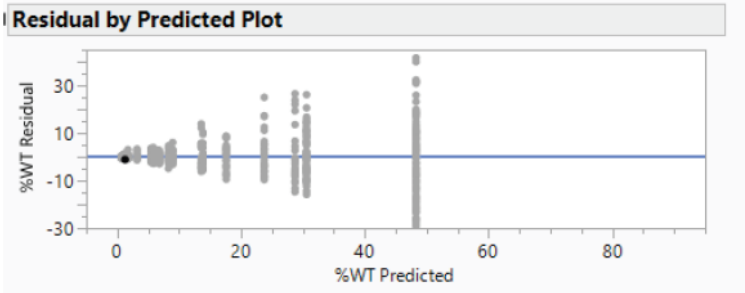

B Studentized residuals of %WT are not normally distributed

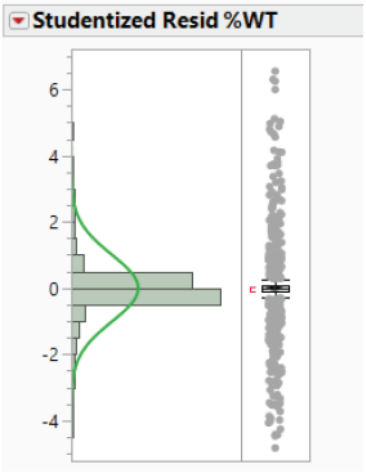

D After transformation, Residuals of %WT have a homoskedastic distribution

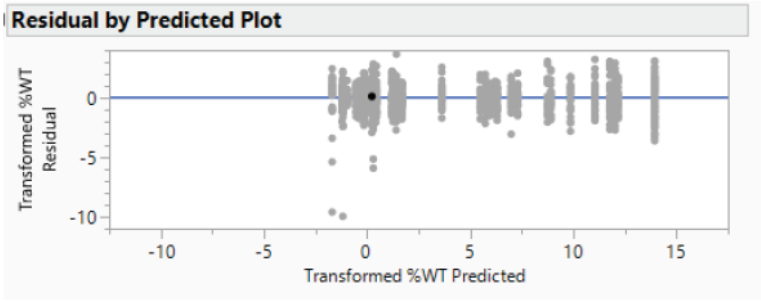

E After transformation, the distribution of studentized residuals is near normal

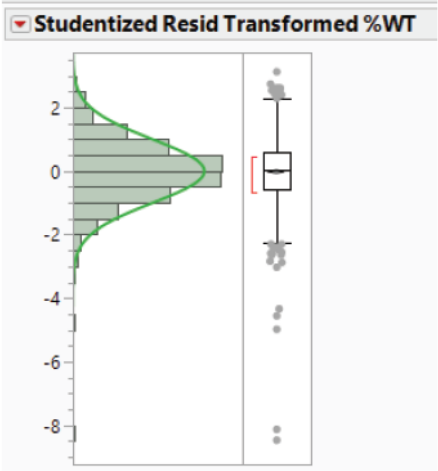

C Box-Cox Transformation Minimizes Discrepancy between dataset and a normal distribution curve

$$y(\lambda) = \begin{cases} \frac{y^{\lambda}-1}{\lambda}, & \text{if } \lambda \neq 0; \\ \log y, & \text{if } \lambda = 0. \end{cases}$$

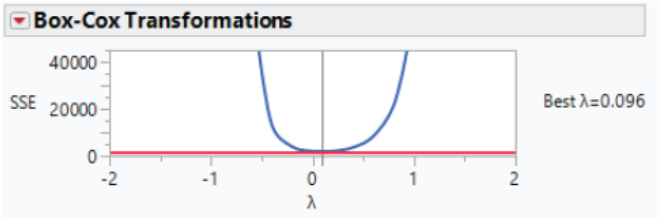

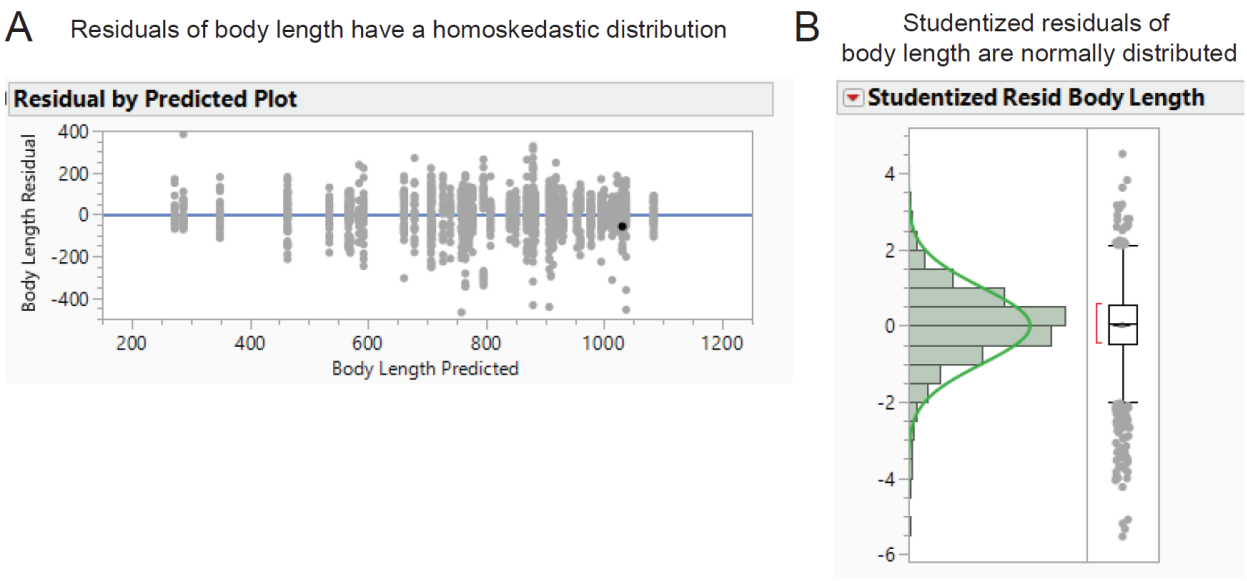

Figure 25. Plots for statistical analysis of body length dataset

(A) The plot of the residuals from a one-way ANOVA with genotype as the independent variable and body length as the dependent variable shows a homoscedastic distribution. **(B)** The distribution of the residuals from (A). The bars represent the residuals, and the green line represents the theoretical normal distribution. This dataset is slightly leptokurtotic but can be considered to be “near normal”.

References

Brenner, S. (1974). The genetics of Caenorhabditis elegans. *Genetics* **77**: 71-94. doi: 10.1093/genetics/77.1.71.

Glass, G. V., Peckham, P. D. and Sanders, J. R. (2016). Consequences of Failure to Meet Assumptions Underlying the Fixed Effects Analyses of Variance and Covariance. *Review of Educational Research* **42**: 237-288. doi: 10.3102/00346543042003237.

Harwell, M. R., Rubinstein, E. N., Hayes, W. S. and Olds, C. C. (2016). Summarizing Monte Carlo Results in Methodological Research: The One- and Two-Factor Fixed Effects ANOVA Cases. *Journal of Educational Statistics* **17**: 315-339. doi: 10.3102/10769986017004315.

Kim, K. W., Thakur, N., Piggott, C. A., Omi, S., Polanowska, J., Jin, Y. and Pujol, N. (2016). Coordinated inhibition of C/EBP by Tribbles in multiple tissues is essential for Caenorhabditis elegans development. *BMC Biol* **14**: 104. doi: 10.1186/s12915-016-0320-z.

Lix, L. M., Keselman, J. C. and Keselman, H. J. (1996). Consequences of Assumption Violations Revisited: A Quantitative Review of Alternatives to the One-Way Analysis of Variance "F" Test. *Review of Educational Research* **66**: 579-619. doi: 10.2307/1170654.

Sakia, R. M. (1992). The Box-Cox Transformation Technique A Review. *Journal of the Royal Statistical Society* **41**: 169-178.

Sarin, S., Prabhu, S., O'Meara, M. M., Pe'er, I. and Hobert, O. (2008). Caenorhabditis elegans mutant allele identification by whole-genome sequencing. *Nat Methods* **5**: 865-867. doi: 10.1038/nmeth.1249.